

# REPORT

EWI Project No. 46211GTH  
Electronic File Name: 41633R85.pdf

## Internal Repair of Pipelines Final Technical Report

Reporting Period:  
September 30, 2002 through December 31, 2005

Principal Authors:  
Bill Bruce, Matt Boring, Nancy Porter, George Ritter, Dennis Harwig, Ian Harris,  
Joe Dierksheide, Bill Mohr, Mark Lozev, Robin Gordon, Chris Neary, and Mike Sullivan

Report Issued: December 2005  
Revised: February 2006  
Revision n/a

DOE Award No.: DE-FC26-02NT41633

Submitted By:  
Edison Welding Institute  
1250 Arthur E. Adams Drive  
Columbus, OH 43221

Significant Subcontractor:  
Pacific Gas & Electric  
3400 Crow Canyon Road  
San Ramon, CA 94583



## DISCLAIMER

This report was prepared as an account of work sponsored by an agency of the United States Government. Neither the United States Government nor any agency thereof, nor any of their employees, makes any warranty, express or implied, or assumes any legal liability or responsibility for the accuracy, completeness, or usefulness of any information, apparatus, product, or process disclosed or represents that its use would not infringe privately owned rights. Reference herein to otherwise does not necessarily constitute or imply its endorsement, recommendation, or favoring by the United States Government or any agency thereof. The views and opinions of authors expressed herein do not necessarily state or reflect those of the United States Government or any agency hereof.

Measurement Units -- SI Metric System of Units are the primary units of measure for this report followed by their U.S. Customary Equivalents in parentheses ( ).

Note: SI is an abbreviation for "Le Systeme International d'Unites."

## ABSTRACT

Fiber-reinforced composite liner repair, deposited weld metal repair, adhesively bonded steel patch repair, and adhesively bonded/helically wound steel strip repair were reviewed and evaluated for potential application for internal repair of gas transmission pipelines.

In terms of performance requirements for internal repair, the following summarizes principal conclusions from a survey of natural gas transmission industry pipeline operators.

- Most attractive for river crossings/other bodies of water, in difficult soil conditions, under highways/congested intersections, and under railway crossings.
- Strong potential advantage vs. the high cost of horizontal direct drilling.
- Typical travel distances can be divided into three distinct groups: up to 305 m (1,000 ft.); between 305 m and 610 m (1,000 ft. and 2,000 ft.); and beyond 914 m (3,000 ft.). All three groups will require pig-based deployment systems.
- The most common pipe size diameter range for 80% to 90% of operators surveyed is 508 mm (20 in.) to 762 mm (30 in.), with 95% using 558.8 mm (22 in.).

Hydrostatic pressure testing was conducted on pipe sections with simulated corrosion damage repaired with glass fiber-reinforced composite liners, carbon fiber-reinforced composite liners, weld deposition, an adhesively bonded steel patch, and adhesively bonded/helically wound steel strip. To benchmark pipeline material performance, additional pipe sections were evaluated in the virgin and in the corrosion damaged/un-repaired conditions. Three repair technologies exhibited burst pressures that were greater than the burst pressures of the un-repaired pipe sections: adhesively bonded/helically wound steel strip repair exhibited the highest performance with burst pressures ranging from 0.4% to 144% higher; carbon fiber-reinforced liner repair had burst pressures ranging from 4% to 17% higher; and glass fiber-reinforced liner repair had burst pressures ranging from 1% to 7% higher. Two repair technologies exhibited burst pressures that were lower than the burst pressures of the un-repaired pipe sections: adhesively bonded steel patch repair was 1% lower and weld deposition repair was 10% lower.

Physical testing indicates that adhesively bonded/helically wound steel strip repair is clearly the most promising technology evaluated to-date because of its ability to effectively restore a damaged pipe section to well beyond the pressure that corresponds to 100% of the specified minimum yield strength, it lends itself well to field deployment, and the material itself is inexpensive. Coils can be sized to accommodate any length of corrosion damage, cinched down to allow deployment through pipe bends, and compressed down to a single strip width. Future investigation into this repair technology should be conducted to optimize its application and to develop a prototype repair systems to deploy this repair technology.

# TABLE OF CONTENTS

	<u>Page</u>
DISCLAIMER .....	ii
ABSTRACT .....	iii
TABLE OF CONTENTS .....	iv
LIST OF TABLES .....	vii
LIST OF GRAPHICAL MATERIALS .....	viii
LIST OF EQUATIONS .....	xiv
2.0 - INTRODUCTION .....	1
3.0 - EXECUTIVE SUMMARY .....	9
3.0 - EXPERIMENTAL .....	11
3.3 - Simulated Defect Preparation and Hydrostatic Testing .....	11
3.4 - Weld Deposition Repair Trials .....	18
3.5 - Glass Fiber-Reinforced Liner Repair Trials .....	25
3.6 - Carbon Fiber-Reinforced Liner Repair Trials .....	28
3.7 - Mechanical Testing of Carbon Fiber Liner Material .....	38
3.7 - Steel Patch-Reinforced Liner Repair Trials .....	42
3.8 - Helically Wound Steel Strip Repair Trials .....	46
4.0 - RESULTS AND DISCUSSION .....	52
4.1 - Technology Status Assessment .....	52
4.1.0 - Introduction .....	52
4.1.1 - Background .....	52
4.1.2 - Review and Assessment of Candidate Repair Methods .....	53
4.1.2.0 - Weld Repairs .....	53
4.1.2.1 - Fiber-Reinforced Composite Liners Repair .....	55
<i>General</i> .....	55
<i>External Repair Methods</i> .....	56
<i>Internal Repair Methods</i> .....	56
4.1.3 - Development Needs of Candidate Repair Methods .....	57
Weld Repair Methods .....	58
Fiber-Reinforced Composite Repair Methods .....	58
4.1.4 - Summary .....	58

4.2 - Operators Experience and Repair Needs Survey .....	58
4.2.0 - Repair Needs and Performance Requirements .....	58
4.2.1 - Target Specifications for an Internal Pipeline Repair System .....	59
4.2.2 - Survey Responses .....	61
Part 1: Currently Used Repair Methods.....	61
Part 2: Use/Potential Use of Internal Repair.....	66
Part 3: Need for In-Service Internal Repair.....	77
Part 4: Applicable Types of Damage .....	81
Part 5: Operational & Performance Requirements for Internal Repairs...	85
Part 6: General Comments.....	90
4.2.3 - Identification of Potential Repair Methods.....	91
4.3 - Detailed Test Program .....	97
4.4 - Baseline Material Performance.....	98
Pipe Material Evaluations .....	98
Glass Fiber Liner Material Evaluations.....	107
Carbon Fiber Liner Material Evaluations .....	108
Steel Strip Material Evaluations .....	111
4.5 - Weld Deposition Repair .....	114
Welding Systems Evaluated.....	115
Welding Procedure Development.....	118
Test 01: Weld Repair, 558.8 mm (22 in.) Pipe, Short/Deep Damage.....	127
Effect of Methane on Weld Quality.....	138
Implications of Weld Deposition Repair Trials .....	146
4.6 - Glass Fiber Liner Repairs .....	146
Test 02: GF Liner Repair, 114.3 mm (4.5 in.) Pipe, Long/Shallow Damage .....	147
Test 03: GF Patch Repair, 114.3 mm (4.5 in.) Pipe, Short/Deep Damage.....	150
Implications of GF Liner Repair Trails .....	151
4.7 - Simulation and Analysis of Fiber-Reinforced Liner Repair .....	152
4.8 - Carbon Fiber Reinforced Liner Repairs .....	158
Test 04: Solid/Half-Round/Radial CF Patch (Quasi-Isotropic), Short/Deep Damage, 3M DP460 Adhesive .....	159
Test 05: Thin Radial CF Patch (all 0, 90), Short/Deep Damage, 3M DP460 Adhesive.....	164
Optimized Requirements for CF Test Patches .....	167
Test 06: Thin Radial CF Patch (all 0, 90), Short/Deep Damage, 3M DP460 Adhesive.....	168

Test 07: Thick, Axial CF patch (all 0, 90), Long/Shallow Damage, 3M DP460 Adhesive.....	170
4.9 - Adhesively Bonded Steel Patch Repair .....	174
Test 08: Adhesively Bonded Steel Patch Repair, Short/Deep Damage .....	174
4.10 - Selection of Defect Size / Failure Mechanism.....	176
4.11 - Adhesively Bonded Helically Wound Steel Strip Repair Trials.....	177
Test 09: High Strength Steel Strip, Short/Extra Deep Damage, 3M DP460 Epoxy Adhesive.....	178
Test 10: High Strength Steel Strip, Short/Extra Deep Damage, Lord 7542 A/D Adhesive.....	180
Test 11: Low Strength Steel Strip, Short/Extra Deep Damage, 3M DP460 Epoxy Adhesive.....	182
Test 12: High Strength Steel Strip, Short/Extra Deep Damage, 3M DP460 Epoxy Adhesive.....	184
Test 13: High Strength Steel Strip, Short/Extra Deep Damage with Through Hole, 3M DP460 Epoxy Adhesive.....	186
Test 14: High Strength Steel Strip, Extra Long/Shallow Damage, 3M DP460 Epoxy Adhesive.....	189
4.12 - Comparison of All Candidate Repair Technologies .....	193
4.13 - Further Development Needs for Adhesively Bonded Helically Wound Steel Strip Repair.....	195
5.0 - CONCLUSIONS .....	196
6.0 - REFERENCES .....	199
7.0 - BIBLIOGRAPHY .....	200
8.0 - LIST OF ACRONYMS .....	202
9.0 - APPENDICES.....	203
Appendix A: Industry Survey with Cover Letter .....	A-1
Appendix B: Members of the Pipeline Research Council International.....	B-1
Appendix C: List of Natural Gas Pipeline Operating Companies.....	C-1
Appendix D: Lists of Surveyed PRCI Member & Other Gas Transmission Companies.....	D-1

## LIST OF TABLES

	<u>Page</u>
Table 1 - Pipe Materials and Wall Thicknesses .....	11
Table 2 - 2002/03 Natural Gas Transmission Pipeline Incident Summary by Cause .....	11
Table 3 - Metric Unit Welding Parameters for Weld Deposition Repair Test 01 .....	23
Table 4 - U.S. Customary Unit Welding Parameters for Weld Deposition Repair Test 01.....	24
Table 5 - Methane Welding Process Parameters .....	25
Table 6 - Layer Build Schedule for Test 04 CF Patch.....	29
Table 7 - Key to Ratings in Potential Repair Process Matrices (Table 8 - Table 10).....	92
Table 8 - Potential Welding Repair Methods .....	93
Table 9 - Potential Liner Repair Methods .....	94
Table 10 - Potential Surfacing Repair Methods .....	95
Table 11 - Tensile and Yield Strengths of the Pipe Materials .....	99
Table 12 - Pipe Materials/Sizes and Defect Characteristics for Baseline Pipe Sections .....	100
Table 13 - Predicted vs. Actual Hydrostatic Burst Pressure Values for Baselines .....	106
Table 14 - Tensile Testing Results for Glass Polypropylene Liner Material.....	107
Table 15 - Tensile and Interlaminar Shear Properties for CF Composite Panels .....	110
Table 16 - Measured Strength of Steel Strip Materials .....	112
Table 17 - Welding Parameters for Specimens R-01 through R-05 .....	124
Table 18 - Tie-In Quality at Each Clock Position for R-05 .....	125
Table 19 - Ultrasonic Thickness Measurements at Locations in Figure 125.....	133
Table 20 - Summary of Predicted vs. Actual Hydrostatic Burst Pressure Values Test 01 .....	138
Table 21 - Average Weld Metal Hardness and Carbon Content for Methane Weld Trials.....	142
Table 22 - Summary of Predicted vs. Actual Hydrostatic Burst Pressure Values Test 02 .....	149
Table 23 - Summary of Predicted vs. Actual Hydrostatic Burst Pressure Values Test 03 .....	151
Table 24 - Summary of Predicted vs. Actual Hydrostatic Burst Pressure Values Test 04 .....	162
Table 25 - Summary of Predicted vs. Actual Hydrostatic Burst Pressure Values Test 05 .....	167
Table 26 - Summary of Predicted vs. Actual Hydrostatic Burst Pressure Values Test 06 .....	169
Table 27 - Summary of Predicted vs. Actual Hydrostatic Burst Pressure Values Test 07 .....	173
Table 28 - Summary of Predicted vs. Actual Hydrostatic Burst Pressure Values Test 08 .....	176
Table 29 - Summary of Predicted vs. Actual Hydrostatic Burst Pressure Values Test 09 .....	180
Table 30 - Summary of Predicted vs. Actual Hydrostatic Burst Pressure Values Test 10 .....	182
Table 31 - Summary of Predicted vs. Actual Hydrostatic Burst Pressure Values Test 11 .....	184
Table 32 - Summary of Predicted vs. Actual Hydrostatic Burst Pressure Values Test 12 .....	186
Table 33 - Summary of Predicted vs. Actual Hydrostatic Burst Pressure Values Test 13 .....	189
Table 34 - Summary of Predicted vs. Actual Hydrostatic Burst Pressure Values Test 14 .....	192
Table 35 - Summary of Test Series Conducted.....	193

## LIST OF GRAPHICAL MATERIALS

	<u>Page</u>
Figure 1 - Installation of a Full-Encirclement Repair Sleeve .....	2
Figure 2 - External Weld Deposition Repair of Internal Wall Loss in 90° Elbow .....	2
Figure 3 - Osaka Gas System Robotic Welding System .....	3
Figure 4 - Internal Pipeline NDE System (IPNS) .....	3
Figure 5 - Welding and Inspection Steam Operations Robot (WISOR) .....	4
Figure 6 - Explorer II .....	4
Figure 7 - Clock Spring® Fiber-Reinforced Composite Device for Pipeline Repair .....	5
Figure 8 - Installation of a Sectional Liner in a Low-Pressure Pipeline .....	7
Figure 9 - Installation of a Cured-in-Place Liner (Inversion Process).....	8
Figure 10 - Installation of Fold-and-Formed Liner.....	8
Figure 11 - Milling Machine Set-Up Used to Simulate Corrosion Damage on Pipe Sections .....	12
Figure 12 - End Caps Welded on Pipe Section in Preparation for Hydrostatic Testing .....	13
Figure 13 - Pipe Section Attached to Hydrostatic Testing Equipment .....	13
Figure 14 - Long/Shallow Simulated Corrosion Damage for 114.3 mm (4.5 in.) Pipe .....	14
Figure 15 - Short/Deep Simulated Corrosion Damage for 114.3 mm (4.5 in.) Pipe.....	14
Figure 16 - Short/Deep Simulated Corrosion Damage for 508 mm (20 in.) Pipe.....	15
Figure 17 - Long/Shallow Simulated Corrosion Damage for 508 mm (20 in.) Pipe .....	15
Figure 18 - Short/Deep Simulated Corrosion Damage for 558.8 mm (22 in.) Pipe.....	16
Figure 19 - Short, Extra Deep Simulated Corrosion Damage for 609.6 mm (24 in.) Pipe .....	16
Figure 20 - Short, Extra Deep Damage with Through Hole for 609.6 mm (24 in.) Pipe.....	17
Figure 21 - Through Hole in Short/Extra Deep Damage in 609.6 mm (24 in.) Pipe.....	17
Figure 22 - Pipe Section in the 5G Horizontal Position.....	18
Figure 23 - Bortech Motion Mechanism for Continuous Spiral Deposition.....	18
Figure 24 - Bortech Controller.....	19
Figure 25 - OTC Robot Set-Up for Internal Welding .....	19
Figure 26 - Kobelco PC-350 Variable Polarity Fuzzy Logic Power Supply .....	20
Figure 27 - Magnatech Pipeliner II Welding Tractor .....	21
Figure 28 - Magnatech Control Pendant.....	21
Figure 29 - Panasonic AE 350 Power Supply .....	22
Figure 30 - Lay-Up and Forming of GF-Reinforced Composite Liner .....	25
Figure 31 - Insertion of GF Liner into 114.3 mm (4.5 in.) Diameter Pipe .....	26
Figure 32 - Silicon Rubber Bag Inserted into GF Liner .....	26
Figure 33 - Oven Used to Heat Pipe and GF Liner to 200°C (392°F).....	27



Figure 34 - GF Liner Installed in 114.3 mm (4.5 in.) Diameter Pipe .....	27
Figure 35 - Pipe Section Used for Carbon Fiber Patch Test 04.....	28
Figure 36 - Mylar-Lined Semi-Circular Mold for Test 04 CF Patch .....	30
Figure 37 - Dry Pack of Quasi-Isometric Fiber.....	30
Figure 38 - Breather Cloth Frame Draped Around Pack.....	31
Figure 39 - Mylar Top Shown Draped .....	31
Figure 40 - Vacuum Bag Film Draped Over Entire Pack .....	32
Figure 41 - Completed Test 04 CF Patch with Grit-Blasted OD .....	33
Figure 42 - Application of 3M DP460 Adhesive to Grit-Blasted ID of Test 04 Pipe.....	33
Figure 43 - Application of Adhesive to Test 04 CF Patch .....	34
Figure 44 - Installation of Test 04 CF Patch .....	34
Figure 45 - Clamping Bars Used to Hold Test 04 CF Patch in Place.....	35
Figure 46 - Adhesive Fillet Around Test 04 CF Patch.....	35
Figure 47 - Test 05 "Pressure Bandage" CF Patch .....	36
Figure 48 - Test 06 Thin CF Patch.....	37
Figure 49 - Test 07 CF Patch for Long/Shallow Defect Evaluation.....	38
Figure 50 - Mylar Over Release-Coated Plate .....	39
Figure 51 - Rim of Breather Added $\cong$ 76.2 mm (3 in.) Wide.....	39
Figure 52 - Dry Stack Before Lay-Up .....	40
Figure 53 - Top Breather Added .....	40
Figure 54 - Vacuum Bag Added Over Sealer Tape .....	41
Figure 55 - Wet Panel Under Applied Vacuum .....	41
Figure 56 - Three-Point Bending Test Set Up for ILS Testing .....	42
Figure 57 - Test 08 Steel Patch Prior to Epoxy Curing .....	43
Figure 58 - Test 08 Steel Patch Prior to Epoxy Curing (Long Seam) .....	43
Figure 59 - Test 08 Steel Patch Prior to Epoxy Curing (Circumferential Fillet).....	44
Figure 60 - Rubber Sheet Protecting Inflatable Bladder From Epoxy for Test 08.....	44
Figure 61 - Bladder Prior to Pressurization for Test 08.....	45
Figure 62 - Bladder Pressurized at 206 kPa (30 psi) for Test 08.....	45
Figure 63 - Test 08 Steel Patch with Circumferential Adhesive Fillet .....	46
Figure 64 - Test 09 Helically Wound Steel Strip with 3M DP460 Epoxy Applied.....	47
Figure 65. ID of Demonstration Pipe (similar to Test 09) with 3M DP460 Epoxy Applied.....	47
Figure 66 - Helically Wound Steel Strip Inserted into Pipe (similar to Test 09).....	48
Figure 67 - Helically Wound Steel Strip Expanded to Fit Pipe ID (similar to Test 09).....	49
Figure 68 - Inflatable Bladder Inserted in Pipe (similar to Test 09).....	49
Figure 69 - Bladder Pressurized to 206 kPa (30 psi) (similar to Test 09) .....	50

Figure 70 - Currently Used Repair Methods .....	62
Figure 71 - Criteria Affecting Choice of Repair Method .....	64
Figure 72 - Decision Factors for Internal Pipe Repair .....	67
Figure 73 - Specific Geographic Locations and Special Situations .....	69
Figure 74 - Distance Repair System Required to Travel Down Pipe .....	71
Figure 75 - Range of Pipe Diameters Used .....	72
Figure 76 - Potential Obstructions to be Negotiated .....	73
Figure 77 - Cost Comparative Breakpoint for Internal Repair .....	74
Figure 78 - Estimated Number of Internal Repairs Required Per Year .....	76
Figure 79 - Importance of Repair While Pipeline Remains In-Service .....	77
Figure 80 - Still Attractive if Pipeline Must be Shut Down (Depressurized and Evacuated) .....	78
Figure 81 - Still Attractive if Pipeline Must be Depressurized but Not Evacuated .....	79
Figure 82 - Still Attractive if Pipeline Must be Out of Service but Pressurized? .....	80
Figure 83 - External Coatings Used .....	82
Figure 84 - Maintenance on Coating Integrity .....	83
Figure 85 - Is CP System Capable of Compensating for Small Coating Breaches .....	84
Figure 86 - Inspectable by Pigging .....	85
Figure 87 - How Far Could the Repair Protrude Into Pipe Before Interference .....	86
Figure 88 - NDE Required for Repair to an Existing Weld .....	87
Figure 89 - NDE Required for Base Metal Repair .....	88
Figure 90 - Would Internal Repair be Attractive Even as a Temporary Repair? .....	89
Figure 91 - Weighted Scores of Potential Repair Methods .....	96
Figure 92 - 114.3 mm (4.5 in.) Pipe with Un-Repaired Long/Shallow Damage after Burst Test	101
Figure 93 - 114.3 mm (4.5 in.) Pipe with Un-Repaired Short/Deep Damage after Burst Test ..	101
Figure 94 - 508.0 mm (20 in.) Virgin Pipe After Burst Testing .....	102
Figure 95 - 508.0 mm (20 in.) Pipe with Un-Repaired Damage After Burst Testing .....	102
Figure 96 - 558.8 mm (22 in.) Virgin Pipe After Burst Testing .....	103
Figure 97 - 558.8 mm (22 in.) Pipe with Un-Repaired Damage After Burst Testing .....	103
Figure 98 - 609.6 mm (24 in.) Pipe with Un-Repaired Extra Long/Shallow Damage After Burst Testing .....	104
Figure 99 - Pressure vs. Time Plot of 609.6 mm (24 in.) Virgin Pipe Section .....	104
Figure 100 - Pressure vs. Time Plot of 609.6 mm (24 in.) Pipe with Defect .....	105
Figure 101 - Tensile Test Results for GF Polypropylene Liner Material .....	108
Figure 102 - Average Tensile and Modulus Properties for CF Composite Panels .....	111
Figure 103 - Photomicrograph of High Strength Steel Strip at 100X Magnification .....	112
Figure 104 - Photomicrograph of High Strength Steel Strip at 1000X Magnification .....	113

Figure 105 - Photomicrograph of Low Strength Steel Strip at 100X Magnification.....	113
Figure 106 - Photomicrograph of Low Strength Steel Strip at 1000X Magnification.....	114
Figure 107 - Bortech Torch and Torch Height Control.....	116
Figure 108 - OTC Robot Arm and Torch.....	117
Figure 109 - Weld Bead Shape Diagram.....	119
Figure 110 - Tests R-01 - R-04 at 12:00 (Note the Poor Tie-Ins for R-01 through R-03).....	120
Figure 111 - Test R-01 at 12:00 Show Poor Stop-Start Tie-In.....	121
Figure 112 - Tests R-03 and R-04 at 12:00 Show Better Stop-Start Overlap.....	122
Figure 113 - Tests R-01 and R-02 at 3:00 Showing Steady-State Bead Shape.....	123
Figure 114 - Tie-In Tests Using Parameters R-05 Every 30° Around One Ring Deposit.....	126
Figure 115 - Short/Deep Simulated Corrosion on 558.80 mm (22 in.) Pipe for Test 01.....	127
Figure 116 - Soil Box for Weld Deposition Repair Test 01.....	128
Figure 117 - Orientation of Pipe Section with Dirt Box for Weld Deposition Repair Test 01.....	128
Figure 118 - Outline of Simulated Corrosion on ID of Test 01 Pipe Section.....	129
Figure 119 - First Pass of Weld Layer 1 for Test 01.....	129
Figure 120 - Second Pass of Weld Layer 1 of Test 01.....	130
Figure 121 - Third Pass of Weld Layer 1 for Test 01.....	130
Figure 122 - Completed Weld Layer 1 for Test 01.....	131
Figure 123 - First Pass of Weld Layer 2 for Test 01.....	131
Figure 124 - Finished Weld Layer 2 of Test 01.....	132
Figure 125 - Ultrasonic Thickness Measurement Locations on Weld Repair Test 01.....	132
Figure 126 - Simulated Corrosion on Outside of Pipe After Weld Repair Test 01.....	134
Figure 127 - Soil in Contact With Pipe During Weld Repair Test 01.....	134
Figure 128 - Profile of Dent in Outside Pipe Surface After Internal Weld Repair Test 01.....	135
Figure 129 - Magnified Pictures of Dent at Ends and Middle of Test 01 Simulated Damage ...	136
Figure 130 - Test 01 Pipe Section After Hydrostatic Burst Test.....	137
Figure 131 - Set-Up for Welding Thin Wall Pipe with Pressurized Methane Gas.....	139
Figure 132 - Welds Made in Pressurized Methane - Appearance from OD.....	139
Figure 133 - Welds Made in Pressurized Methane - Appearance from ID.....	139
Figure 134 - Metallographic Cross Section of Weld 2M9.....	140
Figure 135 - Eutectic Iron Layer on Backside Surface of Weld 2M9.....	140
Figure 136 - Cracks in Eutectic Iron Layer of Weld 2M9.....	141
Figure 137 - Graphs of Table 21 Hardness Values and Carbon Content.....	143
Figure 138 - Methane Weld Specimen 325-2.....	143
Figure 139 - Methane Weld Specimen 325-3.....	144
Figure 140 - Methane Weld Specimen 325-4.....	144

Figure 141 - Methane Weld Specimen 325-5 .....	144
Figure 142 - Methane Weld Specimen 325-6 .....	145
Figure 143 - Methane Weld Specimen 325-8 .....	145
Figure 144 - Methane Weld Specimen 325-9 .....	145
Figure 145 - RolaTube Bi-Stable Reeled Composite Material .....	147
Figure 146 - Test 02 Pipe with GF Liner Repair of Long/Shallow Damage After Burst Test ....	148
Figure 147 - Cross Section of Test 02 Burst Test Specimen .....	149
Figure 148 - Magnified Cross Section of Test 02 Burst Test Specimen .....	149
Figure 149 - Test 03 Pipe with GF Liner Repair of Short/Deep Damage after Burst Test .....	150
Figure 150 - Relationship Between Modulus and Strength for Carbon Fibers.....	154
Figure 151 - Design Space for Composite Liner .....	156
Figure 152 - Test 04 Pipe With CF Patch Repair After Burst Test.....	161
Figure 153 - Test 04 Failure Initiation Site .....	161
Figure 154 - Magnified Test 04 Failure Initiation Site .....	162
Figure 155 - Test 05 CF Patch with Failure Locations .....	165
Figure 156 - Failure of Test 05 Pipe and Composite Repair.....	166
Figure 157 - Disbondment Between Pipe and Test 05 Patch at Pipe Failure Site.....	166
Figure 158 - Test 06 Damage after Burst Testing.....	169
Figure 159 - Test 07 Damage After Burst Test .....	171
Figure 160 - Inside Surface of Test 07 Pipe Section After Burst Test .....	171
Figure 161 - Test 07 Patch after Burst Testing .....	172
Figure 162 - Test 08 Post-Epoxy Cured Steel Patch Repair .....	174
Figure 163 - Test 08 Damage after Burst Test .....	175
Figure 164 - Inside of Test 08 Pipe Section After Burst Test.....	175
Figure 165 - Completed Helically Wound Steel Strip Repair .....	177
Figure 166 - Close Up of Completed Helically Wound Steel Strip Repair.....	178
Figure 167 - Test 09 Damage after Burst Test .....	179
Figure 168 - Test 10 Damage after Burst Test .....	181
Figure 169 - Large Number of Voids in Urethane Adhesive from Test 10 .....	181
Figure 170 - Test 11 Damage after Burst Test .....	183
Figure 171 - Test 12 Damage after Burst Test .....	185
Figure 172 - Pressure vs. Time Plot for Test 12 .....	185
Figure 173 - Test 13 Damage after Burst Test .....	187
Figure 174 - Close Up of Test 13 Damage after Burst Test.....	187
Figure 175 - Pressure vs. Time Plot for Test 13 .....	188
Figure 176 - Test 14 Damage after Burst Test .....	190

Figure 177 - Close Up of Test 14 Damage after Burst Test..... 190  
Figure 178 - Pressure vs. Time Plot for Test 14 ..... 191  
Figure 179 - % Improvement of Burst Test Results for Repaired vs. Un-Repaired Pipe ..... 194

## LIST OF EQUATIONS

Equation 1 - Length Beyond Which Hoop Stress Can No Longer Distribute Itself Around the End of a Defect .....	12
Equation 2 - Barlow's Formula .....	97
Equation 3 - Tensile Strength of the Fiber $\sigma_{fu}$ in MPa .....	153
Equation 4 - Tensile Strength of the Fiber $\sigma_{fu}$ in ksi .....	153
Equation 5 - Pressure to Reach Stress Equal to the SMYS of the Pipe Material .....	154
Equation 6 - Minimum Allowable Tensile Strength of the Fiber $\sigma_{fu}$ in MPa .....	155
Equation 7 - Minimum Allowable Tensile Strength of the Fiber $\sigma_{fu}$ in ksi .....	155
Equation 8 - Maximum Fiber Modulus in MPa .....	155
Equation 9 - Maximum Fiber Modulus in ksi .....	155
Equation 10 - c as a Function of the Thickness of Both the Pipe and Liner, and the Moduli of Both the Pipe and Liner .....	157
Equation 11 - Shear Stress as a Function of Shear Force .....	157
Equation 12 - Shear Force per Unit Length .....	157

## 2.0 - INTRODUCTION

This report describes work sponsored by the U.S. Department of Energy (DOE) National Energy Technology Laboratory (NETL) to develop internal repair technology for gas transmission pipelines. Lead by Edison Welding Institute (EWI), this project brought together a combination of partners that have a proven track record in developing energy pipeline repair technology: EWI, Pacific Gas & Electric (PG&E), and Pipeline Research Council International (PRCI). Based in Columbus, Ohio, EWI is North America's leading engineering and technology organization dedicated to welding and materials joining. EWI's staff provides materials joining assistance, contract research, consulting services, and training to over 3,300 member company locations representing world-class leaders in the energy pipeline, aerospace, automotive, defense, energy, government, heavy manufacturing, medical, and electronics industries. Based in San Francisco, PG&E is one of the largest combination natural gas and electric utilities in the United States, delivering natural gas and electric service to approximately 15 million people throughout a 70,000-square-mile service area in northern and central California. PRCI is a not-for-profit corporation comprised of energy pipeline companies who conduct a collaboratively-funded technology development program that enables energy pipeline companies around the world to provide safe, reliable, environmentally compatible, and cost-effective service to meet customer energy requirements.

External, corrosion-caused loss of wall thickness is the most common cause of repair for gas transmission pipelines. To prevent an area of corrosion damage from causing a pipeline to rupture, the area containing the corrosion damage must be reinforced. Since corrosion is a time dependent process, as pipelines become older, more repairs are required. Repair methods that can be applied from the inside of a gas transmission pipeline (i.e., trenchless methods) are an attractive alternative to conventional repair methods since pipeline excavation is precluded. This is particularly true for pipelines in environmentally sensitive and highly populated areas.

Several repair methods that are commonly applied from the outside of the pipeline are, in theory, directly applicable from the inside. However, issues must be addressed such as development of the required equipment to perform repairs remotely and the mobilization of said equipment through the pipeline to areas that need to be repaired. In addition, several additional repair methods that are commonly applied to other types of pipelines (e.g., gas distribution lines, water lines, etc.) have potential applicability, but require further development to meet the requirements for repair of gas transmission pipelines.

To prevent a corrosion defect from causing a pipeline to rupture, the area containing the defect must be reinforced to prevent the pipeline from bulging. The most predominant method of reinforcing corrosion defects in transmission pipelines is to install a welded full-encirclement repair sleeve (Figure 1). Full-encirclement sleeves resist hoop stress and can also resist axial stresses if the ends of the sleeves are welded.



**Figure 1 - Installation of a Full-Encirclement Repair Sleeve**

Gas transmission pipeline repair by direct deposition of weld metal, or weld deposition repair, is also a proven technology that can be applied directly to the area of wall loss, e.g., external repair of external wall loss, or to the side opposite to the wall loss, e.g., external repair of internal wall loss (Figure 2).



**Figure 2 - External Weld Deposition Repair of Internal Wall Loss in 90° Elbow**

There are no apparent technical limitations to applying this repair method to the inside of an out-of-service pipeline, e.g., internal repair of external wall loss. It is direct, relatively inexpensive to apply, and requires no additional materials beyond welding consumables. However, application



of this repair method to the inside of an in-service pipeline would require that welding be performed in a hyperbaric environment.

Deposited weld metal repairs are also used to repair circumferentially oriented planar defects (e.g., intergranular stress corrosion cracks adjacent to girth welds) in the nuclear power industry. Although remote welding was developed primarily for the nuclear power industry, working devices have been built for other applications, including repair of gas transmission pipelines. For example, Osaka Gas has developed remote robotic equipment for repair of flaws in the root area of welds of gas transmission lines (Figure 3).



**Figure 3 - Osaka Gas System Robotic Welding System**

Pacific Gas and Electric Company (PG&E) has developed the Internal Pipeline NDE System (IPNS) for internal inspection of gas pipelines (Figure 4). The system incorporates a variety of inspection technologies to characterize girth weld and long seam flaws, corrosion, and dents and gouges.



**Figure 4 - Internal Pipeline NDE System (IPNS)**

Honeybee Robotics and Consolidated Edison have developed the Welding and Inspection Steam Operations Robot (WISOR) system for inspection and repair of flanges in steam piping (Figure 5).



**Figure 5 - Welding and Inspection Steam Operations Robot (WISOR)**

A successfully developed internal repair method could be coupled to an autonomous inspection robot such as the Explorer II (Figure 6) to provide continuous inspection and repair capability for the natural gas infrastructure.



**Figure 6 - Explorer II**

Fiber-reinforced composite repairs are becoming widely used as an alternative to the installation of welded, full-encirclement sleeves for repair of gas transmission pipelines. These repairs typically consist of glass fibers in a polymer matrix material bonded to the pipe using an adhesive. The primary advantage of these repair products over welded, full-encirclement sleeves is that the need for welding is precluded.



**Figure 7 - Clock Spring® Fiber-Reinforced Composite Device for Pipeline Repair**

Glass-fiber based composite systems, such as Clock Spring® (Figure 7), consists of a coil of continuous uniaxial e-glass fibers in a polyester matrix material that is bonded to the pipe using an adhesive. As is the case with welded full-encirclement repair sleeves, adhesive filler is applied to the defect prior to Clock Spring® installation to allow load transfer to the composite material.

The average tensile strength and elastic modulus of the Clock Spring® composite in the hoop direction are 70,000 psi and  $5.5 \times 10^6$  psi, respectively. The elastic modulus of steel is approximately  $30 \times 10^6$  psi. When a pipe with a corrosion defect that has been repaired using Clock Spring® is pressurized, both the steel and the Clock Spring® begin to carry the hoop stress that is generated by the pressure. The Clock Spring®, because it has a lower elastic modulus than steel, begins to carry the load at a reduced proportion compared to the steel. The reason for this is that a material with a lower elastic modulus must experience a greater amount of strain (elongation) to carry an equal amount of load compared to a material with a higher elastic modulus. Once the steel in the vicinity of the defect exceeds its elastic limit, (i.e., begins to yield), the Clock Spring® begins to carry a larger portion of the load while at the same time preventing the defect from bulging. Because yielding is required in order for the Clock Spring® to carry a larger portion of the load, the use of Clock Spring® is not recommended for low toughness pipe or for sharp defects.

When applied to the inside of a pipe with a corrosion defect, a glass-fiber based composite repair system behaves in much the same way as an externally applied Clock Spring® up to the elastic limit of the steel. The composite material is prevented from carrying its share of the load because of the constraint that is provided by the steel pipe around it. The steel prevents the composite from experiencing the strain (elongation) required to carry a significant portion of the load. When the steel in the vicinity of the defect exceeds its elastic limit, (i.e., begins to yield),

the composite begins to carry a larger portion of the load, but since it is applied to the inside of the pipe, cannot prevent the defect from bulging. The adhesive that bonds the composite to the steel and the matrix material of the composite both have low strength in tension compared to the steel and the composite fibers. For external repair, bulging of the pipe wall in the vicinity of the defect places the adhesive in compression. For internal repair, bulging places the adhesive in tension. When the steel in the vicinity of the defect begins to yield, the adhesive and the matrix material fail allowing pressure to act upon the defect.

For internal repair, a composite repair material that has an elastic modulus that is closer to steel is required to protect the defect from experiencing the hoop stress that eventually leads to bulging. Carbon-fiber based composite materials are a more attractive option for internal repair of transmission pipelines, as they have an elastic modulus that is much closer to that of steel than glass-fiber based composite materials. For internal repair, designs that avoid loading the adhesive and the matrix material in tension are also required.

A variety of liners are commonly used for repair of other types of pipelines (e.g., gas distribution lines, sewers, water mains, etc.). These repair methods are primarily used to restore leak-tightness and are not considered structural repairs. Of these, the three that are potentially applicable to internal repair of gas transmission pipelines are sectional liners, cured-in-place liners, and fold-and-formed liners. Sectional liners are typically 0.9 m (3 ft.) to 4.6 m (15 ft.) in length and are installed only in areas that require repairs. The installation of a sectional liner is illustrated in Figure 8. Cured-in-place liners and fold-and-formed liners are typically applied to an entire pipeline segment. Cured-in-place liners are installed using the inversion process (Figure 9), while fold-and-formed liners (Figure 10) are pulled into place and then unfolded so they fit tightly against the inside of the pipe.

Composite liner repair processes and materials require further development before liner repair is a viable option for structural repair of gas transmission pipelines. The strength and stiffness of these materials must be improved, as well as the adhesive systems that bond the liner to the pipe surface. The required material thickness is of particular interest for internal structural reinforcement, as liner thickness can have an adverse affect on the ability to perform subsequent internal inspection and can generate flow restrictions.

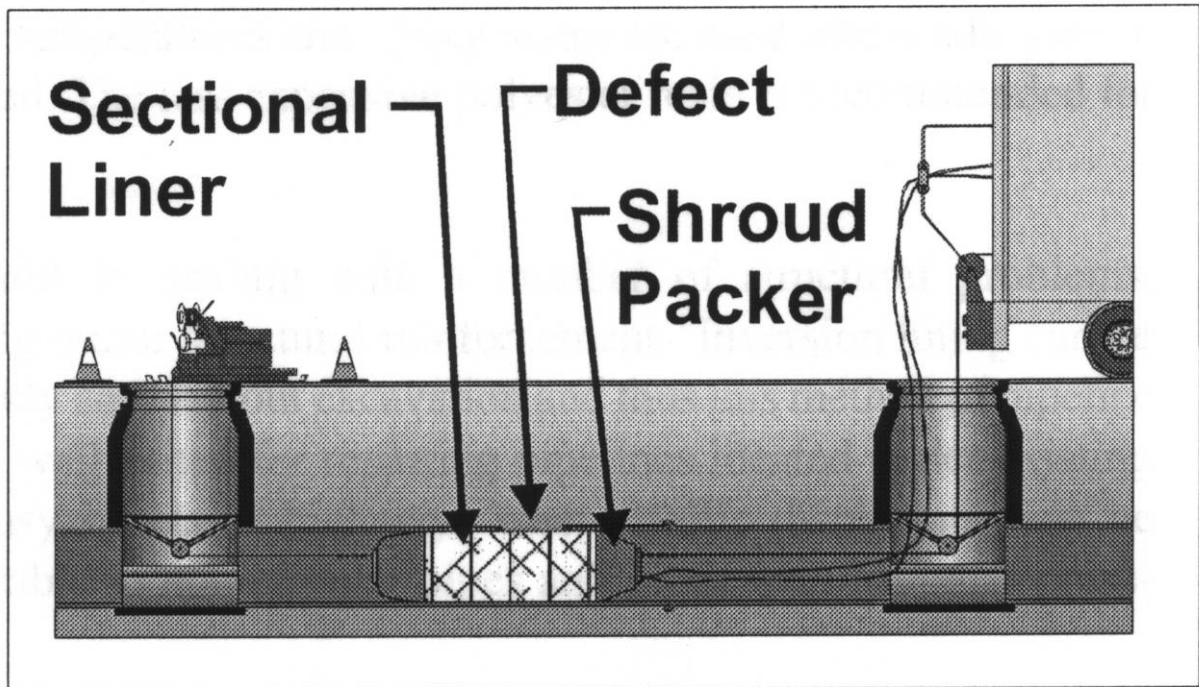
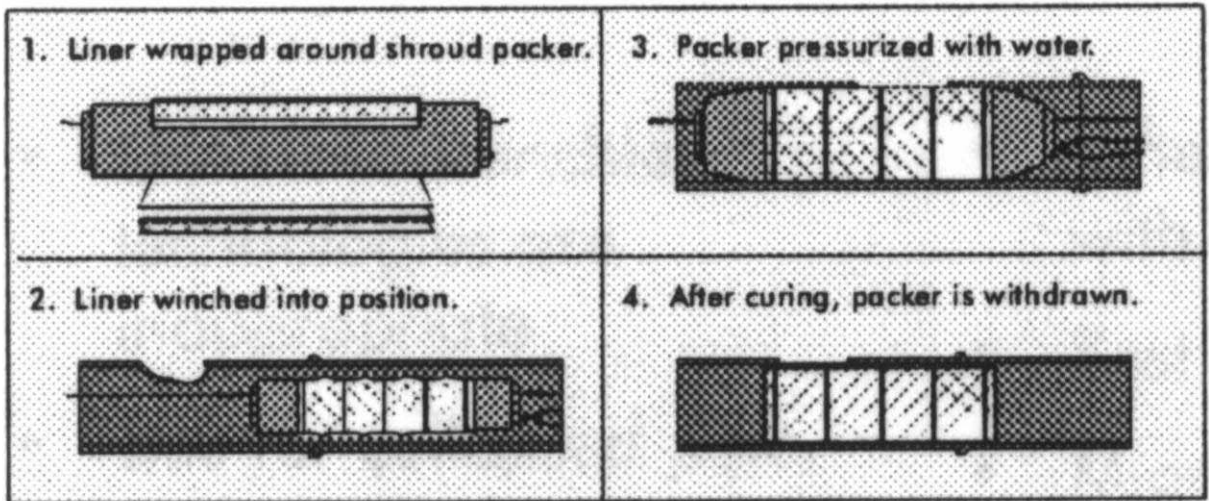


Figure 8 - Installation of a Sectional Liner in a Low-Pressure Pipeline

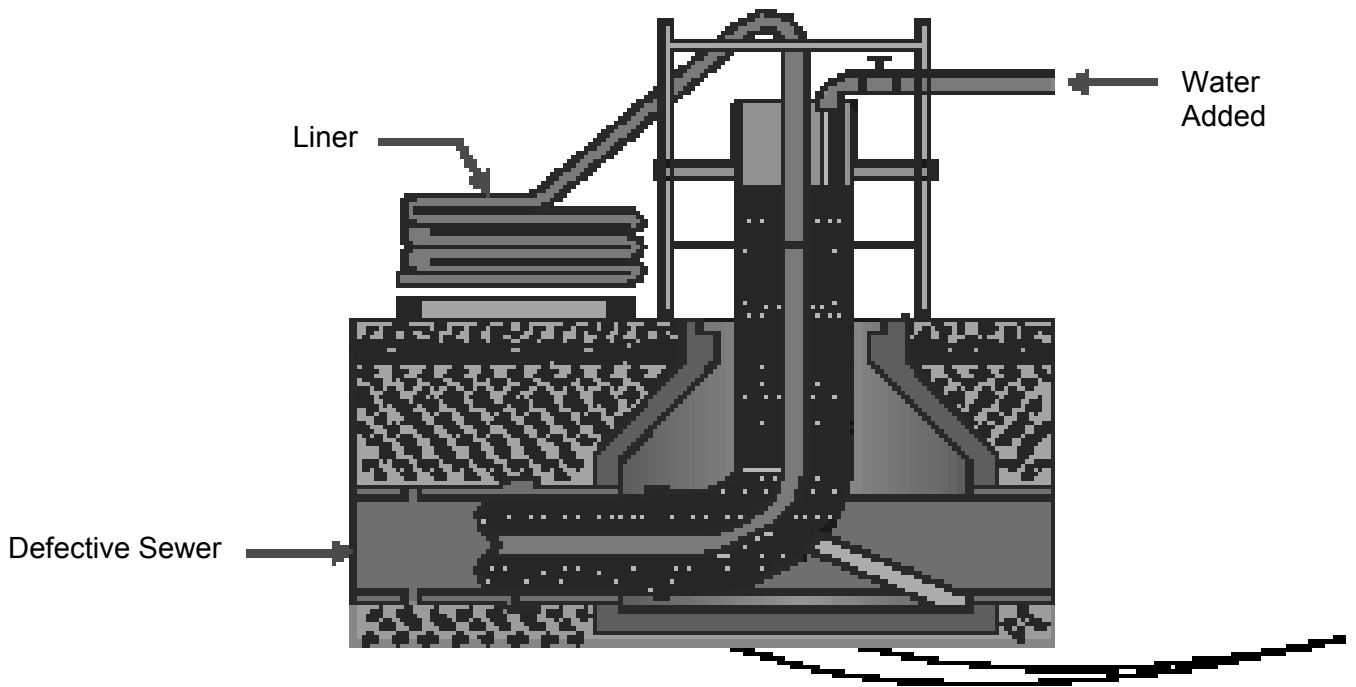


Figure 9 - Installation of a Cured-in-Place Liner (Inversion Process)

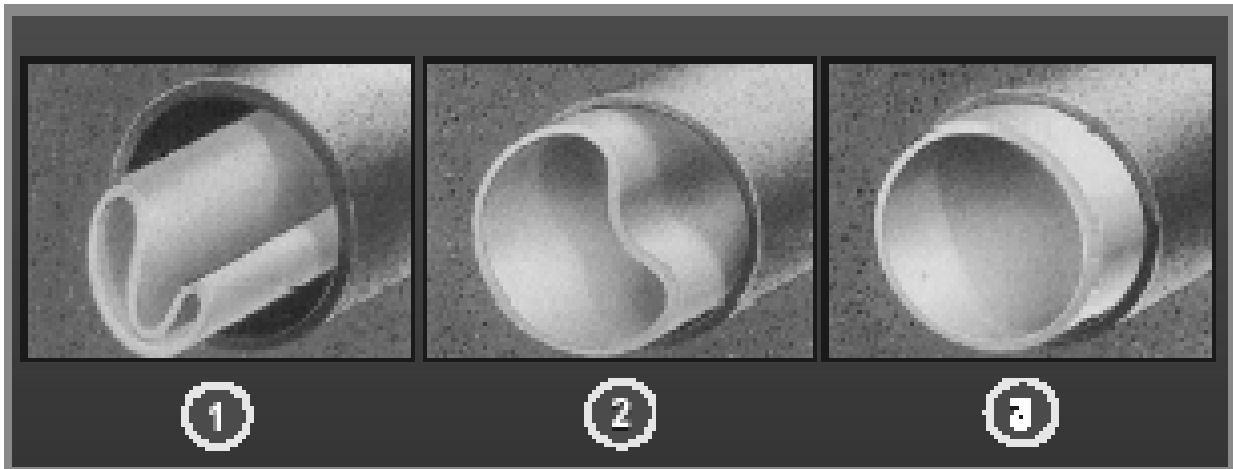


Figure 10 - Installation of Fold-and-Formed Liner

### 3.0 - EXECUTIVE SUMMARY

Fiber-reinforced composite liner repair, deposited weld metal repair, adhesively bonded steel patch repair, and adhesively bonded/helically wound steel strip repair technologies were reviewed, evaluated, and further developed for potential application for internal repair of gas transmission pipelines. Both fiber-reinforced composite liner repair and deposited weld metal repair are used extensively for external repair of energy pipelines. Adhesively bonded steel patch and adhesively bonded/helically wound steel strip repair processes are new innovative technologies that were developed and evaluated during the course of this investigation.

A survey of natural gas transmission industry pipeline operators was conducted to better understand their needs and performance requirements for internal repair. Survey responses produced the following principal conclusions.

- Most attractive for river crossings/other bodies of water, in difficult soil conditions, under highways/congested intersections, and under railway crossings. These repairs tend to be very difficult and very costly if, and where, conventional excavated methods are used.
- Strong potential advantage vs. the high cost of horizontal direct drilling.
- Typical travel distances can be divided into three distinct groups: up to 305 m (1,000 ft.); between 305 m (1,000 ft.) and 610 m (2,000 ft.); and beyond 914 m (3,000 ft.). All three groups require pig-based systems. A despoiled umbilical system would suffice for the first two groups which represents 81% of survey respondents. The third group would require an onboard self-contained power unit for propulsion and welding/liner repair energy needs.
- Pipe diameter sizes range from 50.8 mm (2 in.) through 1,219.2 mm (48 in.). The most common pipe diameter size range for 80% to 90% of operators surveyed is 508 mm (20 in.) to 762 mm (30 in.), with 95% of companies using 558.8 mm (22 in.).

The most frequent cause for repair of gas transmission pipelines was identified as external, corrosion-caused loss of wall thickness.

A test program was developed to evaluate full-size pipe sections repaired with candidate internal repair technologies. Areas of simulated damage were introduced into the outside diameter of pipe sections using methods previously developed at EWI. These damaged pipe sections were then repaired with the most promising candidate technologies. Repaired pipe sections were then hydrostatically pressure tested until rupture to establish performance data for the potential repair processes. Additionally, pipe sections in the virgin (i.e., undamaged) condition and pipe sections with un-repaired simulated corrosion damage were hydrostatically tested until rupture to establish baseline performance data (i.e., to establish a benchmark from which improvements could be measured).

Initially, glass fiber-reinforced composite liners were hydrostatically tested in small-scale pipe sections with simulated damage. Unlined, small-scale pipe sections with simulated damage

were also hydrostatically tested until rupture. The pipe sections with glass fiber-reinforced liners failed at pressures only slightly greater than the pipes with no liners, indicating that the glass fiber-reinforced liners are only marginally effective at restoring the pressure containing capability of a pipeline. Postmortem results indicate that a fiber-reinforced composite liner material that is stiffer would more effectively reinforce steel pipelines, thus allowing the liner to carry its share of the load without putting the interface between the liner and the steel pipe in tension.

Engineering analysis determined that a carbon fiber (CF) reinforced composite liner with a high fiber modulus and shear strength is required for composite liners to resist the types of shear stresses that can occur when external corrosion continues to the point where only the liner carries the stresses from the internal pressure in the pipe. Realistic combinations of composite material and thickness were analytically determined for use in experimental trials. Failure pressures for full-scale pipe repaired with carbon fiber-reinforced composite liner were greater than that of pipe sections without liners, indicating that carbon fiber-reinforced liners were more effective at restoring the pressure containing capabilities of gas transmission pipelines as compared to glass fiber-reinforced composite liners.

Failure pressures for full-scale pipe repaired with an adhesively bonded steel patch were less than that of un-repaired pipe sections, indicating that the adhesively bonded steel patch repair was less than effective at restoring the pressure containing capabilities of a pipeline. Failure pressures for full-scale pipe repaired with the adhesively bonded/helically wound steel strip repair process far exceeded that of un-repaired pipe sections, indicating that the adhesively bonded/helically wound steel strip repair process is capable of restoring the pressure containing capabilities of a pipeline to well beyond the pressure that corresponds to 100% of the SMYS of the pipe.

Specimens of virgin pipe material had the highest hydrostatic burst pressures. Three repair technologies exhibited burst pressures that were greater than the burst pressures of the same diameter pipe material with un-repaired damage: adhesively bonded/helically wound steel strip repair exhibited the highest performance with burst pressures ranging from 0.4% to 144% higher; carbon fiber-reinforced liner repair had burst pressures ranging from 4% to 17% higher; and glass fiber-reinforced liner repair had burst pressures ranging from 1% to 7% higher. Two repair technologies exhibited burst pressures that were lower than the burst pressures of the same diameter pipe material with un-repaired damage: adhesively bonded steel patch repair was 1% lower and weld deposition repair was 10% lower.

Physical testing clearly indicates that adhesively bonded/helically wound steel strip repair is the most promising technology evaluated in this study. It significantly restores the pressure containing capability of damaged pipe, lends itself well to field deployment, and the material is inexpensive. Coils can be sized to accommodate any length of corrosion damage, cinched down to allow deployment through pipe bends, and compressed down to a single strip width. Future investigation into this repair technology should be conducted to optimize its application and to develop a prototype repair systems to deploy this repair technology.



### 3.0 - EXPERIMENTAL

This section describes all experimental methods used during the execution of the project.

#### 3.3 - Simulated Defect Preparation and Hydrostatic Testing

During the course of this investigation, four different pipe diameters and three different pipe materials were used to evaluate the various repair technologies. Table 1 contains a list of all pipe material and wall thickness combinations used.

Diameter		Wall Thickness		Pipe Material	Coating Type
mm	in.	mm	in.		
114.3	4.5	4.8	0.188	API 5L, Grade B	Red FBE
508	20	6.4	0.25	API 5L, X52	Green FBE
558.8	22	7.9	0.312	API 5L, Grade B	Coal Tar
609.6	24	7.9	0.312	API 5L, X65	Bare

**Table 1 - Pipe Materials and Wall Thicknesses**

The test program considered a range of damage types, both internal and external, that are typical of those encountered in pipelines. The U. S. Department of Transportation, Research and Special Programs Administration, Office of Pipeline Safety, compiles statistics on pipeline failure causes<sup>(1)</sup> which are posted on their web site located at [http://primis.rspa.dot.gov/pipelineInfo/stat\\_causes.htm](http://primis.rspa.dot.gov/pipelineInfo/stat_causes.htm). During 2002-2003, DOT statistics indicate that for natural gas transmission pipelines the largest contributor to pipeline damage was clearly corrosion-caused loss of wall thickness (as shown in Table 2). Eventually, the wall thickness decreases to the point where it is not sufficient to contain the stresses from the internal pressure and the pipeline will rupture or burst.

Reported Cause	Number of Incidents	% of Total Incidents	Property Damages	% of Total Damages	Fatalities	Injuries
Excavation Damage	32	17.9	\$4,583,379	7.0	2	3
Natural Force Damage	12	6.7	\$8,278,011	12.6	0	0
Other Outside Force Damage	16	8.9	\$4,687,717	7.2	0	3
Corrosion	46	25.7	\$24,273,051	37.1	0	0
Equipment	11	6.1	\$3,958,904	6.0	0	5
Materials	36	20.1	\$12,130,558	18.5	0	0
Operation	5	2.8	\$286,455	0.4	0	2
Other	21	11.7	\$7,273,647	11.1	0	0
Total	179	-	\$65,471,722	-	2	13

**Table 2 - 2002/03 Natural Gas Transmission Pipeline Incident Summary by Cause**

Given the fact that corrosion was the most significant contributor to natural gas pipelines failures during 2002 and 2003, the two most common types of corrosion, general corrosion and a deep/isolated corrosion pit (with approximately 30% reduction in burst pressure) were selected initially for repair process evaluation. For a specific pipe material and wall thickness combination, RSTRENG® software<sup>(2)</sup> was used to calculate the dimensions of the desired defect. As shown in Figure 11, a milling machine was used to introduce simulated damage into pipe specimens.



**Figure 11 - Milling Machine Set-Up Used to Simulate Corrosion Damage on Pipe Sections**

For the purpose of these defect descriptions, "short" refers to a length that is shorter than the following:

$$L = (20Dt)^{1/2}$$

**Equation 1 - Length Beyond Which Hoop Stress Can No Longer Distribute Itself Around the End of a Defect**

where  $L$  is the defect length,  $D$  is the pipe diameter, and  $t$  is the wall thickness. "Long" refers to a defect that exceeds this length beyond which the hoop stress in the pipe can no longer distribute itself around the end of the defect.

After simulated corrosion damage was introduced in to pipe sections, they were repaired with the appropriate repair technology. End caps were then welded to pipe sections as shown in Figure 12. Following the installation of end caps, pipe sections were hydrostatically pressurized to failure (i.e., burst pressure) using the set-up shown in Figure 13.



**Figure 12 - End Caps Welded on Pipe Section in Preparation for Hydrostatic Testing**

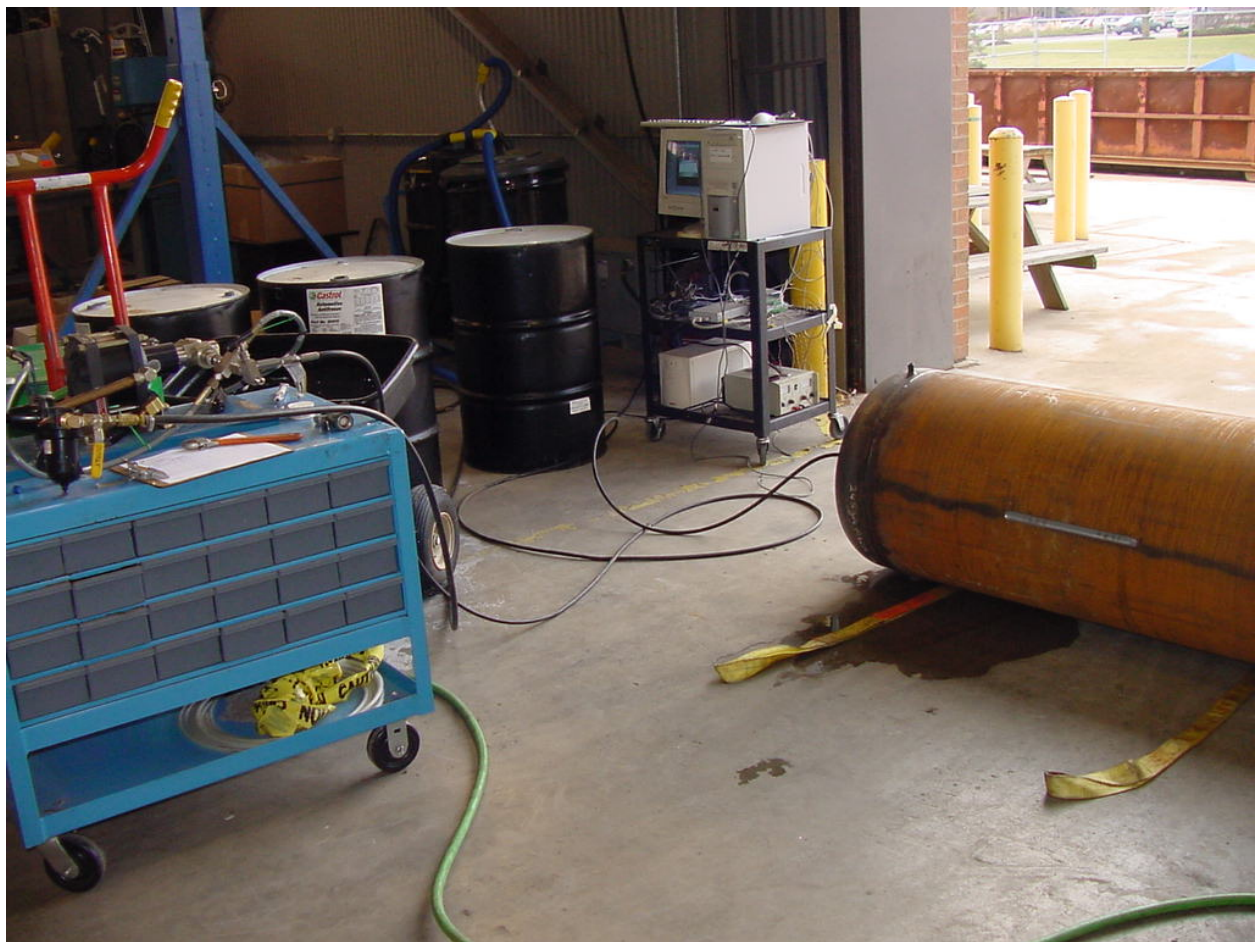


**Figure 13 - Pipe Section Attached to Hydrostatic Testing Equipment**

RSTRENG was used to determine that a long/shallow corrosion defect that represents a 30% reduction in burst strength needs to be 127 mm (5 in.) long by 2.54 mm (0.100 in.) deep for the 114.3 mm (4.5 in.) diameter API-5L, Grade B pipe. An end mill was used to machine a simple slot in the outside diameter (OD) of the pipe sections (Figure 14).



**Figure 14 - Long/Shallow Simulated Corrosion Damage for 114.3 mm (4.5 in.) Pipe**

RSTRENG was also used to determine that a short/deep corrosion pit with 30% reduction in burst pressure needs to be 25.4 mm (1 in.) long by 4.01 mm (0.160 in.) deep for the 114.3 mm (4.5 in.) diameter API 5L Grade B pipe. An end mill with rounded corners was used to machine this simulated corrosion pit in the OD of pipe sections (Figure 15).



**Figure 15 - Short/Deep Simulated Corrosion Damage for 114.3 mm (4.5 in.) Pipe**

Using the same methodology, a short/deep corrosion defect that represents a 25% reduction in burst strength was calculated to be 127 mm (5 in.) long by 3.45 mm (0.136 in.) deep for the

508 mm (20 in.) diameter API 5L X52 pipe. An end mill was used to machine a more stylized slot (i.e., more representative of actual corrosion damage) in the OD of pipe sections as shown in Figure 16. End caps were similarly welded to pipe sections in preparation for burst testing.



**Figure 16 - Short/Deep Simulated Corrosion Damage for 508 mm (20 in.) Pipe**

A long/shallow corrosion defect that represents a 25% reduction in burst strength was calculated to be 381 mm (15 in.) long by 2.74 mm (0.108 in.) deep for the 508 mm (20 in.) diameter API-5L X52 pipe. An end mill was used to machine a simple slot in the OD of the pipe section as shown in Figure 17. End caps were welded to the pipe section in preparation for burst testing.



**Figure 17 - Long/Shallow Simulated Corrosion Damage for 508 mm (20 in.) Pipe**

A stylized short/extra deep defect that represents a 50% reduction in burst strength was calculated to be 127 mm (5 in.) long by 4.75 mm (0.187 in.) deep for the 508 mm (20 in.) diameter API-5L X52 pipe (picture not shown but similar to Figure 16). An end mill was used to machine the defect in the OD of the pipe section. End caps were welded to the pipe section in preparation for burst testing.

A short/deep corrosion defect that represents a 25% reduction in burst strength was calculated to be 190.5 mm (7.5 in.) long by 3.96 mm (0.156 in.) deep for the 558.8 mm (22 in.) diameter API-5L, Grade B pipe. An end mill was used to machine a simple slot in the OD of pipe sections as shown in Figure 18. End caps were welded to pipe sections in preparation for burst testing.



**Figure 18 - Short/Deep Simulated Corrosion Damage for 558.8 mm (22 in.) Pipe**

A short/extra deep corrosion defect that represents a 60% reduction in burst strength was calculated to be 228.6 mm (9 in.) long by 5.94 mm (0.234 in.) deep for the 609.6 mm (24 in.) diameter API-5L X65 pipe. An end mill was used to machine the simple slot in the OD of pipe sections as shown in Figure 19. End caps were welded to pipe sections in preparation for burst testing.



**Figure 19 - Short, Extra Deep Simulated Corrosion Damage for 609.6 mm (24 in.) Pipe**

For the 609.6 mm (24 in.) diameter API-5L X65 pipe, a thru-wall pit was also incorporated into a short/extra deep corrosion defect representing a 60% reduction in burst strength (228.6 mm (9 in.) long by 5.94 mm (0.234 in.) deep). Figure 21 is a close up view of the through hole in the 609.6 mm (24 in.) pipe section. An end mill was used to machine the slot and the through-wall pit in the OD of the pipe section as shown in Figure 20. End caps were welded to pipe sections in preparation for burst testing.



**Figure 20 - Short, Extra Deep Damage with Through Hole for 609.6 mm (24 in.) Pipe**

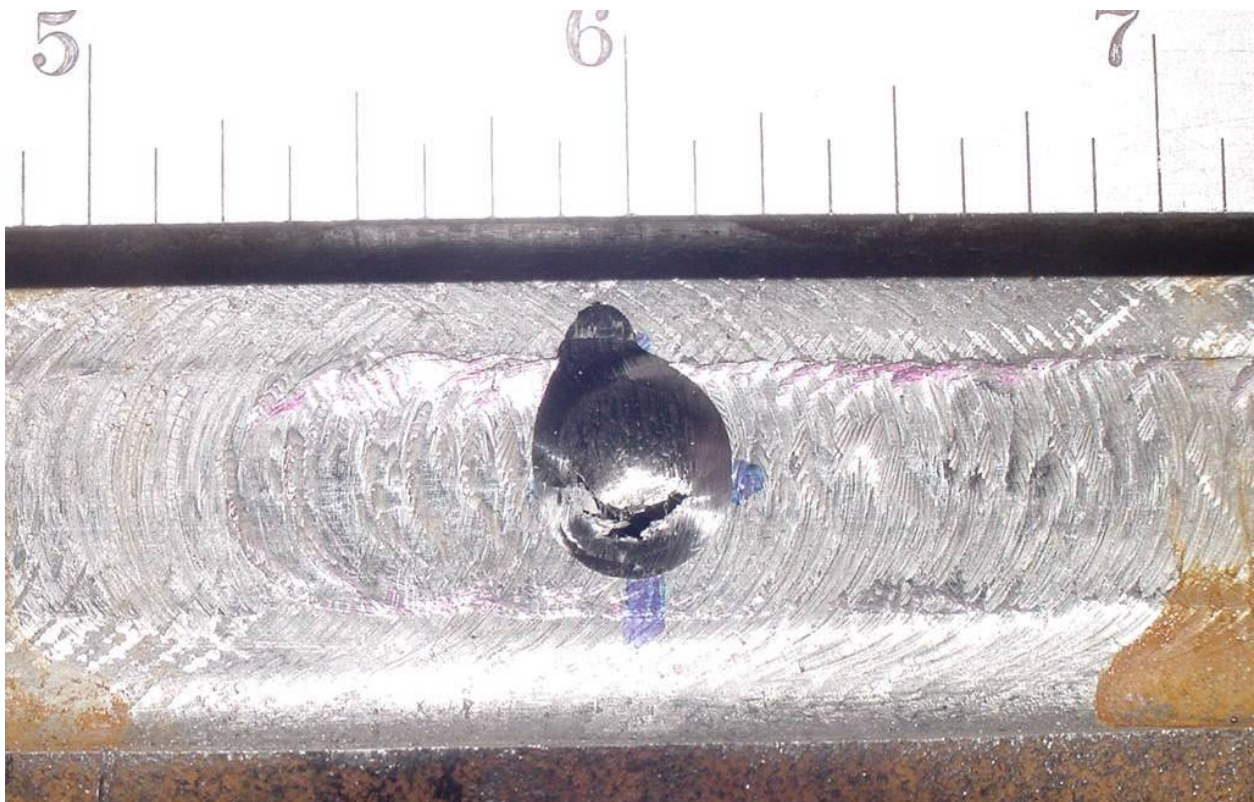


**Figure 21 - Through Hole in Short/Extra Deep Damage in 609.6 mm (24 in.) Pipe**

A long/shallow corrosion defect that representing a 60% reduction in burst strength was calculated to be 381 mm (15 in.) long by 5.66 mm (0.223 in.) deep for the 609.6 mm (24 in.) diameter API-5L X65 pipe. An end mill was used to machine the slot in the OD of pipe sections. End caps were welded to pipe sections in preparation for burst testing.

### 3.4 - Weld Deposition Repair Trials

All weld deposition repair trials used short-circuit gas metal arc welding (GMAW) Welding was conducted on 558.8 mm (22 in.) diameter API 5L, Grade B pipe sections. During all welding trials, the pipe axis was fixed in the 5G (i.e., horizontal) position as illustrated in Figure 22.

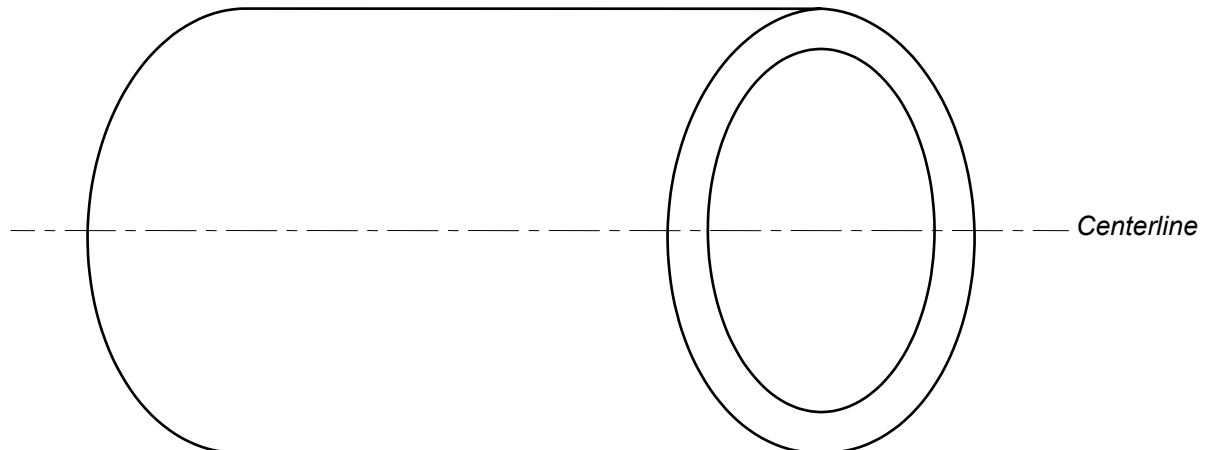


**Figure 22 - Pipe Section in the 5G Horizontal Position**

The following welding systems were evaluated for internal repair of pipelines:

- Internal bore cladding system (Bortech)
- 6-axis robot capable of complex motion control (OTC Daihen)
- Orbital welding tractor configured for inside welding (Magnatech Pipeliner)

The internal bore cladding system manufactured by Bortech (Figure 23) was designed for spiral cladding the inside of pipe that is preferably in the vertical position.



**Figure 23 - Bortech Motion Mechanism for Continuous Spiral Deposition**





Figure 24 - Bortech Controller



Figure 25 - OTC Robot Set-Up for Internal Welding

The OTC Daihen robot was interfaced to an advanced short-circuit welding power supply, the Kobelco PC-350 shown in Figure 26.



Figure 26 - Kobelco PC-350 Variable Polarity Fuzzy Logic Power Supply

The Magnatech Pipeliner II welding tractor was designed to weld the inside diameter of 508 mm (22 in.) pipe. Figure 28 shows the Magnatech control pendant.



Figure 27 - Magnatech Pipeliner II Welding Tractor



Figure 28 - Magnatech Control Pendant

The Magnatech tractor was interfaced to a Panasonic AE 350 power supply, which is shown in Figure 29.



Figure 29 - Panasonic AE 350 Power Supply

The Magnatech Pipeliner II was used to make the weld deposition repair of a short/deep, stylized corrosion defect (Figure 18) evaluated in Test 01. Test 01 welding was done with a shielding gas mixture of 95% Argon (Ar) and 5% Carbon Dioxide (CO<sub>2</sub>). Filler metal was a GMAW 0.89 mm (0.035 in.) diameter AWS ER70S-6 electrode. Welding parameters are shown in Table 3 and Table 4.

Layer	Pass	Wire Feed Speed (mpm)	Current (amps)	Volts	Length (mm)	Time (sec)	Travel Speed (mpm)	Heat Input (kJ/mm)
1	1	5.44	100	19.9	158.750	165	0.058	2.07
	2	5.51	97	19.8	165.100	175	0.057	2.04
	3	5.46	96	19.9	171.450	173	0.059	1.93
	4	5.49	98	19.8	165.100	173	0.057	2.03
	5	5.46	98	19.8	168.275	185	0.055	2.13
	6	5.46	99	20.0	171.450	191	0.054	2.21
	7	5.38	98	19.9	171.450	192	0.054	2.18
	8	5.46	99	19.8	174.625	200	0.052	2.24
	9	5.44	98	19.8	171.450	200	0.051	2.27
	10	5.38	98	19.5	174.625	197	0.053	2.16
	11	5.46	100	19.6	174.625	192	0.055	2.16
2	1	5.49	96	19.9	155.575	179	0.052	2.20
	2	5.41	98	19.8	165.100	179	0.055	2.11
	3	5.38	99	19.9	155.575	171	0.055	2.17
	4	5.51	98	19.8	161.925	187	0.052	2.24
	5	5.46	104	19.6	160.274	176	0.055	2.24
	6	5.44	101	19.8	165.100	189	0.052	2.29
	7	5.46	98	19.8	165.100	189	0.052	2.22
	8	5.46	96	19.9	163.576	199	0.049	2.32
	9	5.46	100	19.8	166.624	204	0.049	2.42
	10	5.49	101	19.8	169.545	205	0.050	2.42

**Table 3 - Metric Unit Welding Parameters for Weld Deposition Repair Test 01**

Weld Layer	Pass	Wire Feed Speed (ipm)	Current (amps)	Volts	Length (in)	Time (sec)	Travel Speed (ipm)	Heat Input (kJ/in)
1	1	214	100	19.9	6.25	165	2.27	52.5
	2	217	97	19.8	6.50	175	2.23	51.7
	3	215	96	19.9	6.75	173	2.34	49.0
	4	216	98	19.8	6.50	173	2.26	51.6
	5	215	98	19.8	6.63	185	2.15	54.2
	6	215	99	20.0	6.75	191	2.12	56.0
	7	212	98	19.9	6.75	192	2.11	55.4
	8	215	99	19.8	6.88	200	2.06	57.0
	9	214	98	19.8	6.75	200	2.02	57.6
	10	212	98	19.5	6.88	197	2.09	54.8
	11	215	100	19.6	6.88	192	2.15	54.7
2	1	216	96	19.9	6.13	179	2.06	55.8
	2	213	98	19.8	6.50	179	2.18	53.5
	3	212	99	19.9	6.13	171	2.15	55.1
	4	217	98	19.8	6.38	187	2.04	57.0
	5	215	104	19.6	6.31	176	2.15	57.0
	6	214	101	19.8	6.50	189	2.06	58.1
	7	215	98	19.8	6.50	189	2.06	56.4
	8	215	96	19.9	6.44	199	1.94	59.0
	9	215	100	19.8	6.56	204	1.93	61.5
	10	216	101	19.8	6.68	205	1.95	61.5

**Table 4 - U.S. Customary Unit Welding Parameters for Weld Deposition Repair Test 01**

The Magnatech Pipeliner II was also used to weld trials with a shielding gas containing various levels of methane to determine the effect of methane on resultant weld quality. For each weld specimen, a single GMAW weld (i.e., a bead on plate) was deposited on the ID of a 558.80 mm (22 in.) diameter API 5L Grade B pipe in the 6:00 or flat welding position. Filler metal was a GMAW 0.89 mm (0.035 in.) diameter AWS ER70S-6 electrode.

Shielding gas was supplied by two independent gas bottles: one bottle contained a mixture of 95% Ar + 5% CO<sub>2</sub>; the other bottle contained a mixture of 10% methane with a balance of 95% Ar + 5% CO<sub>2</sub>. The amount of methane was raised by increasing the flow rate on the flow meter of the bottle containing methane. Linear travel speeds of the welds were not recorded as they were held constant for all weld trials. The welding parameters for these trials are shown in Table 5.

Weld ID	Shielding Gas Flow Rate				Voltage (volts)	Current (amps)	Wire Feed Speed	
	95% Ar + 5% CO <sub>2</sub>		10% Methane + 4.5% CO <sub>2</sub> + 85.5% Ar				(mpm)	(ipm)
	(m <sup>3</sup> /hr)	(ft <sup>3</sup> /hr)	(m <sup>3</sup> /hr)	(ft <sup>3</sup> /hr)				
325-2	1.41	50	0.00	0	23.4	111	5.36	211
325-6	1.22	43	0.20	7	23.4	104	5.23	206
325-3	1.13	40	0.28	10	23.3	108	5.28	208
325-8	0.99	35	0.28	10	23.2	101	5.26	207
325-4	0.99	35	0.42	15	23.4	99	5.08	200
325-9	0.85	30	0.42	15	23.1	97	5.56	219
325-5	0.85	30	0.57	20	23.1	96	5.41	213

**Table 5 - Methane Welding Process Parameters**

### 3.5 - Glass Fiber-Reinforced Liner Repair Trials

For Test 02 and Test 03, RolaTube developed a modified version of their bi-stable reeled glass fiber (GF) composite product, which uses nine plies of a glass-polypropylene material in the form of overlapping, pre-pregnated tapes of unidirectional glass and polymer. Glass-high density polyethylene (HDPE) material was also considered. The glass-polypropylene material was selected after problems were encountered bonding the glass-HDPE material to steel. Heat and pressure were used to consolidate the glass-polypropylene material into a liner (Figure 30). The resulting wall thickness of the liner is 2.85 mm (0.11 in.).



**Figure 30 - Lay-Up and Forming of GF-Reinforced Composite Liner**

For Test 02, a 114.3 mm (4.5 in.) diameter API 5L Grade B pipe with a long/shallow corrosion defect (Figure 14) was used. For Test 03, a 114.3 mm (4.5 in.) diameter API 5L Grade B pipe

with a short/deep corrosion pit defect (Figure 15) was used. Both Test 02 and Test 03 were repaired with the RolaTube GF liner.

The inside surface of each 1.2 m (4 ft.) long section of 114.3 mm (4.5 in.) diameter API 5L Grade B pipe was degreased prior to installing the GF liners (Figure 31).



**Figure 31 - Insertion of GF Liner into 114.3 mm (4.5 in.) Diameter Pipe**

The installation process consisted of locating the GF liner inside the pipe and inserting a silicon rubber bag inside the liner (Figure 32). The silicon bag was then inflated to press the liner against the inside diameter (ID) of the pipe wall.



**Figure 32 - Silicon Rubber Bag Inserted into GF Liner**

Each pipe section was then heated to 200°C (392°F) in an oven (Figure 33) to fuse the liner to the pipe wall.



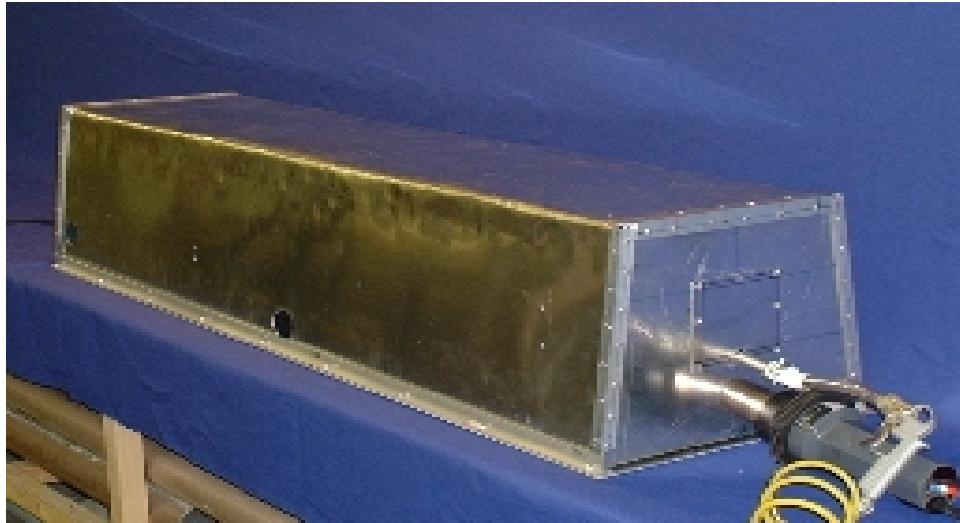


**Figure 33 - Oven Used to Heat Pipe and GF Liner to 200°C (392°F)**

An installed liner is shown in Figure 34.



**Figure 34 - GF Liner Installed in 114.3 mm (4.5 in.) Diameter Pipe**

### 3.6 - Carbon Fiber-Reinforced Liner Repair Trials

For Test 04, a 508 mm (20 in.) diameter X52 pipe with a short/deep, stylized corrosion defect (Figure 16) was used on the pipe section shown in Figure 35.



**Figure 35 - Pipe Section Used for Carbon Fiber Patch Test 04**

For the medium grade carbon fiber (CF) patch used in Test 04, EWI procured raw CF material and fabricated a semi-circular 11.42 mm (0.45 in.) thick reinforcement patch.

The raw materials used to create the patch Test 04 were a standard 6K-tow, 5-harness weave carbon fiber fabric and a vinylester resin, catalyzed with methyl ethyl ketone peroxide (MEKP) and promoted with cobalt naphthenate. The resin had a gel time of 1.0 - 1.5 hours. The fabric was cut to give a quasi-isotropic lay-up with  $\pm 45$  degrees for the outer layers, interleaved with 0, 90 degree layers. A 567 g (20 oz.) woven roving, glass fabric outer layer was employed for the outer face (i.e., on the inside diameter of the patch). The inner glass face (i.e., outside diameter of the patch) was included to act as a galvanic corrosion barrier between the carbon fiber composite and the steel.

The composite patch was fabricated using a wet lay-up process followed by vacuum bagging. To develop the technique, the first trial was a flat panel, approximately 254 mm (10 in.) by 254 mm (10 in.). It was determined that additional layers of fabric were needed to increase section thickness. This was accomplished by including extra 0, 90 degree internal layers in the patch.

The half-round composite patch (Test 04) had an outside diameter that matched the internal diameter of the pipe section. The patch was 711 mm (28 in.) in length, 254 mm (10 in.) wide, by 11.42 mm (0.45 in.) thick. The semi-circular patch lay-up consisted of 27 layers; layers 1 and 27 were glass woven roving. The remainder consisted of alternating layers of  $\pm 45$  degree (i.e.,

quasi-isotropic) and 0, 90 degree (fiber orientation) to produce the patch (Table 6). A semi-circular mold was produced from a cut half-round of 508 mm (20 in.) diameter pipe (Figure 36). Figure 37 shows the dry pack of quasi-isometric fiber build. Figure 38 is the breather cloth frame draped around the pack. The Mylar top is draped next as shown in Figure 39, which is followed by the application of the top breather draped over the pack. Figure 40 is the vacuum bag film draped over entire pack.

<b>Patch Build Layer</b>	<b>Regular 9.65 mm (0.38 in.)</b>	<b>Thicker 11.43 mm (0.45 in.)</b>
1	Glass	Glass
2	Bias	Bias
3	Regular	Regular
4	Bias	Bias
5	Regular	Regular
6	Bias	Bias
7	Regular	Regular
8	Bias	Bias
9	Regular	Regular
10	Bias	Bias
11	Regular	Regular
12	Bias	Regular
13	Regular	Regular
14	Bias	Bias
15	Regular	Regular
16	Bias	Regular
17	Regular	Regular
18	Bias	Bias
19	Regular	Regular
20	Bias	Bias
21	Regular	Regular
22	Bias	Bias
23	Glass	Regular
24		Bias
25		Regular
26		Bias
27		Glass

**Table 6 - Layer Build Schedule for Test 04 CF Patch**

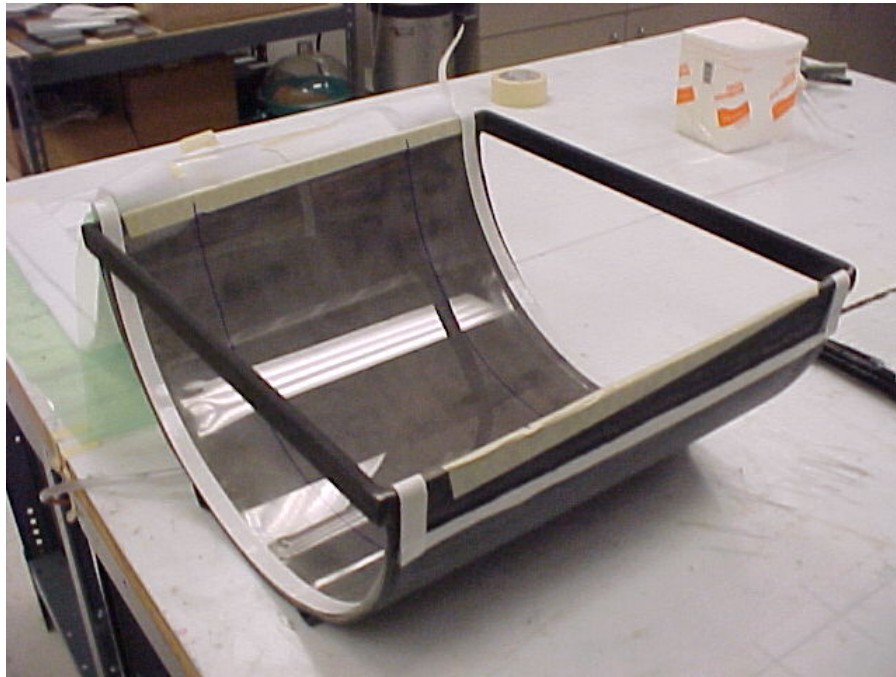


**Figure 36 - Mylar-Lined Semi-Circular Mold for Test 04 CF Patch**

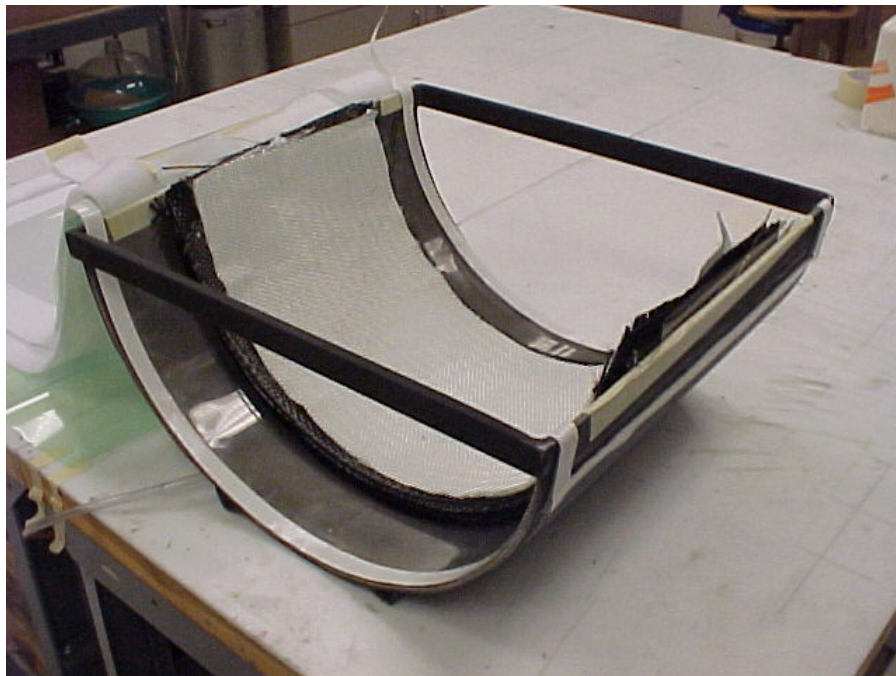


**Figure 37 - Dry Pack of Quasi-Isometric Fiber**

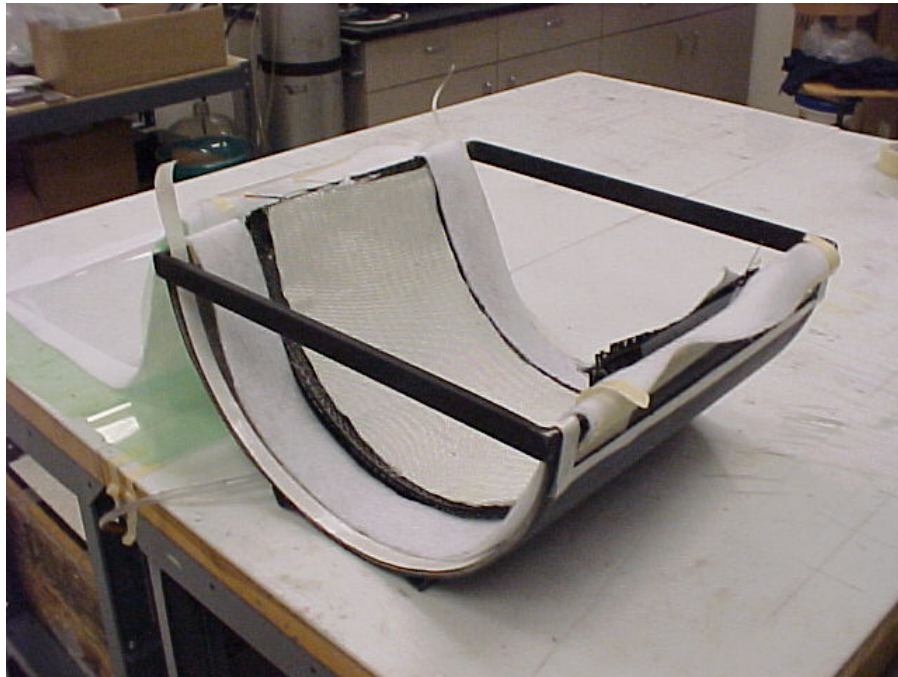


**Figure 38 - Breather Cloth Frame Draped Around Pack**

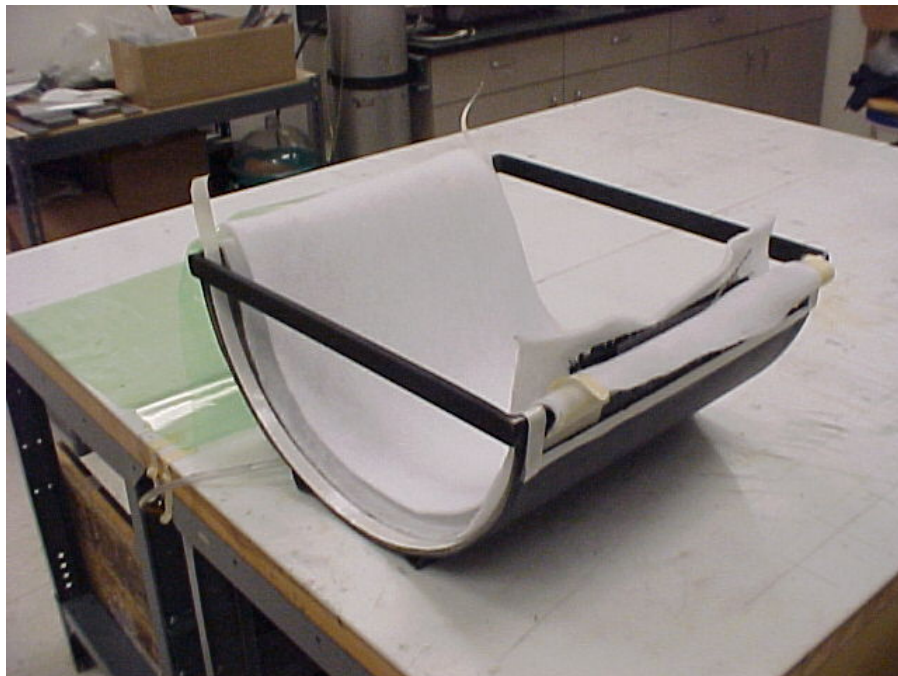


**Figure 39 - Mylar Top Shown Draped**



**Figure 40 - Vacuum Bag Film Draped Over Entire Pack**

FiberGlast 1110 vinylester resin was catalyzed at 1.25% MEKP (9% Oxygen equivalent). The assembly required about 1,600 g (56.43 oz.) of catalyzed resin giving a cup gel time of 75 minutes. Each layer was pre-impregnated with resin as the lay-up proceeded. The hand lay-up was prepared inside the mold with the applied vacuum being maintained until gellation and initial cure was assured (approximately 4 hours). The assembly was then cured overnight. After excising the cured panel, it was trimmed to insertion dimensions. Forced post-cure was not required to maintain dimensions. The calculated fiber volume was between 40% - 45%.

To facilitate Test 04 patch installation, the outer surface of the patch was grit-blasted using 50 - 80 grit Alumina to remove surface resin (Figure 41). Similarly, the installation area inside the pipe was grit-blasted to a near-white blast with 50 - 80 grit Alumina (Figure 42). After cleaning, a liberal coating of 3M DP460 epoxy adhesive was applied to the internal faying surface and a thin coating was applied to the patch faying surface (Figure 43).



**Figure 41 - Completed Test 04 CF Patch with Grit-Blasted OD**



**Figure 42 - Application of 3M DP460 Adhesive to Grit-Blasted ID of Test 04 Pipe**



**Figure 43 - Application of Adhesive to Test 04 CF Patch**

The patch and pipe section were mated as shown in Figure 44.

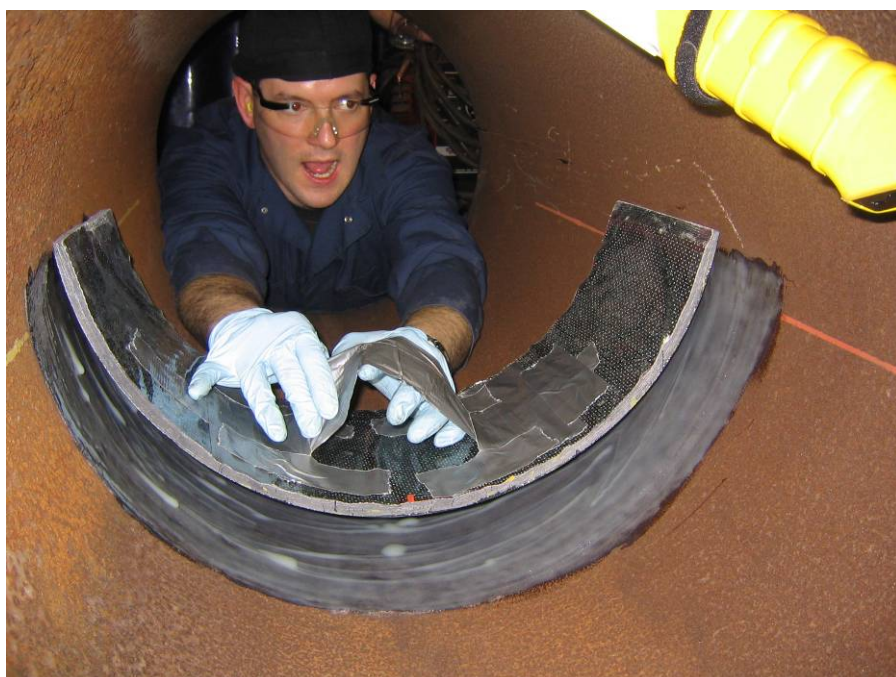


**Figure 44 - Installation of Test 04 CF Patch**



Bar clamps were used along the axis of the pipe to hold the patch in place for cure. Figure 45 shows the adhesive squeeze-out being removed prior to forming a fillet as shown in Figure 46.



**Figure 45 - Clamping Bars Used to Hold Test 04 CF Patch in Place**



**Figure 46 - Adhesive Fillet Around Test 04 CF Patch**

Approximately two weeks after the Test 04 patch cured, the pipe section with the carbon fiber-reinforced liner was hydrostatically tested to failure.

For Test 05, a 508 mm (20 in.) diameter X52 pipe with a short/deep, stylized corrosion defect (Figure 16) was used on a pipe section similar to that shown in Figure 35. The Test 05 patch was fabricated/installed with the same materials and procedures developed for the Test 04 patch. As shown in Figure 47, the Test 05 patch resembles a "pressure bandage" wherein there is a solid 254 mm (10 in.) long by 254 mm (10 in.) wide by 11.43 mm (0.45 in.) thick solid thickness of composite in the middle with wings of composite material that neck down toward the outside of both ends. This gives the "pressure bandage" patch a total overall length of 711.2 mm (28 in.). All 0, 90 construction was used with 27 layers (layers 1 and 27 were glass woven roving). Calculated fiber volume was 50% - 55%. The "pressure bandage" patch was allowed to cure for approximately two weeks after fabrication. After the patch was installed in the pipe section, it was allowed to cure for another week before hydrostatic testing to failure.



**Figure 47 - Test 05 "Pressure Bandage" CF Patch**

For Test 06, a 508 mm (20 in.) diameter X52 pipe with a short/deep, stylized corrosion defect (Figure 16) was used on a pipe section similar to that shown in Figure 35. As compared to the Test 05 patch, the Test 06 patch was thinner. Test 06 patch consisted of all 0, 90 construction fabricated/installed with the same materials and procedures developed for the Test 04 patch.

As shown in Figure 48, Test 06 patch was 254 mm (10 in.) long by 711.2 mm (28 in.) wide by 7.62 mm (0.3 in.) thick and consisted of 18 layers (layers 1 and 18 were glass woven roving).

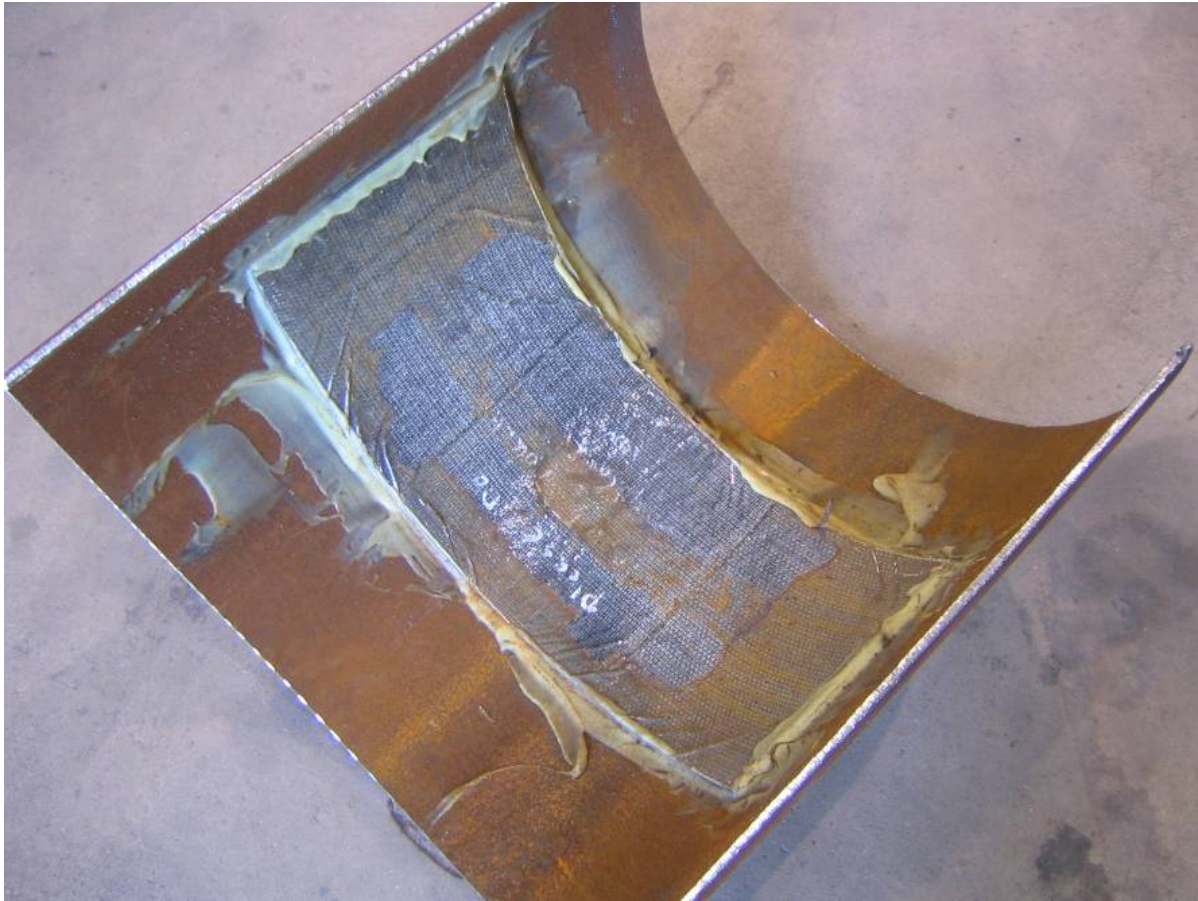


**Figure 48 - Test 06 Thin CF Patch**

For Test 07, a 508 mm (20 in.) diameter X52 pipe with a long/shallow corrosion defect (Figure 17) was used on a pipe section similar to that shown in Figure 35. The Test 06 patch was the same thickness as the Test 07 patch, which consisted of all 0, 90 construction and was fabricated/installed with the same materials and procedures developed for the Test 04 patch. As shown in Figure 49, the Test 07 patch was 711.2 mm (28 in.) long by 254 mm (10 in.) wide by 7.62 mm (0.3 in.) thick and consisted of 18 layers (layers 1 and 18 were glass woven roving). This test was included to evaluate the performance of a CF patch on a defect that exceeds the length beyond which the hoop stress in the pipe can no longer distribute itself around the end of the defect.



**Figure 49 - Test 07 CF Patch for Long/Shallow Defect Evaluation**

### **3.7 - Mechanical Testing of Carbon Fiber Liner Material**

Three composite lay-up structures were designed to evaluate the mechanical properties of the carbon fiber material:

- Quasi-isotropic lay-up with alternating layers of 0, 90 and  $\pm 45$  with extra 0, 90 near the thickness-center
- 0, 90 only lay-up
- Uniaxial 0 only lay-up

The thicknesses of the quasi-isotropic and the 0, 90 panels were 11.43 mm (0.45 in.). The thickness of the uniaxial panel was 8.89 mm (0.35 in.). For the first two, fiberglass close-out layers were included on the “steel side” as a proposed corrosion barrier at the steel/carbon fiber interface and as the top layer (bag side). The uniaxial panel had no fiberglass. The carbon-glass constructions produce ~40% w/w carbon fiber, with a density of 1.47-1.51 g/cc. The uniaxial panel contains >70% carbon fiber w/w, so a higher tensile modulus is anticipated (its density was measured at 1.44 g/cc, reflecting mostly the absence of fiberglass).

All panels were produced using a combined hand lay-up vacuum bagging technique and were cured at least one month under ambient conditions before testing or were post cured at 70°C (158°F) for 2 hours. Figure 50 through Figure 55 show the panel fabrication process.



**Figure 50 - Mylar Over Release-Coated Plate**



**Figure 51 - Rim of Breather Added  $\cong$  76.2 mm (3 in.) Wide**



**Figure 52 - Dry Stack Before Lay-Up**

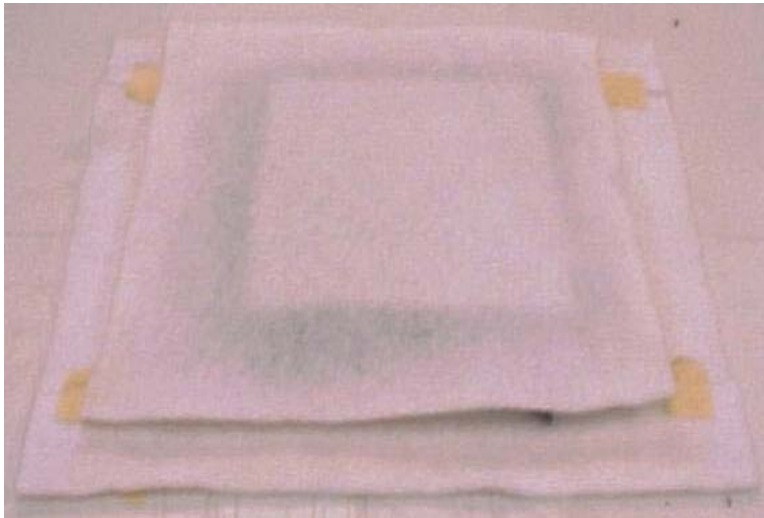


**Figure 53 - Top Breather Added**



**Figure 54 - Vacuum Bag Added Over Sealer Tape**

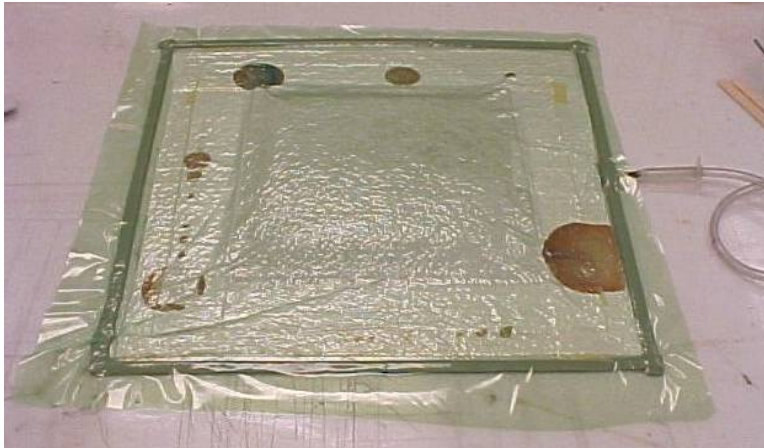


**Figure 55 - Wet Panel Under Applied Vacuum**

The tensile testing samples were cut as a standard ASTM D638 Type-1 sample.

Interlaminar shear (ILS) samples were taken from a separate panel in which a portion of one middle layer was omitted and replaced with a Teflon release sheet. This produced a molded-in defect notch for three-point bending tests (see Figure 56). The ILS panel was built with 0, 90 layers only.

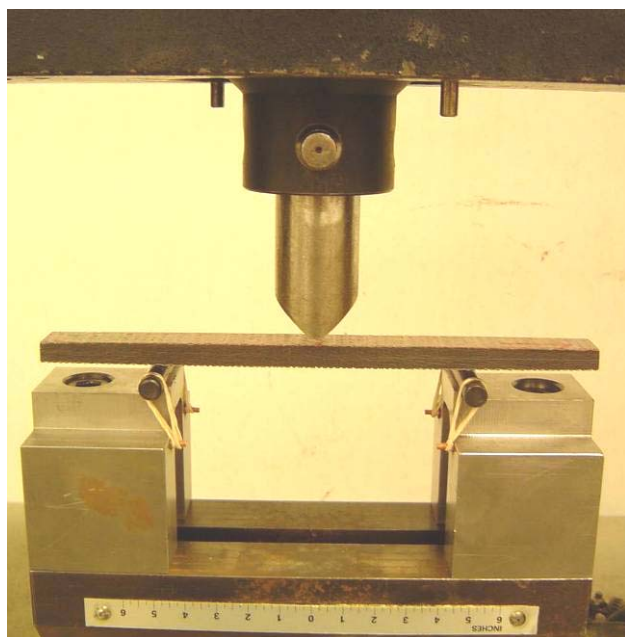


**Figure 56 - Three-Point Bending Test Set Up for ILS Testing**

### **3.7 - Steel Patch-Reinforced Liner Repair Trials**

For Test 08, a 508 mm (20 in.) diameter by 6.35 mm (0.25 in.) wall, API 5L-X52 pipe with a short/deep, stylized corrosion defect (as shown in Figure 16) was used on a pipe section similar to that shown in Figure 35. The Test 08 patch was steel. The steel patch and the pipe section it was installed in were both taken from the same longer pipe section.

The steel patch was custom rolled to a 495.3 mm (19.5 in.) OD so the patch would fit snugly into the 508 mm (20 in.) OD pipe with simulated corrosion. The overall dimensions of the patch were 254 mm (10 in.) long by 711.2 mm (28 in.) wide; the same dimensions of composite patch design 3.

The patch and ID of the pipe were sandblasted and cleaned prior to assembly. The steel patch was installed in the pipe section using the same epoxy adhesive (3M DP460) that was used for CF liner Tests 04 - 07. The epoxy was applied to both the patch and the ID of the pipe. Figure 57 through Figure 59 show various views of the steel patch inside the pipe section before the epoxy was cured.





**Figure 57 - Test 08 Steel Patch Prior to Epoxy Curing**



**Figure 58 - Test 08 Steel Patch Prior to Epoxy Curing (Long Seam)**



**Figure 59 - Test 08 Steel Patch Prior to Epoxy Curing (Circumferential Fillet)**

For this and subsequent tests, an inflatable bladder was used to facilitate the installation process. Figure 60 shows the rubber sheet that was placed over the steel patch to protect the inflatable bladder from epoxy that leaked from around the patch.



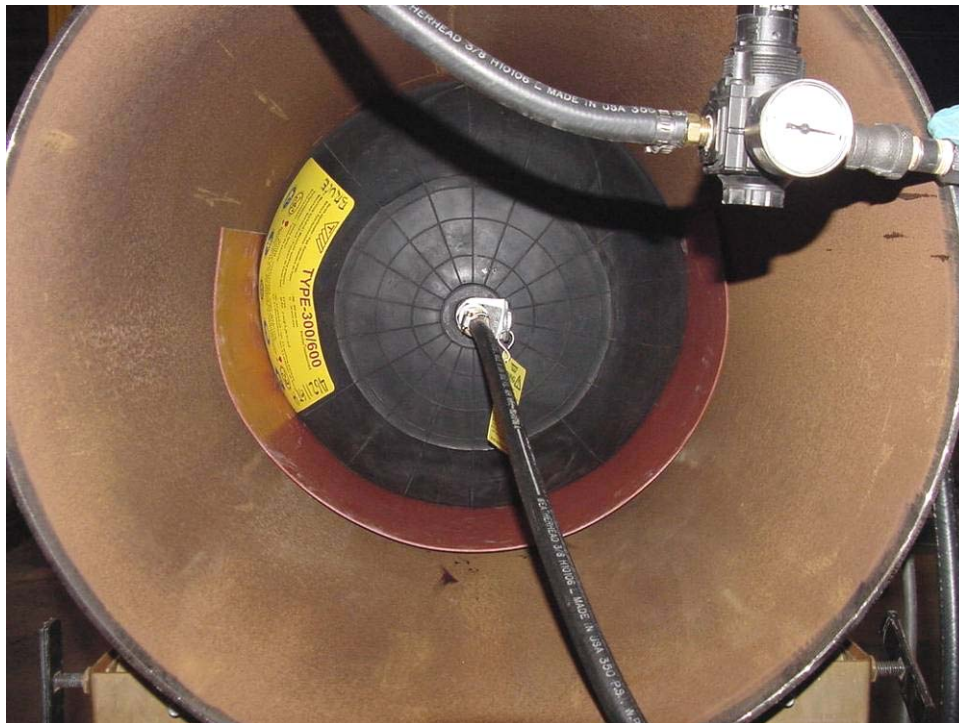
**Figure 60 - Rubber Sheet Protecting Inflatable Bladder From Epoxy for Test 08**

The inflatable bladder was then inserted into the pipe, pressurized to 206 kPa (30 psi), and held overnight to assure a sound bond between the steel patch and the ID of the pipe (Figure 61).



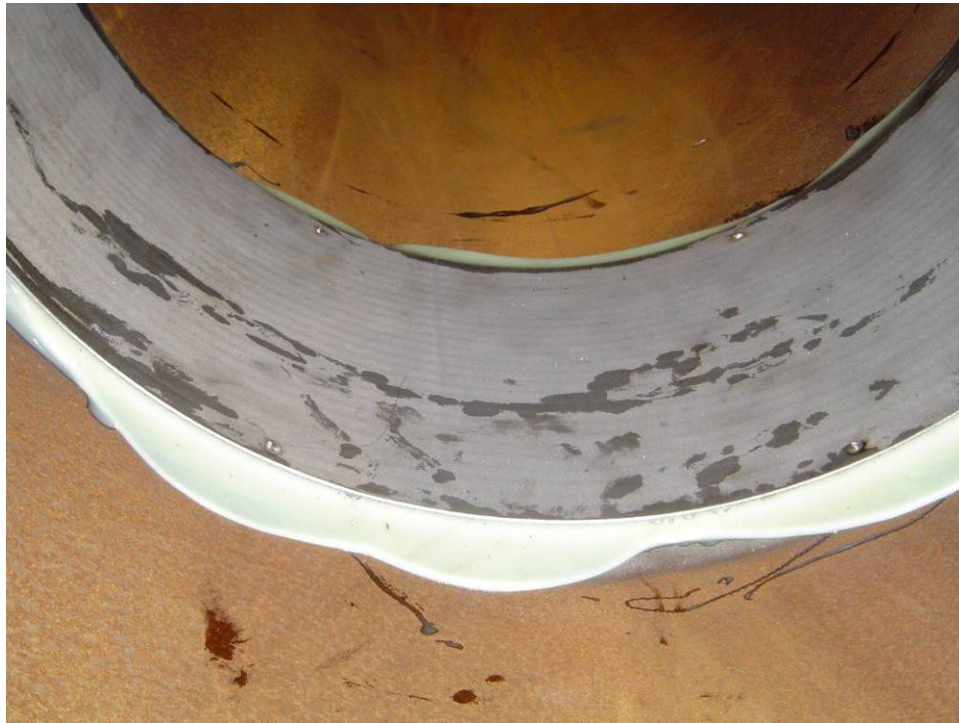
**Figure 61 - Bladder Prior to Pressurization for Test 08**

Figure 62 shows the bladder pressurized to 206 kPa (30 psi) prior to epoxy cure.



**Figure 62 - Bladder Pressurized at 206 kPa (30 psi) for Test 08**

Figure 63 shows the Test 08 steel patch after the epoxy has cured.



**Figure 63 - Test 08 Steel Patch with Circumferential Adhesive Fillet**

### **3.8 - Helically Wound Steel Strip Repair Trials**

Test 09 used a 508 mm (20 in.) diameter by 6.35 mm (0.25 in.) wall, API 5L X52 pipe with a stylized/short, extra deep corrosion defect similar to that shown in Figure 16. For Test 09, the 127 mm (5 in.) long defect was 4.75 mm (0.187 in.) deep not 3.45 mm (0.136 in.) deep as shown in Figure 16. For Test 09, the "patch" consisted of helically wound steel strip.

The steel strip consisted of 50.8 mm (2 in.) wide by 1.12 mm (0.044 in.) thick commercial banding material. The measured ultimate tensile strength (UTS) of this material is 987.95 MPa (143.25 ksi). Prior to installation, the strip was custom rolled with a permanent 533.4 mm (21 in.) diameter helix.

The OD of the strip and the ID of the pipe were sandblasted using the same procedures used for Tests 04 - 08. The same epoxy (3M DP460) used for Tests 04 - 08 was also applied to the OD of the strip and to the ID of the pipe (in a similar manner to that shown in Figure 64 and Figure 65).



**Figure 64 - Test 09 Helically Wound Steel Strip with 3M DP460 Epoxy Applied**



**Figure 65. ID of Demonstration Pipe (similar to Test 09) with 3M DP460 Epoxy Applied**

Prior to installation, the helically wound steel strip was cinched down to a diameter that was just smaller than the ID of the pipe. Adhesive tape (Figure 63) was used to hold the shape of the steel strip during installation.



**Figure 66 - Helically Wound Steel Strip Inserted into Pipe (similar to Test 09)**

Once the steel strip was inserted into the pipe, the tape was removed and the steel strip was allowed to spring outward against the ID of the pipe (Figure 67). A rubber sheet was placed over the helically wound steel strip to protect the inflatable bladder from epoxy that leaked from around/between the coils.



**Figure 67 - Helically Wound Steel Strip Expanded to Fit Pipe ID (similar to Test 09)**

An inflatable bladder was then inserted into the ID of the pipe and pressurized to 206 kPa (30 psi) and held overnight to assure sound bonding between the helically wound steel strip and ID of the pipe (Figure 68 and Figure 69).



**Figure 68 - Inflatable Bladder Inserted in Pipe (similar to Test 09)**



**Figure 69 - Bladder Pressurized to 206 kPa (30 psi) (similar to Test 09)**

Using the same technique, two additional layers of helically wound steel strip were installed in the Test 09 pipe for a total of three layers. End caps were welded on the pipe section and the assembly was then hydrostatically testing to failure.

Test 10 used a 508 mm (20 in.) diameter by 6.35 mm (0.25 in.) wall, API 5L-X52 pipe with the same stylized/short, extra deep corrosion defect used for Test 09. Three layers of helically wound steel strip was installed in the Test 10 pipe using the same methodology developed for Test 09. The same 987.95 MPa (143.25 ksi) UTS steel strip was used with a smaller quantity of a new urethane adhesive (Lord 7542 A/D) as opposed to the epoxy adhesive used in previous tests. After the adhesive cured, end caps were welded on the pipe section and the assembly was pressure tested to failure.

Test 11 used a 508 mm (20 in.) diameter by 6.35 mm (0.25 in.) wall, API 5L-X52 pipe with the same stylized/short, extra deep corrosion defect used for Test 09. Three layers of helically wound steel strip were installed in the Test 11 pipe using the same methodology developed for Test 09. For this test, a new lower strength material, cold rolled AISI C1010 steel strip with a UTS of 586.9 MPa (85.1 ksi), was used. The physical dimensions of the new strip were 50.8 mm (2 in.) wide by 1.17 mm (0.050 in.) thick. A smaller quantity of the old adhesive (3M DP460) was also used for Test 11. After the adhesive cured, end caps were welded on the pipe section and the assembly was pressure tested to failure.

Test 12 used a 609.6 mm (24 in.) diameter by 7.9 mm (0.312 in.) wall, API 5L X65 pipe with the short/extra deep slot shown in Figure 19. Three layers of helically wound steel strip were installed in the Test 12 pipe using the same methodology developed for Test 09. The 987.95 MPa (143.25 ksi) UTS steel strip was used with a normal quantity of the old adhesive (3M DP460). After the adhesive cured, end caps were welded on the pipe section and the assembly was pressure tested to failure.



Test 13 used a 609.6 mm (24 in.) diameter by 7.9 mm (0.312 in.) wall, API 5L X65 pipe featuring a short/extra deep slot with a through hole as shown in Figure 20 and Figure 21. Three layers of helically wound steel strip were installed in the Test 13 pipe using the same methodology developed for Test 09. The 987.95 MPa (143.25 ksi) UTS steel strip was used with a normal quantity of the old adhesive (3M DP460). After the adhesive cured, end caps were welded on the pipe section and the assembly was pressure tested to failure.

Test 14 used a 609.6 mm (24 in.) diameter by 7.9 mm (0.312 in.) wall, API 5L X65 pipe with a long/shallow slot (381 mm (15 in.) long by 5.66 mm (0.223 in.) deep). Three layers of helically wound steel strip were installed in the Test 14 pipe using the same methodology developed for Test 09. The 987.95 MPa (143.25 ksi) UTS steel strip was used with a normal quantity of the old adhesive (3M DP460). After the adhesive cured, end caps were welded on the pipe section and the assembly was pressure tested to failure.

## **4.0- RESULTS AND DISCUSSION**

This section is a presentation of the results and a discussion of their significance.

### **4.1 - Technology Status Assessment**

#### **4.1.0 - Introduction**

A repair method that can be applied from the inside of a gas transmission pipeline (i.e., a trenchless repair) is an attractive alternative to conventional repair methods since the need to excavate the pipeline is precluded. This is particularly true for pipelines in environmentally sensitive and highly populated areas. Several repair methods that are commonly applied from the outside of the pipeline are, in theory, directly applicable from the inside; however, issues such as development of the required equipment to perform repairs remotely and mobilization of equipment through the pipeline to areas that require repair need to be addressed. Several additional repair methods that are commonly applied to other types of pipelines (gas distribution lines, water lines, etc.) also have potential applicability for internal repair of gas transmission pipelines. Many of these require further development to meet the requirements for repair of gas transmission pipelines. The following section is the status of existing pipeline repair technology that can be applied to the inside of a gas transmission pipeline. This section includes results from a comprehensive computerized literature search, together with information obtained from discussions with companies that are currently developing or evaluating novel pipeline repair methods.

#### **4.1.1 - Background**

The most common cause for repair of gas transmission pipelines is external, corrosion-caused loss of wall thickness. To prevent an area of corrosion damage from causing a pipeline to rupture, the area containing the corrosion damage must be reinforced. Other pipeline defects that commonly require repair include internal corrosion, original construction flaws, service induced cracking, and mechanical damage. Defects oriented in the longitudinal direction that have a tendency to fail from hoop stress (pressure loading) must be reinforced in the circumferential direction, while defects oriented in the circumferential direction that have a tendency to fail from axial stresses (e.g., pipeline settlement) must be reinforced in the longitudinal direction. The most commonly used method for repair of gas transmission pipelines is the full-encirclement steel repair sleeve. These sleeves resist hoop stress and, if the ends are welded to the pipeline, can resist axial stresses.

Current repair methods that are commonly applied from the outside of the pipeline are typically done so while the pipeline remains in service. While this would be desirable for internal repair, many of the repair methods that are applicable to the inside of the pipeline would require that the pipeline be taken out of service. Most of the repair methods that are commonly applied to

the inside of other types of pipelines, which typically operate at low pressure, are done so to restore leak tightness. These repair methods would typically require further development to restore the strength of a gas transmission pipeline.

#### **4.1.2 - Review and Assessment of Candidate Repair Methods**

A review of common external repair methods for gas transmission pipelines and repair methods that are typically applied to the inside of other types of pipelines resulted in the identification of two broad categories of exiting technologies that are potentially applicable to repair of gas transmission pipelines from the inside:

- Weld Deposition Repair
- Fiber-Reinforced Composite Liner Repair

##### **4.1.2.0 - Weld Repairs**

Gas transmission pipeline repair by direct deposition of weld metal, or weld deposition repair, is a proven technology that can be applied directly to the area of wall loss (e.g., external repair of external wall loss) or to the side opposite the wall loss (e.g., external repair of internal wall loss). There are no apparent technical limitations to applying this repair method to the inside of an out-of-service pipeline. Application of this repair method to the inside of an in-service pipeline would require that the welding be carried out in a hyperbaric environment, however. It is direct, relatively inexpensive to apply, and requires no additional materials beyond welding consumables. Deposited weld metal repairs are also used to repair circumferentially oriented planar defects (e.g., intergranular stress corrosion cracks adjacent to girth welds) in the nuclear power industry. Remote welding has been developed primarily by needs in the nuclear power industry, though working devices have been built for other applications.

Osaka Gas has developed remote robotic equipment for repair of flaws in the root area of welds of gas transmission lines. Work on the equipment dates back to 1985. The robot is self-propelled via wheels with umbilical cable for control and power and is able to perform work up to 152.4 m (500 ft.) from the pipeline entry point. The power supply for welding equipment is located at the entry point, which limits the working range. The working range is also limited by the ability of the robot to pull the umbilical cable. The robot is capable of working in 304.8 mm (12 in.) to 609.6 mm (24 in.) pipe with 90° bends. It does not remove the root flaws from the pipe prior to welding; it is limited to grinding of the pipe wall to remove impurities that can disrupt the welding arc. Welding is performed using the GMAW process and the torch travel path is programmed prior to welding. Welding filler metal is carried onboard, while shielding gas is supplied via the umbilical. The robot incorporates features such as wire cutting and nozzle cleaning. All inspection is visual using video cameras located on the robot. Welding is controlled to avoid damage to pipeline coating. Approximately 4 hours are required to grind, weld, and inspect a 609.6 mm (24 in.) weld. Osaka Gas has been using the robots to perform

field repairs since 1995. Continuing development work is believed to focus on improving arc stability and robot range by placing the welding power supply on the robot.

Welding Services, Incorporated, has developed a series of welding devices for remote welding. Of these, the device most applicable to pipeline repair is a machine developed for remote weld cladding of Cold Reheat Piping in nuclear power plants. The machine has no locomotive capability as the pipe sections to be clad are large in diameter (1.1 m (42 in.) is common) and have nearby access, permitting technicians to assemble the machine within the pipe section to be clad. Each weld bead is deposited axially along the pipe for distances up to 3.7 m (12 ft.) and then the weld head steps a short distance in the circumferential direction and begins depositing the next bead. This process is continued until the entire inside surface is clad. All welding is controlled remotely via video feed. High reliability and high weld deposition rates have been demonstrated with this machine, and thousands of pounds of weld metal have been deposited since its introduction. The machine has no machining or inspection capability since pipe sections are manually cleaned by abrasive blasting prior to welding and visual inspection can be performed after welding.

Honeybee Robotics and Consolidated Edison are developing the WISOR (Welding and Inspection Steam Operations Robot) system for inspection and repair of flanges in steam piping. Development commenced in 1995 and the system is expected to enter field trials in the near future. The robot is self-propelled using tracks with an umbilical cable for control and power. It is designed to operate in the presence of steam at temperatures up to 275°F and can perform work up to 41.1 m (135 ft.) from the pipeline entry point. The power supply for the welding equipment is located at the entry point, which limits the working range. The robot is capable of working in 0.4 m (16 in.) to 0.6 m (24 in.) pipe. A grinding operation is used to prepare a 6.35 mm (0.25 in.) deep weld groove. Welding is performed using GMAW process and the torch is manually controlled. A steam guard is incorporated into the robot to allow welding in the presence of residual steam. Welding filler metal is carried onboard, while shielding gas is supplied via the umbilical. All inspection is visual using video cameras located on the robot.

Fermi National Accelerator Laboratory has developed their VRW (Visual Robotic Welding) system for the repair of highly radioactive proton beam transport pipes. The prototype system was developed in 1998 and is successfully performing field repairs. Most repairs performed have involved depositing weld metal to seal leaks from corrosion, but one repair was made by welding a small patch plate in place. The welding control system is innovative in that the GMAW welding gun is mounted on a robotic arm that duplicates the movements of an operator using a control arm to simulate welding a mockup of the work area. The robot is towed into position with umbilical cable for control and power and is capable of traversing straight pipe only. Work can be performed in excess of 304.8 m (1,000 ft.) from the pipeline entry point. Preliminary conceptual work was done to allow welding at distances up to 3 km(10,000 ft.). The robot is capable of working in 304.8 mm (12 in.) to 457.2 mm (18 in.) pipe and can prepare surfaces for welding by grinding or wire brushing, using an arm controlled in the same manner

as the welding. Welding is performing using GMAW process. All inspection is visual using video cameras located on the robot.

Pacific Gas and Electric Company (PG&E) has developed the Internal Pipeline NDE System (IPNS) for internal inspection of gas pipelines. The system incorporates a variety of inspection technologies to characterize girth and long seam flaws, corrosion, and dents and gouges. The system also incorporates a grinder for preparation of areas of interest. The system has been in field use since 1996 and has a maximum range of 2500 ft. The robot is self-propelled using tracks and is able to traverse 90° bends in pipe from 558.8 mm (22 in.) to 609.6 mm (24 in.) in diameter. An umbilical is used to supply power and to control the device. Preliminary development work was performed for a companion system to perform machining and welding of defective welds. While not a welding system, IPNS demonstrates the practicality of performing work inside gas pipelines at extended distances from the entry point.

Siemens AG, Nuclear Power Generation in Erlangen, Germany has developed and deployed a family of robotic equipment for making repairs to the inside of piping for the nuclear power industry. The equipment can be inserted into the pipe through a disassembled valve and can move through 152.4 mm (6 in.) to 1.02 m (40 in.) diameter pipe for a distance of 80 m (262.5 ft.) or more at speeds up to 4.6 m/min. (15 ft./min.). It can travel through multiple, 90°, short radius elbows. It consists of one or more driving modules and one working module joined by flexible couplings. Power, control and communication, are provided through an umbilical attached to the rear of the last driving module. The system has been used to perform remote inspection, machining, and welding. This system is very flexible and can be configured for a variety of inspection, machining, welding, and object retrieval tasks. It is designed specifically to operate in power plant piping and is not capable of traveling long distances needed for pipeline repair. The equipment includes interchangeable wheeled or “inch-worm” driving modules that are capable of horizontal or vertical travel. Interchangeable working modules are capable of milling, grinding, GTAW welding, debris removal, visual inspection, and eddy current and ultrasonic inspection.

#### **4.1.2.1 - Fiber-Reinforced Composite Liners Repair**

##### ***General***

Fiber-reinforced composite repairs are becoming widely used as an alternative to the installation of welded, full-encirclement sleeves for repair of gas transmission pipelines. These repairs typically consist of glass fibers in a polymer matrix material bonded to the pipe using an adhesive. Adhesive filler is applied to the defect prior to installation to allow load transfer to the composite material. The primary advantage of these repair products over welded, full-encirclement sleeves is that the need for welding is precluded.

A variety of liners are commonly used for repair of other types of pipelines (gas distribution lines, sewers, water mains, etc.). Of these, the three that are potentially applicable to internal

repair of gas transmission pipelines are sectional liners, cured-in-place liners, and fold-and-formed liners. Sectional liners are typically 0.9 m (3 ft.) to 4.6 m (5 ft.) in length and are installed only in areas that require repairs. Cured-in-place liners, and fold-and-formed liners are typically applied to an entire pipeline segment. Cured-in-place liners are installed using the inversion process, while fold-and-formed liners are pulled into place and then inverted so that they fit tightly against the inside of the pipe. In addition to repair, continuously-applied liners could be used to increase the operating pressure (i.e., up-rate) an existing pipeline.

Composite reinforced line pipe (CRLP) is also being considered for new construction of gas transmission pipelines. CRLP is a patented process that applies glass-resin reinforcement to steel pipe, which forms an outer protective barrier with additional hoop strength, prior to installation. In the winter of 2001, a 2 km (1.2 miles) section of 609.6 mm (24 in.) outside diameter (OD) CRLP pipe was installed in northwestern Canada and is presently being tested by TransCanada Pipelines. Composite reinforced pressure vessels are also being developed for gas transport modules (GTMs), which can be used to transport stranded gas to market areas. Composite materials are also being used for coiled tubing and offshore risers.

### ***External Repair Methods***

The three fiber-reinforced composite devices most commonly used for external repair of gas transmission pipelines are the Clock Spring®, StrongBack®, and Armor Plate® methods.

Clock Spring® is a coil of high-strength composite material whose configuration allows it to wrap tightly around the pipe. When properly installed, the resulting repair provides circumferential reinforcement of the corroded area. The first units were placed in service in the 1980s. Over 50,000 permanent repairs have been made with the Clock Spring® system. Because the fibers are oriented uniaxially, Clock Spring® devices are not recommended for repair of circumferentially oriented defects. The Clock Spring® device in its present form is not suited to internal repair.

StrongBack® is a resin-impregnated tape wrap that is applied directly to the prepared damaged pipeline area. The wrap is activated by immersion in water or external application of water and thus has the advantage of being applicable to wet lines.

Armor Plate® Pipe Wrap repair is similar to StrongBack®, except that the hardening agent is chemical rather than water activated.

### ***Internal Repair Methods***

The repair methods that are applicable for internal repair of pipelines include cured-in-place liners, fold-and-formed liners, and bi-stable reeled composite pipe liners.

Cured-in-place pipe (CIPP) liners typically consist of a resin-impregnated felt tube. The inversion process is driven by either air or water pressure which results in the tube fitting tightly against the inside of the pipe. Depending on the product, the resin is cured using heated water or steam, or heat from one of a variety of other sources. Most of these products are intended to restore leak-tightness only. Several products could potentially be used to restore strength, one of which is manufactured by Inpipe in Sweden. Instead of felt, the Inpipe system uses braided tube consisting of resin-impregnated glass fibers. Once in place, the tube is cured using ultraviolet light. The cured liner is reported to have a tensile strength of 130 MPa (18.8 ksi) and a modulus of elasticity of 10,000 MPa (1,450 ksi). Another cured-in-place product that contains glass fibers is manufactured by IHCTM Rehabilitation Products in Pinehurst, Texas, which incorporates a technology known as Intralaminar Heat Cure or IHCTM. IHC hybrid composites contain conductive elements that cure the laminate through resistive heating. In 1995, PG&E began an exhaustive program to evaluate the performance of CIPP liners for gas distribution main and service applications. The program focused on the Paltem liner developed by Insituform Technologies in Chesterfield, Missouri, which is also based on a braided tube design. While the program was a technical success, PG&E concluded that a number of obstacles remain to be overcome before wide spread acceptance of this technology as a practical pipe rehabilitation method.

Fold and form liners are installed using a process that involves collapsing a liner into a "U" or "C" shape either in the manufacturing plant or on site. After insertion, typically using a winch, the liner is reverted to a "close fit" using air pressure and/or heat. For pressure pipe renovation, liners based on polyethylene (PE) are typically used. Insituform has developed a polyester fiber reinforced polyethylene (PRP) liner that can achieve a 1.03 MPa (150 psi) independent pressure rating at a thickness of just a few mm. The product is factory folded into a "C" shape and transported to site on a reel.

Bi-stable Reeled Composite Pipe/Liner is a prototype product developed by Wellstream, Inc. (Division of Halliburton Energy Services Group). This is a bi-stable reeled composite product offering the potential to make strong, lightweight, composite pipes and pipe linings. As the composite liner is unreeled it changes shape from a flat strip to an overlapping circular strip that can be pulled into position in the pipe or pipeline. The liner is referred to as bi-stable because it is reeled as a flat strip but deployed as an overlapping circular strip. Once the liner is deployed it is longitudinally seam welded on site using a containerized system. The adhesive for the Wellstream product is activated and cured using induction heating. One example of a cured 100 mm (4 in.) diameter pipe with a wall thickness 2.5 mm (0.10 in.) is said to have a 6 MPa (870 psi) short-term burst pressure.

#### **4.1.3 - Development Needs of Candidate Repair Methods**

Further development work is needed for both weld deposition repair and fiber-reinforced composite liner repair.

## **Weld Repair Methods**

The important characteristics of a useful internal weld repair system include the ability to operate at long range from the pipe entry point (i.e., 610+ m (2,000+ ft.)), the ability to transverse bends and miters, machining capability to prepare the weld joint, a grinding system for cleaning and preparation, and a high deposition robust welding process. Although many of these features are incorporated in the existing systems, there is no single system that possesses all the required characteristics. Further work is required to develop a system with all of these features.

## **Fiber-Reinforced Composite Repair Methods**

Further development of fiber-reinforced composite repairs/liners with sufficient strength is required prior to application to internal, local structural repair of gas transmission pipelines. Ideally, these products would combine the strength of currently used external repair products or CRLP with the installation process currently used for liners in other types of pipelines. Adhesion of the liner to the pipe surface, which is important for structural reinforcement but not restoration of leak tightness, also needs to be addressed. The required thickness of a repair for structural reinforcement and the potentially adverse effect on internal inspection and flow restriction will also need to be addressed.

### **4.1.4 - Summary**

Two broad categories of existing repair technology that are potentially applicable to gas transmission pipelines from the inside have been identified and reviewed; deposited weld metal repairs and fiber-reinforced composite repairs. Both are used to some extent for other applications and could be further developed for internal, local, structural repair of gas transmission pipelines.

## **4.2 - Operators Experience and Repair Needs Survey**

With cost share funding provided by Pipeline Research Council International (PRCI), EWI conducted an extensive survey of pipeline companies to determine the operators experience, repair needs, and situations where internal repair would be the preferred repair method for gas transmission pipelines.

### **4.2.0 - Repair Needs and Performance Requirements**

The pipeline operators experience and repair needs survey was divided into the following parts:

- Currently-Used Repair Methods
- Use/Potential Use of Internal Repair
- Need for In-Service Internal Repair



- Applicable Types of Damage
- Operational and Performance Requirements for Internal Repairs

The survey ([Appendix A](#)) primarily focused on pipeline operating companies (gas transmission) that are members of the Pipeline Research Council International ([Appendix B](#)). The survey was also sent to other pipeline operating companies ([Appendix C](#)). A detailed list of contact information for surveyed individuals can be found in [Appendix D](#).

Following receipt of completed surveys, follow-up telephone calls were made to further identify the range of pipeline sizes, materials and coating types in most common use and the types of pipeline damage and remediation/upgrades (to more stringent code requirements) that are most frequently encountered. The pipeline companies were also asked to define specific operational and performance requirements for internal repairs, including post repair inspection and future pipeline inspection (i.e., pigging). Additionally, the survey determined operating requirements such as the minimum and maximum distance a repair system needs to be able to travel inside a pipe to facilitate internal repair and potential obstructions such as elbows, bends, branches, and taps that may limit access.

Companies that offer in-line inspection services were also surveyed to determine the maximum geometric variations associated with internal repairs (particularly internal build-up, liner thickness, etc.) that can be tolerated by current and next generation in-line inspection vehicles (a.k.a. smart pigs).

#### **4.2.1 - Target Specifications for an Internal Pipeline Repair System**

The results of the survey were collected and analyzed. Target specifications for an internal Pipeline Repair System were identified.

##### ***General Specifications***

- The most frequently cited potential application would be for out-of-service use under river crossings, lakes, swamps, highways, high population density areas, and railway crossings.
- Use of internal repair as a temporary repair is of limited interest and is only attractive in seasonal climates where excavation and permanent repair would occur during the summer months.
- The repair system should have the ability to effect permanent internal repairs within the range of 508 mm to 762 mm (20 in. to 30 in.) diameter pipe as identified by 90% of survey respondents (559 mm (22 in.) diameter is the most commonly used size).

### ***Deployment Distance Specifications***

- One excavation should be required to insert internal repair device into the pipe. From this insertion point, the repair device should travel in each direction from the excavation.
- 81% of all respondents would be served by a pig-based system (with despoiled umbilicals) capable of traveling 610 m (2,000 ft.) which would suffice for all highway and river crossings. A river crossing of up to 1,219 m (4,000 ft.) could be accessed from an insertion point on either side of the river.

### ***Inspection Specifications***

- The repaired pipeline must be inspectable by pigging after repair per DOT code 49 CFR 192.150<sup>(3)</sup> which states, "each new transmission line and each line section of a transmission line where the line pipe, valve, fitting, or other line component is replaced must be designed to accommodate the passage of instrumented inspection devices."
- Repairs made by the system must be inspectable via nondestructive evaluation (NDE) pigging, preferably radiographic testing (RT), with ultrasonic testing (UT) as an acceptable alternative. Inspection requirements should meet those specified in the following codes:
  - ASME B31.8
  - ASME B31.4
  - CSA Z662
  - DOT Part 192 NDE

### ***Coatings Specifications***

- Repairs must not compromise cathodic protection effectiveness after completion.
- Preservation of pipeline coating integrity must meet DOT 192/195 requirements

### ***Geometric Specifications***

- System must be capable of effecting circumferential and/or patch type repairs.
- System must be capable of negotiating bends in the range of 1.5D maximum to 6D minimum (3D is the most common).
- Repair reinforcement, or protrusion into the pipeline, should not exceed 1% - 2% of the inside diameter. For example, a 914 mm (36 in.) outside diameter pipe with a 12.7 mm (0.5 in.) wall thickness has an inside diameter of 888.6 mm (35 in.). The maximum protrusion into this pipe must be equal to or less than 17.77 mm (0.7 in.).

## 4.2.2 - Survey Responses

The following survey responses are summarized in categories that correspond to the sections and questions asked in the survey itself. The questions are repeated (and presented in bold type to distinguish them) within each section to avoid the need to continually refer to Appendix A. In most instances, the data collected is presented in the form of a bar chart for easy interpretation.

Most respondents answered all the survey questions, but this was not always the case. As such, in many cases there were twenty responses to a particular question, in others there were less, and in some cases, such as the types of coatings used on pipelines, there were many more, since most companies have used several coating types over the years.

### Part 1: Currently Used Repair Methods

- 1. Describe the corrective actions your company has taken due to degradation (corrosion, cracking, etc.) of transmission pipelines, especially repair or replacement actions.**

Figure 70 summarizes the responses received. The most common type of repair is a welded external steel sleeve, which was mentioned fourteen times, followed closely by "cut-out and replace" which was listed thirteen times. ClockSpring®, grind-out repairs, and composite wraps were all mentioned eight times.

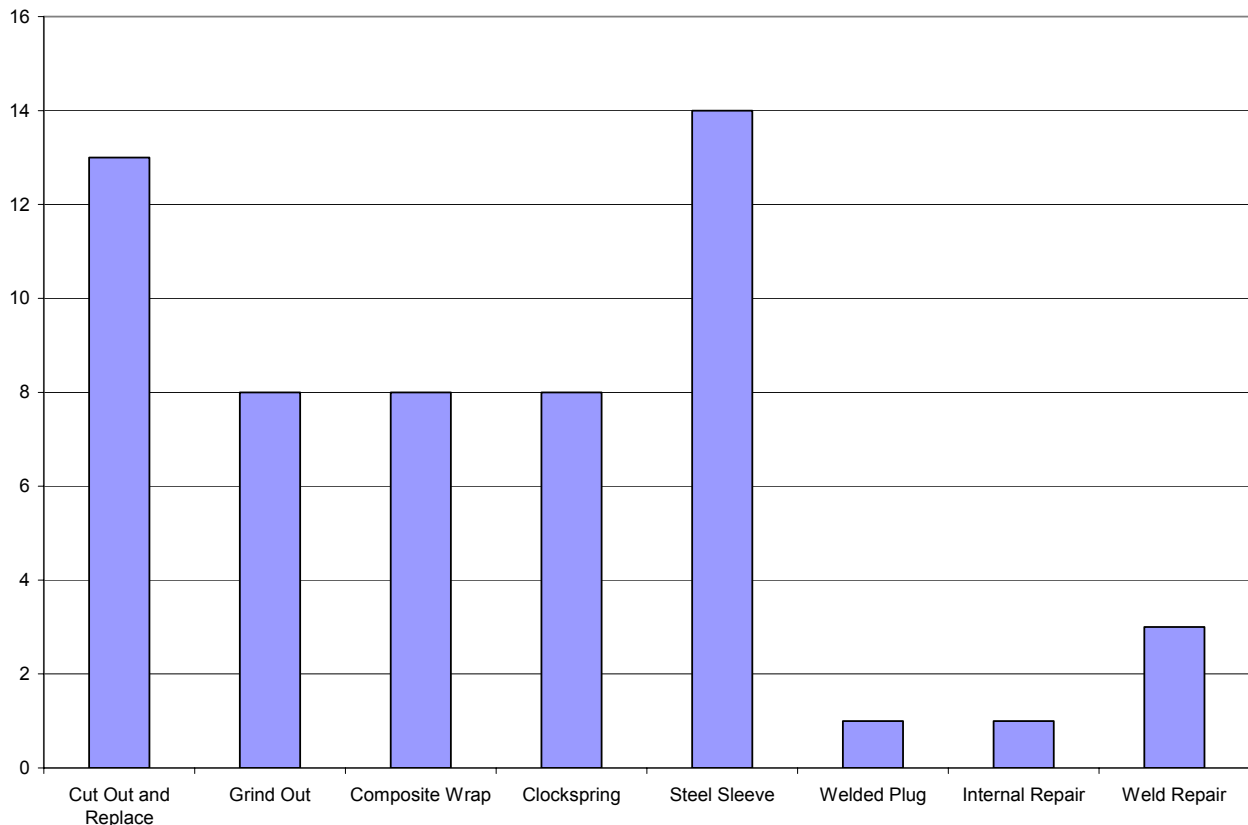


**Figure 70 - Currently Used Repair Methods**

One response summarized the company’s perspective in the following fashion: cut-out and replace cylinder (seldom), full encirclement steel sleeves (most common), direct deposition of weld metal (seldom, but frequency may increase), grinding to remove gouges (common), and welding a plugged fitting like a Threadolet over the damage.

After the degradation is detected by whatever means, repair protocols are used. For general corrosion these include steel sleeves or composite sleeves. For stress corrosion cracking (SCC), gouges, and sharp corrosion profiles, grinding is often used. Typically gouges are ground until the cold worked material has been removed and are sleeved where necessary. For cracks, much of the time these are cut out, however, there are times that cracks are ground out using in-house protocols. Repair of dents is carried out with steel reinforcement sleeves. All respondents indicated that excavations and repairs involve the replacement of the existing coating with liquid applied epoxy coating.

One reply indicated that the first step was evaluation to ASME B31G. For repairs needed in lines that can be taken out of service, the solution is to either replace the damaged section as a "cylinder" or attach a sleeve. In the past, sleeves were exclusively steel, as technology has evolved, fiberglass wraps have been used. For low pressure lines leak clamps are used where appropriate.

In the case of internal corrosion, on-stream cleaning, chemical treatment, in-situ coating and in-situ polyethylene (PE) sleeve repairs have been applied. Recently, an internal repair approach of a 914 m (3,000 ft.) long, 607 mm (24 in.) diameter, river crossing was considered (<http://www.unisert.com>) using an internal fiberglass sleeve supported by a grouted annulus. Ultimately, a new HDD river crossing option was selected because of loss of cover in the river bottom.

Another respondent stated that a variety of repair methods are used, with the selection of the method dependent on several factors including class location, type of damage, operating pressure, and operational considerations.

Corrosion is repairable by a variety of repair methods dependent upon the conditions. Options include band clamp, mechanical sleeve, weld-on sleeve, ClockSpring®, and replacement. External repair methods used by one company include sleeves (reinforcing, pressure containment), grinding (cracks) and pipe replacement. Another company indicated that they normally use ClockSpring® to re-enforce external corrosion areas, whereas cracks that exceed code limitations require an automatic cut-out (which is the last option to consider). Yet another company uses external repair techniques that include a simple blast and recoat, grind and recoat, ClockSpring® repair, welded sleeve repair or pipe replacement.

## **2. Have you used methods other than external sleeving or pipe replacement to repair different types of degradation?**

The responses to this question were split 50% "no" and 50% "yes." The "yes" responses typically gave examples, which are summarized as follows:

- Grinding is used to remove gouges (common), cracks, SCC, and sharp anomalies.
- Plugs are fitted and welded over the damage, e.g. a Threadolet.
- Composite wraps are used.
- ClockSpring® is used.
- Direct deposition welding has been used to repair wall loss
- "Encapsulating" a malfunctioning or defective area has been used.
- Taps have been used for small defects.
- Leak clamps have also been used.

Seven of the responses mentioned grinding of one type of defect or another and was the most common other type of repair. Three examples of different types of welding solution

were cited, of which only one involved direct deposition of weld metal on the outside of the pipe.

### 3. What criteria (including ease of pipe access) affect choice of the specific repair method to be used?

The compiled answers to this question are represented in Figure 71 and show twelve responses, of which cost and the availability of the repair method were those most frequently cited. The next important consideration is the position of the defect, and whether the line had to be out-of-service as the next most frequently mentioned criteria.

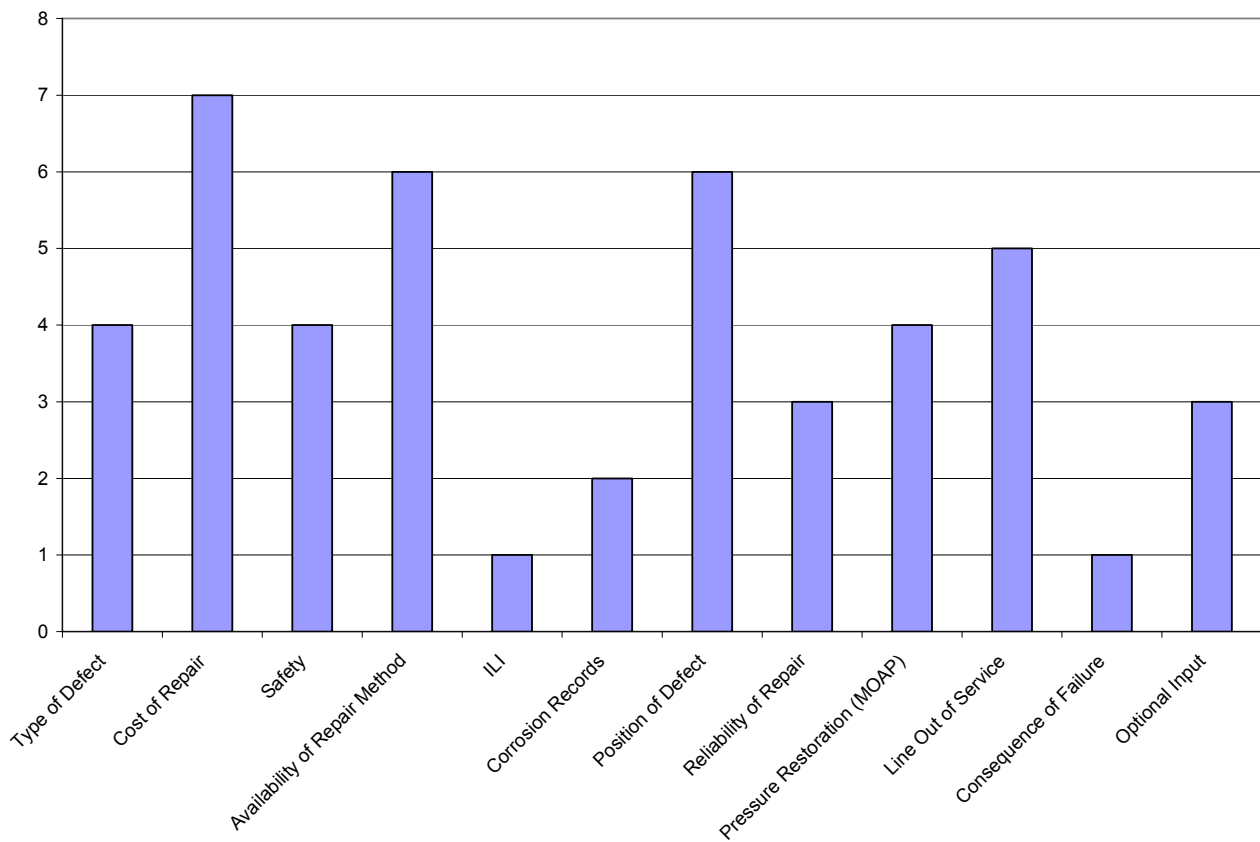


**Figure 71 - Criteria Affecting Choice of Repair Method**

One respondent summarized the evaluated criteria as follows:

- Consequence of failure
- Position of defect (on bend, weld, top/bottom, etc.)
- Impact of a pressure restriction
- Cost of repair
- Type of defect

- Availability of repair method, crews, expertise, etc.

Another response listed the following criteria:

- Maximum allowable operating pressure (MAOP) and possible future increases
- Maximum operating pressure (MOP) at time of repair
- Pipeline specified minimum yield strength (SMYS)
- Downstream demand
- Ability to remove the pipeline from service
- Cost
- Projected life of the pipeline

The size of flaw (surface area), the ability to shut in and replace the damaged section, the ratio of estimated failure pressure to MAOP, and the ability to stop additional degradation (in the case of internal corrosion) were stated as important criteria by another respondent.

Other responses follow:

- Must make repairs without taking the line out of service since it is not looped.
- Need to have the line out-of-service or at less pressure during repair work
- Can the pipeline be taken out-of-service, gas loss?
- Leak history
- Corrosion records
- ILI (in-line inspection) logs
- Cost (access, out-of-service time, mobilization time, etc.)
- Reliability (how reliable is the repair method to fix the problem, permanent repair, temp. repair)
- Safety issues
- Operator qualification
- Type and depth
- Material properties and type of pipes, e.g. electric resistance welded (ERW), seamless, etc.
- Coating
- Location (proximity to housing or public facilities)
- Operational timing (ability to take line out-of-service, i.e. impacts to customers and system)

- Type or severity of defect, access to site, time constraints in regards to length of line outage or restriction, soil conditions (e.g. swamp, rock, etc.), environmental issues (wetlands, streams, etc.).
- Pressure, Department of Transportation (DOT) status (we operate many rural gathering lines), contents of line, risk to public
- Location, pipe condition, operating pressure/SMYS, pipe geometry (e.g. straight, over-bend, sag, etc.)

#### **4. Comments pertaining to currently used repair methods.**

Not unexpectedly, comments ranged from:

- Most of our line has easy access
- The use of sleeves for the repair of external flaws has been satisfactory to date
- Most existing methods have been effective
- The ClockSpring® has been a very useful repair method in the last few years
- Many are very difficult in swamp or underwater locations

Cut-out repair is considered the last resort due to flow disruption and overall cost. External faults are more readily repaired using sleeves than internal anomalies. Internal damage requiring repair in bends equate to a pipe replacement. The threshold for pipe replacement versus repair decreases once the first replacement in a section is justified.

Live repair methods require a reduction in operating pressure. Normally the excavation trench requires tight sheeting and shoring, a certified welder, and qualified maintenance welding procedure with low hydrogen procedures (e.g. E7018 low hydrogen electrodes).

### **Part 2: Use/Potential Use of Internal Repair**

#### **1. Has your company attempted repair of a transmission line from inside the pipe?**

Of the nineteen responses to this question, only one was "yes." Another company indicated that they considered the use of the PG&E tool for weld repair on the internal diameter, but the expense was said to be large and the diameter range was limited. Other companies raised the question of how to ensure the quality of the repair.



**If so, describe the repair(s)**

Plastic tight liners were used and for lower pressure lines (less than 100 psig MAOP) slip lined plastic liners have been used. Both of these methods require the line to be out of service when repair is made.

**2. There are many factors that affect the decision to repair or replace pipe. What circumstances would favor performing a repair from inside the pipe using only one or two excavations rather than excavating the entire length of pipe?**

Figure 72 shows the primary factor for choice of an internal repair method is road and river crossings. Confidence in repair method, presence of numerous but localized areas of damage, inability to excavate large areas because of environmental permitting issues, economics/cost and availability of a proven, industry (and regulator) accepted internal method were also factors mentioned.

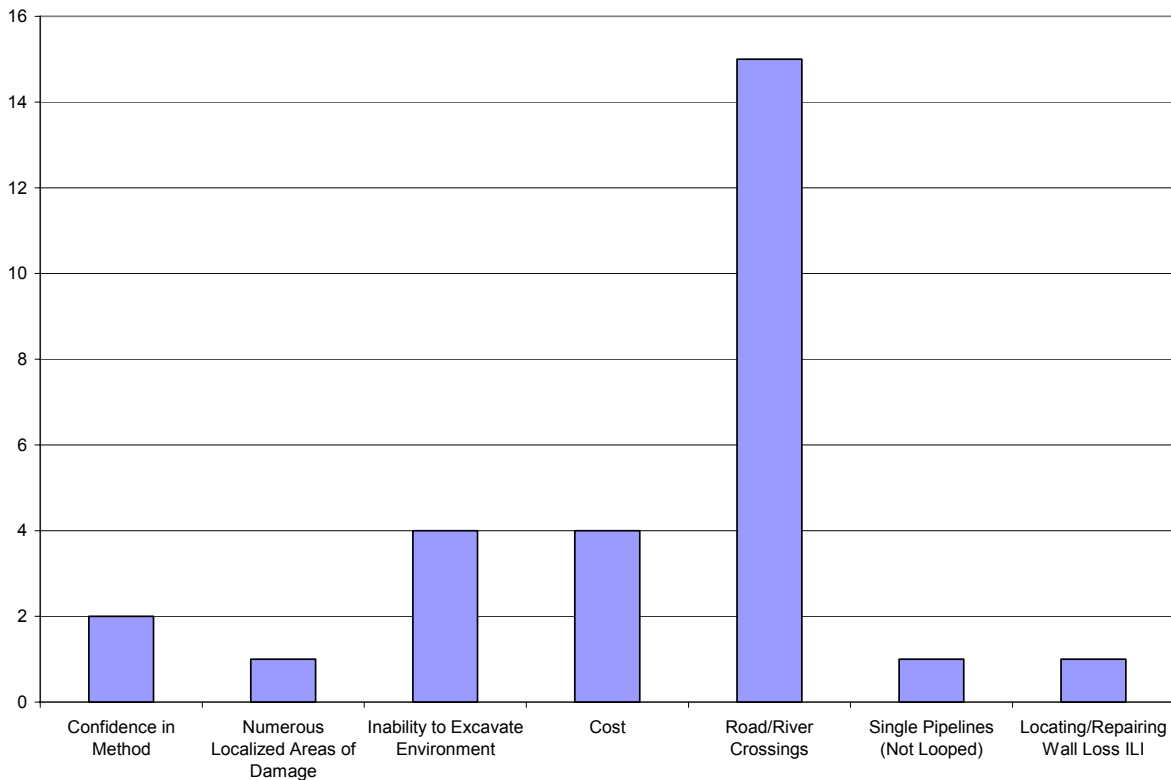


**Figure 72 - Decision Factors for Internal Pipe Repair**

Specific comments follow:

- Depending on the depth of burial and the presence of over-bends, sag bends or side-bends or road/river crossings etc., then an internal repair may be much more preferable than cutting out the piece of affected pipe. Single barrel

pipelines (versus looped lines) are more difficult to remove from service (customer interruption).

- Factors, such as, class location, environmentally sensitive areas, in crossings, under waterways or rugged terrain would be some of the major factors influencing this decision; an anomaly found inside a casing might be (a factor), under a road, irrigation canal, or railroad tracks; difficult to excavate locations (e.g. rocky conditions, caliche soils, etc.); and cost would be another factor influencing the decision. This potential technology would also be useful for locating and repairing internal wall loss identified by ILI inspections without excavation of the entire pipeline and numerous cuts to the line.
- Property damages, contractor costs, inaccessible right-of-way, lack of temporary workspace, road, railroad, and stream crossings sometimes must be replaced just because indicated damage cannot be directly measured highway crossings, railroad crossings, and heavy traffic intersections.
- Highly congested areas that impact risk to other pipelines or utilities and proximity to structures.
- Possibly a pipeline under water or a permanent structure where the pipeline is not easily accessible
- Where the pipe repair is located under a road or body of water where access is limited.
- Pipelines that are under paved areas, or in narrow or confined rights-of-way where space is limited. Crossings at roads, railroads, lakes, and rivers, and water cover, such as, marsh or swamp.
- If the cost of an internal repair plus the outage restriction was less than the cost of an external repair. For example, if the defect was in the middle of a major water crossing or swamp which would normally require ice road construction for access.
  - High traffic areas
  - Federal, state, city or county roadway restoration requirements
  - Environmental concerns
  - Railway crossings

**3. If the technology were available to perform a repair from the inside, would your company consider using the technology?**

One "no" response was received. The other seventeen responses were "yes" and some were qualified with additional comments as follows:

- We would want to review testing and possibly witness a demonstration

- Only if proven
- If cost is reasonable
- Particularly if DOT compatible
- Depending on the site-specific conditions

One response indicated that the company transports non-corrosive natural gas, so the probability of an internal flaw is highly unlikely. While this may be true for many companies in terms of internal corrosion, it misses the point that the internal repair can be used for repair of external damage.

**If so, for what application(s) – e.g., specific geographic locations and special situations?**

Figure 73 summarizes the answers to this question. River crossings and populated areas with highway crossings were most frequently cited. Use for repair of flaws found by pigging, included internal or external corrosion pitting, gouges, seam or weld flaws (if detectable by pigging).

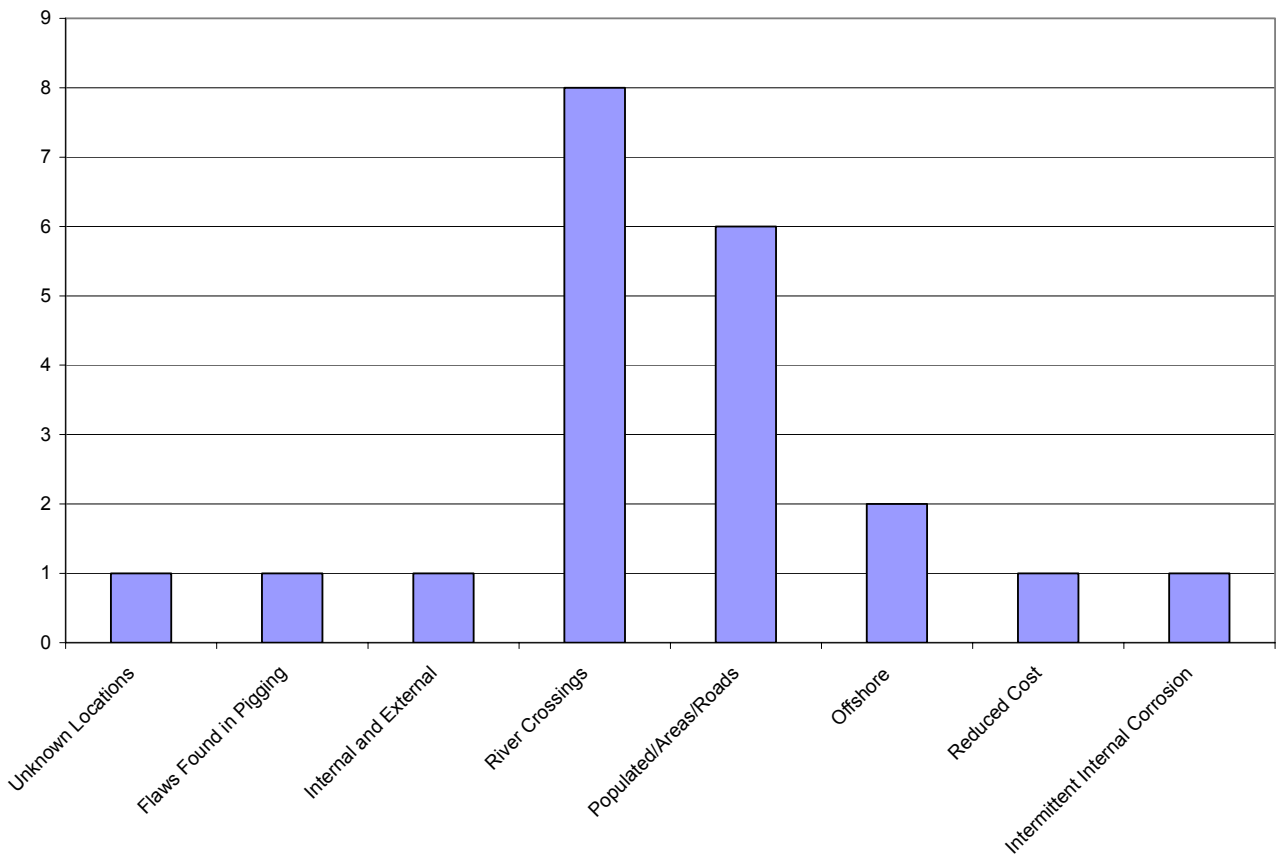


**Figure 73 - Specific Geographic Locations and Special Situations**

Seven responses mentioned river crossings and this was the most common response to this question. Others cited pipelines that are under paved areas, or in narrow or confined rights-of-way where space is limited, crossings at roads, railroads, lakes, swamp areas, and difficult access due to physical barriers inherent to high population density and congested areas (e.g., numerous utilities, building, streets, etc.).

One response mentioned concerns regarding the use of internal repair on a direction bored crossing of a freeway, because of unknown future cathodic protection (CP) effectiveness after welding.

Another response referred to applications where it is not cost effective to repair or replace the pipe conventionally, provided the internal repair is an equivalent repair. Probably the best application in this case would be offshore.

**4. At least one excavation will be required to insert the internal repair device into the pipe. From this excavation, the repair device could travel in each direction from the excavation. About how far from the insertion point should the repair device be able to travel?**

Answers ranged from 15 m (50 ft.) to 113 km (70 miles); the latter for offshore operation, with most answers being in the 305 m to 915 m (1,000 ft. to 3,000 ft.) range. The array of responses is summarized in Figure 74, showing that there are discrete lengths of 305 m (1,000 ft.) and 610 m (2,000 ft.) "umbilicals" (or travel distances) for certain categories of repairs or related requirements. The typical travel distances required are divided into three groups; up to 305 m (1,000 ft.); between 305 m to 610 m (1,000 ft. and 2,000 ft.); and beyond 915 m (3,000 ft.), and are indicated by the dotted lines in Figure 74. In concept, all these systems would be pig-based. Systems with despoiled umbilicals could be considered for the first two groups, while the last group would be better served with a self propelled system with self-contained onboard power and welding system.

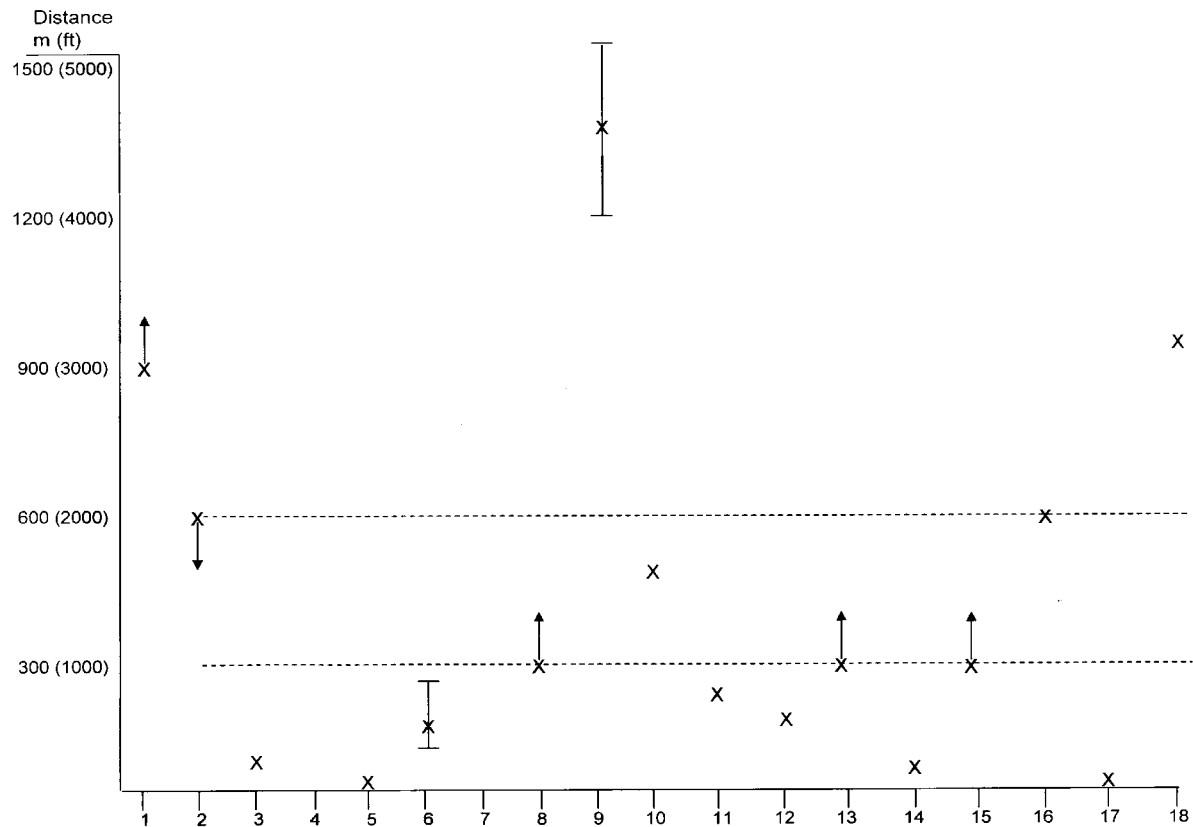


**Figure 74 - Distance Repair System Required to Travel Down Pipe**

152 m (500 ft.) appears to be adequate to cross most interstate highway crossings and 610 m (2,000 ft.) for all river crossings. A major river crossing would require the device to travel up to 610 m (2,000 ft.). In one case it was stated that the longest section of pipe which is not accessible (directional bore) is approximately 1,219 m (4,000 ft.), so the need would be to access the pipe a distance of approximately 610 m (2,000 ft.) from either end.

Longer distances, probably from 915 m (3,000 ft.) to several miles or more would require the technology to travel in a similar way as an inspection pig. Realistically, such a system would have to be based on an onboard propulsion device using gas line pressure as the motive force. A self-contained, inverter-based welding power source and welding system would also be required.

**In what range of pipe diameters should the repair device be capable of operation?**

A wide range of pipe sizes were cited, both within a particular company, and between various companies. The results are summarized in Figure 75 show that pipe size range requirements run from 51 mm (2 in.) through 1,219 mm (48 in.) diameter. The common size range for 80% to 90% of operators surveyed is 508 mm to 762 mm (20 in. to 30 in.) diameter, with 95% using 559 mm (22 in.) diameter pipe.

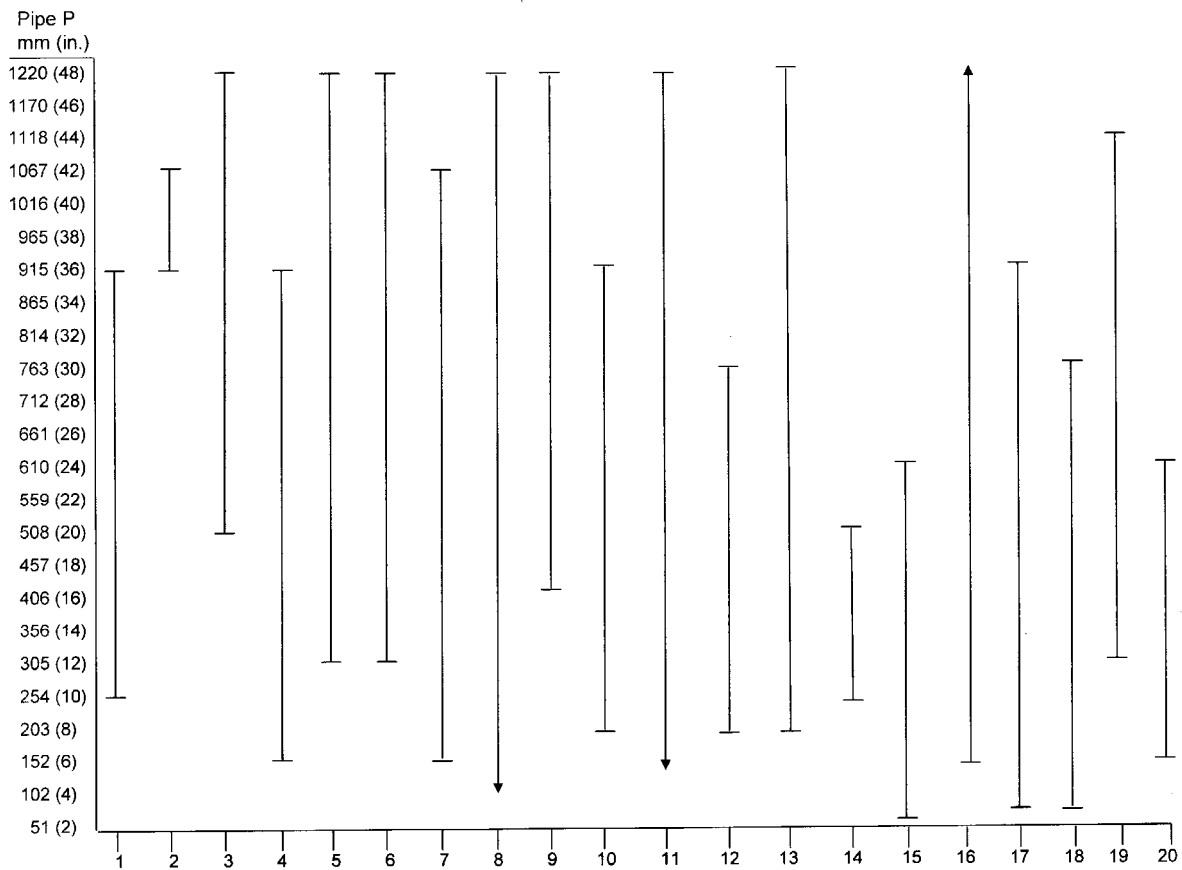


**Figure 75 - Range of Pipe Diameters Used**

**5. What potential obstructions such as elbows, bends, branches, and taps should the repair system be able to negotiate?**

The answers to this question were quite varied and are summarized in Figure 76. Pipe bends of various radii were most commonly mentioned including 1.5 times the diameter (1.5D), 3 times the diameter (3D), and 6 times the diameter (6D), with 3D pipe bends being the most commonly used. Elbows were mentioned in three responses. It is interesting to note that the answer "all" was given four times.

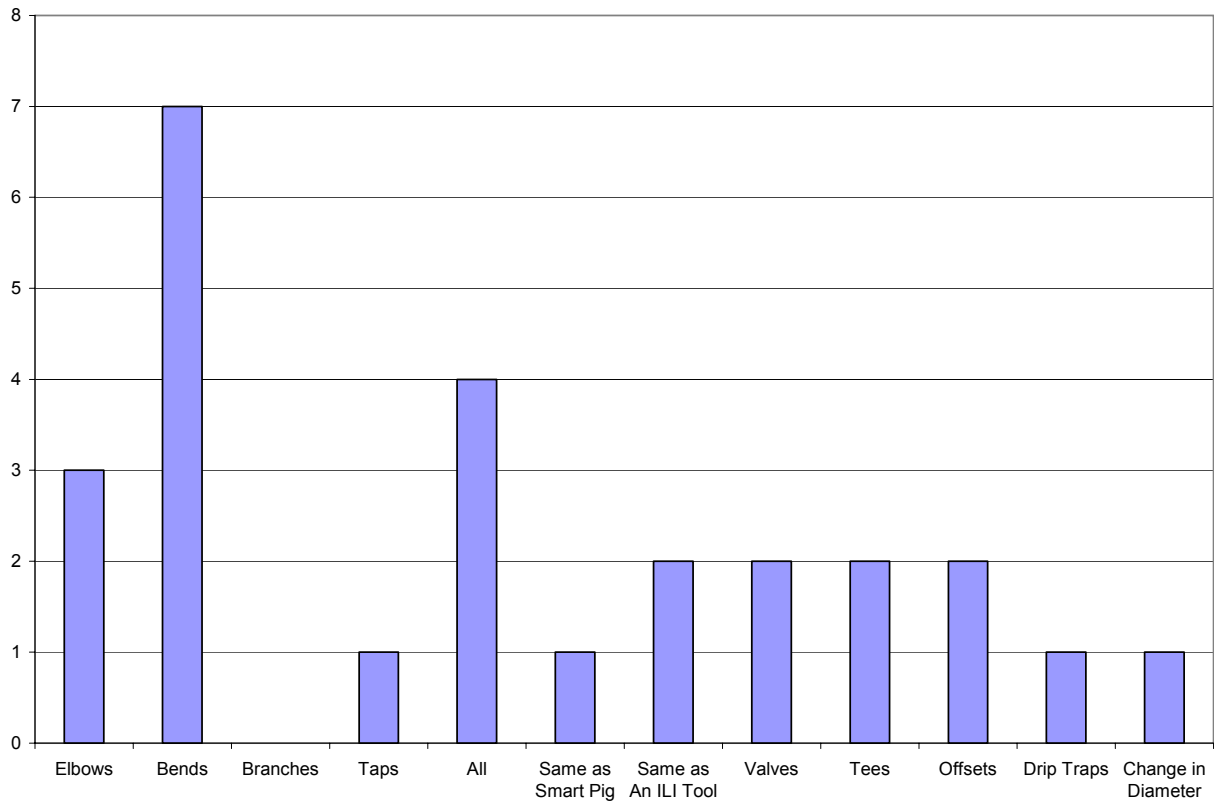


**Figure 76 - Potential Obstructions to be Negotiated**

**6. For the situations described in Question #3, at what approximate cost would an internal repair method become competitive with existing repair options?**

Statements and cost figures varied widely from \$25,000 to \$1,000,000 depending on the perspective of the survey respondent and the terrain that their pipeline systems crossed (see Figure 77).

- Case by case basis
- \$1,000/0.3 m (\$1,000/ft.) is the benchmark for internal repair as this is the cost for HDD
- Road crossing/HDD cost is \$50,000 to \$1,000,000 depending on pipe size & distance
- \$25,000 per repair site
- \$30,000 - \$60,000 per repair site
- \$50,000 - \$70,000 per repair site
- \$200,000 per repair site
- Permanent repair less up to \$1,000,000
- Twice the cost of conventional repair
- Half the cost of conventional repair

### Figure 77 - Cost Comparative Breakpoint for Internal Repair

One reply indicated that internal repair probably would not be competitive with external repair/replacement except in river crossings. Anything cheaper than a new HDD and tie-in would be economical in that case.

One company indicated that the cost is related directly to the amount of time the pipeline would be out of service. For major river/road crossings the technology would be competing with HDD @ \$1,000/305 m (\$1,000/ft.). On land, if one can dig up the area and cut out the affected piece of pipe faster than repairing it, then this is what companies would do since the cost of the pipe and a couple of field welds is inconsequential compared with the cost of having the pipeline out of service. The potential cost option could be the reconstruction of a river crossing or other directionally bored crossing.

One respondent indicated that pipe repairs without external access are typically expensive, thus limiting the types of repairs to critical service lines. Repair costs, if the repair can be quickly mobilized (i.e. leaking system) and be confidently applied, can approach \$1,000,000. Therefore the repair would have to serve as a permanent repair.

Another company noted that existing external methods are relatively inexpensive. Repairs required in an area that is inaccessible to current external repair methods can be very expensive and vary by the pipe size, length, and situation. The advantage will be to repair multiple locations or hard to reach locations with minimal excavation. Quite reasonably, several respondents answered that this would have to be examined on a case-by-case basis.



Yet another response indicated that an internal repair tool would be valuable where the pipe is inaccessible. Replacing a road crossing/directional bore could range from \$50,000 to \$1,000,000 depending on the size of pipe/distance. Other quantitative replies were within the wide range of about \$30,000 to \$60,000 per repair site in one case; for repairs other than in crossings, about \$25,000 per site total including excavation, recoating and backfill; and another reply mentioned about \$200,000, while a another response indicated that an internal repair would have to be 50% to 75% of the cost for a conventional repair/replacement to be competitive.

**7. Have new regulatory requirements created a need to improve the fitness for service of existing transmission lines via localized repair or removal of conditions that are acceptable under previous criteria?**

Responses to this question were varied, with six "no" responses and nine "yes" responses. Specific remarks are listed below:

- Not in Canada – new requirements only change documentation effort.
- Regulations will require companies to prove the fitness for purpose of their pipelines rather than improve. There maybe circumstances with HCA's where repairs are now required.
- Some, but I see this as having little impact on the use of this technology. The newly proposed pipeline integrity regulation will make us more aware more quickly to the extent of repair required.
- Under the current Texas Railroad Commission Integrity Rule, and the pending DOT integrity rule, operators are in-line inspecting more pipe than has been done in the past. More repairs may be necessary as a result of more inspections.
- Upcoming inspection requirements may result in the discovery of defects requiring repairs that would not otherwise have been discovered. Increased cost of excavation restoration has been imposed by various municipalities.

**8. What is the estimated number of repairs per year that could potentially be performed by internal repair in your company for the reasons discussed in Questions #3 and #7?**

Responses varied from "none," through "1 repair in 5 years," and in one case, "10-75 repairs per site." These answers are summarized in Figure 78, which shows that answers from "1 repair in 5 years," up to "5 repairs per year" were by far the most common response. This indicates a limited expected requirement for such a system, particularly based on expected relative cost to purchase and operate. This supports the suggestion that pigging operators would be the best source to supply and operate such equipment on a contracted basis.

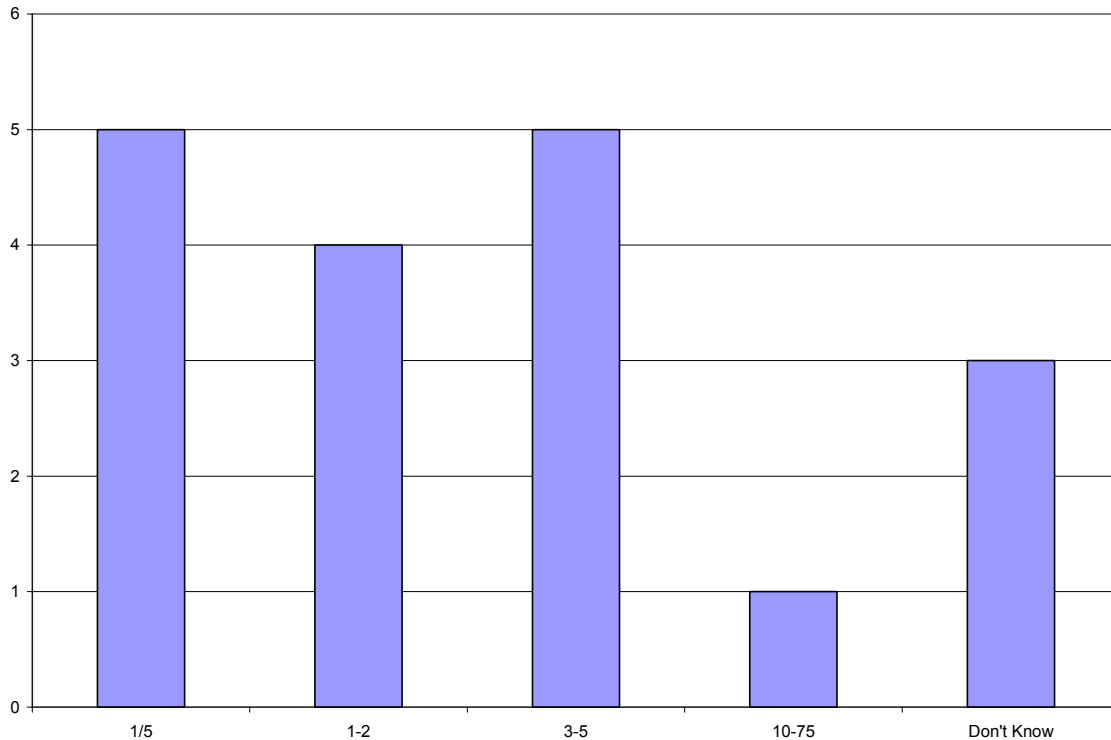


**Figure 78 - Estimated Number of Internal Repairs Required Per Year**

**9. Comments pertaining to the use/potential use of internal repair.**

Significant individual responses follow:

- Internal methods would be hard to accept as it would be difficult for QA/QC and direct inspection.
- It would have to provide a permanent repair and be piggable to be worthwhile.
- Reinforcing weld joints internally for the in-service pipelines built using welding process, which produced joints with incomplete penetration and lack of fusions.
- Any internal repair sites would have to still be capable of passing an ILI tool and be visible to that tool.
- Internal repair could not impede the ability to pig lines and still be a viable option.
- The major concern would be not to obstruct subsequent ability to assess the pipeline's integrity through internal inspection schemes.
- It is a good to have, whenever necessary.
- A method of inspection of the repaired area may need to be devised.
- It would seem that internal repair methods would have minimal use unless long distances need repaired in congested locations.

- Offshore or underwater (e.g. river crossings, swamps, etc.) offer best economics.
- It would be a valuable tool to have; however, I see no advantage to the process for pipe, which is accessible. The only value would be where pipe is inaccessible in a road/stream.
- The use of an internal repair would probably be driven by the discovery of unacceptable corrosion in an inaccessible location. We are currently unaware of this situation in our system.

### Part 3: Need for In-Service Internal Repair

#### 1. How important is the ability to perform a repair from the inside the pipe while the pipeline remains in service?

The majority of survey respondents considered the ability for the pipeline to remain in service while the repair was conducted to be very important (Figure 79), especially if their system was not looped. Companies with looped pipeline systems presumably account for the respondents that considered this to be only somewhat important.

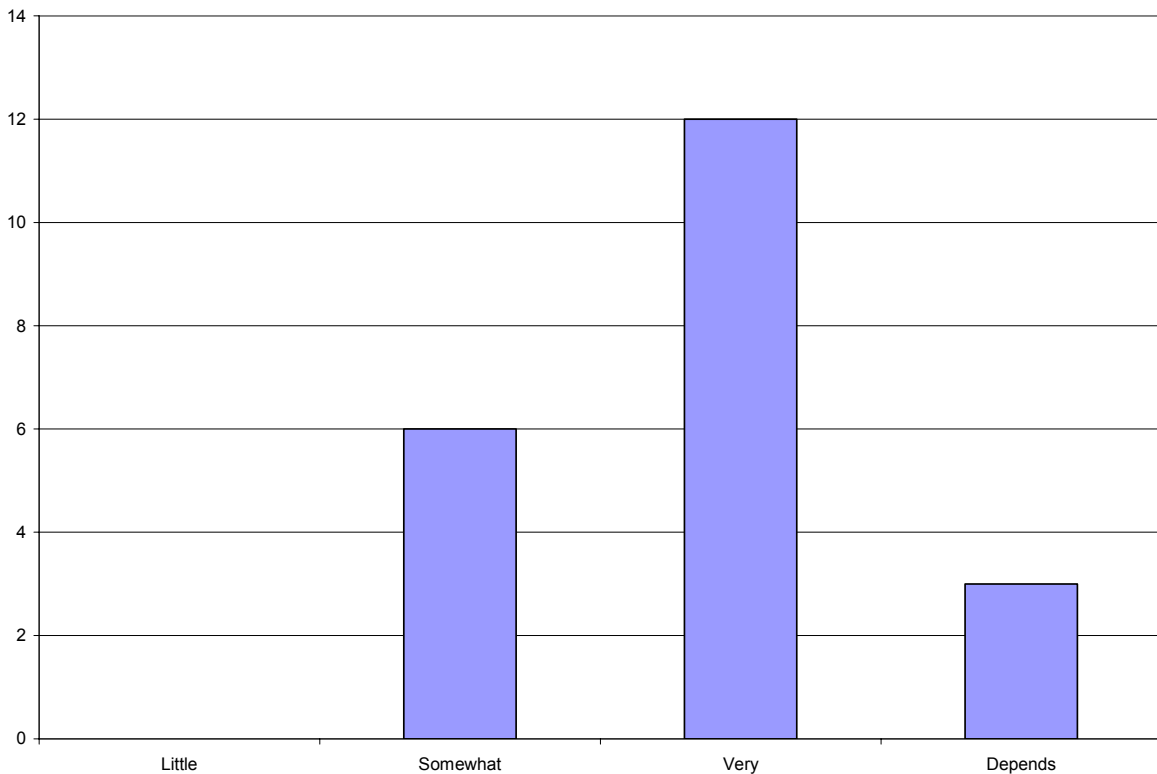


Figure 79 - Importance of Repair While Pipeline Remains In-Service

Significant individual responses:

- If the pipeline could remain in service the probability of using the tool would be very greatly increased.
- The ability to keep a pipeline in service during repair work would be an important factor when considering internal repair as a possible option.
- Very important for the economics of a large diameter transmission line. Keeping the line in-service is a distinct advantage over cut-out.
- For us it would be important because we are not looped.
- Because this may compete with external sleeving, I think that this is real important.
- This repair method would save gas that would normally be lost and would allow service to be uninterrupted. It is very important.
- Minimizing business disruptions to key customers is important. This ability would make such a repair method very important.
- For those pipelines where service cannot be interrupted and where welding is impractical, it is very important.

**2. Would internal repair remain attractive if it was necessary to completely shut down the pipeline (depressurized and evacuated) during the repair?**

The answers summarized in Figure 80 include six "yes" and three "no," with a variety of other responses in between.

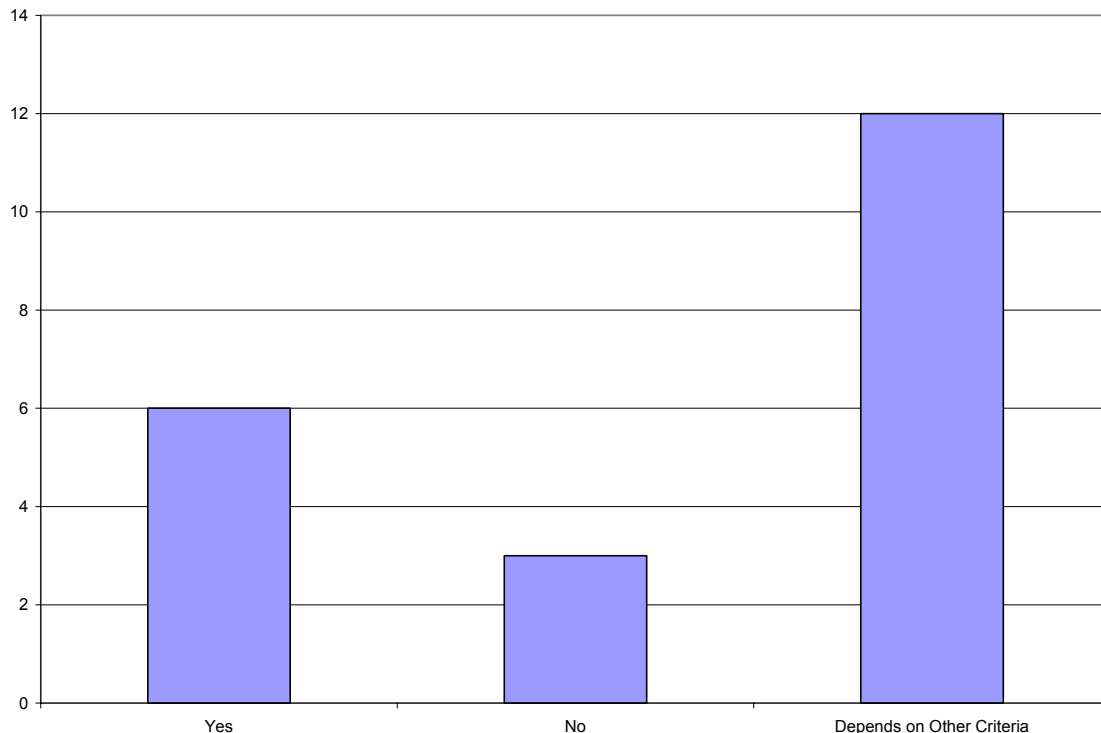


**Figure 80 - Still Attractive if Pipeline Must be Shut Down (Depressurized and Evacuated)**

Twelve respondents collectively indicated that this depends on a number of other criteria. It would remain attractive if:

- It could eliminate the need to build an ice road in the swamp or dam and flume a river
- in highly congested areas it could be attractive
- Could be where it is too hard to get to the defect location directly like under a river, lake, for offshore and underwater.
- For offshore environments, shut-in is possible, blow-down probably an extra \$100k minimum dependant upon gas prices.
- To depressurize and evacuate the gas adds cost that would affect how attractive this type of repair would be.

### Depressurized but not evacuated?

Responses are presented in Figure 81: there were eight "yes" responses and two "no" responses.

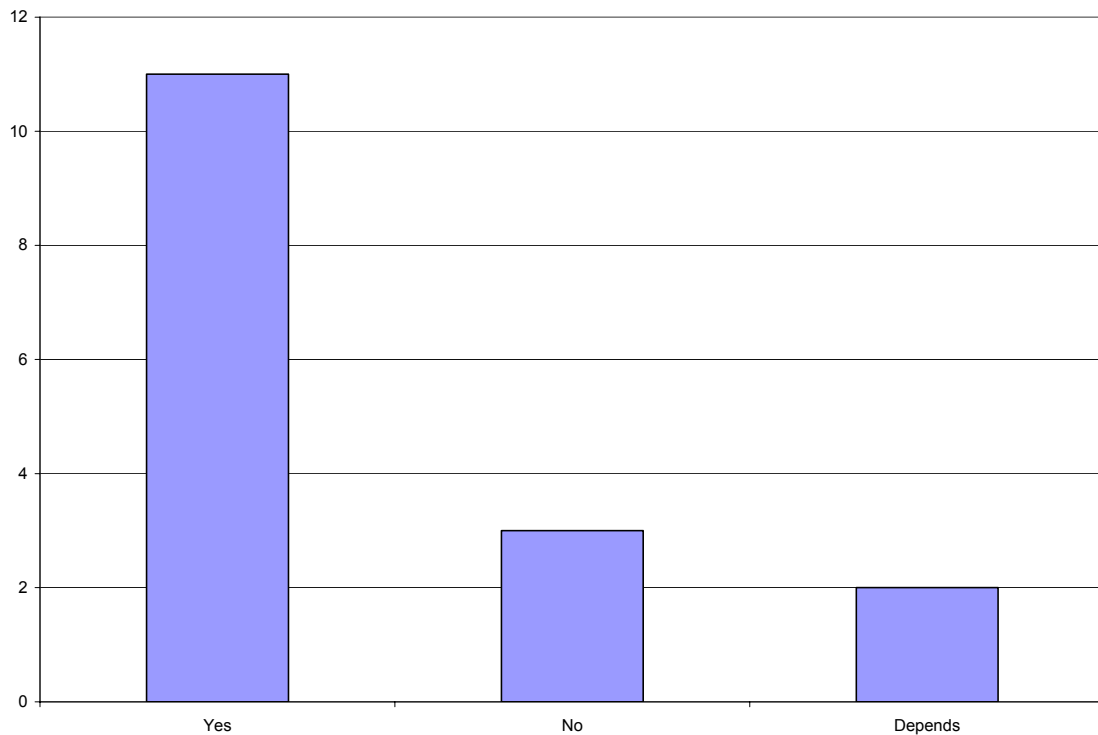


Figure 81 - Still Attractive if Pipeline Must be Depressurized but Not Evacuated

Individual responses:

- Depressurized but still flowing is better.
- Depressurized and not flowing is poor; usually the cost of excavation is minor compared to the outage.
- It is typically not possible to depressurize without a blow down and would not be as attractive.
- There could still possibly be applications but would then be much more a function of the cost of the internal repair versus the cost of external repair or replacement.

### Out-of-service (no flow), but remain pressurized?

Responses are summarized in : there were eleven "yes" responses and two "no" responses. If the pipeline must be out-of-service, the amount of pressure remaining and whether or not it is evacuated are probably far lesser considerations.

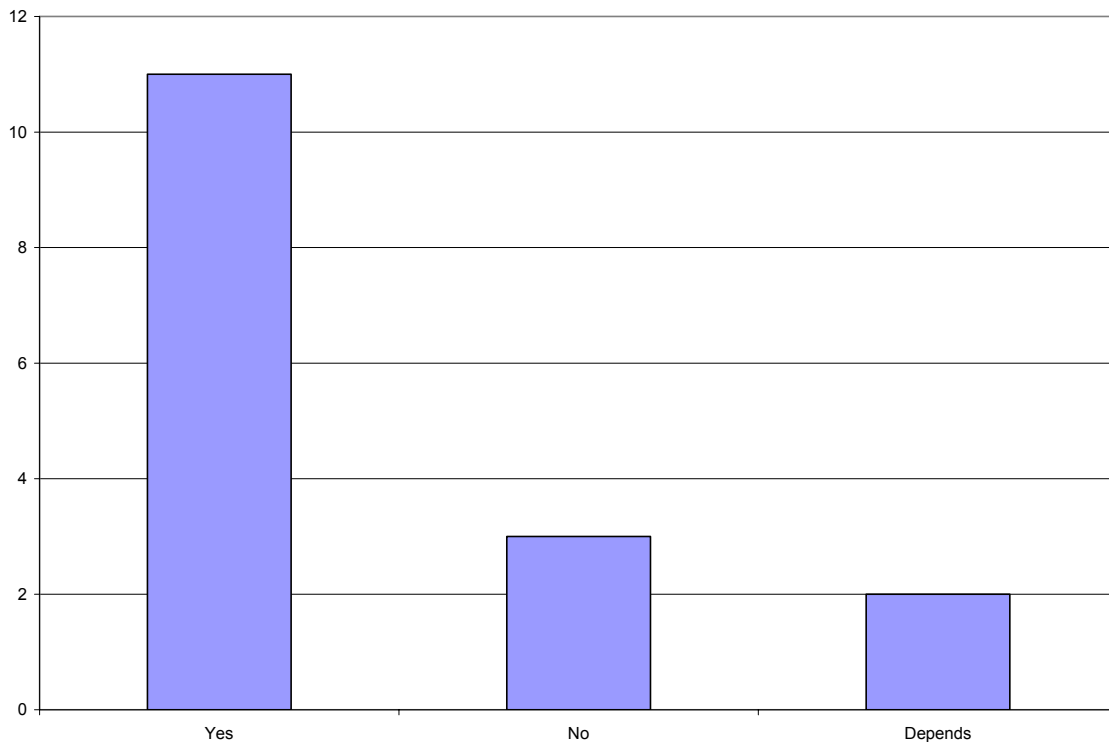


**Figure 82 - Still Attractive if Pipeline Must be Out of Service but Pressurized?**

Specific responses:

- This is more attractive than the previous two.
- It would be an attractive repair technology under these conditions.
- Leaving the line pressurized would reduce the gas lost, and reduce the potential cost of the repair.

### **3. Comments pertaining to the need for in-service internal repair.**

One response commented that hopefully internal repair would only be required for operators who transport wet or corrosive products. This comment refers to their lack of internal corrosion damage, but also indicates a lack of understanding that the internal repair could be used to repair external corrosion damage. An internal repair appears to be attractive if it reduces the potential for gas lost from blowing down a pipeline, and reduces cost, and/or reduces out-of-service time. Obviously, as the price of gas increases each of the above options will have more impact.

## **Part 4: Applicable Types of Damage**

### **1. What types of external coatings would be found on transmission lines owned by your company?**

A wide variety of coatings were cited ranging from none (bare steel pipe) through a wide range of bitumastic, coal tar, wax; plastic and composite tapes and wraps; to POWERCRETE® and concrete. The number of responses indicating the use of each coating type is summarized in Figure 83. The top three coating types mentioned were fusion bonded epoxy (FBE), coal tar, and concrete/POWERCRETE®.

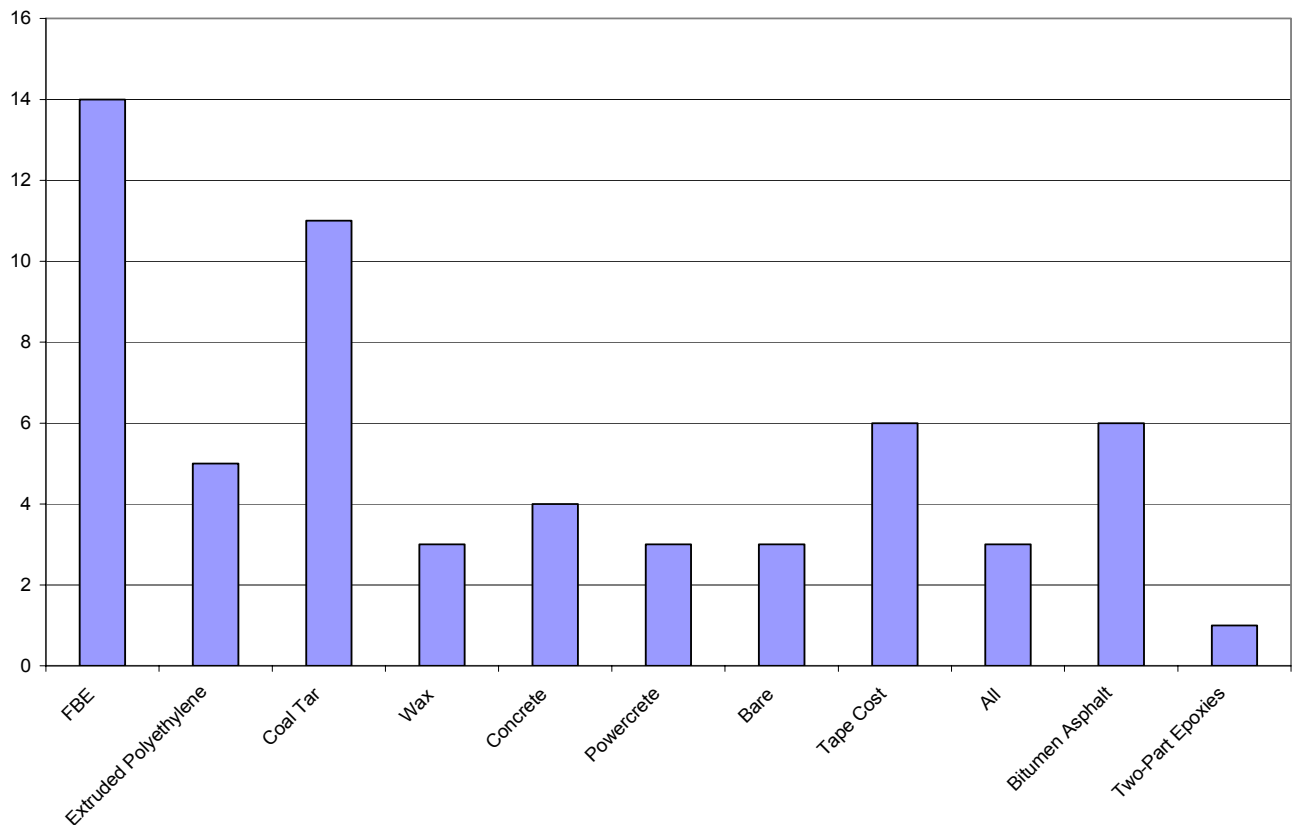


**Figure 83 - External Coatings Used**

**2. If a repair involving welding from the inside was performed, how important is it to preserve the integrity of the coating?**

The ten responses are summarized in Figure 84. There were ten responses to this question. One company indicated a level of importance of "important," six companies listed the level as "very important," and three indicated a level of "critical/essential." Five respondents commented that preserving the coating integrity was not very important, as the CP system was considered capable of taking care of local degradation in these instances.



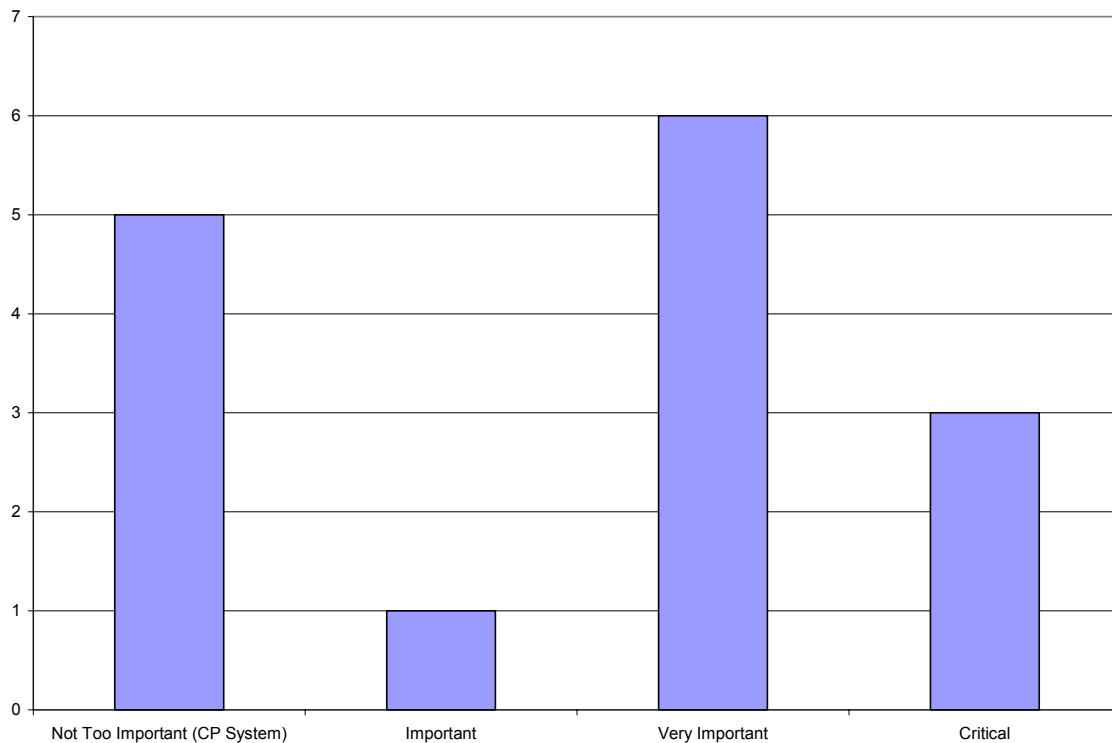


**Figure 84 - Maintenance on Coating Integrity**

Individual responses:

- It is of utmost importance.
- If the existing coating cannot be maintained, then additional excavations will be necessary and the coating repaired.
- It is very important for large damaged areas since access to site to repair the coating may be difficult.
- It is necessary to try to preserve as much coating as possible since the repair may be applied to an area of external corrosion and we would not be able to assess the root cause of the corrosion or know if it is mitigated.
- An offshore pipeline operator suggested that perhaps considering attaching an anode if necessary, but then again, reasonable access would be required. In offshore applications, a small amount of coating damage is not too much of a problem.

**3. Is your cathodic protection system capable of compensating for relatively small breaches in the coating?**

The results here are shown in Figure 85. All respondents said that the CP system is capable of compensating for relatively small breaches in the coating: there were thirteen "yes" responses and five qualified "yes" responses.

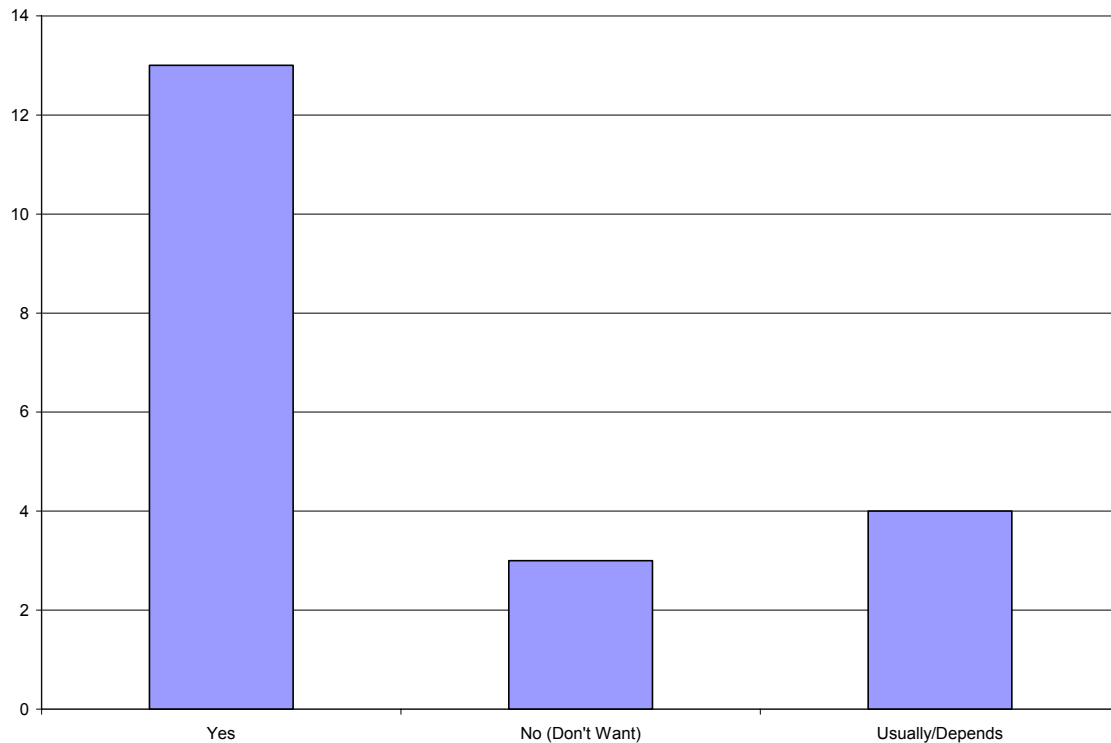


**Figure 85 - Is CP System Capable of Compensating for Small Coating Breaches**

Comments received:

- Preservation of external coating must be a major consideration.
- Not for disbonded coating.
- It would not meet DOT code requirements under 192/195.
- We do not want any breaches or holidays in their coatings. Coating damage would reduce the attractiveness of this repair system.

One company stated that the CP system can normally compensate, but that one would have to consider that if you had an external corrosion anomaly at the repair site, you may repair it and still have an active external corrosion site. The internal repair would have to be fully pressure containing. Also, if the weld damages good coating, and there

is some localized issues with CP protection, that may set-up an active corrosion site at the weld sites (especially if damaged coating is left disbonded and shielded from CP).

#### 4. Comments pertaining to applicable types of damage.

The following three comments were received:

- I would not want to trade a known likelihood of external coating damage in order to permit an internal repair.
- I do not think the industry or the regulators would accept a repair method that damages the coating and leaves it in worse shape than originally found
- If the coating is damaged and CP shielding occurs, then problems would be great. It may be possible to install a Magnesium (Mg) anode at the repair location to spot protect damage to the coating.

### Part 5: Operational and Performance Requirements for Internal Repairs

1. **Two general categories of repairs are being considered, (1) using weld metal to restore a surface and (2) installing an internal sleeve, either metallic or nonmetallic, to provide structural reinforcement of leak tightness. Is it important that the line remain inspectable by pigging after repair?**

The responses are summarized in Figure 86, which shows the unanimous response was "yes."

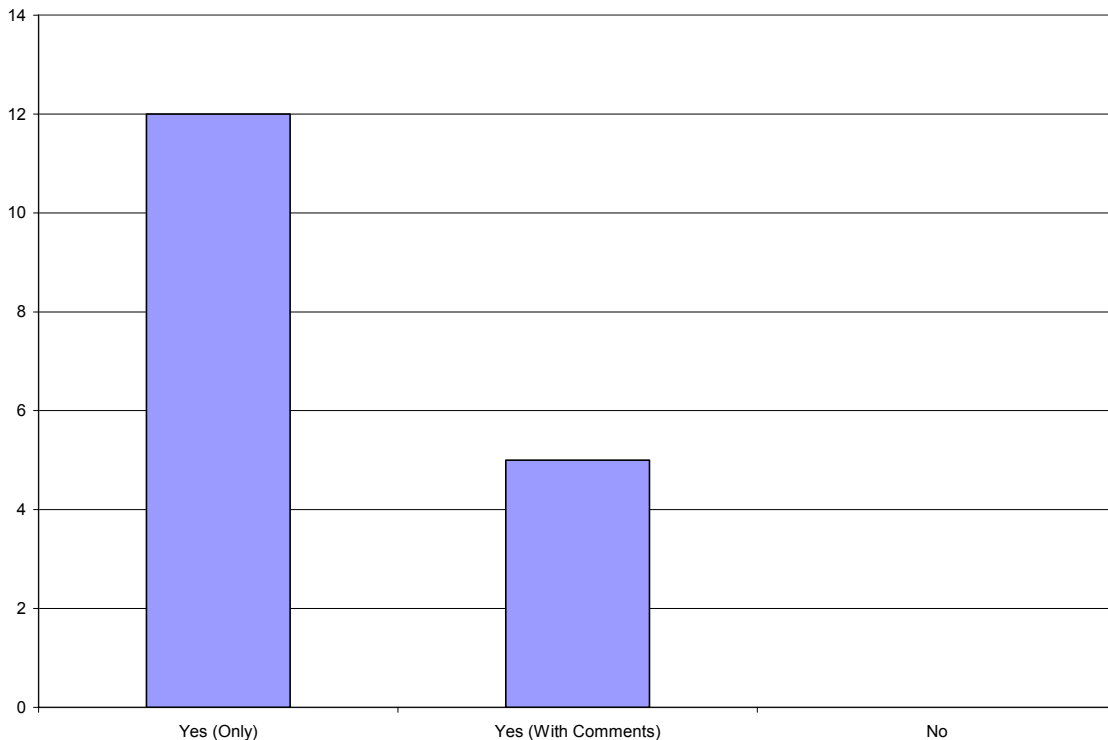


Figure 86 - Inspectable by Pigging

The five "yes" responses contained the following comments:

- Maybe not for a temporary repair. One scenario that comes to mind is in the mountains where there is too much snow to access. A temporary repair could be made and not worry about ILI restriction. Would perform cut-out in the summer.
- Yes, if original line was piggable.
- DOT code 49 CFR 192.150 states that all new lines, or line repaired, will be able to accommodate the passage of an ILI device. Additionally, with the new integrity management rules requiring regular pigging of pipelines, any internal repair would have to allow the passage of a pig.
- Under existing DOT codes it would seem that being able to inspect the line is required. New pipeline integrity regulations may allow for alternative methods.
- For some lines, being "smart- piggable" after repair would be mandatory.

**About how far could the repair protrude into the pipe before it would interfere with pigging?**

The responses are summarized in Figure 87. Six responses gave a range in the region of 5% to 10% of nominal pipe diameter. Even for relatively small diameter pipe this amount of protrusion could be quite large.

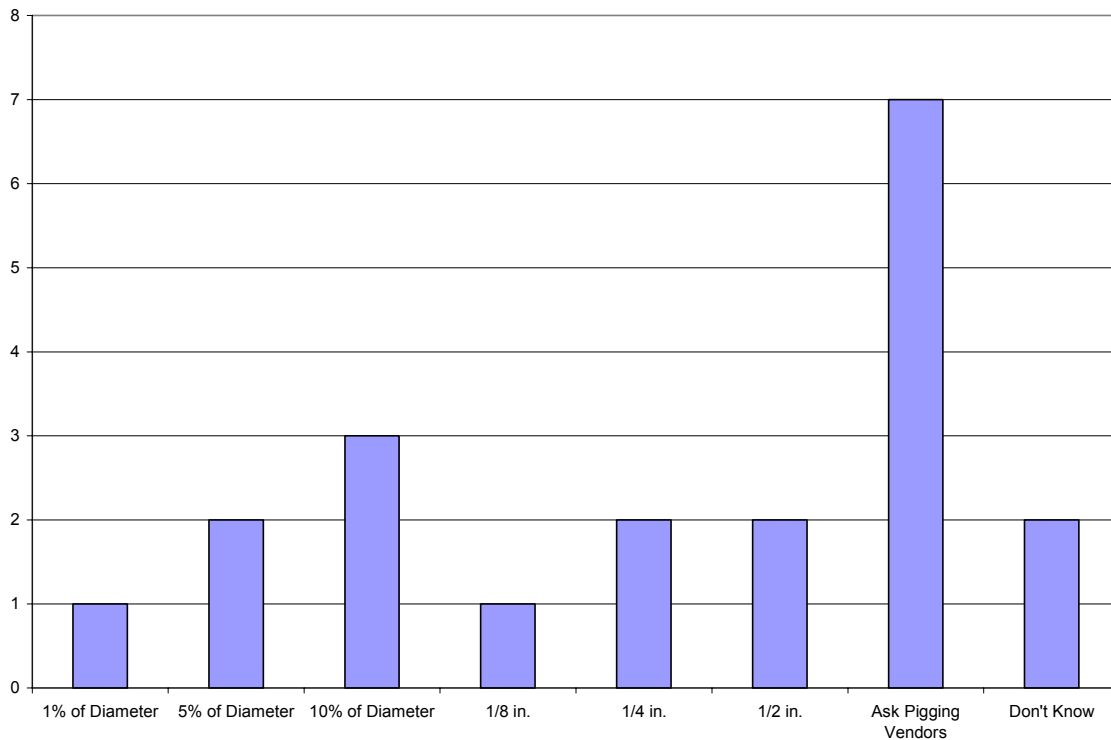


**Figure 87 - How Far Could the Repair Protrude Into Pipe Before Interference**

Seeking guidance from pigging vendors was suggested by seven of the responses. An amount of 1% of diameter was considered a good number as a rule of thumb in one case. In another, about 1.5 mm (0.6 in.) for a 914 mm (36 in.) pipe (2% of diameter) was mentioned. Several responses mentioned that the type of pig is an important consideration when considering an answer to this question. A "smart pig" was said to be able to accommodate a 10% reduction in diameter.

One response stated that the acceptable protrusion varies depending on the type of pig, pipe size, geometry, and longitudinal length of the restriction. Another response stated that this is dependent upon the type of pigging utilized (e.g., traditional versus smart).

**2. What NDE would your utility require for a repair to an existing longitudinal or circumferential weld?**

Thirteen survey respondents included radiographic testing (RT) or indicated that only radiographic inspection was used or allowed; five indicated that ultrasonic testing (UT) is also permitted; and two responses indicated that magnetic particle inspection (MPI) is also allowed (see Figure 88).

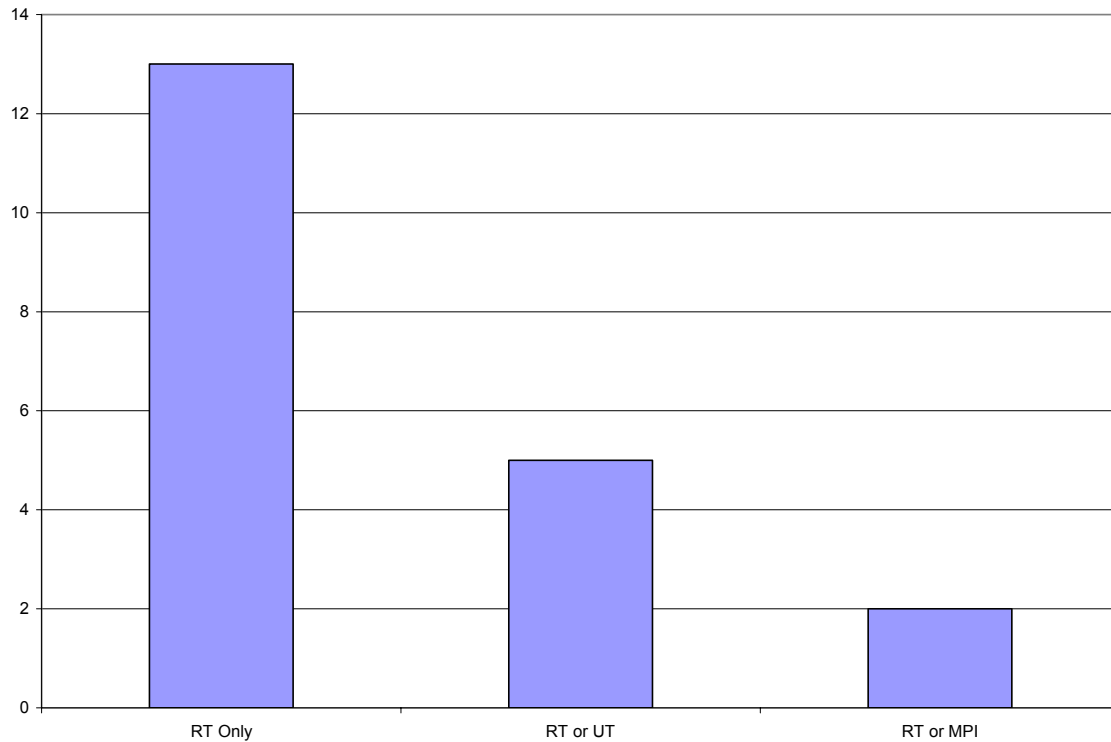


**Figure 88 - NDE Required for Repair to an Existing Weld**

UT or RT acceptability is judged to code acceptance criteria; specifically ASME B31.8 or B31.4, and CSA Z662 codes were mentioned. In one case it was noted that all welds below 40% SMYS are repaired with a reinforcement sleeve/canopy or removed from the system. In another, it was stated that inspection must comply with Part 192 NDE requirements.

**What NDE would your utility require for a welded repair to base metal (e.g. corrosion pitting)?**

Figure 89 summarizes the NDE requirements for weld repair to base metal: seven responses include or only use/allow RT, three responses include UT as an acceptable alternative to RT, and three responses include MPI. UT or RT acceptability to code acceptance criteria ASME B31.8 or ASME B31.4 were also mentioned. In one case, it was noted that, at a minimum, all weld repairs are visually inspected and soap tested. Another response indicated that all welds must meet the acceptability standards of the currently referenced edition of the API 1104.

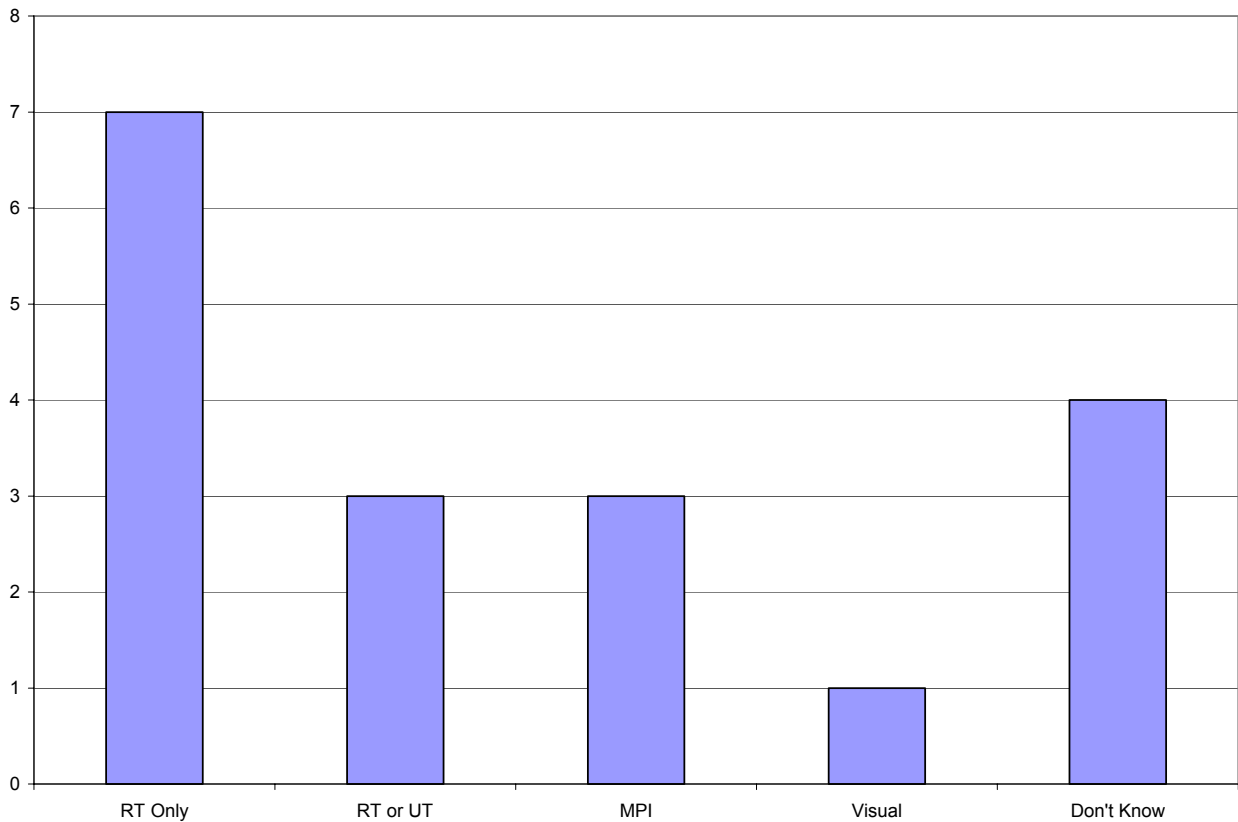


**Figure 89 - NDE Required for Base Metal Repair**

**Could a visual or magnetic particle examination be substituted for radiography in these special circumstances?**

The answers to the question were evenly distributed. There were three "yes" only responses, three qualified "yes" answers, three "MPI not visual," three "maybe," three "no," and three "don't know."

Specific comments:

- On fillet welds to the base metal, yes. For the long seam repair, probably not.
- Below 40% SMYS repairs utilizing pre-qualified components with a manufacturer established MAOP require both a visual and a soap test.
- I am not sure how the MPI would be done remotely, but it would have value.

**3. Would the use of internal repair be attractive even if it were considered a temporary repair?**

The answers to this question were mixed, as summarized in Figure 90: eight were "no" responses, three were "yes" only, and eight were qualified "yes" responses.

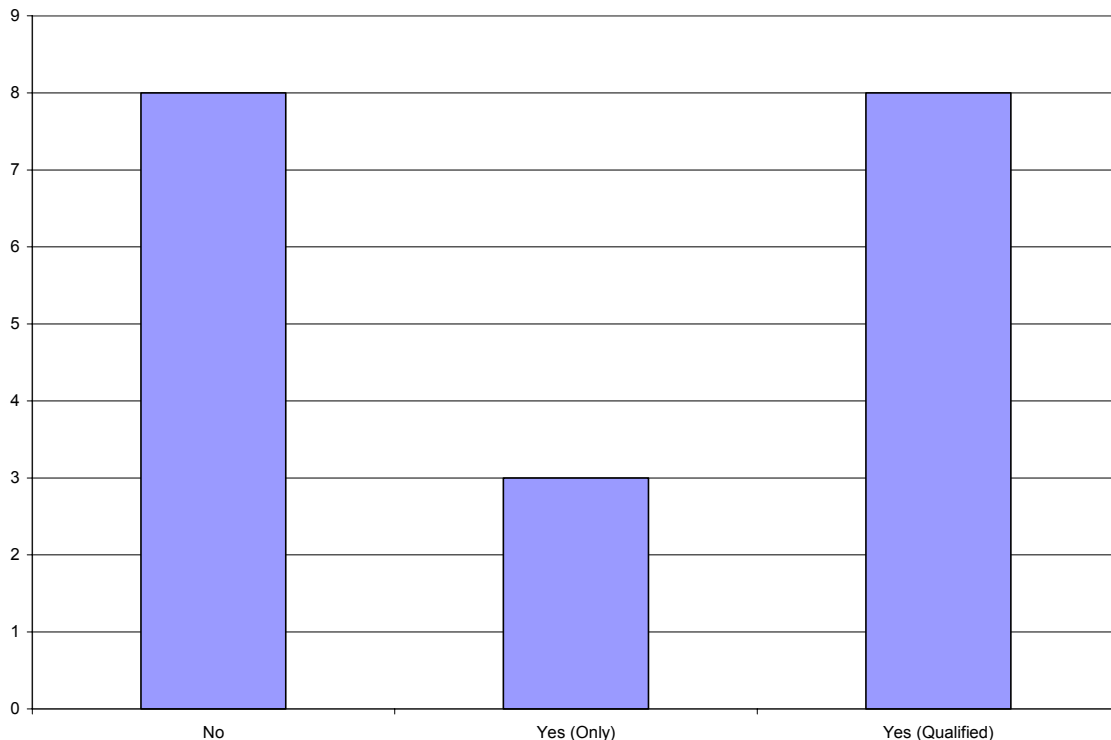


**Figure 90 - Would Internal Repair be Attractive Even as a Temporary Repair?**

Individual comments:

- In some circumstances, especially in seasonal climates (Canada, mountains, muskeg).
- Yes, if it could be done at relatively low cost (competing with an external sleeve, which is permanent) and with little to no interruption in service.
- Only if the cost was very low.
- If we were using this as a repair, we would rather have a permanent solution.
- Only in a very limited number of cases.
- It could be to allow for scheduling repairs and avoid a shut down during critical times.
- Yes – if it could be accomplished without purging the pipeline.
- Possibly, dependent upon the situation.

#### **4. Comments pertaining to operational and performance requirements for internal repairs.**

Specific responses:

- Repairs would need to be as good as the original pipe; one would not want to create local corrosion cells if the weld filler metal was more/less active than the base metal. This would only be attractive if shutdown is not required and no excavation is required to find the defect.
- The internal repair should provide for a smooth internal surface. The weld repair would not leave an area subject to long term cracking. CP would not be compromised. Repair will not interfere with future inspections.

#### **Part 6: General Comments**

**Please provide any general comments that you may have. For example, comments on an acceptable range of commercial pricing for such a system would be useful (as distinct from a repair cost in Question #6 of Part 2).**

Individual responses follow:

- This would not be a piece of equipment that our company would use often enough to justify us owning it. The most effective management of this system may be through a smart pigging company that could offer this as a follow-on service after inspection.



- The internal repair should return pipe to its original serviceability and safety factor. Pricing would determine selection if the repair was appropriate and proven for the type of defect. The costs are going to be weighed against the cost of excavation and the need to purge the line. Quite often, corrosion damage and even some dents can be repaired with steel sleeves using hot tap procedures so the pipeline does not have to be shut down. In swamp conditions, excavation is very expensive due to special equipment and the need to construct isolation dams to keep out the water and use pumps to dry the hole. Of course, offshore repairs require divers and habitats. The internal repair method would have the best economics for underwater repair locations. Some urban areas may have the same type of economics.
- Having an internal welding tool option would be very advantageous for a given situation. That situation is a totally inaccessible location such as a directional bore. For a busy intersection or street alignment where the pipeline can be accessed by conventional method at a high cost, accessing the pipeline externally would be preferred. The repair method would have to be approved by DOT prior to being used.
- The cost depends mainly on the requirements of the repair as in pipe size, length, customer outages, etc. I would say that it has to be considerably less than the standard repair methods to make the new repair method accepted by industry. Because it is internal and the integrity of the repair has to be assessed through some form of NDE, the actual repair strength will be hard to sell.

#### **4.2.3 - Identification of Potential Repair Methods**

To capture the results of the survey, a Matrix of Potential Repair Methods was created to compare and contrast the collective knowledge of, and interest in, specific repair methods that should be emphasized in the experimental portion of this project.

The five major feasibility categories defined for the Matrix:

- Technical Feasibility
- Inspectability
- Technical Feasibility of the Process while the Pipeline is In-Service
- Cost
- Industry Experience with the Repair Method

Each feasibility category was then subdivided into capabilities or characteristics to rank. Each capability/characteristic was assigned a unique weight factor to distinguish its importance in the overall repair process feasibility. Weight factors were based on the quantity of survey responses associated with the feasibility capability/characteristic, with the sum of all weight factors being 100%.

For each potential repair process, individual feasibility capabilities were rated on a scale from (-1) to (5) as defined in Table 7.

Rating	Definition of Rating
-1	Unacceptable
0	Unknown Potential - High Risk
1	Marginal Potential - High Risk
2	Development Required - High Risk
3	Development Required - Low Risk
4	Acceptable - No Risk
5	Ideal - No Risk

**Table 7 - Key to Ratings in Potential Repair Process Matrices (Table 8 - Table 10)**

Each rating was then multiplied by its unique weight factor to arrive at the weighted score for the individual feasibility capability. Five feasibility characteristics were determined to be "show stoppers," given the fact that an unacceptable rating for these capabilities would negate repair process feasibility.

The five show stoppers were identified as:

- Ability to Perform the Process Out-of-Position
- Technical Feasibility of the Process Itself
- Ability of the Process to Match the Strength of the Base Material
- Technical Feasibility of Performing the Process In-Service
- Material Cost

The rating of each show stopper was multiplied by 25 to produce the corresponding weighted score.

The Matrix of Potential Repair Methods is subdivided into three technology specific tables: Potential Welding Repair Methods (Table 8), Potential Liner Repair Methods (Table 9), and Potential Surfacing Repair Methods (Table 10).

Feasibility Category	Weight Factor	Capability or Characteristic to Rank	Welding Processes													
			GTAW		GMAW		FCAW		SAW		Laser		Explosive			
			Rating	Weighted Score	Rating	Weighted Score	Rating	Weighted Score	Rating	Weighted Score	Rating	Weighted Score	Rating	Weighted Score		
Technical		Out-of-Position Applicability	2	50	3	75	3	75	-1	-25	2	50	1	25		
		Process Technical Feasibility	2	50	3	75	-1	-25	-1	-25	0	0	-1	-25		
	5%	Process Robustness	2	10	3	15	2	10	0	0	2	10	1	5		
	10%	Repair Permanence	2	20	3	30	2	20	0	0	2	20	1	10		
	10%	Process Deployment Risk	2	20	5	50	-1	-10	0	0	1	10	-1	-10		
	5%	Remote Operation Feasibility	2	10	3	15	-1	-5	0	0	1	5	0	0		
		Ability to Match Strength of Pipe Material	3	75	4	100	4	100	0	0	3	75	3	75		
	1%	Ability to Match Pipe Corrosion Resistance	3	3	4	4	4	4	0	0	4	4	3	3		
	1%	Ability to Effect Patch Repair	2	2	3	3	-1	-1	0	0	2	2	-1	-1		
	5%	Ability to Effect Circumferential Repair	2	10	3	15	-1	-5	0	0	2	10	1	5		
	10%	Ability to Negotiate 3D Bends	3	30	3	30	3	30	3	30	0	0	0	0		
	5%	Metallurgical Bond	5	25	5	25	5	25	5	25	5	25	2	10		
	1%	Mechanical Bond	5	5	5	5	5	5	5	5	5	5	2	2		
Inspectability	5%	Ability to Inspect via Pigging	5	25	5	25	-1	-5	0	0	5	25	0	0		
	5%	Radiographic Flaw Detectability	5	25	5	25	5	25	5	25	5	25	-1	-5		
In-Service	7%	Low Power Required (Process Efficiency)	4	28	4	28	4	28	1	7	-1	-7	-1	-7		
	5%	Pipeline Depressurized, But Not Evacuated	2	10	2	10	2	10	0	0	0	0	0	0		
	5%	Pipeline Pressurized	0	0	0	0	0	0	0	0	0	0	-1	-5		
		Technical Feasibility	2	50	2	50	-1	-25	0	0	0	0	2	50		
Cost	5%	Process Development	1	5	3	15	0	0	0	0	1	5	0	0		
	10%	Process Application	1	10	4	40	0	0	0	0	0	0	0	0		
		Material	2	50	4	100	4	100	0	0	1	25	0	0		
History	5%	Industry Experience with Process	0	0	4	20	4	20	0	0	0	0	2	10		
				100%		513		755		376		42		289		142

Table 8 - Potential Welding Repair Methods

Feasibility Category	Weight Factor	Capability or Characteristic to Rank	Liner Processes											
			Fiber-Reinforced Composite		Steel Coil		Shape Memory Alloy		Reeled Composite		Solid Expandable Tubulars			
			Rating	Weighted Score	Rating	Weighted Score	Rating	Weighted Score	Rating	Weighted Score	Rating	Weighted Score		
Technical		Out-of-Position Applicability	2	50	3	75	3	75	2	50	3	75		
		Process Technical Feasibility	2	50	3	75	3	75	2	50	2	50		
	5%	Process Robustness	1	5	2	10	2	10	1	5	2	10		
	10%	Repair Permanence	2	20	3	30	3	30	1	10	2	20		
	10%	Process Deployment Risk	2	20	0	0	0	0	1	10	2	20		
	5%	Remote Operation Feasibility	2	10	1	5	0	0	1	5	2	10		
		Ability to Match Strength of Pipe Material	2	50	1	25	1	25	-1	-25	2	50		
	1%	Ability to Match Pipe Corrosion Resistance	3	3	2	2	2	2	2	2	2	2		
	1%	Ability to Effect Patch Repair	-1	-1	-1	-1	-1	-1	-1	-1	-1	-1		
	5%	Ability to Effect Circumferential Repair	3	15	2	10	2	10	2	10	2	10		
	10%	Ability to Negotiate 3D Bends	3	30	0	0	0	0	1	10	-1	-10		
5%	Metallurgical Bond	0	0	-1	-5	-1	-5	-1	-5	-1	-5			
1%	Mechanical Bond	2	2	0	0	1	1	1	1	2	2			
Inspectability	5%	Ability to Inspect via Pigging	2	10	0	0	2	10	0	0	2	10		
	5%	Radiographic Flaw Detectability	-1	-5	0	0	0	0	-1	-5	0	0		
In-Service	7%	Low Power Required (Process Efficiency)	3	21	3	21	3	21	3	21	2	14		
	5%	Pipeline Depressurized, But Not Evacuated	3	15	2	10	2	10	3	15	2	10		
	5%	Pipeline Pressurized	3	15	2	10	2	10	3	15	1	5		
		Technical Feasibility	3	75	2	50	2	50	3	75	2	50		
Cost	5%	Process Development	3	15	2	10	1	5	3	15	2	10		
	10%	Process Application	3	30	3	30	2	20	3	30	1	10		
		Material	2	50	3	75	-1	-25	3	75	-1	-25		
History	5%	Industry Experience with Process	3	15	3	15	-1	-5	3	15	0	0		
			100%		495		447		318		378		317	

**Table 9 - Potential Liner Repair Methods**

Feasibility Category	Weight Factor	Capability or Characteristic to Rank	Surfacing Processes							
			Electroless Nickel		Thermal Spray		Carburization		Explosive	
			Rating	Weighted Score	Rating	Weighted Score	Rating	Weighted Score	Rating	Weighted Score
Technical		Out-of-Position Applicability	1	25	0	0	0	0	1	25
		Process Technical Feasibility	1	25	1	25	-1	-25	0	0
	5%	Process Robustness	0	0	1	5	0	0	2	10
	10%	Repair Permanence	0	0	1	10	0	0	2	20
	10%	Process Deployment Risk	0	0	0	0	0	0	0	0
	5%	Remote Operation Feasibility	0	0	0	0	0	0	0	0
		Ability to Match Strength of Pipe Material	0	0	-1	-25	0	0	2	50
	1%	Ability to Match Pipe Corrosion Resistance	1	1	2	2	0	0	3	3
	1%	Ability to Effect Patch Repair	0	0	2	2	0	0	0	0
	5%	Ability to Effect Circumferential Repair	0	0	2	10	0	0	2	10
	10%	Ability to Negotiate 3D Bends	0	0	0	0	0	0	0	0
	5%	Metallurgical Bond	2	10	-1	-5	0	0	2	10
1%	Mechanical Bond	2	2	2	2	0	0	1	1	
Inspectability	5%	Ability to Inspect via Pigging	0	0	0	0	0	0	1	5
	5%	Radiographic Flaw Detectability	2	10	2	10	0	0	2	10
In-Service	7%	Low Power Required (Process Efficiency)	0	0	0	0	0	0	0	0
	5%	Pipeline Depressurized, But Not Evacuated	0	0	0	0	0	0	-1	-5
	5%	Pipeline Pressurized	0	0	0	0	0	0	-1	-5
		Technical Feasibility	3	75	1	25	0	0	-1	-25
Cost	5%	Process Development	0	0	0	0	0	0	0	0
	10%	Process Application	0	0	0	0	0	0	0	0
		Material	0	0	0	0	0	0	0	0
History	5%	Industry Experience with Process	-1	-5	1	5	0	0	0	0
		100%		143		66		-25		109

Table 10 - Potential Surfacing Repair Methods

Figure 91 is a bar chart that contains the total weighted scores for each potential repair technology. It is apparent that, of the three broad categories of repair (welding, liners, and surfacing), repair methods that involve welding are generally the most feasible. Of the various welding processes, GMAW is the preferred method. The primary factors that make GMAW the most feasible are process technical feasibility and robustness, and industry familiarity with the process. The second most feasible of the three broad categories is repair methods that involve internal liners. Of these, fiber-reinforced composite liners are the most promising. The primary factors that make fiber-reinforced composite liners the most feasible are the ability to match the strength of the pipe material and negotiate bends, and their corrosion resistance. The advantage of using a fiber-reinforced composite liner is somewhat offset by its material cost which is anticipated to be comparatively higher than that of a steel coil liner.

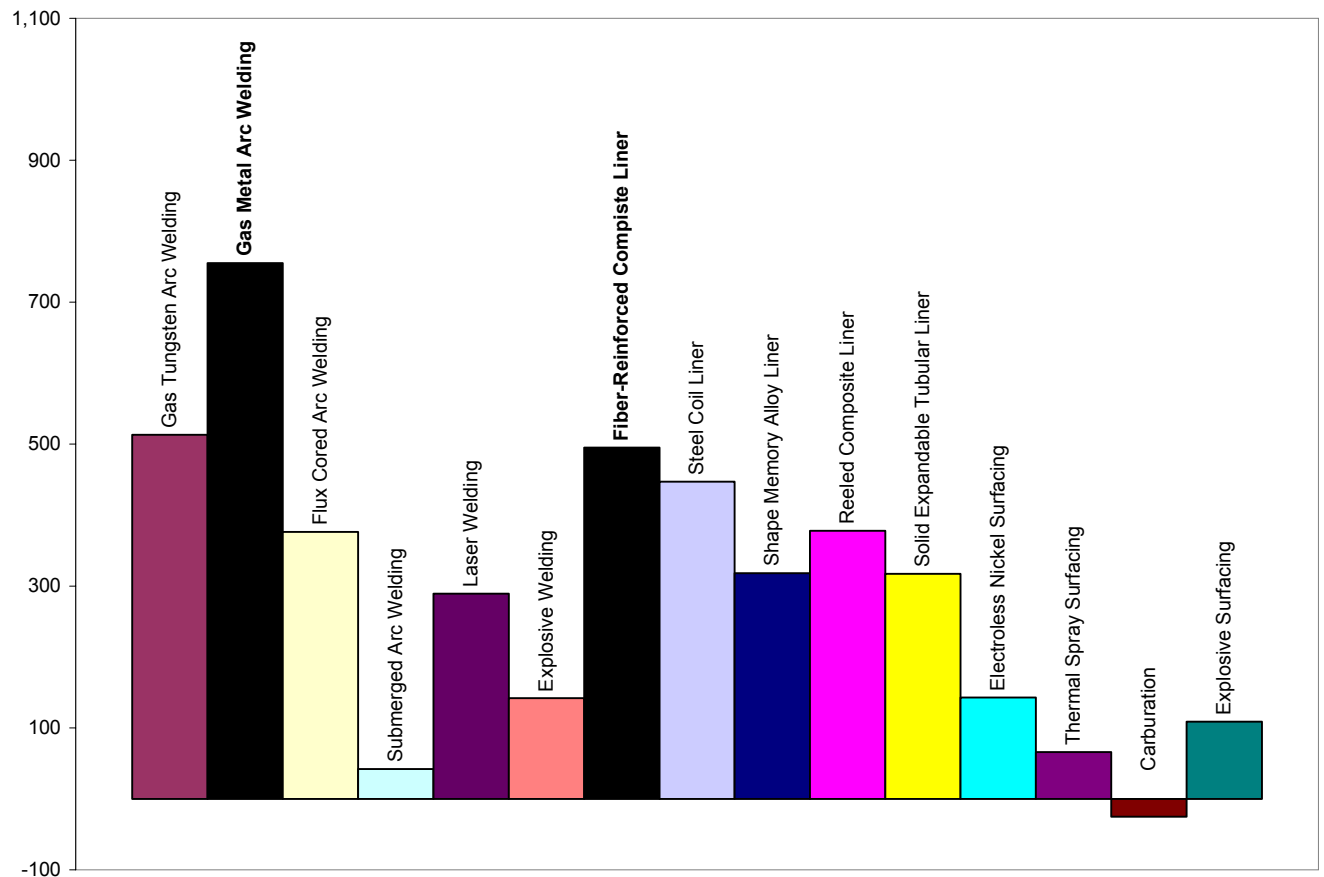


**Figure 91 - Weighted Scores of Potential Repair Methods**

### 4.3 - Detailed Test Program

A detailed test program was developed to evaluate the performance of candidate repair technologies.

Given the fact that corrosion was the most significant contributor to natural gas pipelines failures during 2002 and 2003, the two most common types of corrosion, general corrosion and a deep/isolated corrosion pit (with approximately 30% reduction in burst pressure), were selected initially for repair process evaluations. RSTRENG® was used to calculate the dimensions of simulated corrosion damage that represent the desired reduction in burst pressure.

RSTRENG® was also used to calculate the dimensions of the simulated corrosion damage for the remainder of the evaluations. The DOT/OPS has approved ASME B31G and RSTRENG® as approved technologies for use by pipeline owner/operators and the service companies that work for them. However, RSTRENG® is the preferred technology as it is less conservative than ASME B31G.

The appropriately sized simulated damage was introduced into pipe sections that were subsequently repaired with candidate repair technologies. Elliptical test heads with high-pressure fittings were then welded to the pipe sections and the resultant vessels were hydrostatically pressurized to failure.

To establish baseline material performance for each pipe diameter/material combination, Barlow's equation (Equation 1) was used to calculate the pressure that corresponds to 100% SMYS. To determine the predicted burst pressures for pipe sections in the virgin condition pipes, the measured ultimate tensile strength of each pipe material was used as  $S$  in Equation 1.

$$P = \frac{2St}{D}$$

#### Equation 2 - Barlow's Formula

Where  $P$  is pressure,  $S$  is strength,  $t$  is thickness and  $D$  is diameter.

Physical results, RSTRENG® predictions, and Barlow calculations were used to analyze the performance of each candidate repair technology with respect to pipe sections with simulated corrosion in the un-repaired condition and to pipe sections in the virgin condition.

This detailed test program is directly applicable to the range of pipe sizes, grades, and vintages covered by the program, as well as the range of damage types encountered in cross-country pipelines.

#### 4.4 - Baseline Material Performance

All materials used in this investigation were evaluated to establish physical properties:

- Pipeline Section Material
- Glass Fiber (GF) Reinforced Liner Material
- Carbon Fiber (CF) Reinforced Liner Material
- Steel Strip Material

#### Pipe Material Evaluations

Four different pipe materials, consisting of three different diameters were used in this investigation. In addition to standard tensile testing of the pipe material, hydrostatic pressure tests were conducted for sections of these materials to establish baseline performance data in both the virgin condition and after the introduction of mechanical damage.

The following eleven hydrostatic pressure tests were conducted to establish baseline performance data for the following pipe materials and conditions:

- 114.3 mm (4.5 in.) diameter by 4.78 mm (0.188 in.) wall API 5L Grade B pipe sections:
  - Virgin condition
  - Un-repaired long/shallow simulated corrosion damage
  - Un-repaired short/deep simulated corrosion damage
- 508.0 mm (20 in.) diameter by 6.35 mm (0.25 in.) wall API 5L X52 pipe sections (from material batch TE20L):
  - Virgin condition
  - Un-repaired with stylized, short/deep simulated corrosion damage
- 508.0 mm (20 in.) diameter by 6.35 mm (0.25 in.) wall API 5L X52 pipe sections (from material batch P96):
  - Virgin condition
  - Un-repaired with stylized, short/deep simulated corrosion damage
  - Un-repaired with extra long/shallow simulated corrosion damage
- 558.8 mm (22 in.) diameter by 7.92 mm (0.312 in.) wall API 5L Grade B pipe sections:
  - Virgin condition
  - Un-repaired with stylized, long/shallow simulated corrosion damage
- 609.6 mm (24 in.) diameter by 7.92 mm (0.312 in.) wall API 5L X65 pipe sections:
  - Virgin condition
  - Un-repaired with short, extra deep simulated corrosion damage
  - Un-repaired with extra long/shallow simulated corrosion damage



The results of standard tensile testing of a section taken from each of the pipe materials are shown in Table 11.

Pipe Diameter mm (in.)	Material Batch ID	Ultimate Strength		0.2% Yield Strength		Elongation %
		MPa	ksi	MPa	ksi	
114.3 (4.5)	n/a	461.4	66.9	335.9	48.7	41.5
508.0 (20)	TE20L	601.4	87.2	462.8	67.1	29.9
508.0 (20)	P96	553.1	80.2	413.8	60.0	34.0
558.8 (22)	n/a	384.8	55.8	238.6	34.6	40.3
609.6 (24)	n/a	586.9	85.1	466.9	67.7	33.3

**Table 11 - Tensile and Yield Strengths of the Pipe Materials**

Two different batches of 508 mm (20 in.) diameter API 5L X52 pipe sections were used: TE20L and P96. Test 04 used material from batch TE20L, which was taken from the EWI pipe material stock pile. Test 05 through Test 11 used material from batch P96 which was purchased through a broker.

Table 12 is a summary of pipe materials/sizes and the characteristics of the defect configurations used in this test program.

Test Series No.	02	03	07	04, 05, 06, 08	09, 10, 11	01	12, 13	14
Pipe Outside Diameter	114.3 mm (4.5 in.)	114.3 mm (4.5 in.)	508 mm (20 in.)	508 mm (20 in.)	508 mm (20 in.)	558.80 mm (22 in.)	609.6 mm (24 in.)	609.6 mm (24 in.)
Wall Thickness	4.78 mm (0.188 in.)	4.78 mm (0.188 in.)	6.35 mm (0.250 in.)	6.35 mm (0.250 in.)	6.35 mm (0.250 in.)	7.92 mm (0.312 in.)	7.92 mm (0.312 in.)	7.92 mm (0.312 in.)
API 5L Pipe Material	Grade B	Grade B	X52	X52	X52	Grade B	X65	X65
Type of Simulated Damage	Long/Shallow Slot	Short/Extra Deep	Extra Long/Shallow Slot	Short/Deep	Short/Extra Deep	Long/Shallow	Short/Extra Deep Slot	Long/Shallow Slot
Damage Length	127 mm (5 in.)	25.4 mm (1 in.)	381 mm (15 in.)	127 mm (5 in.)	127 mm (5 in.)	190.50 mm (7.5 in.)	228.6 mm (9 in.)	381 mm (15 in.)
Damage Depth	2.54 mm (0.100 in.)	4.01 mm (0.160 in.)	2.74 mm (0.108 in.)	3.45 mm (0.136 in.)	4.75 mm (0.187 in.)	3.96 mm (0.156 in.)	5.94 mm (0.234 in.)	5.66 mm (0.223 in.)
Pressure corresponding to 100% SMYS	20.16 MPa (2,924 psi)	20.16 MPa (2,924 psi)	8.96 MPa (1,300 psi)	8.96 MPa (1,300 psi)	8.96 MPa (1,300 psi)	6.84 MPa (992 psi)	11.65 MPa (1,690 psi)	11.65 MPa (1,690 psi)
Damage as % of wall thickness	53%	85%	43%	54%	75%	50%	75%	71%
RSTRENG® predicted burst pressure compared to pressure at 100% SMYS	70%	69%	75%	75%	48%	75%	40%	40%

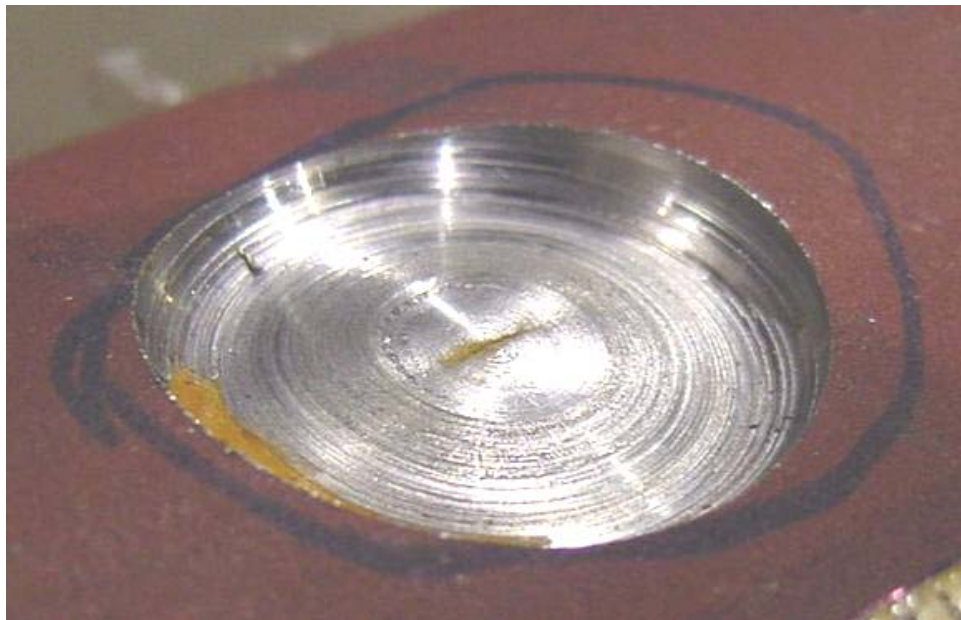
Table 12 - Pipe Materials/Sizes and Defect Characteristics for Baseline Pipe Sections

Figure 92 through Figure 97 show the results of the baseline burst tests for the majority of the pipe materials used in the investigation. Figure 92 shows the 114.3 mm (4.5 in.) diameter specimen with un-repaired long/shallow simulated corrosion damage after burst testing. Calculated with RSTRENG® to represent a 30% reduction in burst strength, defect dimensions were 127 mm (5 in.) long by 2.54 mm (0.100 in.) deep.



**Figure 92 - 114.3 mm (4.5 in.) Pipe with Un-Repaired Long/Shallow Damage after Burst Test**

Figure 93 is the 114.3 mm (4.5 in.) diameter specimen with un-repaired short/deep simulated corrosion damage after burst testing. Calculated with RSTRENG® to represent a 30% reduction in burst pressure, defect dimensions were 25.4 mm (1 in.) long by 4.01 mm (0.160 in.) deep.



**Figure 93 - 114.3 mm (4.5 in.) Pipe with Un-Repaired Short/Deep Damage after Burst Test**

Figure 94 is the 508.0 mm (20 in.) diameter specimen in the virgin condition after burst testing.



**Figure 94 - 508.0 mm (20 in.) Virgin Pipe After Burst Testing**

Figure 95 is the 508.0 mm (20 in.) diameter specimen with a long/shallow, stylized corrosion defect after burst testing. Calculated with RSTRENG® to represent a 25% reduction in burst strength, defect dimensions were 381 mm (15 in.) long by 2.74 mm (0.108 in.) deep.



**Figure 95 - 508.0 mm (20 in.) Pipe with Un-Repaired Damage After Burst Testing**

Figure 96 is the 558.8 mm (22 in.) diameter specimen in the virgin condition after burst testing.



**Figure 96 - 558.8 mm (22 in.) Virgin Pipe After Burst Testing**

Figure 97 is the 558.8 mm (22 in.) diameter specimen with stylized, short/deep corrosion defect. Calculated with RSTRENG® to represent a 25% reduction in burst strength, defect dimensions were 190.5 mm (7.5 in.) long by 3.96 mm (0.156 in.) deep.



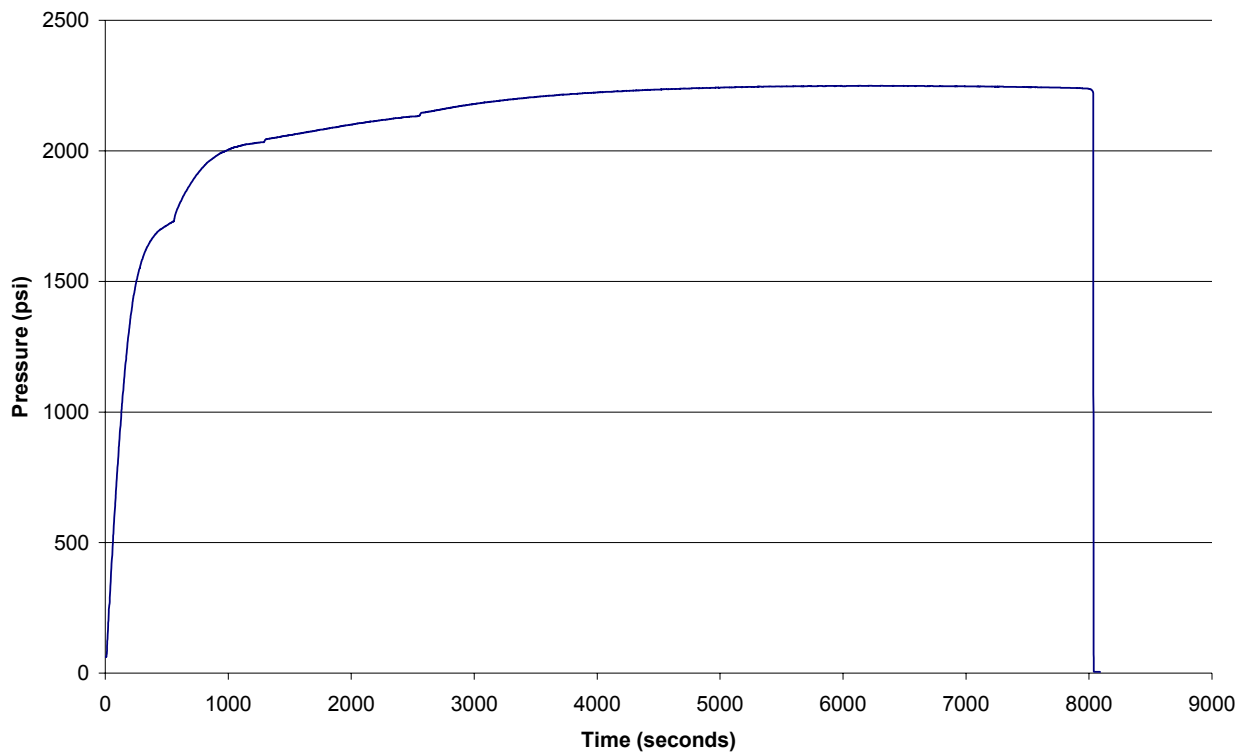
**Figure 97 - 558.8 mm (22 in.) Pipe with Un-Repaired Damage After Burst Testing**

Figure 98 is the 609.6 mm (24 in.) diameter specimen with an extra long/shallow corrosion defect. Calculated with RSTRENG® to represent a 60% reduction in burst strength, defect dimensions were 381 mm (15 in.) long by 5.66 mm (0.223 in.) deep.



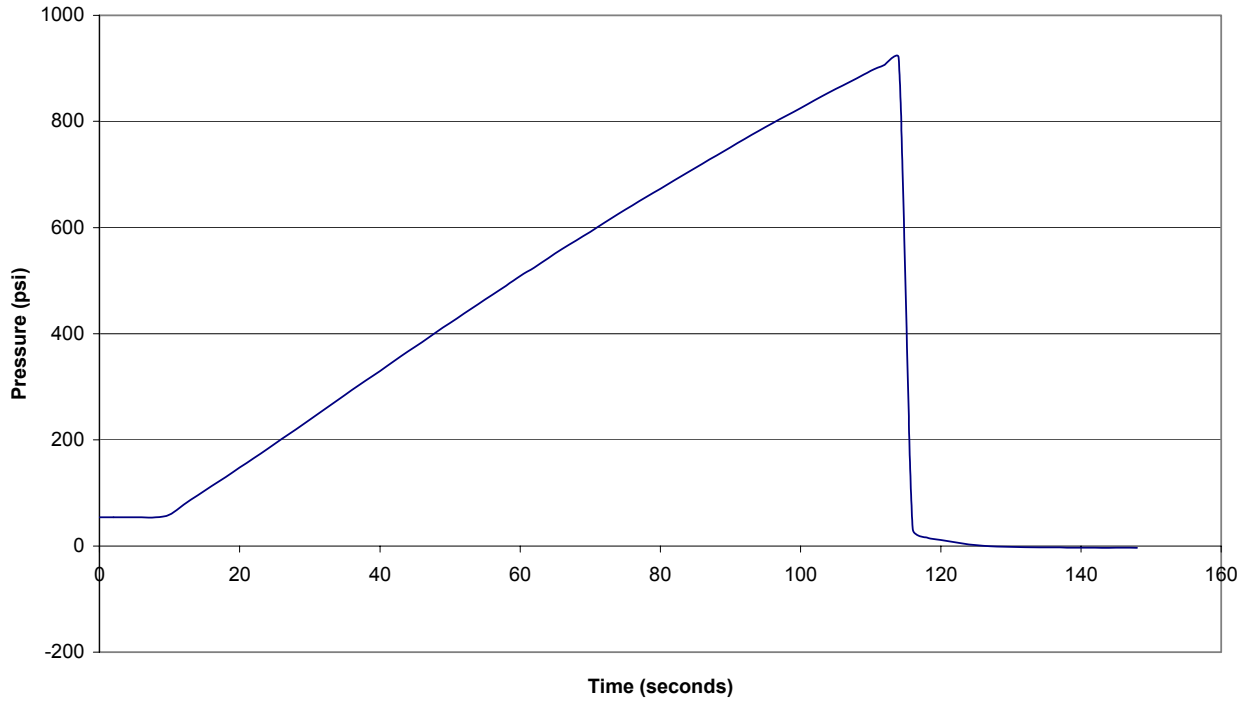
**Figure 98 - 609.6 mm (24 in.) Pipe with Un-Repaired Extra Long/Shallow Damage After Burst Testing**

Figure 99 contains the pressure vs. time plot of the burst test for the 609.6 mm (24 in.) virgin pipe and is representative of the plots obtained for all virgin pipe sections.



**Figure 99 - Pressure vs. Time Plot of 609.6 mm (24 in.) Virgin Pipe Section**

Figure 100 contains the pressure vs. time plot of the burst test for the 609.6 mm (24 in.) pipe with a 228.6 mm (9 in.) long by 5.9 mm (0.234 in.) deep defect and is representative of the plots obtained for all damaged/un-repaired pipe sections.



**Figure 100 - Pressure vs. Time Plot of 609.6 mm (24 in.) Pipe with Defect**

Table 13 contains the predicted and actual burst pressures for all hydrostatic tests conducted to benchmark baseline pipe material performance.

Pipe Diameter	Pipe Condition	Predicted Burst Pressure		Actual Burst Pressure	
		(MPa)	(psi)	(MPa)	(psi)
114.3 mm (4.5 in.)	Virgin	38.66	5,607	-	-
	Simulated Damage Long/Shallow	14.13	2,049	23.66	3,431
	Simulated Damage Short/Deep	13.97	2,026	25.86	3,750
508 mm (20 in.) (TE20L)	Virgin	15.03	2,180	16.03	2,325
	Simulated Damage Short/Deep	6.72	974	14.56	2,112
508 mm (20 in.) (P96)	Virgin	13.82	2,005	14.63	2,122
	Simulated Damage Short/Deep	6.72	974	12.04	1,746
	Simulated Damage Extra Long/Shallow Slot	6.69	970	10.16	1,473
	Simulated Damage Short/Extra Deep	4.31	627	8.95	1,298
558.8 mm (22 in.)	Virgin	10.91	1,583	12.69	1,841
	Simulated Damage Short/Deep	5.15	747	10.78	1,563
609.6 mm (24 in.)	Virgin	15.25	2,212	15.51	2,249
	Simulated Damage Short/Extra Deep	4.65	675	6.34	920
	Simulated Damage Extra Long/Shallow Slot	4.65	674	5.20	754

**Table 13 - Predicted vs. Actual Hydrostatic Burst Pressure Values for Baselines**

As expected, the pipe sections in virgin condition had the highest hydrostatic burst pressures. The most surprising aspect of the baseline hydrostatic burst test results is that fact that the failure pressures for many of the pipe sections with un-repaired damage are significantly greater than the RSTRENG® predicted burst pressures. For example, the RSTRENG® predicted burst pressure for the un-repaired 508 mm (20 in.) X52 pipe (from batch TE20L) with short/deep damage is 6.72 MPa (974 psi), whereas the actual measured burst pressure is 14.56 MPa (2,112 psi). In this case, the actual burst pressure is 117% higher than the RSTRENG® predicted burst pressure.



The results of these experiments illustrate that RSTRENG® predictions tend to be conservative.<sup>(9)</sup> The extent of this conservatism was not understood until after Test 08. Tests 09 through 12 had areas of damage with significantly larger predicted reductions in burst pressure (e.g., 50 to 60% reductions as opposed to 25 to 30% from the initial tests), thus enabling the repairs to better demonstrate their actual ability to restore pressure containing capability of the pipe sections.

### Glass Fiber Liner Material Evaluations

Tensile testing was carried out to determine the modulus of elasticity for the glass/polypropylene liner material that was used for Tests 1 and 2 (Table 14 and Figure 101). The mean value for the modulus of elasticity for the liner material was measured to be approximately 15.2 GPa (2.2 x 10<sup>6</sup> psi).

	<b>Stress at Break MPa (ksi)</b>	<b>Strain at Break (%)</b>	<b>1% Secant Modulus MPa (ksi)</b>
Trial 1	486.6 (70.58)	4.34	15,123.4 (2,193.394)
Trial 2	557.6 (80.88)	4.21	17,166.7 (2,489.741)
Trial 3	492.0 (71.36)	5.21	17,316.5 (2,511.472)
Trial 4	371.5 (53.89)	5.02	14,103.5 (2,045.482)
Trial 5	460.9 (66.85)	4.56	14,347.9 (2,080.924)
Trial 6	154.7 (22.45)	4.51	15,191.0 (2,203.205)
Mean	420.6 (61.00)	4.64	15,541.5 (2,254.036)
S. D.	143.4 (20.81)	0.39	1,384.3 (200.776)
C. V.	235.1 (34.11)	8.45	61.4 (8.907)
Minimum	154.7 (22.45)	4.21	14,103.5 (2,045.482)
Maximum	557.6 (80.88)	5.21	17,316.5 (2,511.472)
Range	402.8 (58.43)	1.00	3,213.0 (465.990)

**Table 14 - Tensile Testing Results for Glass Polypropylene Liner Material**

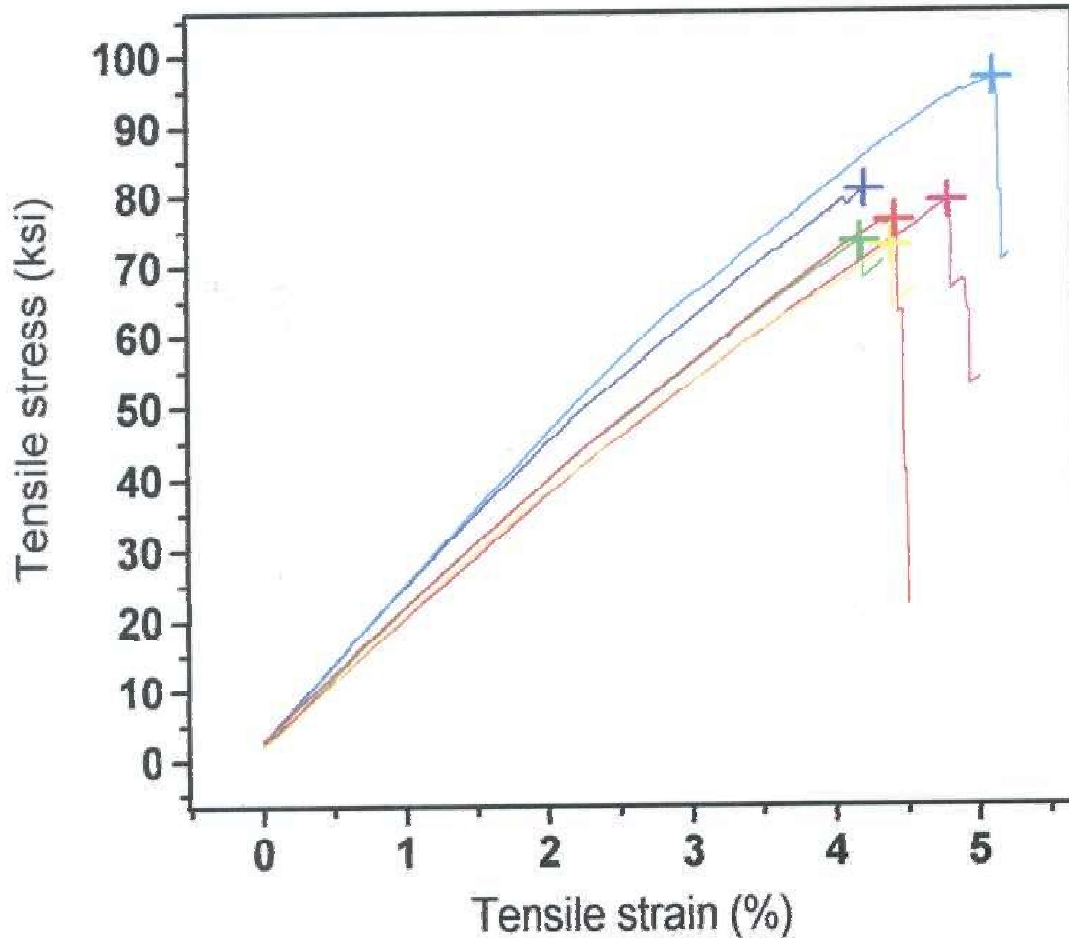


**Figure 101 - Tensile Test Results for GF Polypropylene Liner Material**

### **Carbon Fiber Liner Material Evaluations**

For carbon fiber (CF) patch material testing, three types of composite structures were produced for this program. All were made with carbon fiber cloth and vinylester (VE) resin. The cloth had no special treatment to compatibilize it with the VE resin. The carbon fiber fabric had a nominal weight of 10 oz/yd<sup>2</sup> with 6K tows.

Three composite lay-up structures were designed to evaluate the mechanical properties of the material:

- Quasi-isotropic lay-up (with alternating layers of 0, 90 and  $\pm 45$  with extra 0, 90 near the thickness-center)
- 0, 90 only lay-up
- Uniaxial 0 only lay-up

The thicknesses of the quasi-isotropic and the 0, 90 panels were 11.43 mm (0.45 in.). The thickness of the uniaxial panel was 8.89 mm (0.35 in.). For the first two, fiberglass close-out layers were included on the “steel side” as a proposed corrosion barrier at the steel/carbon fiber interface and as the top layer (bag side). The uniaxial panel had no fiberglass. The carbon-glass constructions produce ~40% w/w carbon fiber, with a density of 1.47-1.51 g/cc. The uniaxial panel contains >70% carbon fiber w/w, so a higher tensile modulus is anticipated (its density was measured at 1.44 g/cc (0.05 lbs./in.<sup>3</sup>), reflecting mostly the absence of fiberglass). The panels were produced using a combined hand lay-up vacuum bagging technique.

The results for the tested systems are shown in Table 15 for both normal and post cured samples (the averages are shown graphically in Figure 102). Post curing produced no significant mechanical advantage over the ambient cure. The most striking differences were the significant increases in tensile strength and modulus for the 0, 90 construction in comparison with the quasi-isotropic construction. The replacement of every other layer with a 0, 90 resulted in a 50% improvement in tensile strength from 367.5 MPa (53.3 ksi) to 581.2 MPa (84.3 ksi) and a 70% improvement in modulus from 36,376 MPa (5,276 ksi) to 64,052 MPa (9,290 ksi). The uniaxial tape sample was subsequently built to see if the trend in tensile and modulus performance would continue upward once *all* the fibers were operating in a tensile mode.

ILS was not affected by panel lay-up architecture. Based on the dimensions and the flexural failure load, the ILS value appears to be about 10.3 MPa (1,500 psi). This is lower than desired, but not unexpected given the lack of fiber treatment for resin compatibility and the notoriously low toughness for VE resins. Notice also the *flexural* modulus ranges from 586,578 MPa (85,076 ksi) to 636,241 MPa (92,279 ksi), meaning the panels are somewhat forgiving in flex.

Mechanical Properties for Carbon-Vinylester Composite							
Sample			Tensile			Flexural (Three Point)	
			Ultimate (ksi)	0.2% Yield (ksi)	Modulus (ksi)	Failure Load (lb)	Modulus (psi)
Not Postcured	Quasi - Iso	T1	56.7	44.5	6036		
		T2	54.1	41.1	5841		
		T3	55.2	42.5	5278		
		T4	47.0	46.4	3948		
		<b>Average</b>	<b>53.3</b>	<b>43.6</b>	<b>5276</b>		
	0, 90	T11	85.6	68.1	9673		
		T12	83.6	65.3	9620		
		T13	84.2	68.4	8748		
		T14	83.8	60.1	9118		
		<b>Average</b>	<b>84.3</b>	<b>65.5</b>	<b>9290</b>		
	0, 90	ILS1				410	91377
		ILS2				400	93688
		ILS3				385	92463
		ILS4				404	91586
		<b>Average</b>				<b>400</b>	<b>92279</b>
Postcured	Quasi - Iso	T5	58.6	50.0	6099		
		T6	54.6	46.0	5683		
		T7	61.2	46.4	7292		
		T8	50.6	44.5	4628		
		<b>Average</b>	<b>56.3</b>	<b>46.7</b>	<b>5926</b>		
	0, 90	T15	81.7	63.9	8803		
		T16	86.9	73.3	8473		
		T18	90.5	74.0	9567		
		T17	87.8		9724		
		<b>Average</b>	<b>86.7</b>	<b>70.4</b>	<b>9142</b>		
	0, 90	ILS5				382	75906
		ILS6				442	91990
		ILS7				411	85773
ILS8		446				86635	
<b>Average</b>		<b>420</b>				<b>85076</b>	

Table 15 - Tensile and Interlaminar Shear Properties for CF Composite Panels

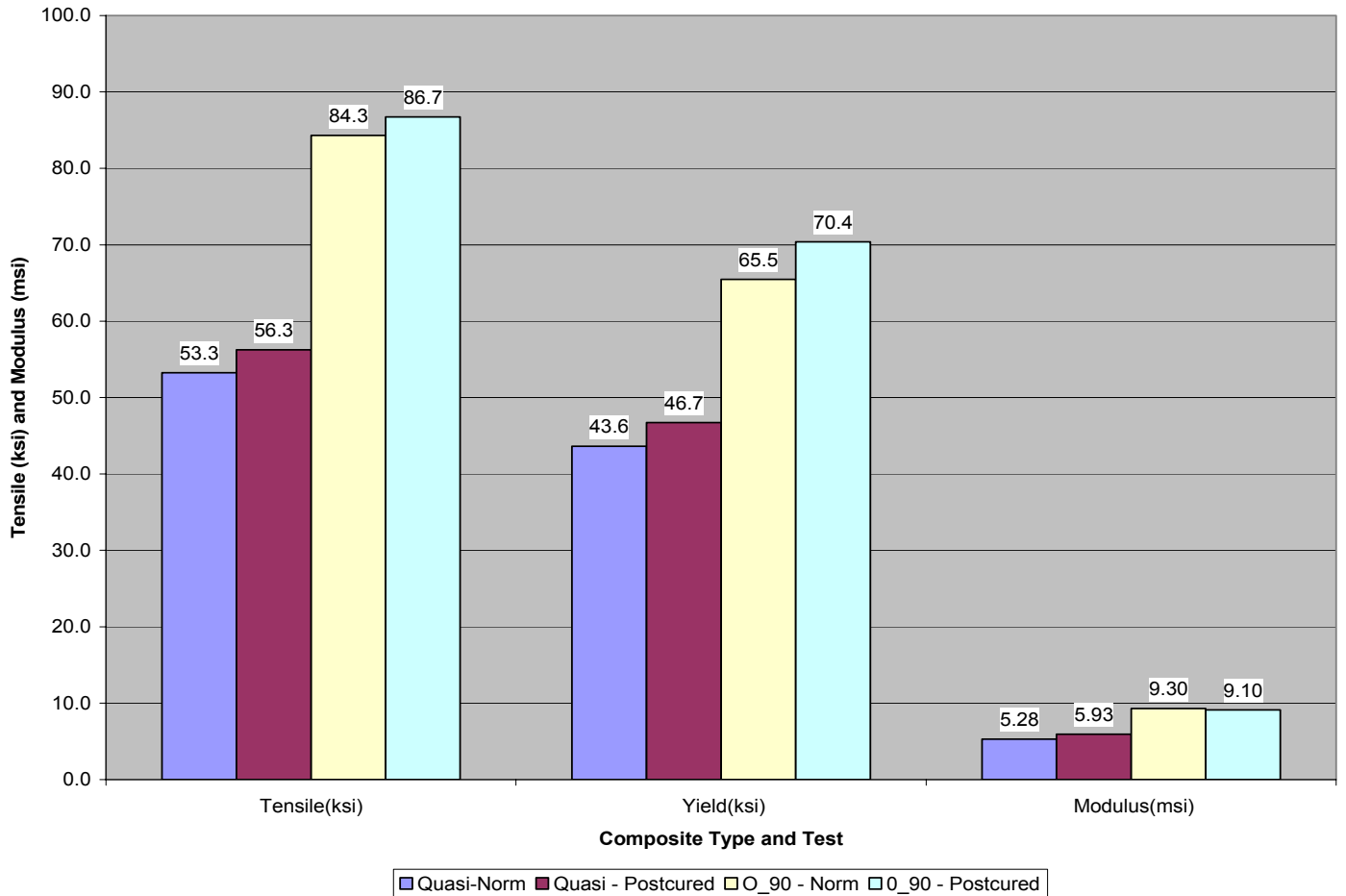


**Figure 102 - Average Tensile and Modulus Properties for CF Composite Panels**

### Steel Strip Material Evaluations

Adhesively bonded/helically wound steel strip repairs (Tests 09 through 12) were conducted with two different steel strip materials: one was high strength and one was low strength. The high strength steel strip was 50.8 mm (2 in.) wide by 1.12 mm (0.044 in.) thick. It was purchased from Allstrap Steel & Poly Strapping Systems. The low strength steel strip was AISI C1010 cold rolled steel strip purchased from Lapham-Hickey Steel. It was 50.8 mm (2 in.) wide by 1.27 mm (0.050 in.) thick and was supplied in the “Half-Hard” condition. Tensile testing results for both steel strip materials are summarized in Table 16.

Strip Specimen ID	Test Temperature		Ultimate Tensile Strength		0.2% Yield Strength		Elongation	Reduction of Area
	°C	°F	MPa	ksi	MPa	ksi		
High Strength	23	73	987.95	143.25	700	101.5	14.6%	77.1%
Low Strength	23	73	413.1	59.9	387.6	56.2	22.9%	74.3%

**Table 16 - Measured Strength of Steel Strip Materials**

Figure 103 is a photomicrograph of the high strength steel strip magnified at 100X. Figure 104 is a photomicrograph of the high strength steel strip magnified at 1000X.

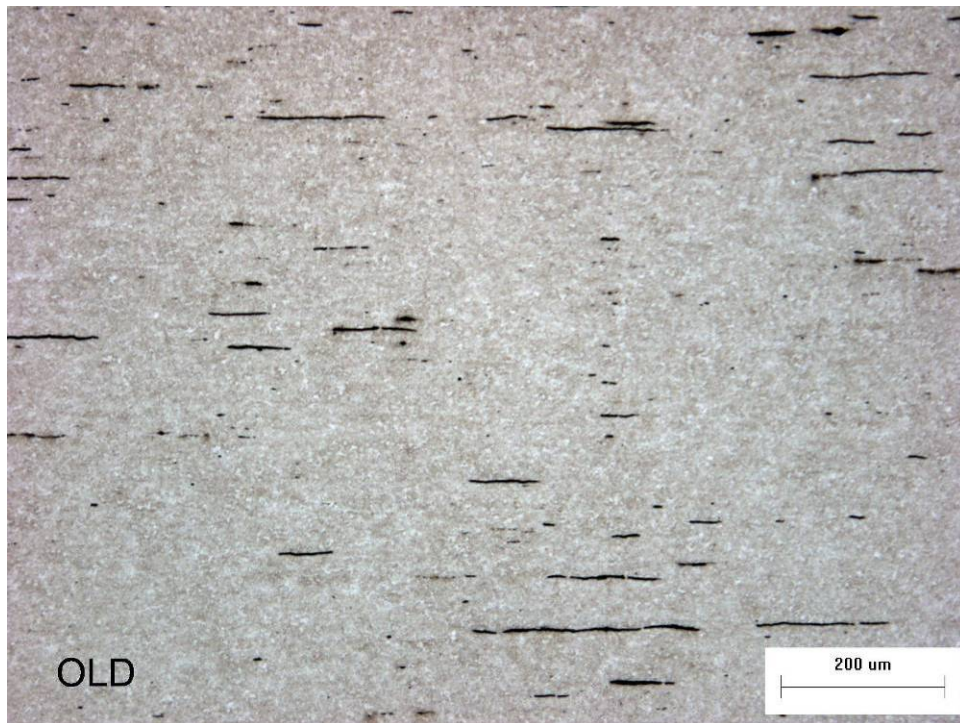


**Figure 103 - Photomicrograph of High Strength Steel Strip at 100X Magnification**

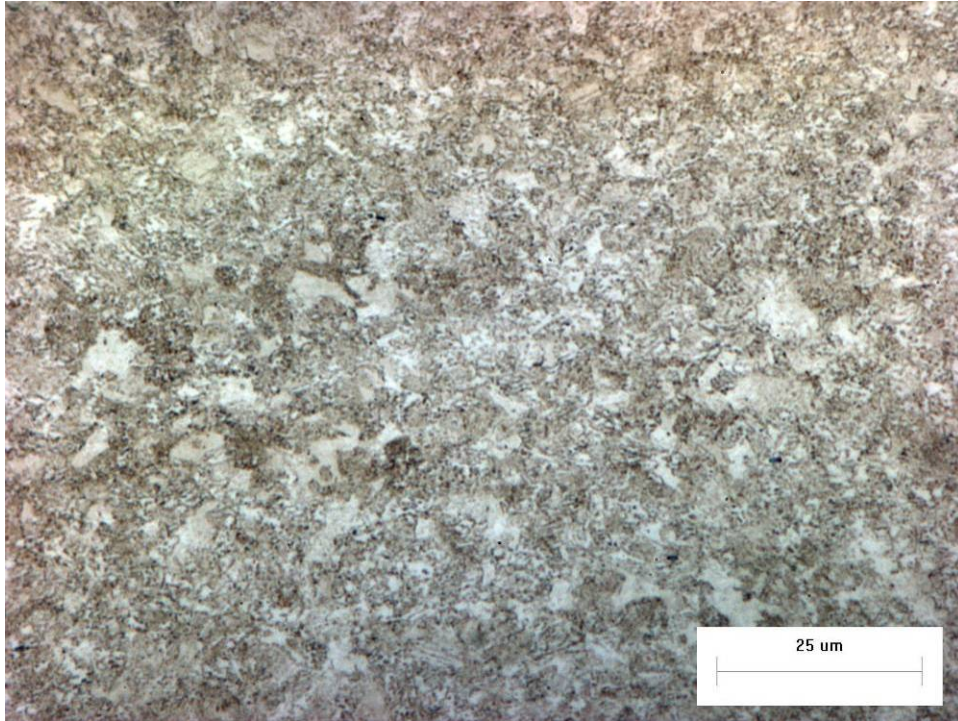


**Figure 104 - Photomicrograph of High Strength Steel Strip at 1000X Magnification**

Figure 105 is a photomicrograph of the low strength steel strip magnified at 100X. Figure 106 is a photomicrograph of the low strength steel strip magnified at 1000X.

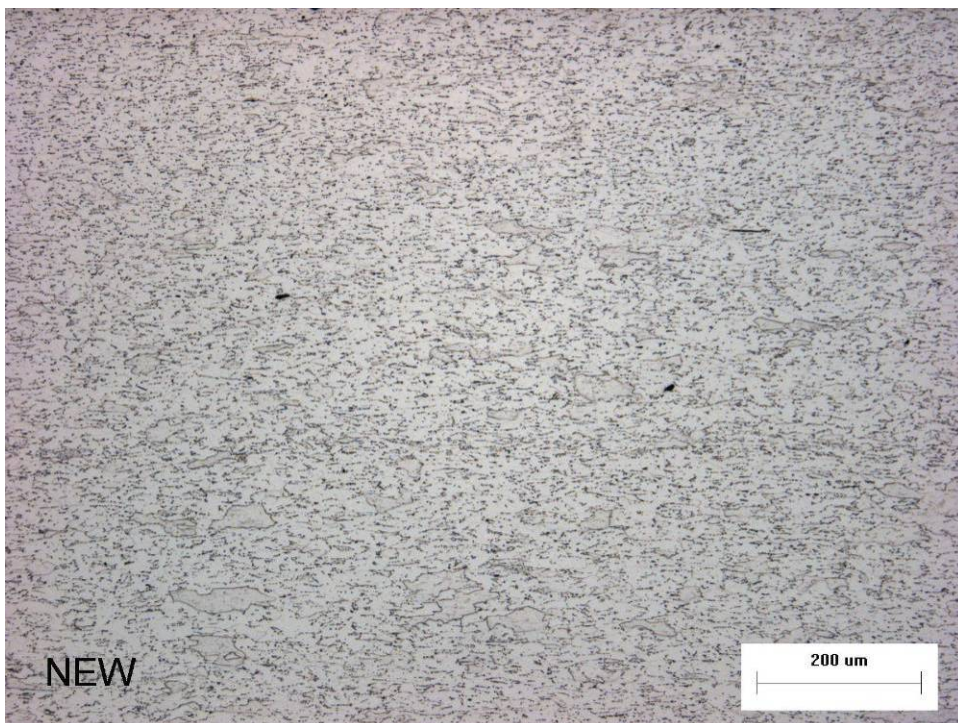


**Figure 105 - Photomicrograph of Low Strength Steel Strip at 100X Magnification**

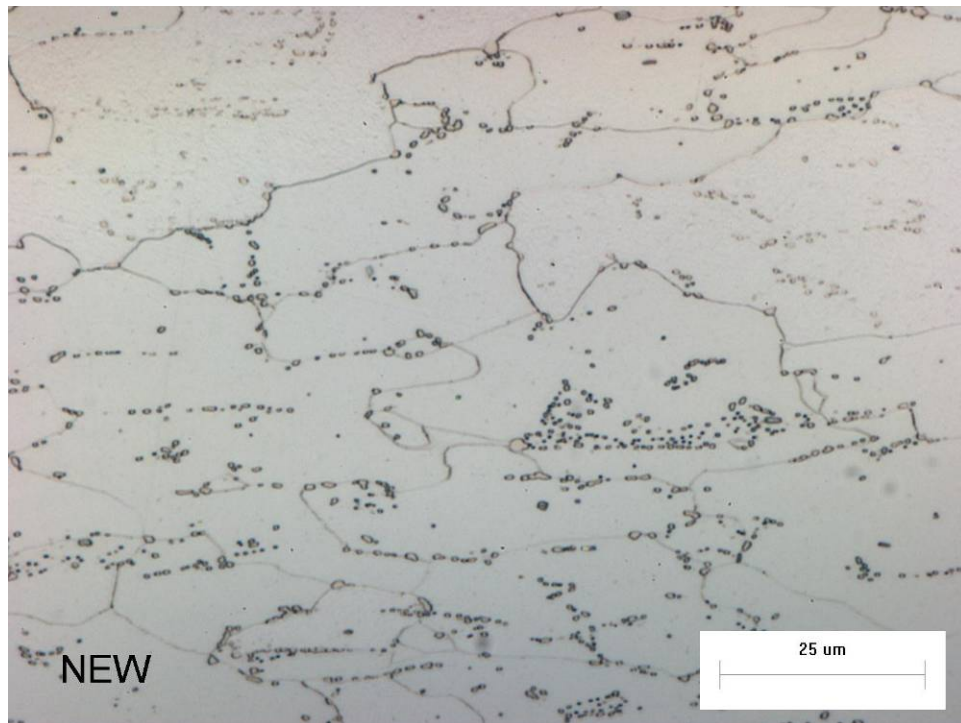


**Figure 106 - Photomicrograph of Low Strength Steel Strip at 1000X Magnification**

#### **4.5 - Weld Deposition Repair**

Arc welding processes offer what appears to be a viable repair method that can be applied from the inside of a gas transmission pipeline. There are several arc welding processes that can be operated remotely. Based on the survey and assessment conducted of candidate arc welding processes, the GMAW process was the most likely choice for this application (Figure 91). GMAW offers a good combination of simplicity, high productivity, robustness, and quality that are required for this welding repair application. Arc welding processes are routinely used to externally repair pipelines.

However, repair from the inside offers new challenges for process control since welding will need to be performed remotely. In addition, since the intent is to leave an unexcavated pipeline in the ground, there are several variables that will affect the welding process and resultant weld quality. Soil conditions have the potential to influence heat removal during welding thereby altering the fusion characteristics, welding cooling rate, and mechanical properties. The effects of welding on the external coating used to protect against corrosion will also affect future pipeline integrity.

If internal welding is performed in-service, the pressure and flow rate of the gas will have a strong effect on the equipment design for the welding process. New process equipment technology will



be required to shield the welding process from methane contamination and to cope with higher gas pressures.

Weld deposition repair evaluations were therefore designed to investigate all of the challenges listed above.

### **Welding Systems Evaluated**

During the development of baseline welding procedures, several welding systems were evaluated for internal weld deposition using GMAW. These evaluations focused on determining whether the systems could make a good internal weld deposit. The pipe axis was fixed in the 5G horizontal position (Figure 22). As welding progressed around the inside diameter, welding position transitioned between flat, vertical, and overhead. The types of envisioned repairs were ring deposits to perhaps reinforce a defective weld, spiral deposits to repair an entire pipeline section, and patches to repair local corrosion damage. Weld deposit motion for the first two types would best be achieved using orbital type welding procedures where welding clocks around the circumference. The patch repair could be accomplished using deposit motion that was either orbital or axial. Motion also required the use of torch weaving, a technique that improves out-of-position (i.e., vertical and overhead) weld pool shape. This is common in vertical-up welding to provide an intermediate shelf on which to progressively build the weld pool deposit. The effects of deposit motion on productivity and quality also required evaluation for this application. With the different welding systems, the preferred metal transfer mode for GMAW was short-circuit transfer. This mode assures drop transfer in all welding positions. Open arc droplet transfer that is provided by spray, pulse spray, and globular transfer are not suitable for spiral overhead welding where gravity promotes spatter instead of metal transfer.

The following welding systems were evaluated for internal repair of pipelines:

- Internal bore cladding system (Bortech)
- 6-axis robot capable of complex motion control (OTC Daihen)
- Orbital welding tractor configured for inside welding (Magnatech Pipeliner II)

Each system had motion control limitations and individually would not be appropriate candidates for an internal repair welding system. The internal bore cladding system manufactured by Bortech (Figure 23 and Figure 86) was designed for spiral cladding the inside of a pipe that is preferably in the vertical position.

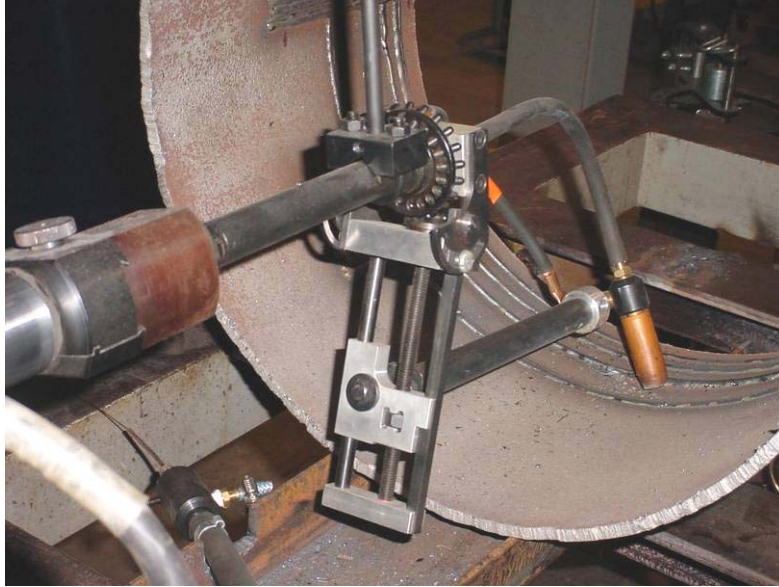


**Figure 107 - Bortech Torch and Torch Height Control**

The Bortech system has simple controls for operating constant voltage (CV) power supplies (Figure 24). This includes the ability to set wire feed speed, voltage, step size (for the spiral motion), and rotation speed (i.e., travel speed). The system is very affordable as it uses simple motors for motion. When positioned inside a horizontal pipe, the rotation drive suffered from significant backlash. Conversations with the supplier led to the purchase and installation of a counterbalance weight that was used to balance the weight of the opposing torch.

Preliminary weld trials with the Bortech system had marginal results. Only stringer beads were successfully deposited using short-circuit transfer in the spiral clad mode. Travel speeds of 3.81 mpm (150 ipm) to 4.45 mpm (175 ipm) were used with a 0.89 mm (0.035 in.) diameter ER70S-6 filler metal (i.e., electrode). With stringer beads, the deposition rate was low since only narrow beads could be deposited. The bead shape suffered the most in the overhead position when starting downhill. Weaving was required to improve weld bead profile thus allowing higher deposition rates and improved fusion. The off-the-shelf system did not permit oscillation, but could if adapted with modern controls. In principle this type of mechanism would be suitable for an internal repair system. Here, anti-backlash servo-motors and gears, and programmable controls would be required to improve the system. Similarly, an additional motor drive that permits control of torch and work angle would also be required to cope with all the possible repair scenarios to optimize bead shape.

Based on the results experienced with the Bortech system, the team decided to develop preliminary welding procedures using a robotic GMAW system. A 6-axis coordinated motion robot (Figure 25) permitted the application of weave beads for spiral cladding or stringer beads in either

direction. An observed limitation was the fact that the system did not have a welding torch current commutator to permit continuous spiral welding.

The standard robot welding torch (Figure 108) could only be used for half a revolution, then it had to be unwound to complete the remainder of each deposit ring. This limitation was acceptable for parameter development since the focus was the welding parameters not high duty cycle welding. The robot was interfaced to an advanced short-circuit power supply, the Kobelco PC-350.



**Figure 108 - OTC Robot Arm and Torch**

The Kobelco PC-350 power supply (Figure 26) uses fuzzy logic pulse waveforms to minimize spatter during metal transfer and permits the application of variable polarity waveforms. Variable polarity combines the rapid, low heat input, melting of negatively charged electrode with the metal transfer stability of electrode positive. Until 1988, all commercial GMAW systems used positively charged electrodes for constant voltage and pulse power supplies. The PC-350 is more advanced than standard variable polarity power supplies, as it uses a fuzzy logic short-circuit anticipation control. On comparable applications that require low heat input, the PC-350 has shown productivity improvements compared to standard short-circuit. This power supply is equipped with waveform algorithms pre-programmed for steel using either 100% Carbon Dioxide (CO<sub>2</sub>) shielding gas or an Argon (Ar) + CO<sub>2</sub> shielding gas mixture for both 0.8 mm (0.035 in.) or 1.2 mm (0.045 in.)

diameter electrodes. The waveform was simply modified by changing the electrode negative ratio on the pendant. Arc length and heat input is changed by an arc length knob on the pendant, which varies the pre-programmed pulse frequency.

The OTC robot welding system was used to develop preliminary repair welding procedures with the intent that they would be transferred to a different system for pipeline repair demonstrations. A range of orbital (i.e., ring motion) weave parameters were developed to establish an operating window, deposit quality, and deposition rate. Preliminary tests were also performed to evaluate bead overlap and tie-in parameters that would be required to make high quality repairs. All the welding tests were performed with a 95% Ar + 5% CO<sub>2</sub> shielding gas mixture using an 0.89 mm (0.035 in.) diameter ER70S-6 electrode.

Several years ago, PG&E purchased a welding tractor (Figure 27) from Magnatech for internal weld repair procedure development. This system was loaned to EWI so it could be used for pipeline repair evaluations, as this equipment is portable where the robot welding system is not.

The Magnatech Pipeliner II welding tractor has orbital motion with controls (Figure 28) for torch oscillation. The system is limited to a finite number of revolutions that can be made before cables must be unwound. The controls are analog and do not have high accuracy; however, they are sufficient for preliminary parameter development and demonstration welding. Programmable controls would be required for an internal repair welding system using a Magnatech tractor. In addition, numerous mechanical changes would be required to accommodate a range of pipeline diameter sizes, since the Pipeliner II was developed specifically for 559 mm (22 in.) diameter pipe.

The Magnatech tractor was interfaced with a Panasonic AE 350 power supply (Figure 29), which provides pulse waveforms and can be operated in a short-circuit mode where artificial intelligence is used to minimize spatter. The current pulsing and short-circuiting helps lower heat input and improve deposition rate in out-of-position welds. Pre-programmed current waveforms are provided by algorithms for steel electrodes and many other materials.

PG&E bought the Magnatech Pipeliner system specifically to repair weld 559 mm (22 in.) diameter pipe. In order to use the PG&E system for this project, Panhandle Eastern supplied approximately 12.19 m (40 ft.) of asphalt covered, 559 mm (22 in.) diameter pipe that was made in the 1930s. Additional lengths of 508 mm (20 in.) diameter pipe of similar vintage were taken from the EWI material inventory.

## **Welding Procedure Development**

Welding procedures were developed using the 6-axis, OTC robot. The objective of these tests was to establish deposit layer parameters that could be used to make ring, spiral or patch repairs. Since the objective for these repairs is to reinforce the wall thickness, the bead shape criteria was

to make flat deposits. If a large area needed repaired, multiple weld beads would be tied to each other. Here, bead overlap parameters need to be developed to optimize the uniformity of the entire repair deposit area. In many ways, the parameters that were developed are similar to cladding procedures. The ideal weld bead shape would have uniform thickness across the weld section except near the weld toes, which should taper smoothly into the base material (Figure 109). Smooth toes promote good tie-ins with subsequent weld beads. The fusion boundary should be uniform and free from defects.

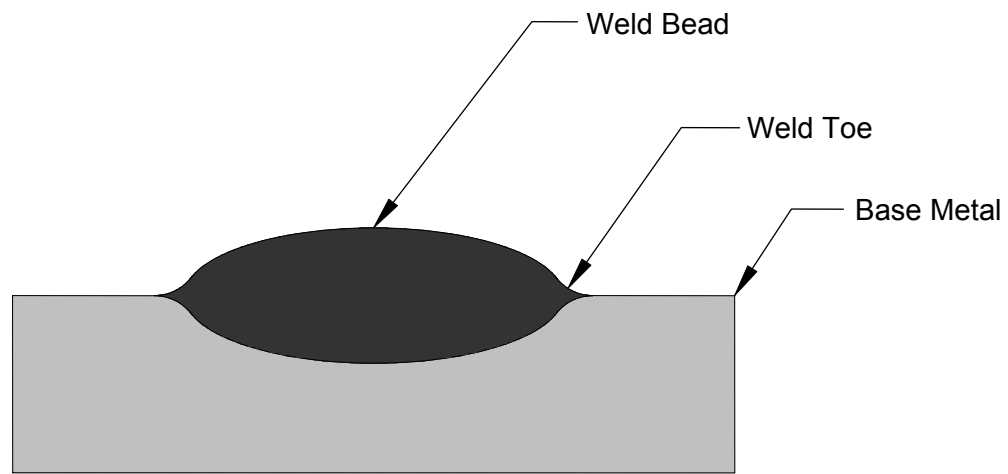


**Figure 109 - Weld Bead Shape Diagram**

Using the robot welding system, ring welding procedures using weaving were developed for several bead widths (Figure 110). This figure shows the location where the first half of the ring was stopped and the second half was started in the overhead position. This was not an ideal stop-start location but was required with the robot to manage the welding cables. If start-stops were required to complete a repair, it would be preferred to have them positioned at a different location around the circumference, ideally in the flat position. Tie-in parameters will need to be optimized for each possible starting position once preferred bead shape weaving parameters are selected. A true orbital bore welding machine, like the Bortech, would have a current and shielding gas commutation system to provide infinite rotations without cable problems thereby minimizing stop-starts.



Figure 110 - Tests R-01 - R-04 at 12:00 (Note the Poor Tie-Ins for R-01 through R-03)

When welding was initiated, the pipe was near room temperature. The weld bead profile at the start (Figure 111 and Figure 112) slowly changed as a steady-state temperatures are built in the material based on the heat input of each welding procedure. In general, most weld starts appeared more convex based on the low starting material temperature. Note that test R-04 was overlapped on test R-03 to provide a larger deposit layer in Figure 112.



Figure 111 - Test R-01 at 12:00 Show Poor Stop-Start Tie-In



Figure 112 - Tests R-03 and R-04 at 12:00 Show Better Stop-Start Overlap



The preferred welding parameters were based on optimizing the bead shape in the steady state (Figure 113). For internal repair of pipelines, a programmable weld controller could be used to use higher welding heat input at the weld start. This would provide better weld bead start quality. Once welding the start parameters could be ramped in the steady-state parameters to provide uniform bead shape.



Figure 113 - Tests R-01 and R-02 at 3:00 Showing Steady-State Bead Shape

Table 17 contains the welding parameters for the weave bead procedures used. Wire feed speeds varied from 5.08 meters per minute (mpm) (200 ipm) to 6.35 mpm (250 ipm). This was better than preliminary tests with the Bortech system, which were at 4.45 mpm (175 ipm) and resulted in stringer beads that had a ropy appearance.

Weld No.	Specimen No.	Wire Feed Speed mpm (ipm)	Voltage (Trim)	Travel Speed mmpm (ipm)	Weave Amplitude mm/side (in/side)	Weave Frequency (Hz)	Dwell Time (seconds)	Comment
1	R-01	5.08 (200)	0	76.2 (3)	9.9 (0.39)	0.6	0.6	Good for a narrow repair.
2		5.08 (200)	0	127 (5)	25.4 (1.00)	0.6	0.2	Too fast. Zigzag pattern results.
3	R-02	6.43 (253)	-4	25.4 (1)	25.4 (1.00)	0.1	0.6	<ul style="list-style-type: none"> <li>• Bad at overhead position</li> <li>• Turned voltage to -4</li> <li>• Dwell is not needed</li> </ul>
4	R-03	6.43 (253)	-4	25.4 (1)	25.4 (1.00)	0.1	0.0	6 mm (0.25 in.) overlap at overhead position to tie two welds together - porosity resulted.
5	R-04	6.43 (253)	-4	25.4 (1)	25.4 (1.00)	0.1	0.0	<ul style="list-style-type: none"> <li>• 6 mm (0.25 in.) overlap at overhead and flat positions.</li> <li>• Centerline is 22 mm (0.88 in.) from previous weld edge (3 mm (0.125 in.) circumferential overlap).</li> <li>• Good circumferential tie on uphill side.</li> <li>• Poor circumferential tie on downhill side.</li> <li>• Need more wire feed speed due to bad fusion on downhill side</li> </ul>
6	R-05	7.62 (300)	-4	25.4 (1)	25.4 (1.00)	0.1	0.0	<ul style="list-style-type: none"> <li>• 6 mm (0.25 in.) overlap at every 30 degrees.</li> <li>• See Table 18 for tie-in quality at each position</li> </ul>

**Table 17 - Welding Parameters for Specimens R-01 through R-05**

Table 18 contains the tie-in quality at each clock position for specimen R-05.

Position (clock)	Tie In Quality (poor/OK/good)
12:00	Poor
1:00	Poor
2:00	Poor
3:00	Poor
4:00	OK
5:00	Good
6:00	Good
7:00	Robot problem
8:00	Good
9:00	Good
10:00	Good
11:00	OK

**Table 18 - Tie-In Quality at Each Clock Position for R-05**

To further improve starting bead shape, some additional tests were performed using 7.62 mpm (300 ipm) wire feed speed (Figure 114). These tests were used by the technician to study the precise location for starting on a "stop" and to evaluate gravity effects. As shown by these tests, start bead shape can be improved through the use of higher wire feed speeds (which produce higher heat input). No additional procedures were developed with the 6-axis robot.



12:00 – Too Much Overlap



1:00 – Too Much Overlap



2:00 – Slightly Better



3:00 – Some Convexity



4:00 – Okay



5:00 – Good



6:00 – Good



7:00 – Bad Appearance Due  
Robot Program Error



8:00 – Good



9:00 – Good



10:00 – Good



11:00 – Okay

**Figure 114 - Tie-In Tests Using Parameters R-05 Every 30° Around One Ring Deposit**

### **Test 01: Weld Repair, 558.8 mm (22 in.) Pipe, Short/Deep Damage**

Test 01 was conducted to determine the feasibility of making weld deposition repairs on the inside diameter (ID) of a pipeline to replace metal loss on the outside diameter (OD) due to corrosion damage.

The Magnatech Pipeliner II was used to make a weld deposition repair on a 558.8 mm (22 in.) diameter API 5L, Grade B pipe section. Test 01 incorporated a short/deep, stylized corrosion defect representing a 25% reduction in burst strength. Defect dimensions were 190.5 mm (7.5 in.) long by 3.96 mm (0.156 in.) deep (pictured in Figure 18). This defect was introduced into the pipe section shown in Figure 115.



**Figure 115 - Short/Deep Simulated Corrosion on 558.80 mm (22 in.) Pipe for Test 01**

Test 01 welding was done with a shielding gas mixture of 95% Ar + 5% CO<sub>2</sub>. Filler metal was a GMAW 0.89 mm (0.035 in.) diameter AWS ER70S-6 electrode. Welding parameters are found in Table 3 and Table 4. The soil box in Figure 116 was used to simulate in-service welding conditions and soil related cooling rates during weld deposition repair.



**Figure 116 - Soil Box for Weld Deposition Repair Test 01**

The pipe section with the soil box was rotated 180° (as shown in Figure 117) to facilitate welding on the ID of the pipe from the 6:00 position (where the weld passes were initiated) to the 9:00 position (where the weld passes were terminated).



**Figure 117 - Orientation of Pipe Section with Dirt Box for Weld Deposition Repair Test 01**

To assure the deposited weld metal completely covered the area of simulated corrosion on the inside of the pipe, an outline of the simulated corrosion was made as shown in Figure 118.

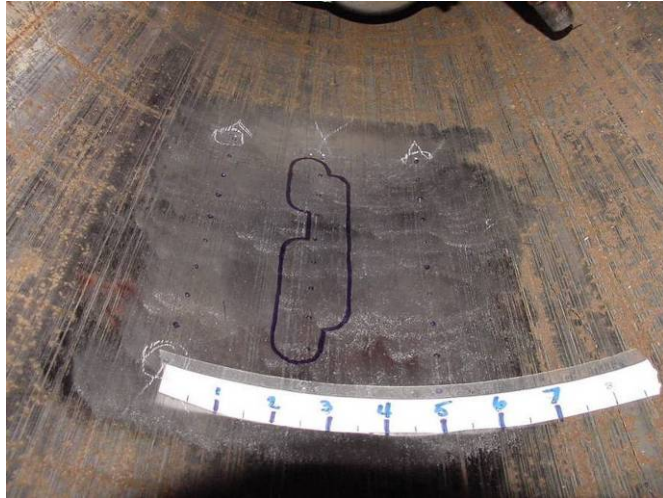


**Figure 118 - Outline of Simulated Corrosion on ID of Test 01 Pipe Section**

The weld deposition repair consisted of two layers of welds. The first pass of weld Layer 1 is shown in Figure 119.



**Figure 119 - First Pass of Weld Layer 1 for Test 01**

For weld Layer 1, each subsequent weld pass overlapped the previous weld pass by 1.5 mm (0.06 in.). The second pass of the Layer 1 is shown in Figure 120.

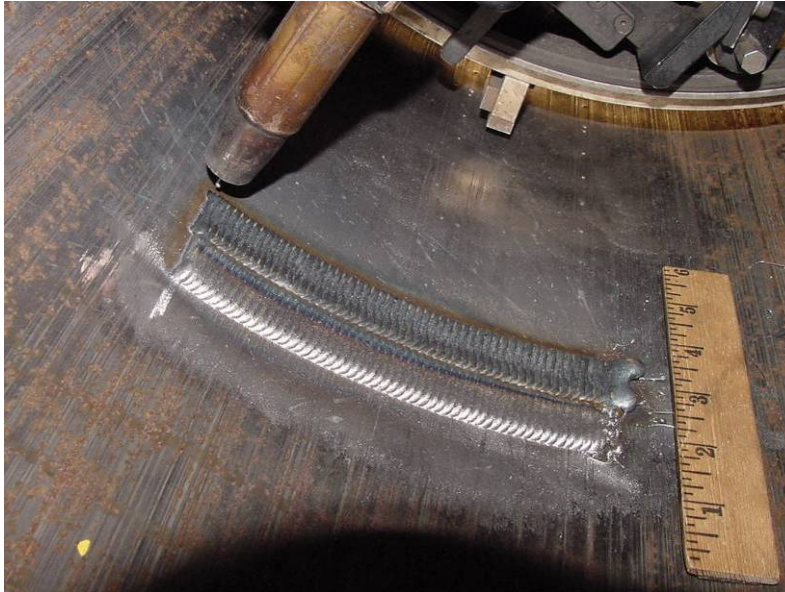


**Figure 120 - Second Pass of Weld Layer 1 of Test 01**

During the deposition of the third pass of weld Layer 1, a small defect was created as indicated in the yellow circle in Figure 121. The defect was repaired with an autogenous (i.e., with no filler metal) gas tungsten arc weld (GTAW).

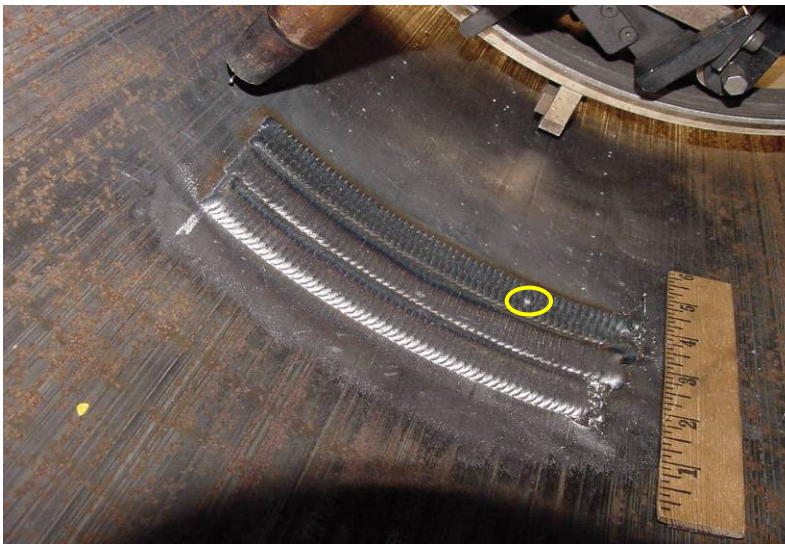


**Figure 121 - Third Pass of Weld Layer 1 for Test 01**



The completed weld Layer 1 is shown in Figure 122. The axial length of Layer 1 exceeded the simulated corrosion by more than 25.4 mm (1.0 in.), which is three times the pipe wall thickness. The rule of thumb for pipeline welding repair is to deposit weld metal such that it exceeds the corrosion area by at least one wall thickness.



**Figure 122 - Completed Weld Layer 1 for Test 01**

First pass of weld Layer 2 is shown in Figure 123. Layer 2 passes were centered over the weld toes of the previous layer.



**Figure 123 - First Pass of Weld Layer 2 for Test 01**

Completed second layer is shown in Figure 124.



**Figure 124 - Finished Weld Layer 2 of Test 01**

After weld Layer 2 was deposited, several ultrasonic thickness measurements were taken to confirm that the weld deposition layers restored the pipe wall back to the original thickness. Locations of thickness measurements are shown in Figure 125.

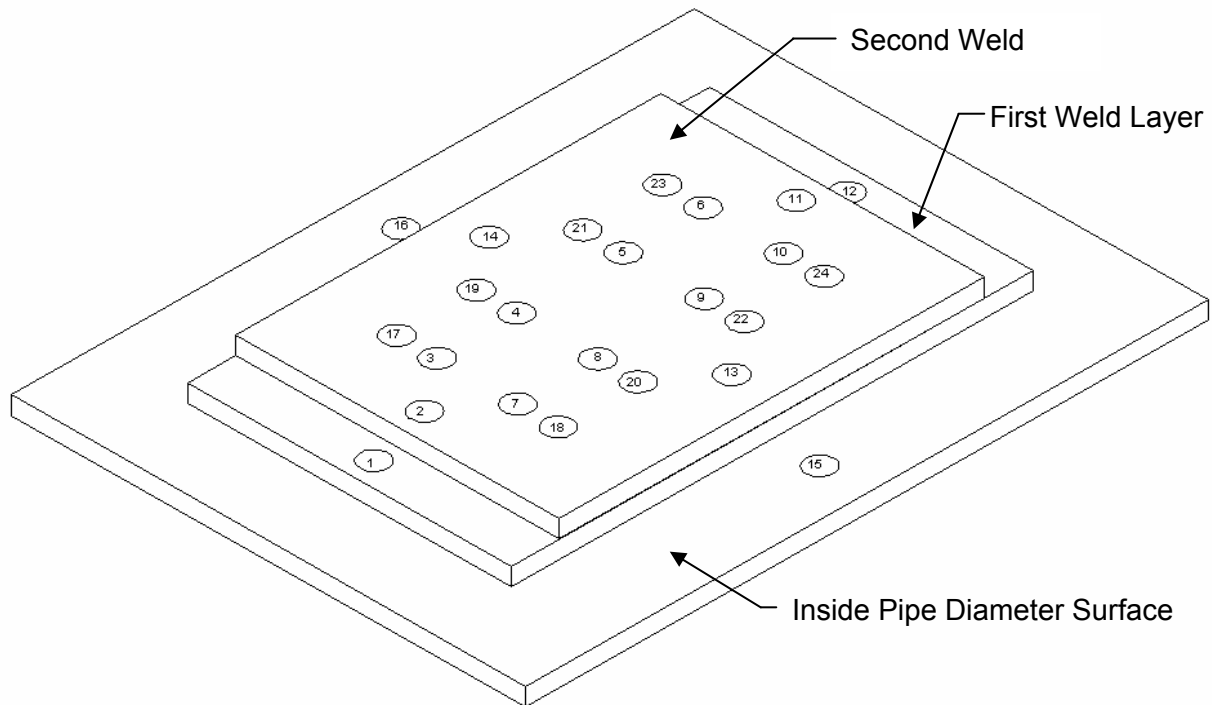


**Figure 125 - Ultrasonic Thickness Measurement Locations on Weld Repair Test 01**

Spacing of the ultrasonic measurements on weld Layer 2 was close enough to assure that the entire simulated corrosion area was evaluated. Locations 15 and 16 were designated as reference measurements.

Five locations were identified that had an apparent thickness values less than reference points 15 and 16 (as seen in Table 19). As a consequence, these areas were ultrasonically scanned to determine the cause of the irregularities. The cause of irregularities was determined to be lack-of-fusion defects between the weld toes of the first layer and the inside diameter of the pipe as opposed to area of insufficient thickness. These defects were oriented along the circumferential direction of the pipe.

The irregularities found in the weld deposition layers were considered inconsequential to hydrostatic testing given their size and circumferential orientation; therefore, hydrostatic burst testing was conducted on the pipe section without repairing the irregularities. Prior to this, additional ultrasonic measurements were taken at four locations with the transducer positioned to the side of the defect. These measurements are shown to the right of the non-conforming measurements (to the right of the slash) in Table 19. The four additional measurements were in excess of reference measurements 15 and 16.

Thickness Measurement Location in Figure 125	Thickness Measurement		Comments
	mm	inches	
1	10.67	0.420	
2	13.13	0.517	
3	5.36 / 9.14	0.211 / 0.360	Lack-of-Fusion
4	13.21	0.520	
5	5.28 / 13.06	0.208 / 0.514	Lack-of-Fusion
6	9.27	0.365	
7	9.37	0.369	
8	9.22	0.363	
9	5.84 / 9.35	0.230 / 0.368	Lack-of-Fusion
10	9.12	0.359	
11	13.67	0.538	
12	10.59	0.417	
13	13.41	0.528	
14	5.20 / 13.34	0.205 / 0.525	Lack-of-Fusion
15	7.89	0.311	Reference Measurement
16	8.18	0.322	Reference Measurement
17	13.21	0.520	
18	9.37	0.369	
19	13.46	0.530	
20	9.25	0.364	
21	5.46	0.215	Lack-of-Fusion
22	9.39	0.370	
23	13.97	0.550	
24	9.37	0.369	

**Table 19 - Ultrasonic Thickness Measurements at Locations in Figure 125**

The area of simulated corrosion on the outside pipe surface is shown after internal weld deposition repair in Figure 126.



**Figure 126 - Simulated Corrosion on Outside of Pipe After Weld Repair Test 01**

After the box with soil was removed from the weld repaired pipe section, an impression of the corrosion damage was left in the soil as shown in Figure 127. The outline of the weld deposition is also clearly visible where the asphalt coating melted and transferred to the surrounding soil during the welding process.



**Figure 127 - Soil in Contact With Pipe During Weld Repair Test 01**

Upon examination of the outside pipe surface (opposite the internal weld repair) prior to hydrostatic testing, it became apparent that a significant amount of weld distortion had occurred (i.e., a "dent" had been produced) as a result of the weld heating and cooling cycles. In Figure 128, a red string is used as a reference against which to measure the extent of the distortion. The red string indicates where the outside surface of the pipe was before welding. The yellow box indicates the location of the simulated corrosion. Figure 129 contains magnified pictures from the middle and ends of the dented area of pipe. The depth of this "dent"

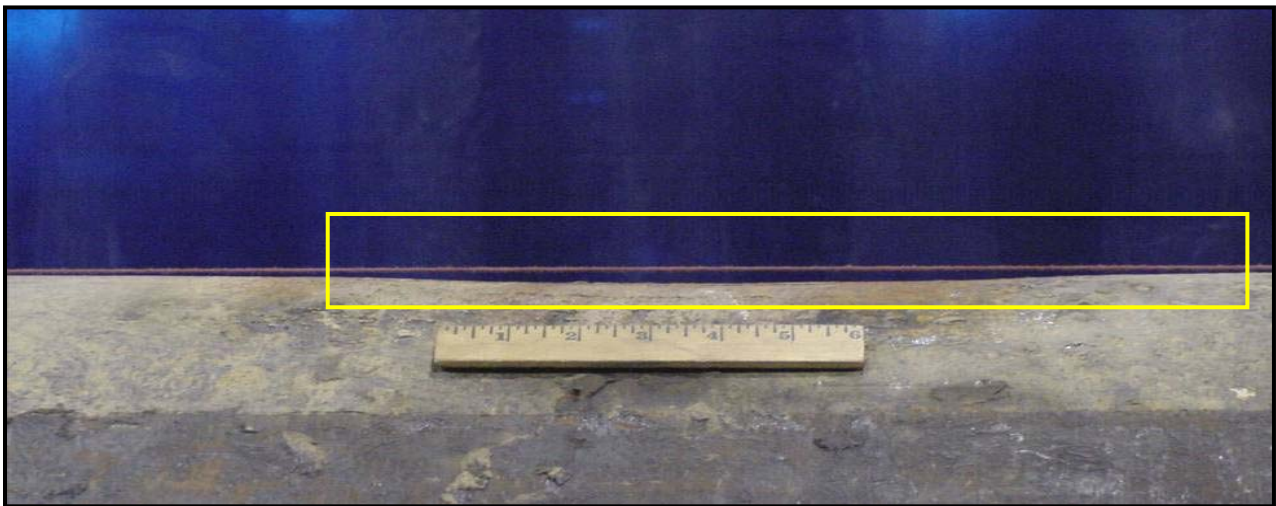


**Figure 128 - Profile of Dent in Outside Pipe Surface After Internal Weld Repair Test 01**

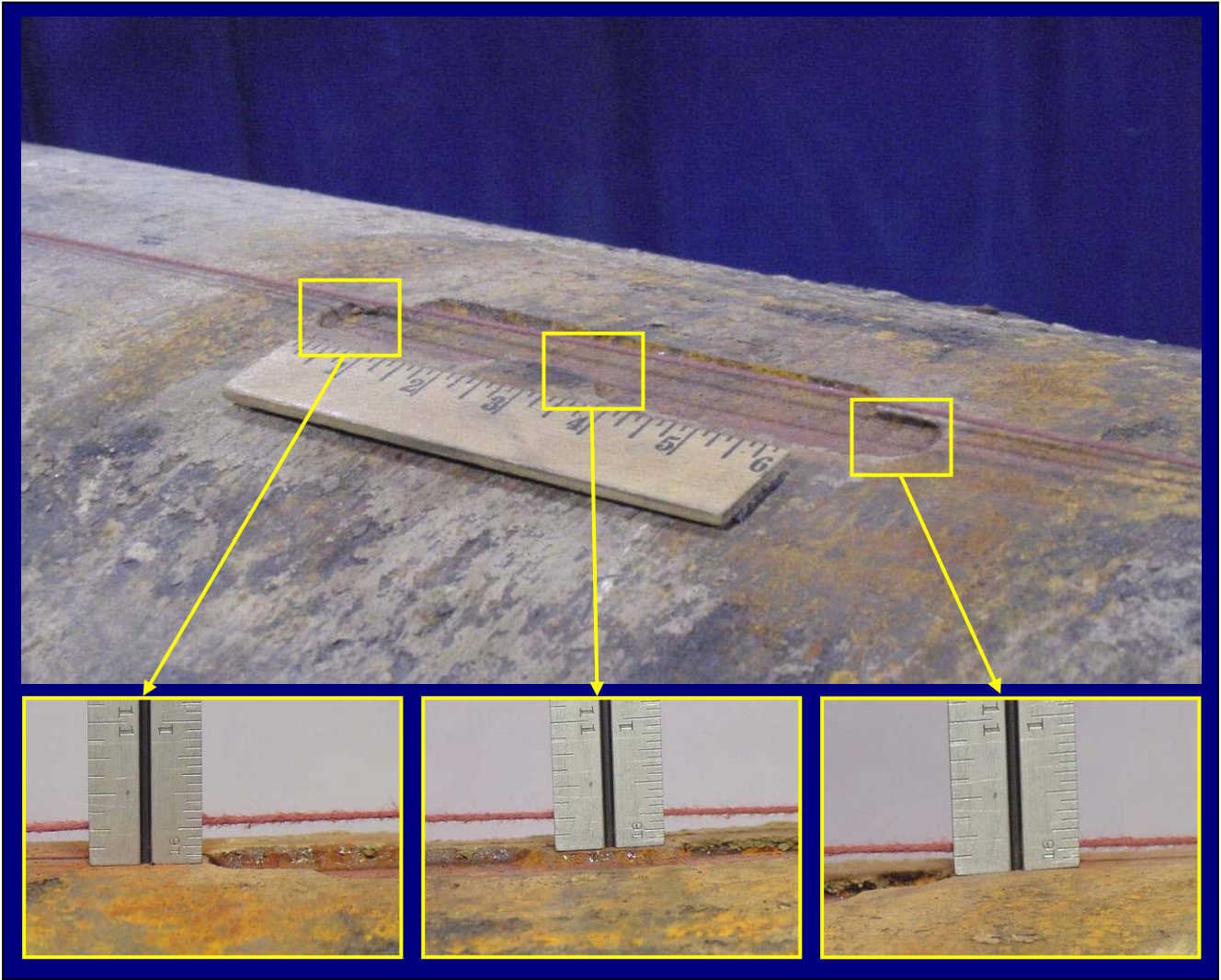


Figure 129 - Magnified Pictures of Dent at Ends and Middle of Test 01 Simulated Damage

Figure 130 is a photo of Test 01 after burst testing. The failure occurred at the toe of the weld repair Layer 1. This weld toe area apparently acted as a stress concentration from which the failure initiated. The failure was also influenced by secondary stresses that were produced as the result of the re-rounding of the "dent".



**Figure 130 - Test 01 Pipe Section After Hydrostatic Burst Test**

Table 20 contains the predicted and measured burst pressures for the 558.8 mm (22 in.) diameter API 5L, Grade B pipe sections in the virgin, un-repaired (short/deep), and Test 01 repaired conditions. The measured burst pressure of the un-repaired pipe section was 24% lower than the measured burst pressure of the virgin pipe section. Although the resultant burst pressure for Test 01 repair was 47% greater than the pressure corresponding to 100% SMYS (6.84 MPa (992 psi)) and 46% higher than the RSTRENG® predicted burst pressure for an un-repaired pipe, the actual measured Test 01 burst pressure was in fact 10% less than the measured performance of the un-repaired pipe section and 24% lower than the measured performance of the virgin pipe.

Pipe Diameter	Pipe Condition	Predicted Burst Pressure		Actual Burst Pressure	
		(MPa)	(psi)	(MPa)	(psi)
558.8 mm (22 in.)	Virgin	10.91	1,583	12.69	1,841
	Simulated Damage Short/Deep Un-Repaired	5.15	747	10.78	1,563
	Simulated Damage Repaired with High Grade CF Liner (Test 01)	-	-	9.68	1,404

**Table 20 - Summary of Predicted vs. Actual Hydrostatic Burst Pressure Values Test 01**

Given the fact that internal weld deposition repair exhibited a 10% lower burst pressure than an un-repaired pipe section, weld deposition repair is clearly a less than desirable candidate for internal repair of gas transmission pipelines..

### Effect of Methane on Weld Quality

During any arc welding operation, the material being welded is exposed to temperatures that range from ambient to well above the melting temperature 1,536°C (2,736°F). When steel at high temperature is exposed to a hydrocarbon gas (such as methane), carburization can occur. When steel at temperatures above 1,130°C (2,066°F) is exposed to methane, eutectic iron can form as the result of diffusion of carbon from the methane into the steel. In previous work at EWI,<sup>(7)</sup> welds were made on the outside of a thin-wall (3.2 mm (0.125 in.)) pipe containing methane gas pressurized to 4.5 MPa (650 psi) with a flow rate of 6.1 m/sec (19.9 ft./sec). Figure 131 shows the equipment set-up used to perform these welding trials.



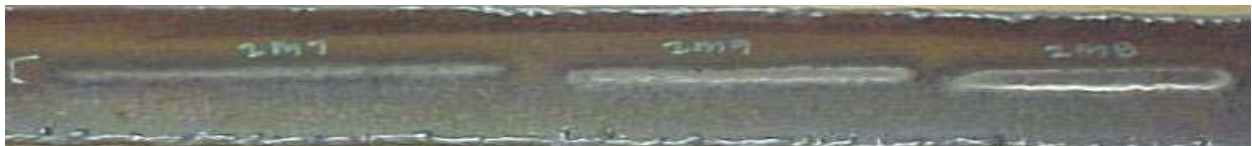


**Figure 131 - Set-Up for Welding Thin Wall Pipe with Pressurized Methane Gas**

Figure 132 shows the external appearance of welds 2M7, 2M9, and 2M8 made on the outside of the thin-wall pipe under these conditions. Figure 133 shows the appearance of these welds from the inside.

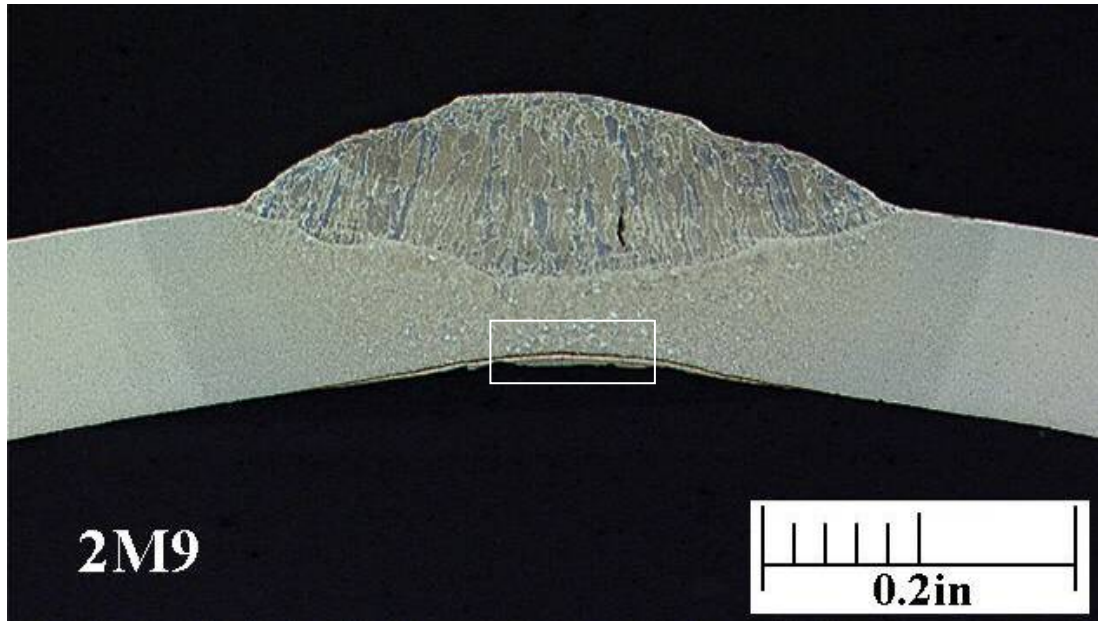


**Figure 132 - Welds Made in Pressurized Methane - Appearance from OD**



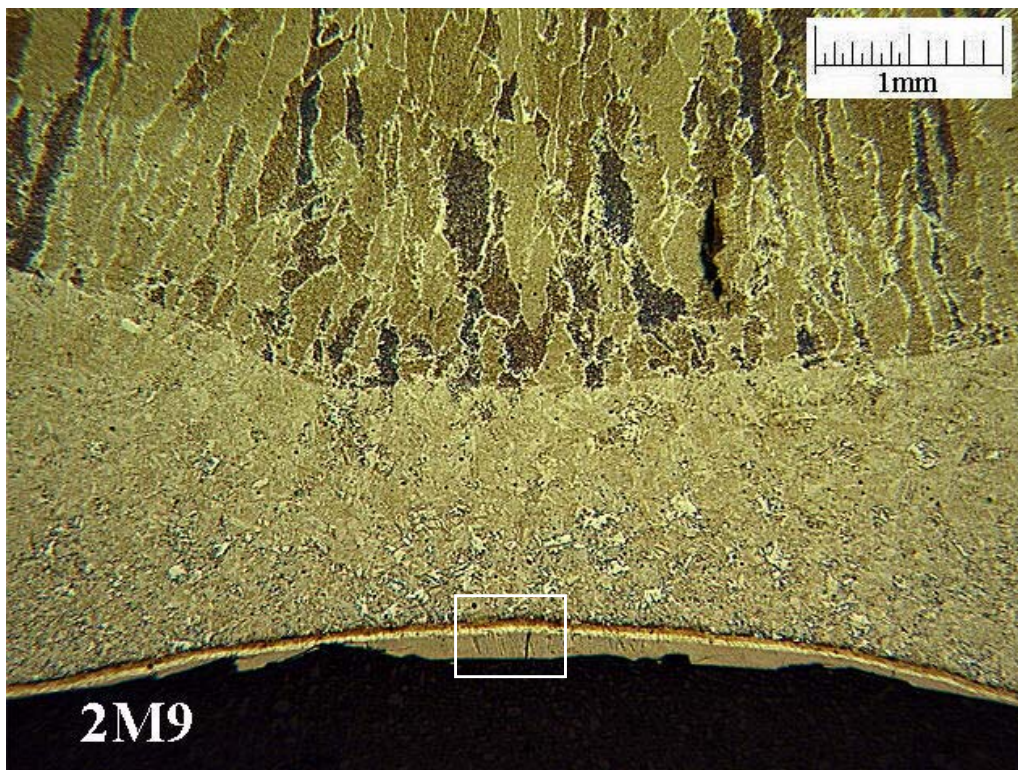
**Figure 133 - Welds Made in Pressurized Methane - Appearance from ID**

Figure 134 is a metallographic cross section thru Weld 2M9 (from Figure 132 and Figure 133).



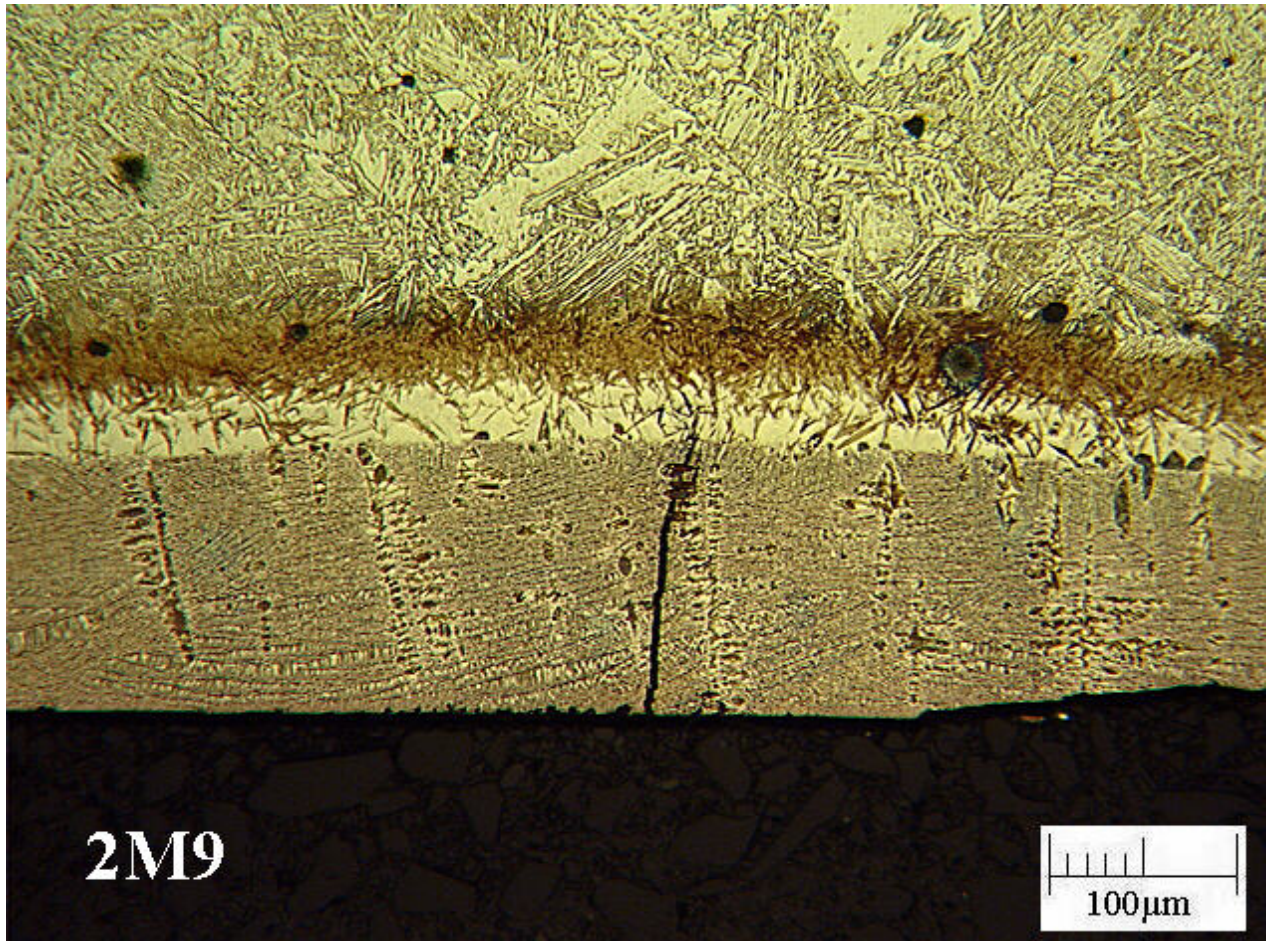
**Figure 134 - Metallographic Cross Section of Weld 2M9**

Figure 135 is a magnified view inside the white box in Figure 134. Figure 135 clearly shows carburization and the formation of thin layer of eutectic iron.



**Figure 135 - Eutectic Iron Layer on Backside Surface of Weld 2M9**

This phenomenon was previously reported by Battelle during experiments with liquid propane.<sup>(5)</sup> Figure 136 is a magnified view inside the white box in Figure 135. Figure 136 shows small cracks associated with the eutectic iron layer, which were attributed to the limited ductility of eutectic iron.



**Figure 136 - Cracks in Eutectic Iron Layer of Weld 2M9**

In a field repair situation, evacuating a pipeline prior to internal weld deposition repair will be particularly difficult. There is a high probability that the weld shielding gas will be contaminated to some degree with methane that remains in the pipe; therefore, weld trials were conducted with a shielding gas containing various levels of methane to determine the effect of methane on resultant weld quality.

The Magnatech Pipeliner II was used to weld seven specimens consisting of a single GMAW weld (i.e., bead on plate weld) deposited on the ID of a 558.80 mm (22 in.) diameter API 5L Grade B pipe in the 6:00 or flat welding position. Filler metal was a 0.89 mm (0.035 in.) diameter AWS ER70S-6 electrode.

Shielding gas was supplied by two independent gas bottles: one bottle contained a mixture of 95% Ar + 5% CO<sub>2</sub>; the other bottle contained a mixture of 10% methane with a balance of 95% Ar + 5% CO<sub>2</sub>. The amount of methane was raised by increasing the flow rate on the flow meter of the bottle containing methane. Linear travel speeds of the welds were not recorded as they were held constant for all weld trials. Methane welding process parameters are found in Table 5.

The resultant welds were then prepared for metallographic examination. Three weld metal hardness measurements were made and the results were averaged for each weld. The chemical composition for each weld was also measured to determine if the presence of methane affected the carbon content of the weld deposit. Table 21 contains a summary of hardness measurements and the percent carbon contents that were measured.

Weld ID	Shielding Gas Flow Rate				Volume Percent Methane	Average Weld Metal Hardness (Hv-10kg)	Weld Metal Carbon Content (%)	Comments
	95% Ar + 5% CO <sub>2</sub>		10% Methane + 4.5% CO <sub>2</sub> + 85.5% Ar					
	(m <sup>3</sup> /hr)	(ft <sup>3</sup> /hr)	(m <sup>3</sup> /hr)	(ft <sup>3</sup> /hr)				
325-2	1.42	50	0.00	0	0.0	169.7	0.073	No Porosity
325-3	1.13	40	0.28	10	2.0	174.7	0.074	No Porosity
325-4	0.99	35	0.42	15	3.0	175.0	0.062	Porosity
325-5	0.85	30	0.57	20	4.0	175.3	0.071	Porosity
325-6	1.22	43	0.20	7	1.4	169.7	0.075	No Porosity
325-8	0.99	35	0.28	10	2.2	176.7	0.071	No Porosity
325-9	0.85	30	0.42	15	3.3	171.3	0.081	Porosity

**Table 21 - Average Weld Metal Hardness and Carbon Content for Methane Weld Trials**

Figure 137 is a graph of the average weld metal hardness values and percent carbon content from Table 21. In Figure 137, the weld metal hardness scale is on the left axis and the percent carbon content of the weld metal is shown on the right axis. From this figure, it can be seen that increasing the volume percent of methane in the shielding gas did not consistently increase either weld metal hardness or percent carbon content of the weld metal.

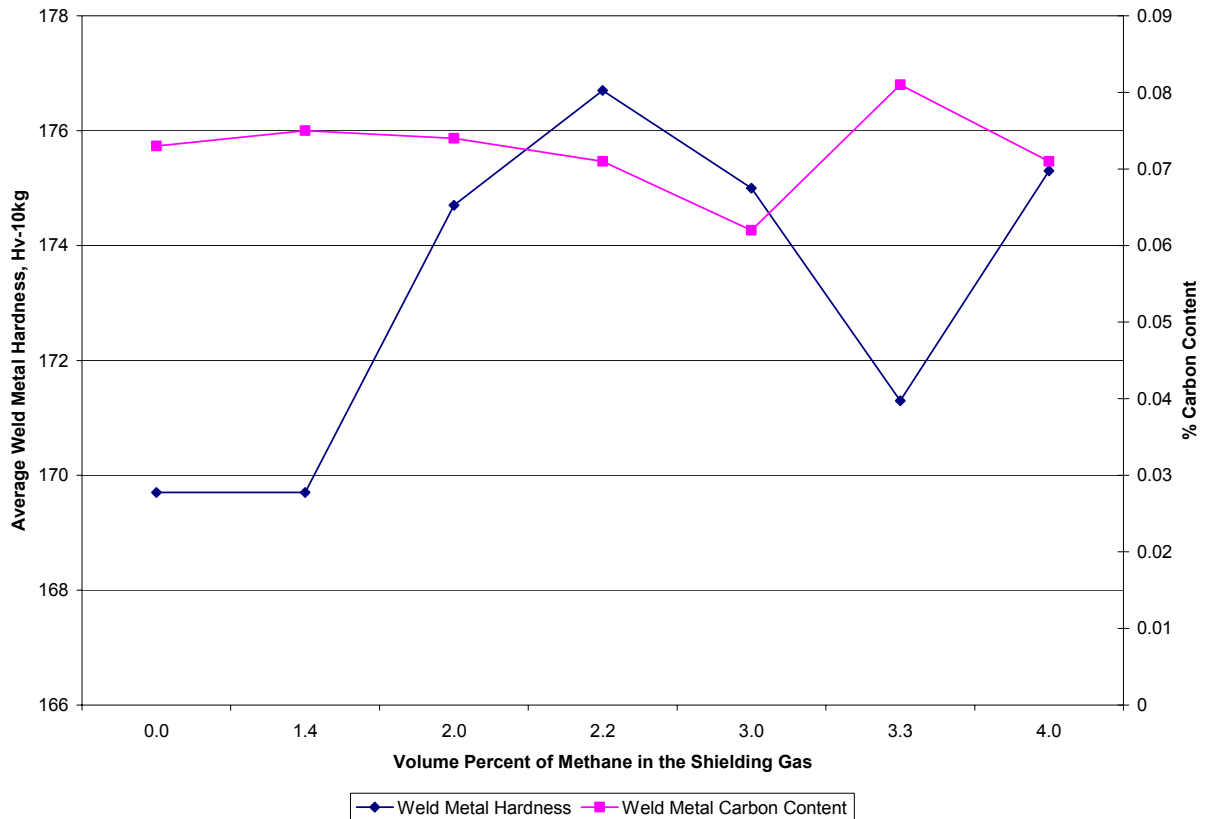


**Figure 137 - Graphs of Table 21 Hardness Values and Carbon Content**

Photos of welds that were made during this portion of the investigation are shown in Figure 138 through Figure 144. A visual examination of the samples revealed that a volume of 3% methane in the shielding gas caused porosity in weld specimens 325-4 (Figure 140), 325-5 (Figure 141), and 325-9 (Figure 144).



**Figure 138 - Methane Weld Specimen 325-2**



**Figure 139 - Methane Weld Specimen 325-3**



**Figure 140 - Methane Weld Specimen 325-4**



**Figure 141 - Methane Weld Specimen 325-5**



Figure 142 - Methane Weld Specimen 325-6



Figure 143 - Methane Weld Specimen 325-8



Figure 144 - Methane Weld Specimen 325-9

These results clearly indicate that an increased volume of methane in the weld shielding gas produces welds with porosity defects that decrease weld quality. Adequate shielding gas protection is critical to creating sound, defect free welds. Providing adequate gas shielding protection during welding in an environment that contains a significant portion of methane will be difficult to achieve in a field repair situation.

### **Implications of Weld Deposition Repair Trials**

Weld deposition, although promising in principal, is less than ideal for internal repair of gas transmission pipelines. The pipe section repaired with weld deposition (Test 01) exhibited a 10% lower burst pressure than that of an un-repaired pipe section. While weld deposition repairs applied to the outside of exposed pipelines are becoming more commonplace in the gas transmission pipeline industry, the application of this technique to the inside of the pipe presents a number of difficulties. When applied to the outside of an exposed pipeline, dents or concavity that result from welding distortion can be overcome by simply applying more weld metal until the outside diameter of the pipe is restored. This is not possible for internal repair where additional weld metal would result in further concavity. In fact, distortion caused by welding residual stresses may have contributed to the lower burst pressures produced by Test 01. In addition to the difficulties that will result from remotely operating welding equipment from great distances, the presence of methane in the welding environment will also cause complications and produce less than desirable weld quality. Weld deposition repair was therefore dropped from the test program.

### **4.6 - Glass Fiber Liner Repairs**

The investigation of glass fiber (GF) reinforced liner repairs resulted in the discovery of several potentially useful commercial fiber-reinforced composite liner products that are directly applicable to internal repair. The GF test program focused on a modified Wellstream-Haliburton/RolaTube product, which was a bi-stable reeled composite material used to make strong, lightweight, composite pipes and pipe linings (Figure 145). When unreeled, this product changes shape from a flat strip to an overlapping circular pipe liner that is pulled into position. One example of this product is 100 mm (4 in.) diameter by 2.5 mm (0.10 in.) thick that has a 5.9 MPa (870 psi) short-term burst pressure.





**Figure 145 - RolaTube Bi-Stable Reeled Composite Material**

Glass-high density polyethylene (HDPE) material was considered. Glass-polypropylene material was selected after problems were encountered bonding the glass-HDPE material to steel.

Prior to the initial trials for GF reinforced composite repairs, RolaTube conducted FEA to determine the required properties of the liner material and fabricated a modified glass-polypropylene product for use in this trial. Heat and pressure were used to consolidate the glass-polypropylene material into a liner (Figure 30). The resulting wall thickness of the liner is 2.85 mm (0.11 in.).

#### **Test 02: GF Liner Repair, 114.3 mm (4.5 in.) Pipe, Long/Shallow Damage**

For Test 02, a 114.3 mm (4.5 in.) diameter API 5L Grade B pipe with a long/shallow simulated corrosion defect (Figure 14) was used. Calculated with RSTRENG® to represent a 30% reduction in burst strength, defect dimensions were 127 mm (5 in.) long by 2.54 mm (0.100 in.) deep. The inside surface of the pipe was degreased prior to installing the GF liners (Figure 31). The installation process consisted of locating the GF liner inside the pipe and inserting a silicon rubber bag inside the liner (Figure 32). The silicon bag was then inflated to press the liner against the inside diameter (ID) of the pipe wall. The pipe section was then heated to 200°C (392°F) in an oven (Figure 33) to fuse the liner to the pipe wall.

After end caps were welded on the ends of the pipe section (Figure 12), the Test 02 pipe was hydrostatically pressurized to failure. The specimen ruptured in the area of simulated corrosion damage as shown in Figure 146.



**Figure 146 - Test 02 Pipe with GF Liner Repair of Long/Shallow Damage After Burst Test**

A postmortem analysis was conducted on the Test 02 burst test specimen. So as not to damage the liner, water jet cutting was used to section the specimen. Results indicate that the liner did rupture (Figure 147 and Figure 148), thus disbonding was not an issue.



**Figure 147 - Cross Section of Test 02 Burst Test Specimen**

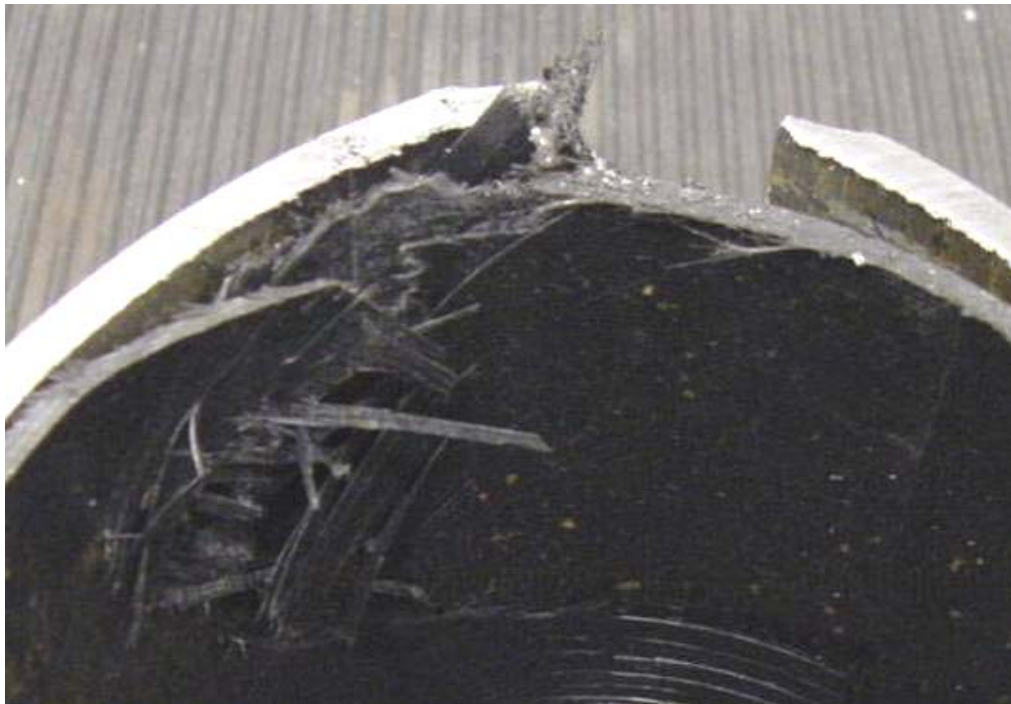


**Figure 148 - Magnified Cross Section of Test 02 Burst Test Specimen**

Table 22 contains the predicted and measured burst pressures for the 114.3 mm (4.5 in.) API 5L Grade B pipe sections in the un-repaired (long/shallow) and Test 02 repaired conditions. Table 22 also contains a predicted burst pressure for virgin pipe based on Barlow's formula using the measured ultimate tensile strength of the pipe material. Although the resultant burst pressure for Test 02 repair was 16% greater than the pressure corresponding to 100% SMYS of 20.16 MPa (2,924 psi) and 41% higher than the RSTRENG® predicted burst pressure for an un-repaired pipe, it was in fact only 1% greater than the measured performance of the un-repaired pipe section and 38% lower than the predicted burst pressure of the virgin pipe.

Pipe Diameter	Pipe Condition	Predicted Burst Pressure		Actual Burst Pressure	
		(MPa)	(psi)	(MPa)	(psi)
114.3 mm (4.5 in.)	Virgin	38.66	5,607	-	-
	Simulated Damage Long/Shallow Un-Repaired	14.13	2,049	23.66	3,431
	Simulated Damage Repaired with High Grade CF Liner (Test 02)	-	-	23.94	3,472

**Table 22 - Summary of Predicted vs. Actual Hydrostatic Burst Pressure Values Test 02**

These results indicate that the liner was ineffective at restoring the pressure containing capability of a pipeline with long/shallow corrosion damage.

### **Test 03: GF Patch Repair, 114.3 mm (4.5 in.) Pipe, Short/Deep Damage**

For Test 03, a 114.3 mm (4.5 in.) diameter API 5L Grade B pipe with a short/deep simulated corrosion pit defect (Figure 14) was used. Calculated with RSTRENG® to represent a 30% reduction in burst strength, defect dimensions were 25.4 mm (1 in.) long by 4.01 mm (0.160 in.) deep. The inside surface of the pipe was degreased prior to installing the GF liners (Figure 31). The installation process consisted of locating the GF liner inside the pipe and inserting a silicon rubber bag inside the liner (Figure 32). The silicon bag was then inflated to press the liner against the inside diameter (ID) of the pipe wall. The pipe section was then heated to 200°C (392°F) in an oven (Figure 33) to fuse the liner to the pipe wall.

After end caps were welded on the ends of the pipe section (Figure 12), the Test 03 pipe was hydrostatically pressurized to failure. The specimen developed a leak in the center of the simulated corrosion damage as shown in Figure 149.



**Figure 149 - Test 03 Pipe with GF Liner Repair of Short/Deep Damage after Burst Test**

Table 24 contains the predicted and measured burst pressures for the 114.3 mm (4.5 in.) API 5L Grade B pipe sections in the un-repaired (short/deep) and Test 03 repaired conditions. Table 23 also contains a predicted burst pressure for virgin pipe based on Barlow's formula using the measured ultimate tensile strength of the pipe material. While the resultant burst

pressure for Test 03 was 27% greater than the pressure corresponding to 100% SMYS of 20.16 MPa (2,924 psi) and 50% higher than the RSTRENG® predicted burst pressure for an un-repaired pipe, it was in fact only 7% greater than the measured performance of the un-repaired pipe section and 28% lower than the predicted burst pressure of the virgin pipe.

Pipe Diameter	Pipe Condition	Predicted Burst Pressure		Actual Burst Pressure	
		(MPa)	(psi)	(MPa)	(psi)
114.3 mm (4.5 in.)	Virgin	38.66	5,607	-	-
	Simulated Damage Short/Deep Un-Repaired	13.97	2,026	25.86	3,750
	Simulated Damage Repaired with High Grade CF Liner (Test 03)	-	-	27.79	4,031

**Table 23 - Summary of Predicted vs. Actual Hydrostatic Burst Pressure Values Test 03**

With a burst pressure of 7% greater than that of an un-repaired pipe section, the liner was only marginally effective at restoring the pressure containing capability of a pipeline with short/deep corrosion damage.

### Implications of GF Liner Repair Trails

Measured burst pressures for pipe sections repaired with the GF liners repairs were 1% higher than an un-repaired specimen with long/shallow damage and 7% higher than an un-repaired specimen with short/deep damage. This clearly indicates that GF liner repair is only marginally effective at restoring the pressure containing capabilities of the pipeline. While these results were initially viewed as discouraging, they do indicate that fiber reinforced composite liners have the potential to increase the burst pressure of pipe sections with external damage.

Analysis of the results indicates that the difference in modulus of elasticity between the steel and the liner material prevents the liner from carrying its share of the load. The modulus of elasticity for steel is approximately 206.8 GPa (30 x 10<sup>6</sup> psi). Tensile testing was carried out to determine the modulus of elasticity for the glass/polypropylene liner material that was used (Table 14 and Figure 101). The mean value for the modulus of elasticity for the liner material was measured to be approximately 15.2 GPa (2.2 x 10<sup>6</sup> psi). Because the GF liner material has a significantly lower modulus of elasticity than the steel pipe, as pressure in the lined pipe increases, the stiffness of the steel prevents the composite liner material from experiencing enough strain to share any significant portion of the load.

Since Test 02 and Test 03 demonstrated that GF liner repairs are not very effective at restoring the pressure containing capabilities of a pipeline, it was anticipated that a liner material with a

modulus of elasticity on the order of 95% of that for steel will be required for effective reinforcement of steel pipelines that have been weakened by external wall loss defects. A liner material with a modulus of elasticity that is slightly less than that of steel would allow the liner to carry its share of the load without putting the interface between the liner and the steel pipe in tension. If the modulus of elasticity for the liner material were greater than that of the steel pipe, as pressure in the pipe increases, the stiffness of the liner would prevent it from expanding with the steel pipe, thus putting the interface between the liner and the steel pipe in tension. If the "adhesive" layer between the pipe and the sleeve are broken, this will allow pressure to enter the annular space between the pipe and liner. The pressure will then act upon the defect-weakened area and render the liner useless. GF composite liners were consequently dropped from the testing program and engineering analysis was employed to identify a fiber-reinforced liner material with desired properties for future testing.

#### **4.7 - Simulation and Analysis of Fiber-Reinforced Liner Repair**

In previous work for PRCI<sup>(6)</sup>, finite element analysis (FEA) was performed to simulate external weld deposition repair of internal wall loss. As indicated above, the difference in modulus of elasticity between the steel and the original GF reinforced liner material prevents the liner from carrying its share of the load. To address this, fiber-reinforced composite liner requirements were determined from the assumed values for an economical carbon fiber (CF) reinforcement with a vinylester resin system. The objective was to define realistic combinations of CF composite material and thickness for use in liner systems for internal repair of natural gas transmission pipelines.

Two simple cases were investigated. The first case was one in which the entire steel pipe has been lost to external corrosion, leaving only the liner to carry the external stress. The second case was one in which shear failure occurs in the matrix material between the layers of fibers. For the engineering analysis, a 508 mm (20 in.) OD pipe with a 6.35 mm (0.25 in.) wall, X65 pipe material was used since it is in the middle of the commonly used pipe size range for transmission pipelines (Figure 75). For this situation, the additional liner material could not be so thick as to prevent subsequent examinations of the adjacent steel pipeline by internal inspection devices, thus the thickness of the simulated liner was limited to less than 12.7 mm (0.5 in.).

Pipeline repairs that use internal addition of material are advantageous for many circumstances where access to the external surface of the pipe is restricted. Transportation of any material that will be added to the pipe wall must be considered, since it must ultimately be introduced from outside the pipe wall. Composites offer the opportunity to tailor the properties of the liner material in different directions to allow the material to be fit through the inside of the pipe and then be reshaped so it can be placed against the wall in the area where repair is desired.

Since repair is contemplated most often for external corrosion that exceeds the allowable limit sizes, we should consider that corrosion on the external surface may continue after the emplacement of the liner. As the external corrosion continues, the situation will get closer and closer to that where only the liner carries the stresses from the internal pressure in the pipe. A simple case can be used for estimation where the entire steel pipe has been lost to external corrosion and only the liner is left to carry the external stress.

We can choose an initial case in the middle of the commonly used range for transmission pipelines: a 508 mm (20 in.) outside diameter pipe with a 6.35 mm (0.25 in.) wall thickness made from X-65. For this pipeline, the additional liner material should not be so thick as to prevent subsequent examinations of the adjacent steel pipeline by internal inspection devices. This roughly limits the thickness of the liner  $t_c$  to less than 12.7 mm (0.5 in.) thickness.

We can define several criteria for the acceptability of the liner repair. One will involve the strength of the liner under a maximum pressure. One simple test case is that the liner should not be at greater risk of bursting than the remote un-repaired pipe under the pressure to reach a stress equal to the standard minimum yield strength of the pipe material. Using Barlow's formula, the pressure  $P$  to reach this hoop stress in the remote pipe is  $SMYS t/R$  or 11.3 MPa (1,646 psi).

Composite materials differ from steel in the expected stress-strain relationship. The composite liner material would be designed to be strong both in the pipe axial and hoop directions. In a strong direction, the composite will have a much lower peak strain before failure than steel, but the stress-strain curve up to that failure point will be much closer to elastic.

Figure 150 shows some estimates of the ranges of tensile strength and modulus for carbon fibers. The strength goes down as the modulus increases, a relationship that can be approximated by a linear relationship between the fiber modulus  $E_f$  and the tensile strength of the fiber  $\sigma_{fu}$

$$\sigma_{fu} = 4,140MPa - 1,380MPa \times \left( \frac{E_f}{29,300MPa} \right)$$

**Equation 3 - Tensile Strength of the Fiber  $\sigma_{fu}$  in MPa**

$$\sigma_{fu} = 600ksi - \left( \frac{200 \times E_f}{42,500} \right)$$

**Equation 4 - Tensile Strength of the Fiber  $\sigma_{fu}$  in ksi**

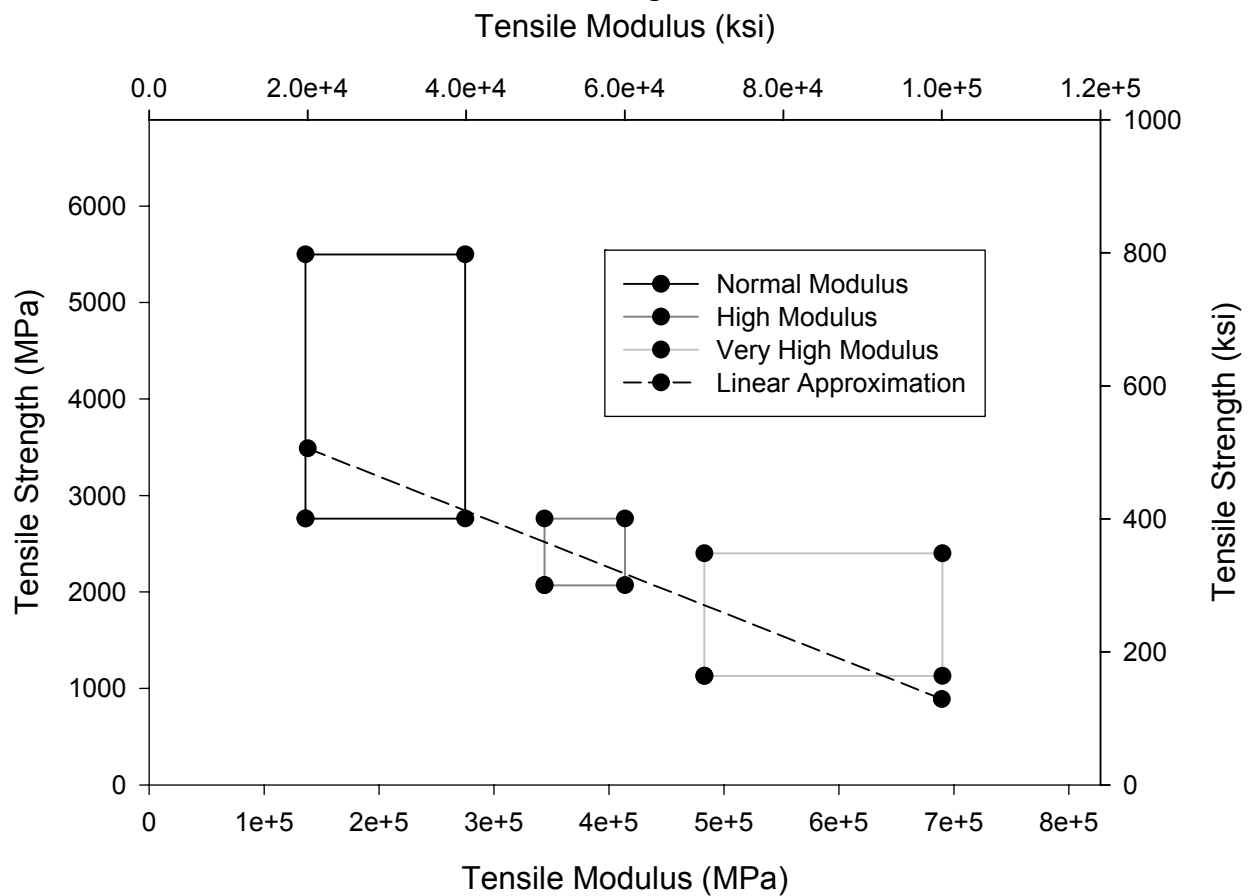


**Figure 150 - Relationship Between Modulus and Strength for Carbon Fibers**

The tensile strength and modulus of the composite can be estimated in the strong direction as 60% of the fiber strength and modulus, respectively. It will be appropriate to use a safety factor (SF) on failure strength in design to keep the strain well below the failure level.

Now the design condition for the composite becomes

$$P < \frac{SF \times 0.6 \times \sigma_{fu} \times t_c}{R - \frac{t}{2} - \frac{t_c}{2}}$$

**Equation 5 - Pressure to Reach Stress Equal to the SMYS of the Pipe Material**

Once SF has been set (with a value of 0.9) then we can determine the relationship between  $\sigma_{fu}$  and  $t_c$  that defines the minimum allowable based on the values chosen above:



$$\sigma_{fu} > 10,500 \text{MPa-mm} \times \left( \frac{1}{t_c} \right) - 10.5 \text{MPa}$$

**Equation 6 - Minimum Allowable Tensile Strength of the Fiber  $\sigma_{fu}$  in MPa**

$$\sigma_{fu} > 60.2 \text{ksi} - \text{in} \times \left( \frac{1}{t_c} \right) - 1.524 \text{ksi}$$

**Equation 7 - Minimum Allowable Tensile Strength of the Fiber  $\sigma_{fu}$  in ksi**

The fiber modulus can thus be given a maximum value using the linear approximation given above. This function is plotted in Figure 151.

$$E_f < \left( \frac{293,000}{1,380} \right) \times \left[ 4,140 - \left\{ 10,500 \times \left( \frac{1}{t_c} \right) - 10.5 \right\} \right] \text{ for } t_c \text{ in mm}$$

**Equation 8 - Maximum Fiber Modulus in MPa**

$$E_f < \left( \frac{42,500}{200} \right) \times \left[ 600 - \left\{ 60.2 \times \left( \frac{1}{t_c} \right) - 1.524 \right\} \right] \text{ for } t_c \text{ in inches}$$

**Equation 9 - Maximum Fiber Modulus in ksi**

If the fiber modulus is above the line in Figure 151, then the strength of the fibers will be too low to achieve the required strength in the composite.

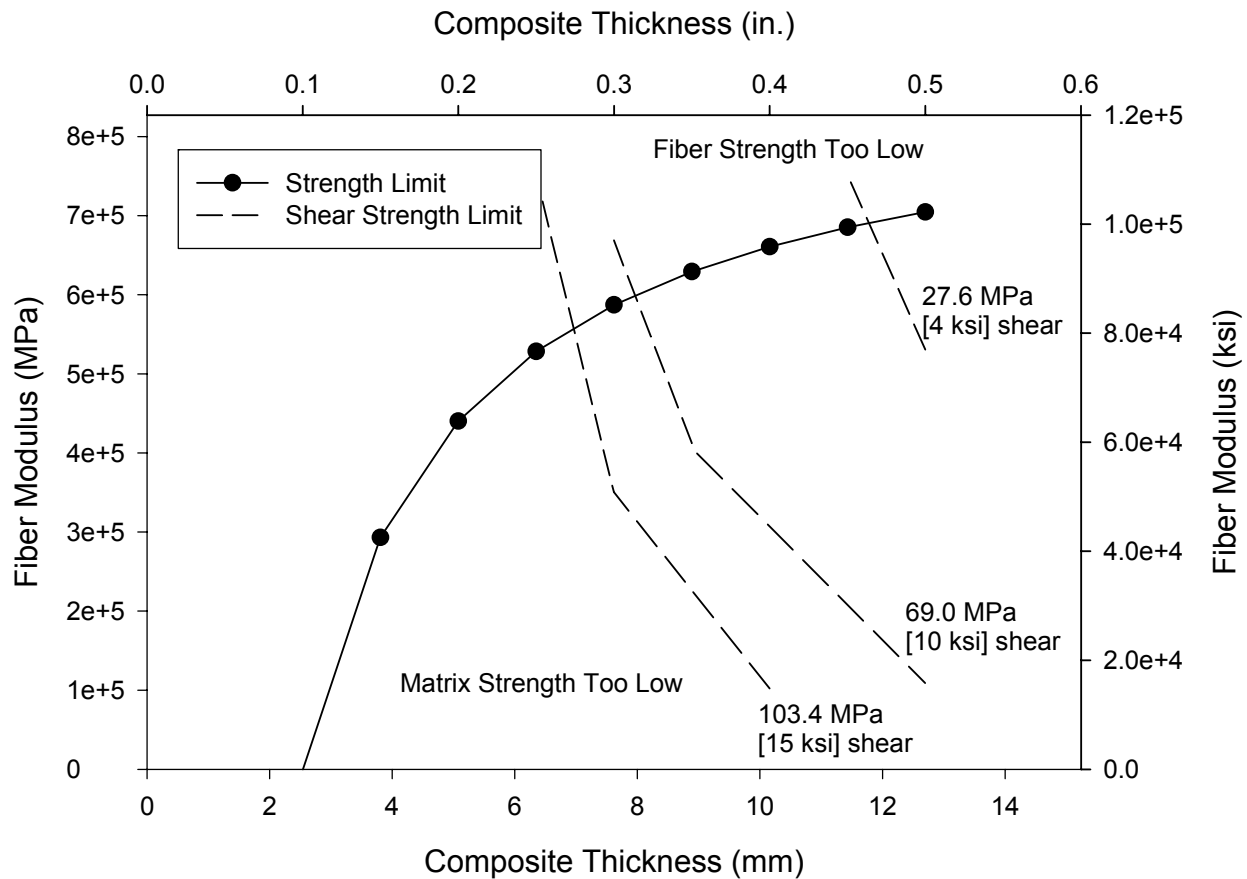


**Figure 151 - Design Space for Composite Liner**

This both limits the minimum thickness of the composite and limits the use of the highest modulus fibers, since they have lower ultimate strengths.

There can also be a problem with failure in shear of the matrix material between the layers of fibers. The simple case described above does not have shear between the fibers, but any case where the steel thickness varies in the hoop direction will have to transfer loads back and forth into the composite and induce shear where those transfers occur.

Again, we assume a simple case. Here the case is a relatively abrupt transition from the full wall thickness of steel to no steel remaining over a small sector of the circumference, with long axial length. In this case we have to transfer all of the load that was carried by the steel into the composite on one side of the loss of wall thickness and back into the steel on the other side. We can assume that all of the transfer occurs within a distance of four times the composite thickness, centered on the transition of the steel wall thickness to zero. Then we can estimate the shear between the composite layers based on an even transfer of the moment across this distance.

The moment per unit length is  $PRc$ , where  $c$  is a function of the thickness of pipe  $t_s$  and composite  $t_c$  and the moduli of the materials  $E_s$  and  $E_c$ . The  $c$  function can be written as

$$c = \frac{t_s \times E_s \times \left( \frac{t_s}{2} + \frac{t_c}{2} \right)}{(t_s \times E_s) + (t_c \times E_c)}$$

**Equation 10 -  $c$  as a Function of the Thickness of Both the Pipe and Liner, and the Moduli of Both the Pipe and Liner**

The shear stress  $\tau$  is as function of the shear force per unit length  $V$

$$\tau = \frac{\left( \frac{4}{3} \right) \times V}{t_c}$$

**Equation 11 - Shear Stress as a Function of Shear Force**

where

$$V = \frac{P \times R \times c}{2 \times t_c}$$

**Equation 12 - Shear Force per Unit Length**

The shear stress must not exceed the shear resistance of the matrix material in the composite. Some examples of shear resistance have been chosen and included in Figure 151.

The combination of the two design cases indicates that there is an optimum modulus of the fibers that allows the smallest thickness to be used. This optimum modulus is a function of the shear strength of the matrix material as well.

The second design case could be refined by finite element modeling, which would better estimate the peak shear forces in the composite.

Two economic limits should also be considered with carbon fiber composites. Higher modulus of the composite can be achieved by choosing high modulus fibers, but at increasing cost. Nevertheless, the more expensive manufacturing process for the highest modulus fibers has prevented wide scale use in infrastructure. The alternative described above is to go to larger thickness. Nevertheless, the larger thickness must be created in the composite by the addition of more sheets or “plies” of the fibers. As the number of plies increases, the manufacturing

difficulties multiply. The “comfort level” for number of plies would today probably be less than that which would be needed for a 12.7 mm (0.5 in.) thick composite liner.

The assessment above has only related to the hoop stress resistance of the composite. Axial strain resistance is also available from the composite because both the axial and hoop directions are strengthened by the fibers.

Composite liners need both high fiber modulus and high shear strength of the matrix, above that for many thermoplastics, to resist the types of shear stresses that can happen in composite liners. There are limits to how high the modulus of the fibers should go, because the strength drops off for the highest modulus fibers.

#### **4.8 - Carbon Fiber Reinforced Liner Repairs**

As compared to the GF reinforced liner trials, CF based composite materials have a much higher modulus of elasticity. The modulus of elasticity for commercial grade raw carbon fiber material is in the 206.8 GPa ( $30 \times 10^6$  psi) range, but this is reduced significantly when a matrix material is introduced. High grade raw carbon fiber materials have a modulus of elasticity that is in the 344.7 to 413.7 GPa ( $50$  to  $60 \times 10^6$  psi) range; however, these high grade raw carbon fiber materials are expensive and scarce. None the less, it may be possible to design a liner material that, when the matrix material is introduced, has a modulus of elasticity on the order of 95% of that for steel.

The cost of a liner composed of high-grade raw carbon fiber material will be high. The results of the survey of pipeline operators suggests that such a repair may still be useful in spite of the high cost for river crossings, under other bodies of water (e.g., lakes and swamps), in difficult soil conditions, under highways, under congested intersections, and under railway crossings.

When the GF polypropylene liner material was evaluated, it was found to be only marginally effective at restoring the pressure containing capabilities of the pipe. The important contributing physical property for a composite repair device is assumed to be an intrinsic modulus approximating that of steel. Based on materials cost and availability, a true match was not possible, so the alternative was to develop a composite having an attainable estimated modulus and adjust section thickness to achieve the desired stiffness.

The second issue is the ability to “access” that stiffness in the form of the composite physical properties. The limiting factor in composite failure is often interlaminar shear strength. A reaction to radial flexure will be a reacted shear stress that will attempt to separate the fabric lamina at the weak link, the resinous interface between fabric layers. A typical value for a “good” composite is an interlaminar shear strength of about 51.7 MPa (7,500 psi).

Taking these two requirements together, engineering analysis was employed to arrive at the composite requirements based on the assumed values for economical carbon fiber reinforcement with a vinylester resin system. It was determined that the patch should be on the order of 11.4 mm (0.45 in.) thick to approximate the stiffness of the steel while still maintaining an interlaminar shear strain below the 51.7 MPa (7,500 psi) benchmark.

#### **Test 04: Solid/Half-Round/Radial CF Patch (Quasi-Isotropic), Short/Deep Damage, 3M DP460 Adhesive**

For Test 04, a section of 508 mm (20 in.) diameter API 5L X52 pipe (Figure 35) with a stylized, long/shallow simulated corrosion defect (Figure 16) was used. Calculated with RSTRENG® to represent a 25% reduction in burst strength, defect dimensions were 127 mm (5 in.) long by 3.45 mm (0.136 in.) deep. A solid, half-round, radial CF patch was adhesively bonded on the ID of the pipe section with a 3M DP460 epoxy adhesive.

The general assembly techniques for Test 04 patch were used to produce patches for Test 04 through Test 07. Variations in fiber lay-up will be documented for each patch type. Resin amounts were modified to allow for the different configurations. The carbon fiber used in the fabrics was a standard 241,317 MPa (35,000 ksi) modulus carbon fiber.

For Test 04, EWI procured raw CF material and fabricated a 11.42 mm (0.45 in.) thick reinforcement patch using a "wet lay-up" process with a vinylester resin system. The carbon fabric was a 5-harness weave pattern with 6K tow ends with a density of 0.34 kg/m<sup>2</sup> (10 oz/yd<sup>2</sup>). The vinylester resin contained a mixture of FiberGlast 1110 vinylester resin and Derakane 510-40 vinylester resin, catalyzed with methyl ethyl ketone peroxide (MEKP). The 1110 resin was supplied pre-promoted. The mixture had a gel time of about 60-75 minutes and gave a typical 100-g cup exotherm at about 2 hours. The fabric was cut to give a quasi-isotropic lay-up with ± 45 degree for the outer layers and 0, 90 degree layers for the interleaves. A 0.57 kg (20 oz.) woven roving, glass fabric outer layer was employed for both faces of the patch. The inner glass face (i.e., outside diameter of the patch) was included to act as a galvanic corrosion barrier between the CF composite and the steel. The other glass layer was a proposed protective face for the exposed portion of the patch.

The Test 04 composite patch was fabricated with a wet lay-up process followed by vacuum bagging. To develop the technique, the first trial was a flat panel, approximately 254 mm (10 in.) by 254 mm (10 in.). It was determined that additional layers of fabric were needed to increase section thickness. This was accomplished by including extra 0, 90 degree internal layers in the semi-circular patch. Once the subscale panel was satisfactory, the same techniques were applied to produce all four full-scale patches (Test 04 through Test 07).

The Test 04 half-round composite patch had an outside diameter that matched the internal diameter of the pipe section. The patch was 711 mm (28 in.) in radial length, 254 mm (10 in.) in axial length, by 11.42 mm (0.45 in.) thick. The semi-circular patch lay-up consisted of 27 layers; layers 1 and 27 were glass woven roving. The remainder consisted of alternating layers of  $\pm 45$  degree and 0, 90 degree (fiber orientation) to produce the quasi-isotropic patch (Table 6). A semi-circular mold was produced from a cut half-round of 508 mm (20 in.) diameter pipe (Figure 43).

The 50/50 mixture FiberGlast 1110 vinylester resin and Derakane® 510A-40 vinylester resin was catalyzed at 1.25% MEKP (9% Oxygen equivalent). The assembly required about 1,600 g (56.43 fl oz.) of catalyzed resin giving a cup gel time of 75 minutes. Each layer was pre-impregnated with resin as the lay-up proceeded. The hand lay-up was prepared inside the mold with the applied vacuum being maintained until gellation and initial cure was assured (approximately 4 hours). The assembly was then cured overnight. After excising the cured panel, it was trimmed to insertion dimensions. Forced post-cure was not required to maintain dimensions, however the panels were usually post cured at 65°C (150°F) to allow them to achieve full cure faster. The calculated fiber volume was between 40% - 45%.

To facilitate Test 04 patch installation, the outer surface of the patch was grit-blasted using 50 - 80 grit Alumina to remove surface resin (Figure 41). Similarly, the installation area inside the pipe was grit-blasted to a near-white blast with 50 - 80 grit Alumina (Figure 42). After cleaning, a liberal coating of 3M DP460 epoxy adhesive was applied to the internal faying surface and a thin coating was applied to the patch faying surface (Figure 43). The patch and pipe section were mated as shown in Figure 44. Bar clamps were used along the axis of the pipe to hold the patch in place for cure. Figure 45 shows the adhesive squeeze-out being removed prior to forming a fillet as shown in Figure 46.

After two weeks of adhesive cure time, end caps were welded on the pipe section and the specimen was hydrostatically tested to failure (Figure 152). Rupture occurred in the area of reduced thickness.



**Figure 152 - Test 04 Pipe With CF Patch Repair After Burst Test**

Figure 153 is a closer view of the failure initiation site. Figure 154 clearly shows that the failure was caused by interlaminar shear mostly between the anti-corrosion glass layer and the carbon layer (1 → 2 layer interfacial failure is common in composites). There was no evidence of disbonding between the pipe and the composite liner.



**Figure 153 - Test 04 Failure Initiation Site**



**Figure 154 - Magnified Test 04 Failure Initiation Site**

Table 24 contains the predicted and measured burst pressures for the 508 mm (20 in.) API 5L X52 pipe sections in the virgin, un-repaired (short/deep), and Test 04 repaired conditions. Table 24 also contains a predicted burst pressure for virgin pipe based on Barlow's formula using the measured ultimate tensile strength of the pipe material. Not surprisingly, the measured burst pressure of the un-repaired pipe section was 9% lower than the measured burst pressure of the virgin pipe section. Although the resultant burst pressure for the Test 05 repair was 41% greater than the pressure corresponding to 100% SMYS of 8.96 MPa (1,300 psi) and 56% higher than the RSTRENG® predicted burst pressure for an un-repaired pipe, it was in fact only 6% less than the measured virgin pipe performance and 28% lower than the predicted virgin pipe performance. As compared to the measured performance of the un-repaired pipe section, Test 04 was actually 4% higher.

Pipe Diameter	Pipe Condition	Predicted Burst Pressure		Actual Burst Pressure	
		(MPa)	(psi)	(MPa)	(psi)
508.0 mm (20 in.)	Virgin	15.03	2,180	16.03	2,325
	Simulated Damage Short/Deep Un-Repaired	6.72	974	14.56	2,112
	Simulated Damage Repaired with Medium Grade CF Liner (Test 04)	-	-	15.13	2,194

**Table 24 - Summary of Predicted vs. Actual Hydrostatic Burst Pressure Values Test 04**



Test 01 (weld repair) had a burst pressure that was 10% lower than the pipe section with un-repaired damage and was 24% lower than the actual burst pressure for virgin pipe. Test 02 (GF liner with long/shallow damage) had a burst pressure that was 1% higher than the pipe section with un-repaired damage and was 38% lower than the predicted burst pressure for virgin pipe. Test 03 (GF liner with short/deep damage) had a burst pressure that was 7% greater than the pipe section with un-repaired damage and was 28% lower than the predicted burst pressure for virgin pipe. Test 04 had a burst pressure that was 4% greater than the pipe section with un-repaired damage and only 6% lower than the actual burst pressure for virgin pipe. In comparison to tests conducted to this point in the research program, Test 04 results indicate that CF liner repair provides marginally improved capability to restore pressure capability of a pipeline as compared to the measured performance of GF liner repair and weld deposition repair.

Test 04 was an excellent evaluation of a CF reinforced liner material. The patch design requires optimization, perhaps allowing a tapered design or smaller dimensions. The vacuum-bagging process also requires refinement. A Vacuum Assisted Resin Transfer Molding (VARTM) approach would be optimal as it could produce far better fiber compaction and would allow the production of more complex patch designs

Fiber-reinforced composite repairs applied to the outside of exposed pipelines have become commonplace in the gas transmission pipeline industry. Based on the results of Tests 01 through 04, the application of CF liner repair technology to internal repair appeared promising, although further development was required to improve material properties and to optimize patch configuration. Another promising aspect of internal pipeline repair using fiber reinforced composite materials is that there is no apparent technical limitation for performing the repairs while the pipeline remains in service.

### **Test 05: Thin Radial CF Patch (all 0, 90), Short/Deep Damage, 3M DP460 Adhesive**

For Test 05, a section of 508 mm (20 in.) diameter API 5L X52 pipe (Figure 35) with a stylized, short/deep simulated corrosion defect (Figure 16) was used. Calculated with RSTRENG® to represent a 25% reduction in burst strength, defect dimensions were 127 mm (5 in.) long by 3.45 mm (0.136 in.) deep. A CF patch in a "pressure bandage" configuration (Figure 47) was adhesively bonded on the ID of the pipe section with a 3M DP460 epoxy adhesive.

As indicated above, the general assembly techniques for Test 04 patch were used to produce patches for Test 04 through Test 07. The carbon fiber used in the fabrics was a standard 241,317 MPa (35,000 ksi) modulus carbon fiber. The patch was 711 mm (28 in.) in radial length, 254 mm (10 in.) in axial length, by 11.42 mm (0.45 in.) thick.

Test 05 patch differed from the Test 04 patch in configuration. Overall patch dimensions were still 711 mm (28 in.) in radial length and 254 mm (10 in.) in axial length; however, the 254 mm (10 in.) by 254 mm (10 in.) center portion of the patch was built to the full 11.43 mm (0.45 in.) thickness using the same quasi-isotropic layout as above. Within that construction, extended layers of 0, 90 plies were interleaved, as part of and preserving the quasi-isotropic lay-up. The extensions served as "wings" for additional bonding of the "pressure bandage" into the pipe. The center portion then had the full 27-layers of quasi-isotropic lay-up while the wing-extensions had 8 layers of 0, 90 layers which compacted under vacuum to about 3.81 mm (0.15 in.).

The Test 05 "pressure bandage" patch was allowed to cure for approximately two weeks before installation. After the patch was installed in the pipe section, it was allowed to cure for another week before hydrostatic testing.

Figure 155 shows the Test 05 CF patch after burst testing. The inset pictures are close up views of failure locations.

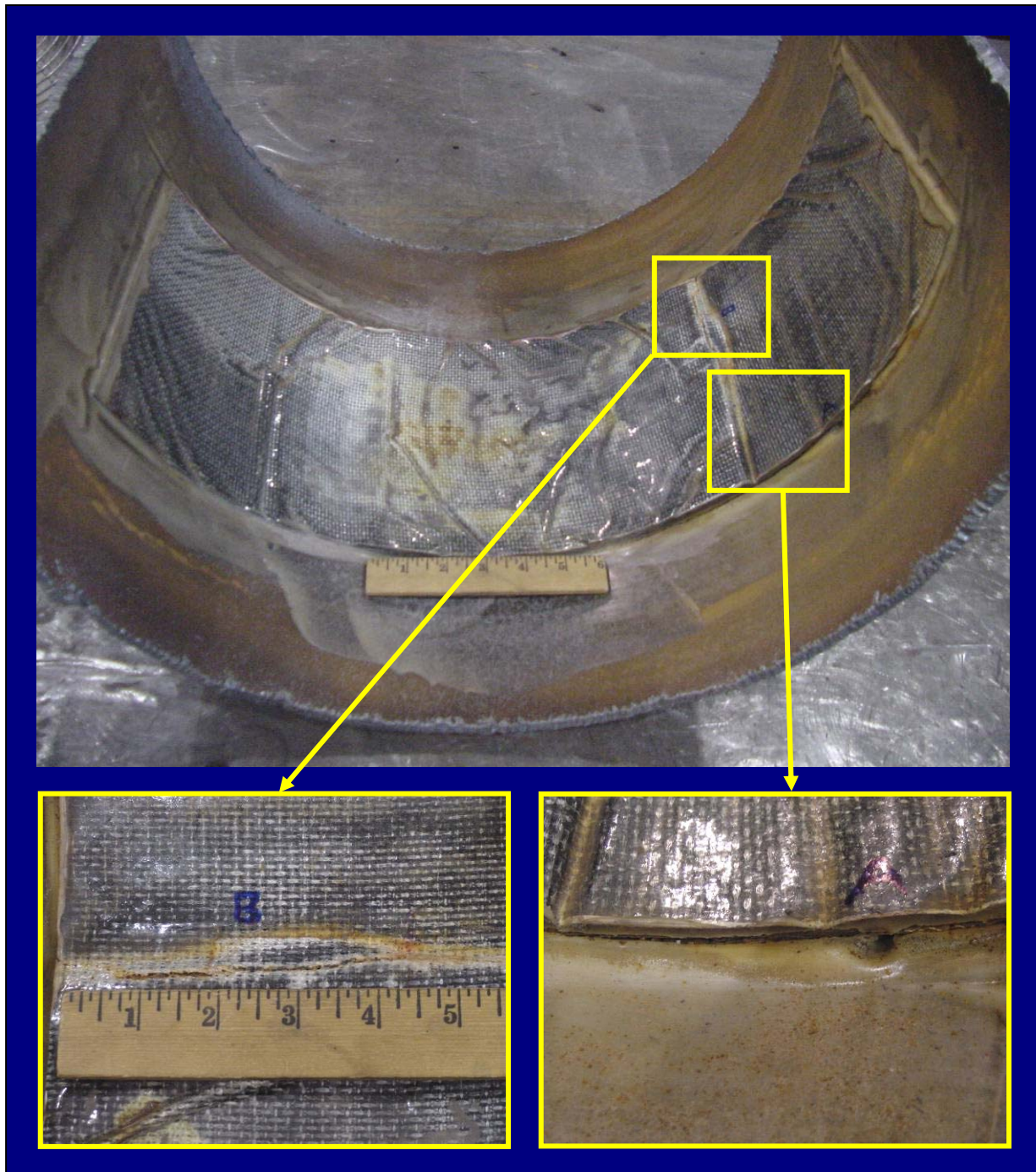


**Figure 155 - Test 05 CF Patch with Failure Locations**

The pipe section with Test 05 patch was then sectioned in the circumferential direction. Figure 156 and Figure 157 show cross sections taken from locations in the area of the simulated corrosion damage. Figure 156 shows a full failure of the pipe and composite repair. Figure 157 shows a failure of the pipe and the disbondment between the ID of the pipe and the composite repair. This failure was caused by interlaminar shear, which appears to have occurred after the steel reached the plastic range (i.e., after the yield point of the steel was exceeded).



**Figure 156 - Failure of Test 05 Pipe and Composite Repair**

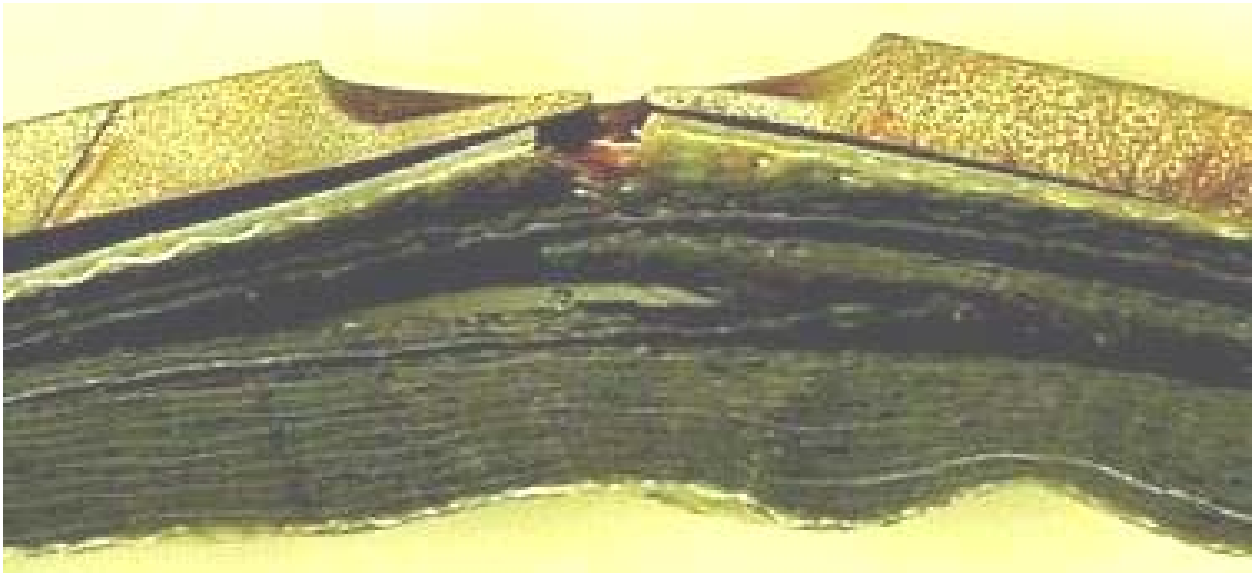


**Figure 157 - Disbondment Between Pipe and Test 05 Patch at Pipe Failure Site**

Table 25 contains the predicted and measured burst pressures for the 508 mm (20 in.) API 5L X52 pipe sections in the virgin, un-repaired (short/deep), and Test 05 repaired conditions. Table 25 also contains a predicted burst pressure for virgin pipe based on Barlow's formula using the measured ultimate tensile strength of the pipe material. The measured burst pressure of the un-repaired pipe section was 18% lower than the measured burst pressure of the virgin pipe section. While the resultant burst pressure for Test 05 repair was 27% greater than the pressure corresponding to 100% SMYS (8.96 MPa (1,300 psi)) and 45% higher than the RSTRENG® predicted burst pressure for an un-repaired pipe, compared to actual results it was 16% less than the measured virgin pipe performance and only 2% greater than the measured performance of the un-repaired pipe section.

Pipe Diameter	Pipe Condition	Predicted Burst Pressure		Actual Burst Pressure	
		(MPa)	(psi)	(MPa)	(psi)
508 mm (20 in.)	Virgin	13.82	2,005	14.63	2,122
	Simulated Damage Short/Deep Un-Repaired	6.72	974	12.04	1,746
	Simulated Damage Repaired with High Grade CF Liner (Test 05)	-	-	12.25	1,777

**Table 25 - Summary of Predicted vs. Actual Hydrostatic Burst Pressure Values Test 05**

Test 04 was a 4% improvement over the un-repaired pipe and a 6% decrease as compared to the performance of a virgin pipe. Test 05 repair was only a 2% improvement over the performance of the un-repaired pipe and a 16% decrease as compared to the performance of a virgin pipe. These results indicate that Test 05 was somewhat less effective than Test 04. Prior to the next round of testing, the CF liner material was evaluated to increase patch performance.

### Optimized Requirements for CF Test Patches

Composite design requirements are based on strength, modulus, and thickness. Composite performance is based on interlaminar shear (resin failure between the layers predominates), modulus (bending under load generates interlaminar shear), and thickness (to provide adequate stiffness to operate the load point below the interlaminar shear value).

For patch material testing, three types of composite structures were produced. All were made with carbon fiber cloth and vinylester (VE) resin. The cloth had no special treatment to compatibilize it with the VE resin. The carbon fiber fabric had a nominal weight of 10 oz/yd<sup>2</sup> with 6K tows.

Three composite lay-up structures were designed to evaluate the mechanical properties of the material:

- Quasi-isotropic lay-up (with alternating layers of 0, 90 and  $\pm 45^\circ$  with extra 0, 90 near the thickness-center); thickness = 11.43 mm (0.45 in.)
- 0, 90 only lay-up; thickness = 11.43 mm (0.45 in.)
- Uniaxial 0 only lay-up; thickness = 8.89 mm (0.35 in.).

For the first two, fiberglass close-out layers were included on the “steel side” as a proposed corrosion barrier at the steel/carbon fiber interface and as the top layer (bag side). The uniaxial panel had no fiberglass. The carbon-glass constructions produce ~40% w/w carbon fiber, with a density of 1.47-1.51 g/cc. The uniaxial panel contains >70% carbon fiber w/w, so a higher

tensile modulus is anticipated (its density was measured at 1.44 g/cc, reflecting mostly the absence of fiberglass). The panels were produced using a combined hand lay-up-vacuum bagging technique.

The results for the tested systems are shown in Table 15 for both normal and post cured samples (the averages are shown graphically in Figure 102). Post curing produced no significant mechanical advantage over the ambient cure. The most striking differences were the significant increases in tensile strength and modulus for the 0, 90 construction in comparison with the quasi-isotropic construction. The replacement of every other layer with a 0, 90 resulted in a 50% improvement in tensile strength and a 70% improvement in modulus.

ILS was not affected by panel lay-up architecture. Based on the dimensions and the flexural failure load, the ILS value appears to be about 10.3 MPa (1,500 psi). This is lower than desired, but not unexpected given the lack of fiber treatment for resin compatibility and the notoriously low toughness for VE resins. Notice also the *flexural* modulus ranges from 586,578 MPa (85,076 ksi) to 636,241 MPa (92,279 ksi), meaning the panels are somewhat forgiving in flex. That may be advantageous for a pipe repair application.

Based on these results, the patch designed for Test 06 (as compared to the Test 05 patch) was a thinner, all 0,90 construction with a higher modulus.

#### **Test 06: Thin Radial CF Patch (all 0, 90), Short/Deep Damage, 3M DP460 Adhesive**

For Test 06, a section of 508 mm (20 in.) diameter API 5L X52 pipe (Figure 35) with a stylized, short/deep simulated corrosion defect (Figure 16) was used. Calculated with RSTRENG® to represent a 25% reduction in burst strength, defect dimensions were 127 mm (5 in.) long by 3.45 mm (0.136 in.) deep. A thin CF patch in a "pressure bandage" configuration (Figure 48) was adhesively bonded on the ID of the pipe section with a 3M DP460 epoxy adhesive.

The general assembly techniques for Test 04 patch were used to produce patches for this test. The carbon fiber used in the fabrics was a standard 241,317 MPa (35,000 ksi) modulus carbon fiber. As compared to the Test 05 patch, the Test 06 patch was a thinner all 0,90 construction with a higher modulus, that was produced with 16 layers of carbon fabric along with the two glass layers as 1<sup>st</sup> and 18<sup>th</sup> plies to produce a panel. The patch was 711 mm (28 in.) in radial length, 254 mm (10 in.) in axial length, and approximately 7.62 mm (0.3 in.) thick.

The Test 06 patch was allowed to cure for approximately two weeks before installation. After the patch was installed in the pipe section, it was allowed to cure for another week before hydrostatic testing.

Figure 158 shows the failure of the Test 06 patch from the OD of the pipe section.



**Figure 158 - Test 06 Damage after Burst Testing**

Postmortem analysis indicate that the Test 06 patch failed due to interlaminar shear, which appears to have occurred after the steel reached the plastic range (i.e., after the steel's yield point was exceeded). This failure mode was very similar to that of the Test 05 patch.

Table 26 contains the predicted and measured burst pressures for the 508 mm (20 in.) API 5L X52 pipe sections in the virgin, un-repaired (short/deep), and Test 06 repaired conditions. Table 26 also contains a predicted burst pressure for virgin pipe based on Barlow's formula using the measured ultimate tensile strength of the pipe material. Although the resultant burst pressure for the Test 05 repair was 33% greater than the pressure corresponding to 100% SMYS (8.96 MPa (1,300 psi)) and 78% higher than the RSTRENG® predicted burst pressure for an un-repaired pipe, it was in fact 18% less than the measured virgin pipe performance and 17% higher than the measured performance of the un-repaired pipe section.

Pipe Diameter	Pipe Condition	Predicted Burst Pressure		Actual Burst Pressure	
		(MPa)	(psi)	(MPa)	(psi)
508.0 mm (20 in.)	Virgin	13.82	2,005	14.63	2,122
	Simulated Damage Short/Deep Un-Repaired	6.69	970	10.16	1,473
	Simulated Damage Repaired with High Grade CF Liner (Test 06)	-	-	11.93	1,730

**Table 26 - Summary of Predicted vs. Actual Hydrostatic Burst Pressure Values Test 06**

Test 04 (quasi-isotropic CF patch) was a +4% improvement over the un-repaired pipe and a -6% decrease as compared to the performance of a virgin pipe. Test 05 (thin, all 0, 90 CF patch) was only a +2% improvement over the performance of the un-repaired pipe and a -16% decrease as compared to the performance of a virgin pipe. Test 06 (thinner, all 0, 90 CF patch) was a +17% increase over the un-repaired pipe and a -18% decrease as compared to the performance of a virgin pipe. These results indicate that Test 06 was more effective than previous CF liner repairs Test 04 and Test 05.

### **Test 07: Thick, Axial CF patch (all 0, 90), Long/Shallow Damage, 3M DP460 Adhesive**

The next round of testing was conducted to evaluate the ability of the CF reinforced composite liner to overcome damage that exceeds the length for which hoop stress can redistribute itself around the ends of the damage. This length is defined in Equation 1 in terms of pipe diameter  $d$  and wall thicknesses  $t$ . For a 508 mm (20 in.) diameter pipe with a 6.35 mm (0.25 in.) wall thickness,  $L$  is equal to 254 mm (10 in.) in Equation 1. In order to perform an experiment to that evaluates the ability of carbon fiber-reinforced repair system to restore the pressure-containing ability of the pipe with a long/shallow defect, an area of simulated damage in excess of a 254 mm (10 in.) in length is required. A simulated defect of 381 mm (15 in.) long by 2.54 mm (0.1 in.) deep was therefore introduced into the pipe sections for this investigation.

For Test 07, a section of 508 mm (20 in.) diameter API 5L X52 pipe (Figure 35) with a long/shallow simulated corrosion defect (Figure 17) was used. Calculated with RSTRENG® to represent a 25% reduction in burst strength, defect dimensions were 381 mm (15 in.) long by 2.74 mm (0.108 in.) deep. A thick CF patch was adhesively bonded on the ID of the pipe section with a 3M DP460 epoxy adhesive.

The general assembly techniques for Test 04 patch were used. The carbon fiber used in the fabrics was a standard 241,317 MPa (35,000 ksi) modulus carbon fiber. As compared to the Test 06 patch, the Test 07 patch was an all 0, 9- construction (same thickness) with an all 0, 90 construction with the long axis oriented axially rather than radially (see Figure 49). The patch was (10 in.) in radial length, 711 mm (28 in.) in axial length, and 7.62 mm (0.3 in.) thick, consisting of 18 layers (layers 1 and 18 were glass woven roving). Calculated fiber volume was 50% - 55%.

The Test 07 patch was allowed to cure for approximately two weeks before installation. After the patch was installed in the pipe section, it was allowed to cure for another week before hydrostatic testing.

Figure 159 shows the OD of the Test 07 pipe section with long/shallow simulated damage after burst testing.





**Figure 159 - Test 07 Damage After Burst Test**

Figure 154 and Figure 155 show the ID of the Test 07 pipe section and the OD of the patch, respectively, after burst testing.



**Figure 160 - Inside Surface of Test 07 Pipe Section After Burst Test**



**Figure 161 - Test 07 Patch after Burst Testing**

Postmortem analysis of Test 07 indicates that the adhesive between the outside of the patch and the inside of the pipe failed in shear when the pipe material began to globally yield.

Table 27 contains the predicted and measured burst pressures for the 508 mm (20 in.) API 5L X52 pipe sections in the virgin, un-repaired (long/shallow), and Test 07 repaired conditions. Table 26 also contains a predicted burst pressure for virgin pipe based on Barlow's formula using the measured ultimate tensile strength of the pipe material. Although the resultant burst pressure for the Test 07 repair was 14% greater than the pressure corresponding to 100% SMYS (8.96 MPa (1,300 psi)) and 53% higher than the RSTRENG® predicted burst pressure for an un-repaired pipe, it was in fact 30% less than the measured virgin pipe performance and essentially the same as the measured performance of the un-repaired pipe section.

Pipe Diameter	Pipe Condition	Predicted Burst Pressure		Actual Burst Pressure	
		(MPa)	(psi)	(MPa)	(psi)
508.0 mm (20 in.)	Virgin	13.82	2,005	14.63	2,122
	Simulated Damage Long/Shallow Un-Repaired	6.69	970	10.16	1,473
	Simulated Damage Repaired with High Grade CF Liner (Test 07)	-	-	10.26	1,488

**Table 27 - Summary of Predicted vs. Actual Hydrostatic Burst Pressure Values Test 07**

Test 04 (quasi-isotropic CF patch) was a 4% improvement over the un-repaired pipe and a 6% decrease as compared to the performance of a virgin pipe. Test 05 (thin, all 0, 90 CF patch) was only a 2% improvement over the performance of the un-repaired pipe and a -16% decrease as compared to the performance of a virgin pipe. Test 06 (thinner, all 0, 90 CF patch) was a 17% increase over the un-repaired pipe and a 18% decrease as compared to the performance of a virgin pipe. Test 07 (axial orientation of Test 06 patch for long/shallow defect) was essentially the same as the un-repaired pipe and a 30% decrease as compared to the performance of a virgin pipe. These results indicate that Test 07 was much less effective at restoring the pressure containing capability of a pipeline as compared to Test 04 through Test 06.

#### 4.9 - Adhesively Bonded Steel Patch Repair

As a result of the May 12, 2005 project review meeting at NETL, the project team was directed to investigate the feasibility of using a steel patch, instead of a composite patch, to internally repair an external defect.

##### Test 08: Adhesively Bonded Steel Patch Repair, Short/Deep Damage

For Test 08, a section of 508 mm (20 in.) diameter API 5L X52 pipe with a stylized, short/deep simulated corrosion defect (Figure 16) was used. Calculated with RSTRENG® to represent a 25% reduction in burst strength, defect dimensions were 127 mm (5 in.) long by 3.45 mm (0.136 in.) deep. A steel patch (Figure 162) was adhesively bonded on the ID of the pipe section with a 3M DP460 epoxy adhesive.

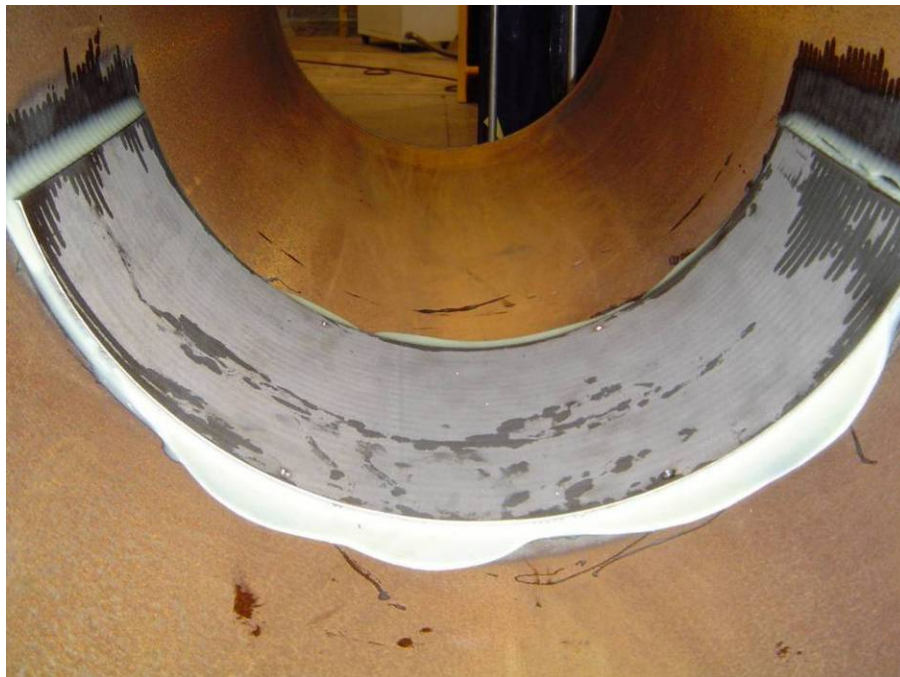


**Figure 162 - Test 08 Post-Epoxy Cured Steel Patch Repair**

The steel patch was fabricated from a section of the same 508 mm (20 in.) diameter by 6.35 mm (0.25 in.) thick API 5L X52 pipe as the pipe section that was prepared with simulated corrosion. The steel patch was custom rolled to a 495.3 mm (19.5 in.) diameter so the patch would fit snugly inside the 508 mm (20 in.) diameter pipe section with simulated corrosion. The same epoxy used for the composite repairs was used to install the steel patch inside the pipe section. After the patch was installed in the pipe section, it was allowed to cure for a week before hydrostatic testing.

Figure 163 and Figure 164 show the OD and ID, respectively, of the Test 08 pipe section with steel patch repair after burst testing.



**Figure 163 - Test 08 Damage after Burst Test**



**Figure 164 - Inside of Test 08 Pipe Section After Burst Test**

Postmortem analysis indicates that, as in Test 07, the adhesive between the outside of the patch and the inside of the pipe failed in shear when the pipe material began to globally yield.

Table 28 contains the predicted and measured burst pressures for the 508 mm (20 in.) API 5L X52 pipe sections in the virgin, un-repaired (short/deep), and Test 08 repaired conditions. Table 26 also contains a predicted burst pressure for virgin pipe based on Barlow's formula using the measured ultimate tensile strength of the pipe material. Although the resultant burst pressure for the Test 08 repair was 33% greater than the pressure corresponding to 100% SMYS (8.96 MPa (1,300 psi)) and 78% higher than the RSTRENG® predicted burst pressure for an un-repaired pipe, it was in fact 18% less than the measured virgin pipe performance and essentially the same as the measured performance of the un-repaired pipe section.

Pipe Diameter	Pipe Condition	Predicted Burst Pressure		Actual Burst Pressure	
		(MPa)	(psi)	(MPa)	(psi)
508.0 mm (20 in.)	Virgin	13.82	2,005	14.63	2,122
	Simulated Damage Short/Deep Un-Repaired	6.72	974	12.04	1,746
	Simulated Damage Repaired with High Grade CF Liner (Test 08)			11.96	1,734

**Table 28 - Summary of Predicted vs. Actual Hydrostatic Burst Pressure Values Test 08**

Test 08 exhibited a performance that was essentially the same as the un-repaired pipe and a -18% decrease as compared to the performance of a virgin pipe. These results are comparable to the average performance of a CF patch repair and indicate that Test 08 was less than effective at restoring the pressure containing capability of a pipeline for the defect geometry that was used.

#### **4.10 - Selection of Defect Size / Failure Mechanism**

Tests 04 through 08 provided some interesting insight into the ability of pipe sections with wall loss to withstand internal pressure and the conservative nature of RSTRENG. Even though the burst pressures predicted using RSTRENG represent a 30 to 40% reduction, the actual burst pressures are quite high, often well above the pressure that corresponds to 100% SMYS prior to repair. The target level of performance for other repair methods that have been developed for gas transmission pipelines is for the repair to be able to withstand a pressure that corresponds to 100% of SMYS. In each of the preceding tests, the burst pressures for pipe with repairs exceeded the pressure that corresponds to 100% of SMYS. Without the defects being

significant enough to impinge upon the pressure that corresponds to 100% of SMYS, improvements in performance are difficult to measure.

Analysis of the results indicates that for a 5.0-in. long by 0.136-in. deep defect in 20-in. diameter by 0.250-in. thick API 5L-X52 pipe, failure of defect is preceded by onset of global yielding of the pipe material (i.e., the defect is not significant enough to fail prior to yield strength being exceeded) even though RSTRENG predicts a 25% reduction in burst pressure. This is significant in terms of the performance of internal repairs that are adhesively bonded. When pipe material begins to globally yield, the adhesive tends to fail by shear allowing pressure to act upon the defect. Therefore, the selection of defect sizes for Tests 04 through 08 may have been unfortunate. In other words, these defects were not significant enough to allow the ability of the repairs to restore pressure containing capability to be effectively demonstrated. Defects that are more significant would have allowed improvement in burst pressure to be demonstrated. For the subsequent tests, defects that represent a 50 to 60% reduction in RSTRENG-predicted burst pressure were used.

#### **4.11 - Adhesively Bonded Helically Wound Steel Strip Repair Trials**

Inspired by the steel patch repair, EWI conceived a concept whereby helically wound steel strip material was adhesively bonded on the ID of a pipe section. Theoretically, several layers of steel strip material could be added to restore material loss on the OD. A demonstration was then conducted on a short section of 609.6 mm (24 in.) pipe that would not be hydrostatically tested to develop the installation procedure. The helically wound steel strip was installed with the same epoxy used for the CF liners and the steel patch (3M DP460). Figure 165 is a picture of one layer of the helically wound steel strip installed in a demonstration pipe section.

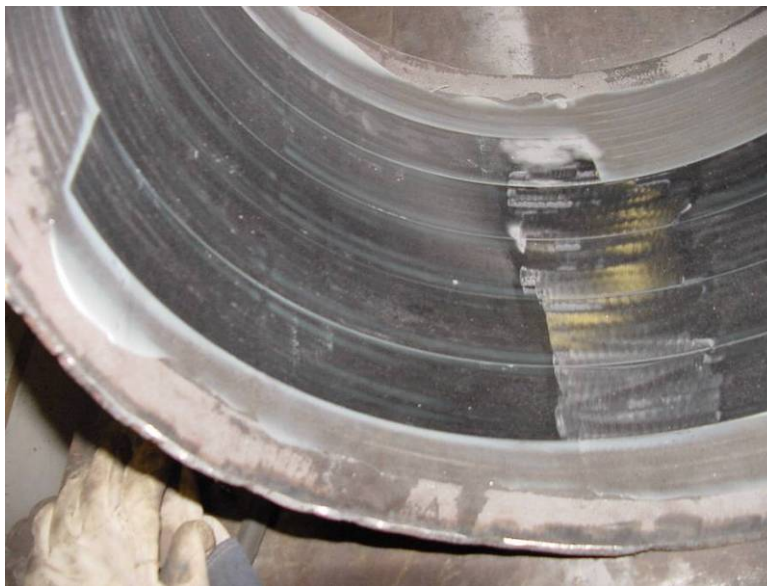


**Figure 165 - Completed Helically Wound Steel Strip Repair**

Figure 166 is a close up of the same installation which shows good intimate contact between the adjacent windings of the steel strip and between the OD of the helically wound steel strip and the ID of the pipe.



**Figure 166 - Close Up of Completed Helically Wound Steel Strip Repair**

Based on the successful mating and adhesion achieved in the demonstration trial, the next test was designed to evaluate the performance of this repair method.

#### **Test 09: High Strength Steel Strip, Short/Extra Deep Damage, 3M DP460 Epoxy Adhesive**

For Test 09, a section of 508 mm (20 in.) diameter API 5L X52 pipe with a short/extra deep simulated corrosion defect was used. Calculated with RSTRENG® to represent a 50% reduction in burst strength, defect dimensions were 127 mm (5 in.) long by 4.75 mm (0.187 in.) deep. The same epoxy used for the CF liner repairs (3M DP460) was used to install three layers of helically wound steel strip inside the pipe section.

The steel strip material was 50.8 mm (2 in.) wide by 1.1 mm (0.044 in.) thick. It had an ultimate tensile strength of 965.27 MPa (140 ksi) (Table 16) and is referred to as the "high strength" strip material throughout this report. The strip was custom rolled to form a 533.4 mm (21 in.) diameter helix. After the three layers of steel strip were adhesively bonded in the pipe section, it was allowed to cure for one week before hydrostatic testing.



Figure 167 shows the defect on the OD of the Test 09 pipe section with helically wound steel strip repair after burst testing.



**Figure 167 - Test 09 Damage after Burst Test**

Postmortem analysis indicates that Test 09 also failed when the pipe material began to globally yield. Upon doing so, the adhesive failed in either tension or shear, which allowed a leak path through the layers of helically wound steel strip to develop. This in turn allowed pressure to act upon the defect, after which it failed. It is interesting to note that the failure was a leak (as shown in Figure 161) as opposed to a rupture.

Table 29 contains the predicted and measured burst pressures for the 508 mm (20 in.) API 5L X52 pipe sections in the virgin, un-repaired (short/extra deep), and Test 09 repaired conditions. Table 29 also contains a predicted burst pressure for virgin pipe based on Barlow's formula using the measured ultimate tensile strength of the pipe material. Although the resultant burst pressure for the Test 09 repair was 34% greater than the pressure corresponding to 100% SMYS (8.96 MPa (1,300 psi)) and 178% higher than the RSTRENG® predicted burst pressure for an un-repaired pipe, it was actually 18% lower than the measured virgin pipe performance. The failure pressure was, however, a significant 34% higher than the measured performance in the un-repaired pipe section.

Pipe Diameter	Pipe Condition	Predicted Burst Pressure		Actual Burst Pressure	
		(MPa)	(psi)	(MPa)	(psi)
508.0 mm (20 in.)	Virgin	13.82	2,005	14.63	2,122
	Simulated Damage Short/Extra Deep Un-Repaired	4.32	627	8.94	1,298
	Simulated Damage High Strength Steel Strip 3M DP460 Adhesive Repair (Test 09)	-	-	12.01	1,743

**Table 29 - Summary of Predicted vs. Actual Hydrostatic Burst Pressure Values Test 09**

Test 09 exhibited a 34% increased performance over the over the un-repaired pipe and an 18% decrease as compared to the performance of a virgin pipe. These results far exceed the average performance of a CF patch repair and indicate that Test 09 vastly increased the pressure containing capability of a damaged pipeline. Test 09 was the most promising repair technology evaluated thus far in the test program. The next test was designed to evaluate the effect of a more elastic adhesive system on the helically wound steel strip repair technology.

**Test 10: High Strength Steel Strip, Short/Extra Deep Damage, Lord 7542 A/D Adhesive**

For Test 10, a section of 508 mm (20 in.) diameter API 5L X52 pipe with a short/extra deep simulated corrosion defect was used. Calculated with RSTRENG® to represent a 50% reduction in burst strength, defect dimensions were 127 mm (5 in.) long by 4.75 mm (0.187 in.) deep. A less-brittle urethane adhesive (Lord 7542 A/D) was used to install three layers of high strength helically wound steel strip inside the pipe section. The strip was custom rolled to form a 533.4 mm (21 in.) diameter helix as in Test 09. The three layers of steel strip were adhesively bonded in the pipe section with a smaller quantity of adhesive. The resultant repair was allowed to cure for a week before hydrostatic testing.

Figure 168 shows the defect on the OD of the Test 10 pipe section with helically wound steel strip repair with Lord 7542 A/D adhesive after burst testing.



**Figure 168 - Test 10 Damage after Burst Test**

Post mortem analysis of the Test 10 specimen revealed a large number of voids in the adhesive layer between the steel strip and the pipe ID (Figure 169). It was not clear whether this was the result of the shorter cure time associated with the urethane adhesive as compared to the epoxy adhesive or the result of having used a smaller quantity of adhesive.



**Figure 169 - Large Number of Voids in Urethane Adhesive from Test 10**

Table 30 contains the predicted and measured burst pressures for the 508 mm (20 in.) API 5L X52 pipe sections in the virgin, un-repaired (short/extra deep), and Test 10 repaired conditions. Table 29 also contains a predicted burst pressure for virgin pipe based on Barlow's formula using the measured ultimate tensile strength of the pipe material. The resultant burst pressure for the Test 10 repair was essentially the same as the pressure corresponding to 100% SMYS (8.96 MPa (1,300 psi)). It was 108% higher than the RSTRENG® predicted burst pressure for an un-repaired pipe, 63% lower than the measured virgin pipe performance and essentially the same as the measured performance of the un-repaired pipe section.

Pipe Diameter	Pipe Condition	Predicted Burst Pressure		Actual Burst Pressure	
		(MPa)	(psi)	(MPa)	(psi)
508.0 mm (20 in.)	Virgin	13.82	2,005	14.63	2,122
	Simulated Damage Short/Extra Deep Un-Repaired	4.32	627	8.94	1,298
	Simulated Damage High Strength Steel Strip Lord 7542 A/D Adhesive Repair (Test 10)	-	-	8.98	1,303

**Table 30 - Summary of Predicted vs. Actual Hydrostatic Burst Pressure Values Test 10**

Test 10 exhibited a 0.4% increased performance over the over the un-repaired pipe and a 63% decrease as compared to the performance of a virgin pipe. Again, it was not possible to determine the actual effectiveness of this repair given the large quantity of voids in the adhesive layer between the coils and between the coil and the pipe ID. This test did, however, illustrate the importance of the installation procedure (i.e., making sure that a significant number of voids are avoided). The next test was designed to evaluate the affect of lower strength steel strip with the original epoxy adhesive (3M DP460).

**Test 11: Low Strength Steel Strip, Short/Extra Deep Damage, 3M DP460 Epoxy Adhesive**

For Test 11, a section of 508 mm (20 in.) diameter API 5L X52 pipe with a short/extra deep simulated corrosion defect was used. Calculated with RSTRENG® to represent a 50% reduction in burst strength, defect dimensions were 127 mm (5 in.) long by 4.75 mm (0.187 in.) deep. The old adhesive (3M DP460) was used to install three layers of low strength helically wound steel strip inside the pipe section. The strip was custom rolled to form a 533.4 mm (21 in.) diameter helix as in Tests 09 and 10. The three layers of steel strip were also adhesively bonded in the pipe section, again using a smaller quantity of the adhesive. The resultant repair was allowed to cure for a week before hydrostatic testing.

The "low strength" steel strip was AISI C1010 cold rolled steel strip purchased from Lapham-Hickey Steel. It has an ultimate tensile strength of 413.1 MPa (59.9 psi) (Table 16). It was 50.8 mm (2 in.) wide by 1.27 mm (0.050 in.) thick and was supplied in the "Half-Hard" condition. This material was selected to have tensile properties that were close to those of the steel pipe.

Figure 170 shows the defect on the OD of the Test 11 pipe section with the low strength helically wound steel strip repair after burst testing.



**Figure 170 - Test 11 Damage after Burst Test**

As with Test 10, postmortem analysis of the Test 11 specimen revealed a large number of voids in the adhesive layer between the steel strip and the pipe ID. It is not clear whether the performance of this repair was adversely affected by these voids, which were apparently the result of having used a smaller quantity of adhesive, or by the lower strength steel strip material.

Table 30 contains the predicted and measured burst pressures for the 508 mm (20 in.) API 5L X52 pipe sections in the virgin, un-repaired (short/extra deep), and Test 11 repaired conditions. Table 30 also contains a predicted burst pressure for virgin pipe based on Barlow's formula using the measured ultimate tensile strength of the pipe material. The resultant burst pressure for the Test 11 repair was 13% greater than the pressure corresponding to 100% SMYS (8.96 MPa (1,300 psi)). It was 133% higher than the RSTRENG® predicted burst pressure for an un-repaired pipe, 45% lower than the measured virgin pipe performance, but 13% higher than the measured performance of the un-repaired pipe section.

Pipe Diameter	Pipe Condition	Predicted Burst Pressure		Actual Burst Pressure	
		(MPa)	(psi)	(MPa)	(psi)
508.0 mm (20 in.)	Virgin	13.82	2,005	14.63	2,122
	Simulated Damage Short/Extra Deep Un-Repaired	4.32	627	8.94	1,298
	Simulated Damage Low Strength Steel Strip 3M DP460 Adhesive Repair (Test 11)	-	-	10.09	1,464

**Table 31 - Summary of Predicted vs. Actual Hydrostatic Burst Pressure Values Test 11**

Test 11 exhibited a 13% increased performance over the over the un-repaired pipe and a 45% decrease as compared to the performance of a virgin pipe. Again, it was not possible to determine the actual effectiveness of this repair given the large quantity of voids in the adhesive layer between the coils and between the coil and the pipe ID. Even with the compromised integrity of the adhesive bond, Test 11 was relatively effective at restoring the pressure containing capability of a damaged pipe section. The next test was designed to confirm performance of the higher strength steel strip with a normal quantity of the original 3M DP460 epoxy adhesive using a more significant defect geometry.

**Test 12: High Strength Steel Strip, Short/Extra Deep Damage, 3M DP460 Epoxy Adhesive**

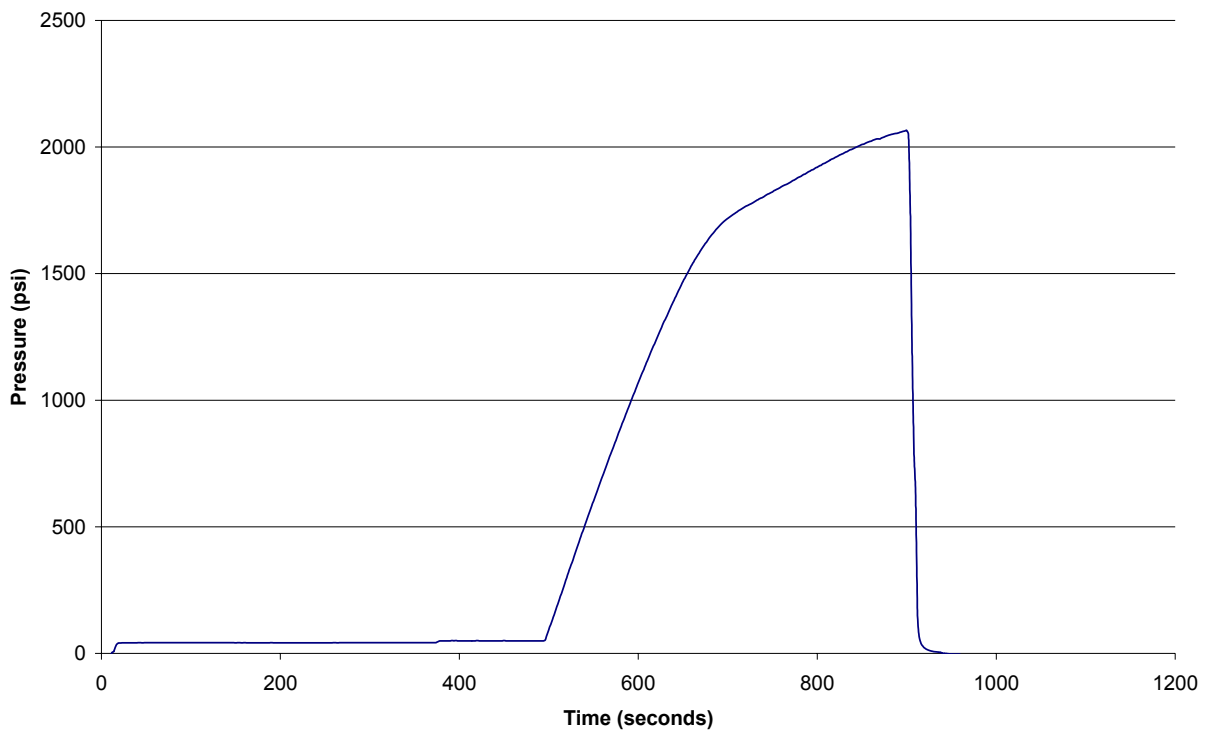
For Test 12, a section of 609.6 mm (24 in.) diameter, 7.92 mm (0.312 in.) wall, API 5L X65 pipe with a short/extra deep simulated corrosion defect was used. Calculated with RSTRENG® to represent a 60% reduction in burst strength, defect dimensions were 228.6 mm (9 in.) long by 5.9 mm (0.234 in.) deep (Figure 19). A normal quantity of 3M DP460 epoxy adhesive was used to install three layers of the high strength helically wound steel strip inside the pipe section. The strip was custom rolled to form a 635.0 mm (25 in.) diameter helix. After the three layers of steel strip were adhesively bonded in the pipe section, it was allowed to cure for a week before hydrostatic testing.

Figure 171 shows the defect on the OD of the Test 12 pipe section with helically wound steel strip repair after burst testing.



**Figure 171 - Test 12 Damage after Burst Test**

Post mortem analysis indicates that Test 12 developed a leak along the length of the simulated corrosion damage after the pipe steel experienced a significant amount of global yielding (i.e., well beyond the point where the yield strength was exceeded). Figure 172 contains the pressure vs. time plot for Test 12.



**Figure 172 - Pressure vs. Time Plot for Test 12**

Table 32 contains the predicted and measured burst pressures for the 609.6 mm (24 in.) diameter API 5L X65 pipe sections in the virgin, un-repaired (extra long/shallow), and Test 12 repaired conditions. Table 32 also contains a predicted burst pressure for virgin pipe based on Barlow's formula using the measured ultimate tensile strength of the pipe material. The

resultant burst pressure for the Test 12 repair was 22% greater than the pressure corresponding to 100% SMYS (11.65 MPa (1,690 psi)) and 206% higher than the RSTRENG® predicted burst pressure for an un-repaired pipe. In fact, it was only 9% lower than the measured virgin pipe performance. The most significant aspect of this test was that the resultant burst pressure for the Test 12 repair was 124% higher than the measured performance of the un-repaired pipe section (2065 psi compared to 920 psi).

Pipe Diameter	Pipe Condition	Predicted Burst Pressure		Actual Burst Pressure	
		(MPa)	(psi)	(MPa)	(psi)
609.6 mm (24 in.)	Virgin	15.25	2,212	15.51	2,249
	Simulated Damage Extra Long/Shallow Un-Repaired	4.65	675	6.34	920
	Simulated Damage High Strength Steel Strip 3M DP460 Adhesive Repair (Test 12)	-	-	14.24	2,065

**Table 32 - Summary of Predicted vs. Actual Hydrostatic Burst Pressure Values Test 12**

Test 12 exhibited a significant 124% increased performance over the over the un-repaired pipe and only a 9% decrease as compared to the performance of a virgin pipe.

**Test 13: High Strength Steel Strip, Short/Extra Deep Damage with Through Hole, 3M DP460 Epoxy Adhesive**

Test 13 featured a section of 609.6 mm (24 in.) diameter, 7.92 mm (0.312 in.) wall, API 5L X65 pipe with a through-wall hole of approximately 6.35 mm (0.26 in.) diameter in the middle of a short/extra deep simulated corrosion defect. Calculated with RSTRENG® to represent a 60% reduction in burst strength (without the through hole), defect dimensions were 228.6 mm (9 in.) long by 5.9 mm (0.234 in.) deep (see Figure 20 and Figure 21). A normal quantity of 3M DP460 epoxy adhesive was used to install three layers of the high strength helically wound steel strip inside the pipe section. The strip was custom rolled to form a 635.0 mm (25 in.) diameter helix. After the three layers of steel strip were adhesively bonded in the pipe section, it was allowed to cure for a week before hydrostatic testing.

Figure 173 and Figure 174 show the defect on the OD of the Test 13 pipe section with helically wound steel strip repair after burst testing.





**Figure 173 - Test 13 Damage after Burst Test**



**Figure 174 - Close Up of Test 13 Damage after Burst Test**

Post mortem analysis indicates that Test 13 developed a leak along the length of the simulated corrosion damage after the pipe steel experienced a significant amount of global yielding (i.e., well beyond the point where the yield strength was exceeded). Figure 175 contains the pressure vs. time plot for Test 13.

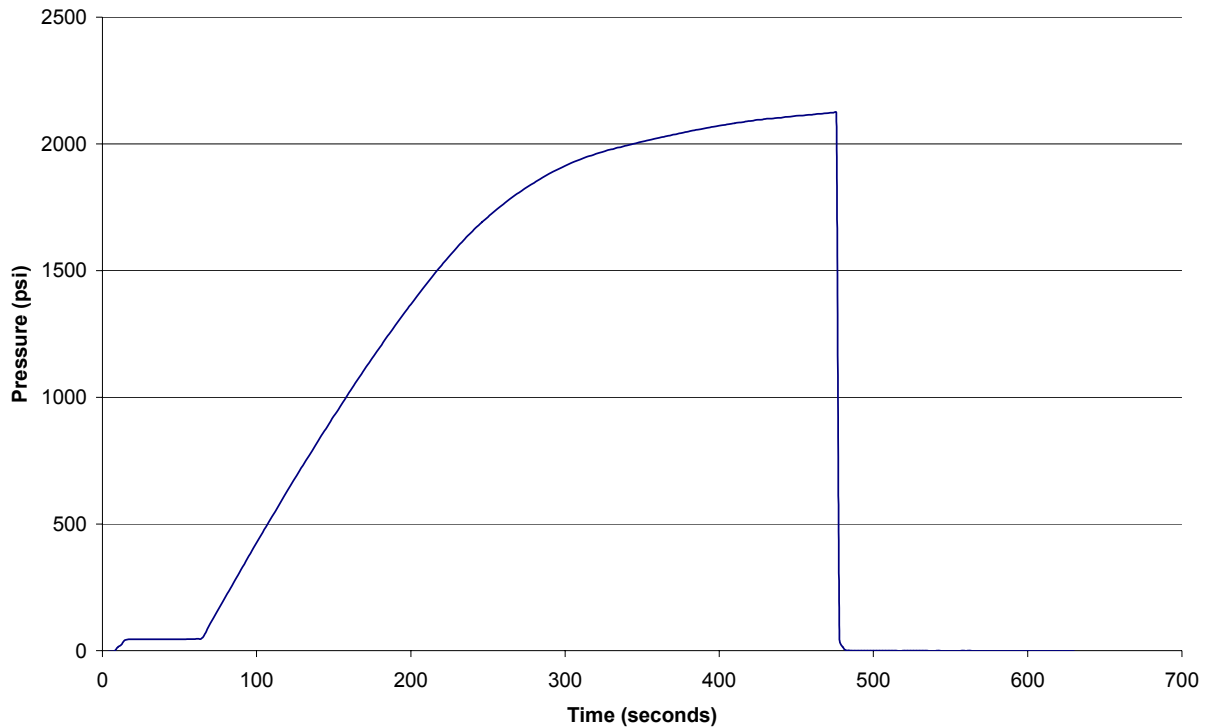


**Figure 175 - Pressure vs. Time Plot for Test 13**

Table 33 contains the predicted and measured burst pressures for the 609.6 mm (24 in.) diameter API 5L X65 pipe sections in the virgin, un-repaired (short/extra deep), Test 12 repaired conditions, and Test 13 (through-wall hole) repaired conditions. Table 33 also contains a predicted burst pressure for virgin pipe based on Barlow's formula using the measured ultimate tensile strength of the pipe material. The resultant burst pressure for the Test 13 repair was 26% greater than the pressure corresponding to 100% SMYS (11.65 MPa (1,690 psi)) and 215% higher than the RSTRENG® predicted burst pressure for an un-repaired pipe. In fact, it was only 8% lower than the measured virgin pipe performance and 3% higher than the Test 12 without a through hole. The most significant aspect of this test was that the resultant burst pressure for the Test 13 repair was 131% higher than the measured performance of the un-repaired pipe section (2,124 psi compared to 920 psi).

Pipe Diameter	Pipe Condition	Predicted Burst Pressure		Actual Burst Pressure	
		(MPa)	(psi)	(MPa)	(psi)
609.6 mm (24 in.)	Virgin	15.25	2,212	15.51	2,249
	Simulated Damage Short/Extra Deep Un-Repaired	4.65	675	6.34	920
	Simulated Damage Short/Extra Deep High Strength Steel Strip 3M DP460 Adhesive Repair (Test 12)	-	-	14.24	2,065
	Simulated Damage Short/Extra Deep with Through Hole High Strength Steel Strip 3M DP460 Adhesive Repair (Test 13)	-	-	14.64	2,124

**Table 33 - Summary of Predicted vs. Actual Hydrostatic Burst Pressure Values Test 13**

Test 13 exhibited a significant 131% increased performance over the over the un-repaired pipe and only a 8% decrease as compared to the performance of a virgin pipe. Surprisingly, Test 13 (with a through hole) was 3% stronger than the same repair/defect conditions with no through hole (Test 12). Overall, Test 13 exhibited the best performance of any repair method evaluated in this study.

**Test 14: High Strength Steel Strip, Extra Long/Shallow Damage, 3M DP460 Epoxy Adhesive**

Test 14 featured a section of 609.6 mm (24 in.) diameter, 7.92 mm (0.312 in.) wall, API 5L X65 with an extra long/shallow simulated corrosion defect. Calculated with RSTRENG® to represent a 60% reduction in burst strength, defect dimensions were 381 mm (15 in.) long by 5.66 mm (0.223 in.) deep. A normal quantity of 3M DP460 epoxy adhesive was used to install three layers of the high strength helically wound steel strip inside the pipe section. The strip was custom rolled to form a 635.0 mm (25 in.) diameter helix. After the three layers of steel strip were adhesively bonded in the pipe section, it was allowed to cure for a week before hydrostatic testing.

Figure 176 and Figure 177 show the defect on the OD of the Test 14 pipe section with helically wound steel strip repair after burst testing.



**Figure 176 - Test 14 Damage after Burst Test**



**Figure 177 - Close Up of Test 14 Damage after Burst Test**

Post mortem analysis indicates that Test 14 developed a leak along the length of the simulated corrosion damage after the pipe steel experienced a noticeable amount of global yielding (i.e., beyond the point where the yield strength was exceeded). Figure 178 contains the pressure vs. time plot for Test 14.

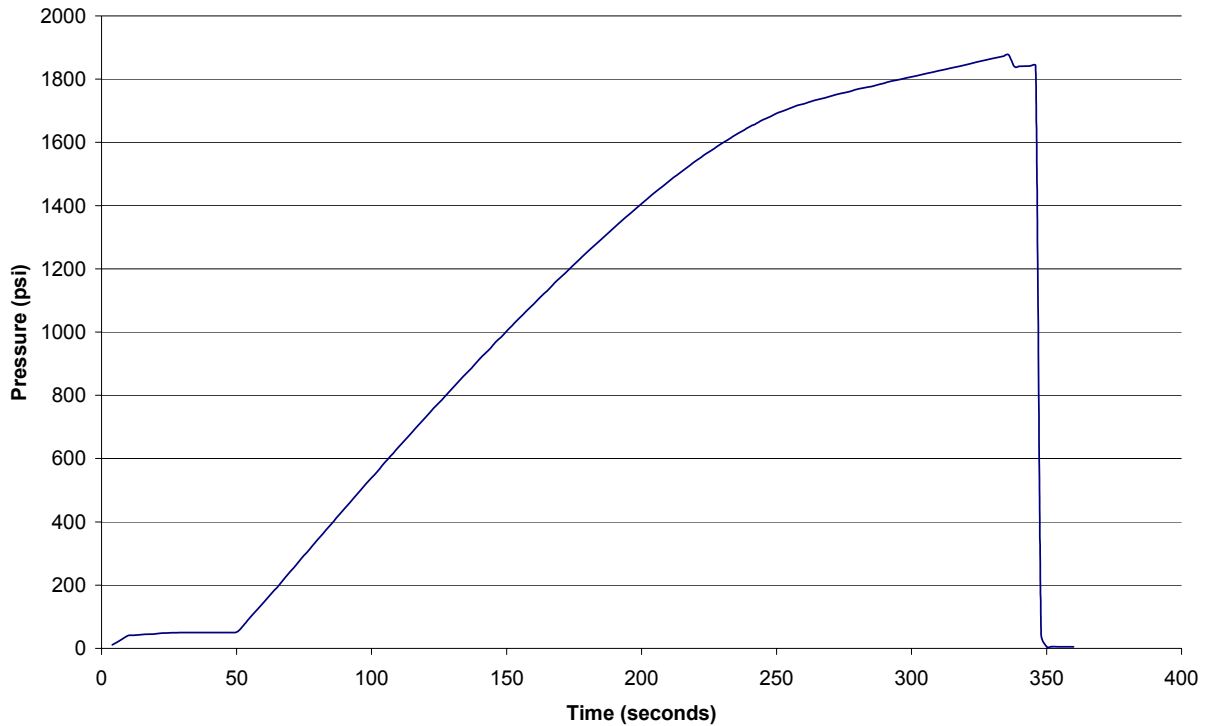


**Figure 178 - Pressure vs. Time Plot for Test 14**

Table 34 contains the predicted and measured burst pressures for the 609.6 mm (24 in.) diameter API 5L X65 pipe sections in the virgin, un-repaired (extra long/shallow), and Test 14 repaired conditions. Table 33 also contains a predicted burst pressure for virgin pipe based on Barlow's formula using the measured ultimate tensile strength of the pipe material. The resultant burst pressure for the Test 14 repair was 9% greater than the pressure corresponding to 100% SMYS (11.65 MPa (1,690 psi)) and 173% higher than the RSTRENG® predicted burst pressure for an un-repaired pipe. The resultant burst pressure was 22% lower than the measured virgin pipe performance. The most significant aspect of this test was that the resultant burst pressure for the Test 14 repair was 144% higher than the measured performance of the un-repaired pipe section (1,842 psi compared to 754 psi).

Pipe Diameter	Pipe Condition	Predicted Burst Pressure		Actual Burst Pressure	
		(MPa)	(psi)	(MPa)	(psi)
609.6 mm (24 in.)	Virgin	15.25	2,212	15.51	2,249
	Simulated Damage Extra Long/Shallow Un-Repaired	4.65	674	5.20	754
	Simulated Damage High Strength Steel Strip 3M DP460 Adhesive Repair (Test 14)	-	-	12.70	1,842

**Table 34 - Summary of Predicted vs. Actual Hydrostatic Burst Pressure Values Test 14**

Test 14 exhibited a significant 144% increased performance over the over the un-repaired pipe and a 22% decrease as compared to the performance of a virgin pipe. Test 14 results confirm that adhesively bonded, helically wound high strength steel strip repair technology is the best method of internal repair evaluated in this study for restoring the pressure containing capability of a damaged pipeline.

The three layer repair did not perform quite as well for the extra long damage as it did for the long damage. The reason for this can be explained based on the defect length beyond which hoop stress can no longer be distributed beyond the ends of the defect. For short defects, a repair only needs to prevent the defect from bulging, which is a precursor to failure. For long defects, the defect-weakened area tends to act like a thin-wall pipe in the vicinity of the defect. The design of the repair for Tests 12 through 14 was identical (three layers of 1.27 mm (0.050 in.) thick steel strip). While this was obviously sufficient to prevent bulging of the defect during Tests 12 and 13, it was less effective for Test 14 where the hoop stress was unable to distribute itself around the end of the extra long defect. For defects that exceed the length beyond which hoop stress can no longer be distributed beyond the ends of the defect, it may be necessary to design the thickness of the repair according to the defect depth. In Test 14 for example, a 6.35 mm (0.250 in.) thick repair (five layers) may have been more appropriate for a 5.66 mm (0.223 in.) deep defect as opposed to a 3.81 mm (0.150 in.) thick (three layer) repair. It may be possible to take advantage of the steel strip's higher strength compared to the strength of the pipe, whereby a 5.08 mm (0.200 in.) thick repair (four layers) may have been adequate for Test 14.

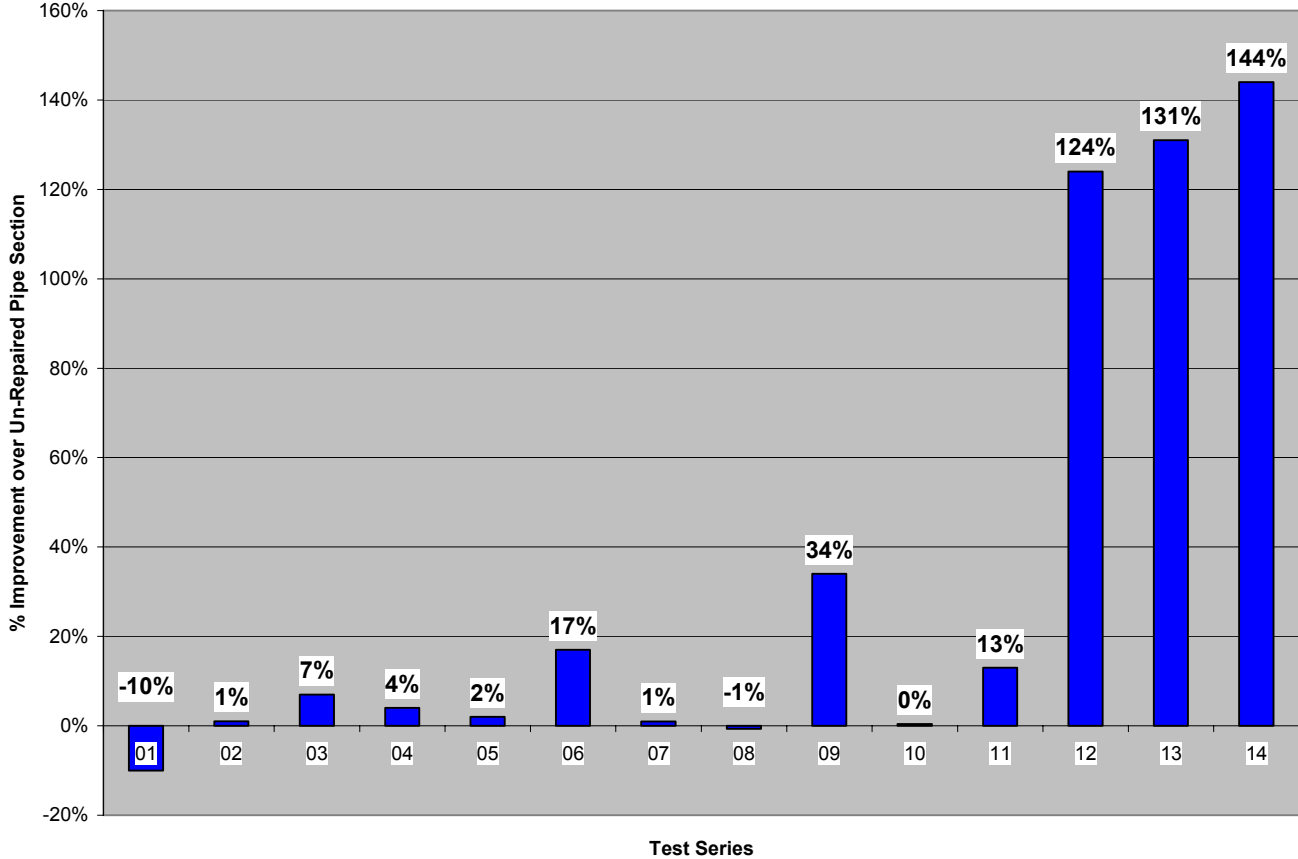
#### 4.12 - Comparison of All Candidate Repair Technologies

Table 35 contains a summary description of all burst test series conducted in this study.

Test No.	Repair Material	Damage Type	Damage as a Percent of Wall Thickness
01	Weld Deposition	Short/Deep	50%
02	GF Patch	Long/Shallow	53%
03	GF Patch	Short/Extra Deep	85%
04	Solid, Half-Round, Radial CF Patch (Quasi-Isotropic) 3M DP460 Adhesive	Short/Deep	54%
05	Thin, "Pressure Bandage", Radial CF Patch, (all 0, 90) 3M DP460 Adhesive	Short/Deep	54%
06	Thin, Radial CF Patch, (all 0, 90), 3M DP460 Adhesive	Short/Deep	54%
07	Thick, Axial CF Patch (all 0, 90), 3M DP460 Adhesive	Long/Shallow	43%
08	Steel Patch, 3M DP460 Adhesive	Short/Deep	54%
09	High Strength, Helically Wound Steel Strip, 3M DP460 Adhesive	Short/Extra Deep	75%
10	High Strength, Helically Wound Steel Strip, Lord 7542 A/D Adhesive Smaller Quantity of Adhesive	Short/Extra Deep	75%
11	Low Strength, Helically Wound Steel Strip, 3M DP460 Adhesive Smaller Quantity of Adhesive	Short/Extra Deep	75%
12	High Strength, Helically Wound Steel Strip, 3M DP460 Adhesive	Short/Extra Deep Slot	75%
13	High Strength, Helically Wound Steel Strip, 3M DP460 Adhesive	Short/Extra Deep Slot with Through Hole	75%
14	High Strength, Helically Wound Steel Strip, 3M DP460 Adhesive	Extra Long/Shallow Slot	71%

**Table 35 - Summary of Test Series Conducted**

For each series of burst tests in Table 35, the percentage of performance improvement for each series of repaired pipe compared to pipe in the un-repaired condition is plotted in Figure 179.



**Figure 179 - % Improvement of Burst Test Results for Repaired vs. Un-Repaired Pipe**

Weld deposition (Test 01) was eliminated early on due to extremely poor performance. GF liner repair (Test 02 and 03) was eliminated from the research program, but these repairs opened the door for exploring CF liner repairs with a higher modulus material. After Test 04, CF liner repair was seen as the most promising process and was developed during Tests 05 through 07 with mostly disappointing results. An adhesively bonded steel patch was evaluated in Test 08 with less than impressive performance; however, this led to the idea of an adhesively bonded/helically wound steel strip repair (Test 09) which produced the best results to that point of the study. Tests 10 through 11 investigated variations of this repair method with varying success. A repeat of Test 09 using a more significant defect geometry, Test 12 produced outstanding performance. This outstanding performance was repeated in Test 13, which was identical to Test 12 except that the through-wall hole was included in the center of the defect. Test 14 showed that the technique is promising for defects that exceed the length beyond which hoop stress can no longer be distributed beyond the ends of the defect, although further work is required to optimize the design of the repair for this application. Based on these results, adhesively bonded/helically wound steel strip repair is by far the most promising repair technology evaluated by this study.



Not only is the helically wound steel strip repair technique attractive in that it has the ability to significantly restore the pressure containing capability of damaged pipe, it is also a technique that lends itself well to deployment in the field. The coils can also be sized to accommodate any length of corrosion damaged pipeline. The steel strip material can be cinched down so that it is possible to deploy the coils through bend sections. The coils can even be compressed so that, prior to deployment, the length of the coil is equal to a single width of the steel strip material. Another attractive aspect of the helically wound steel strip repair technique is that the steel strip material is inexpensive.

#### **4.13 - Further Development Needs for Adhesively Bonded Helically Wound Steel Strip Repair**

Future investigation into this repair technology should be conducted to optimize its application, to investigate its effectiveness for a wider variety of applications, and to develop a prototype repair systems to deploy this repair technology.

Other aspects of the technique that require further investigation include the development of a pre-applied adhesive that can be activated upon deployment (e.g., a hot melt adhesive that is activated by heating coils in the bladder) and the long-term compatibility of the adhesive material in a methane environment.

## 5.0 - CONCLUSIONS

The most common cause for repair of gas transmission pipelines is external, corrosion-caused loss of wall thickness<sup>(6)</sup>. To prevent an area of corrosion damage from causing a pipeline to rupture, the area containing the corrosion damage must be reinforced. Other pipeline defects that commonly require repair include internal corrosion, original construction flaws, service induced cracking, and mechanical damage.

Defects oriented in the longitudinal direction have a tendency to fail from hoop stress (pressure loading) and must be reinforced in the circumferential direction. Defects oriented in the circumferential direction have a tendency to fail from axial stresses (due to pipeline settlement, etc.) and must be reinforced in the longitudinal direction. Full-encirclement steel repair sleeves resist hoop stress and, if the ends are welded to the pipeline, can also resist axial stresses.

### Technology Status Assessment

The Technology Status Assessment indicates that the most commonly used method for repair of gas transmission pipelines is the full-encirclement steel repair sleeve. This and other repair methods commonly applied from the outside of the pipeline are typically executed with the pipeline in-service. While in-service application would be desirable for internal repair, many of the repair methods that are applicable to the inside of the pipeline require that the pipeline be taken out-of-service. Extensive high risk research and development would be required to make these repair processes suitable for in-service natural gas pipeline application. Most of the repair methods that are commonly applied to the inside of other types of pipelines, which typically operate at low pressure, are done so to only restore leak tightness. These repair methods would also require extensive research and development in order for them to have the ability to restore the strength of a gas transmission pipeline. Given the budget and time restraints of this program, efforts were focused on evaluating internal repair technologies for application while the pipeline is out-of-service.

### Survey of Industry Needs for Internal Pipeline Repair

The responses to the operator needs survey produced the following principal conclusions:

1. Use of internal weld repair is most attractive for river crossings, under other bodies of water such as lakes and swamps, in difficult soil conditions, under highways and in congested intersections, and under railway crossings. All these areas tend to be very difficult and very costly, if, and where conventional excavated repairs may be currently used.

2. Internal pipe repair offers a strong potential advantage to the high cost of HDD when a new bore must be created to solve a leak or other problem in a water/river crossing.
3. Typical travel distances can be divided into three distinct groups: up to 305 m (1,000 ft.); between 305 m (1,000 ft.) and 610 m (2,000 ft.); and beyond 914 m (3,000 ft.). All three groups require pig-based systems. A despoiled umbilical system would suffice for the first two groups which represents 81% of survey respondents. The third group would require an onboard self-contained power unit for propulsion and welding/liner repair energy needs.
4. Pipe diameter sizes range from 50.8 mm (2 in.) through 1,219.2 mm (48 in.). The most common size range for 80% to 90% of operators surveyed is 508 mm (20 in.) to 762 mm (30 in.), with 95% using 558.8 mm (22 in.) pipe.
5. Based on the frequency of expected use by many operators, the issue of acceptable system cost for a deployable solution could best be tackled through selling such technology as an additional service through existing "smart pig" vendors/operators.
6. There has been almost no use of internal repair to date and the concept is currently fairly alien to pipeline operators. Even the potential for internal repair of external damage using such a system needs further promotion/education within the industry as a whole.
7. Most operators were open to the economic potential an internal repair system may offer in terms of reducing interruption to product flow, particularly if they did not have looped lines.
8. The top three items of concern for selecting a repair method were cost, availability of the repair method (time/cost), and the position of the defect(s).
9. A wide range of pipe coatings were cited as being deployed in the field. The top three mentioned were FBE, coal tar, and concrete/POWERCRETE®.
10. The majority of operators considered the ability for the pipeline to remain in service while the repair was conducted to be very important.
11. RT is by far the most accepted method for pipeline NDE. UT was the second most common process cited.

In summary, the important characteristics of a useful internal pipeline repair system would include the ability to operate at a long range from the pipe entry point, the agility to transverse bends and miters, and the ability to make a permanent repair that is subsequently inspectable via pigging.

### **Potential Repair Methods Identified Through Survey**

Figure 91 is a bar chart that contains the total weighted scores for each potential repair technology that was considered. It is apparent that, of the three broad categories of repair (welding, liners, and surfacing), repair methods that involve welding are generally the most

feasible. The second most feasible of the three broad categories is repair methods that involve internal liners. Of these, fiber-reinforced composite liners are the most promising.

### **Evaluation of Repair Methods**

Burst pressures for GF liner repair were only slightly greater than that of pipe sections without liners, indicating that this type of liner is only marginally effective at restoring the pressure containing capabilities of pipelines.

Burst pressures for CF liner repair were also marginally greater than that of a pipe section with un-repaired simulated damage without a liner, indicating that this type of liner is only marginally effective at restoring the pressure containing capabilities of pipelines.

Pipe repaired with weld deposition failed at pressures lower than that of un-repaired pipe in both the virgin and damaged conditions, indicating that this repair technology is less effective at restoring the pressure containing capability of pipe than both GF and CF liner repairs.

An adhesively bonded steel patch failed at pressures slightly lower than that of un-repaired pipe, exhibiting a higher capability than weld deposition repair, but significantly lower than both GF and CF liner repairs.

Based on the results of several tests, adhesively bonded/helically wound steel strip repairs exhibited burst pressures that greatly exceeded the burst pressures of un-repaired pipe, indicating that this repair process is extremely promising for restoring the pressure containing capability of a damaged pipe section.

### **Most Promising Repair Technology**

Physical testing indicates that adhesively bonded/helically wound steel strip repair is clearly the most promising technology evaluated to-date, because of its ability to restore a damaged pipe section to near full pressure containing capability and because of its characteristically low profile that will allow inspection by pigging. Future investigation into this repair technology should be conducted to optimize its application and to develop a prototype repair system to deploy this technology.

## 6.0 - REFERENCES

- (1) U. S. Department of Transportation, Research and Special Programs Administration, Office of Pipeline Safety, "Pipeline Failure Causes," [http://primis.rspa.dot.gov/pipelineInfo/stat\\_causes.htm](http://primis.rspa.dot.gov/pipelineInfo/stat_causes.htm) (Washington, DC: U. S. Department of Transportation, Research and Special Programs Administration, Office of Pipeline Safety, 17 June 2004)
- (2) Kiefner, J. F. and Vieth, P. H., "A Modified Criterion for Evaluating the Remaining Strength of Corroded Pipe" Final Report to A.G.A. Pipeline Corrosion Supervisory Committee, Project PR-3-805, Battelle, Columbus, OH, December 1989.
- (3) U. S. Department of Transportation, Research and Special Programs Administration, "§192.150 Passage of internal inspection devices," DOT 49 CFR Part 192 - Transportation of Natural & Other Gas by Pipeline: Minimum Safety Standards, July 1998.
- (4) Bruce, W. A., "Welding onto In-Service Thin Wall Pipelines," Final Report for EWI Project No. 41732CAP to PRC International, Contract No PR-185-9908, July 2000.
- (5) Kiefner, J. F., Barnes, C. R., Gertler, R. C., Fischer, R. D., and Mishler, H. W., "Experimental Verification of Hot Tap Welding Thermal Analysis. Final Report - Phase II - Volume 2, Liquid Propane Experiments," Repair and Hot Tap Welding Group, Battelle Columbus Laboratories, May 1983.
- (6) Wang, Y.-Y., and Bruce, W. A., "Examination of External Weld Deposition Repair for Internal Wall Loss," Final Report for EWI Project No. 07723CAP to PRC International, Contract No PR-185-9633, March 1998.
- (7) Eiber, R. J., Bubenik, T. A., and Leis, B. N., "Pipeline Failure Mechanisms and Characteristics of the Resulting Defects," Eighth Symposium on Line Pipe Research, Paper No. 7 (Houston, TX: American Gas Association, 1993).

## 7.0 - BIBLIOGRAPHY

- U. S. Department of Transportation, Research and Special Programs Administration, Office of Pipeline Safety, "Pipeline Failure Causes," [http://primis.rspa.dot.gov/pipelineInfo/stat\\_causes.htm](http://primis.rspa.dot.gov/pipelineInfo/stat_causes.htm) (Washington, DC: U. S. Department of Transportation, Research and Special Programs Administration, Office of Pipeline Safety, 17 June 2004). This web site provides comprehensive information about the U.S. transportation pipeline infrastructure. It is developed and maintained by the Office of Pipeline Safety (OPS) of the U.S. Department of Transportation's Research and Special Programs Administration.
- Kiefner, J. F. and Vieth, P. H., "A Modified Criterion for Evaluating the Remaining Strength of Corroded Pipe" Final Report to A.G.A. Pipeline Corrosion Supervisory Committee, Project PR-3-805, Battelle, Columbus, OH, December 1989. This report documents a modified criterion for evaluating the corrosion level of a pipeline based on pipeline stress calculations (available as a PC program) as a less conservative alternative to ANSI / ASME B31G.
- U. S. Department of Transportation, Research and Special Programs Administration. "§192.150 Passage of internal inspection devices." *DOT 49 CFR Part 192 - Transportation of Natural & Other Gas by Pipeline: Minimum Safety Standards*. Amdt. 192-72, 59 FR 17281, Apr 12, 1994, as amended by Amdt. 192-85, 63 FR 37502, July 13, 1998. This code describes minimum safety requirements for pipeline facilities and the transportation of gas, including pipeline facilities and the transportation of gas within the limits of the outer continental shelf as that term is defined in the Outer Continental Shelf Lands Act (43 U.S.C. 1331).
- Bruce, W. A., "Welding onto In-Service Thin Wall Pipelines," Final Report for EWI Project No. 41732CAP to PRC International, Contract No PR-185-9908, July 2000. This report discusses special welding difficulties and the extra care required to ensure safe operating procedures and sound welds due to repairs and modifications to in-service, thin walled pipelines.
- Kiefner, J. F., Barnes, C. R., Gertler, R. C., Fischer, R. D., and Mishler, H. W., "Experimental Verification of Hot Tap Welding Thermal Analysis. Final Report - Phase II - Volume 2, Liquid Propane Experiments," Repair and Hot Tap Welding Group, Battelle Columbus Laboratories, May 1983. This report documents the verification of two thermal analysis models of hot tap welding on pressurized pipelines. With velocity input modified as shown, the models are capable of predicting maximum temperatures in the pipe wall especially at the inside surface and critical cooling rates in the heat-affected zones within the range of heat inputs that are practical for shielded metal arc welding.

Wang, Y.-Y., and Bruce, W. A., "Examination of External Weld Deposition Repair for Internal Wall Loss," Final Report for EWI Project No. 07723CAP to PRC International, Contract No PR-185-9633, March 1998. This report discusses the deposition of weld metal on the external surface of straight sections of pipe, field bends, tees and elbows as a potentially useful method for in-service repair of internal wall loss.

Eiber, R. J., Bubenik, T. A., and Leis, B. N., "Pipeline Failure Mechanisms and Characteristics of the Resulting Defects," Eighth Symposium on Line Pipe Research, Paper No. 7 (Houston, TX: American Gas Association, 1993). This report discusses four broad categories of pipeline failure mechanisms: outside forces, environmentally induced defects, manufacturing/materials defects, and operator error or miscellaneous defects.

## 8.0 - LIST OF ACRONYMS

ANSI	American National Standards Institute
API	American Petroleum Institute
ASME	American Society of Mechanical Engineers
CAE	Computer Aided Engineering
CP	Cathodic Protection
CRLP	Composite Reinforced Line Pipe
CSA	Canadian Standards Association
CV	Constant Voltage
DOE	Department of Energy
DOT	Department of Transportation
ERW	Electric Resistance Welded
EWI	Edison Welding Institute
FBE	Fusion Bonded Epoxy
FEA	Finite Element Analysis
FRCP	Fiber-Reinforced Composite Pipe
Glass-HDPE	Glass-High Density Polyethylene
GMAW	Gas Metal Arc Welding
HDD	Horizontal Direct Drilling
HDPE	High Density Polyethylene
ILI	In-Line Inspection
ILS	Interlaminar Shear
IR	Infra-Red
MAOP	Maximum Allowable Operating Pressure
MEKP	Methyl Ethyl Ketone Peroxide
MOP	Maximum Operating Pressure
MPI	Magnetic Particle Inspection
NDE	Nondestructive Examination
NETL	National Energy Technology Laboratory
OD	Outside Diameter
PC	Personal Computer
PE	Polyethylene
PG&E	Pacific Gas & Electric Co.
PRCI	Pipeline Research Council International
QA	Quality Assurance
QC	Quality Control
RT	Radiographic Testing
SCC	Stress Corrosion Cracking
SMYS	Specified Minimum Yield Strength
UT	Ultrasonic Testing
VARTM	Vacuum Assisted Resin Transfer Molding



## 9.0 - APPENDICES

**Appendix A: Industry Survey with Cover Letter**

April 11, 2003

<<<FIELD 1>>>

**EWI Project No. 46211GTH, "Internal Repair of Pipelines"**

Dear <<<FIELD 2>>>:

Enclosed is a survey of operator experience and industry needs pertaining to internal repair of pipelines. EWI is conducting this survey as part of a project being funded by the National Energy Technology Laboratory. The objectives of this project are to evaluate, develop, demonstrate, and validate internal repair methods for pipelines.

Please complete this survey at your earliest convenience.<sup>1</sup> Your participation is greatly appreciated. If you have questions or require additional information, please contact me at 614-688-5059 or [bill\\_bruce@ewi.org](mailto:bill_bruce@ewi.org)

Sincerely,

William A. Bruce, P.E.  
Principal Engineer  
Materials section

Enclosure

---

<sup>1</sup> A copy of this survey was also sent to <<<FIELD 3>>> at your company. You may want to coordinate your response.

# **Internal Repair of Pipelines Survey of Operator Experience and Industry Needs**

conducted for:

**National Energy Technology Laboratory  
Morgantown, WV**

Project No. 46211GTH

on

**Internal Repair of Pipelines – Survey of  
Operator Experience and Industry Needs**

for

**National Energy Technology Laboratory**  
Morgantown, WV

April 11, 2003

**EWI**  
1250 Arthur E. Adams Drive  
Columbus, OH 43221

# Internal Repair of Pipelines – Survey of Operator Experience and Industry Needs

## 1.0 Introduction

A repair method that can be applied from the inside of a gas transmission pipeline (i.e., a trenchless repair) is an attractive alternative to conventional repair methods since the need to excavate the pipeline is precluded. This is particularly true for pipelines in environmentally sensitive and highly populated areas. Several repair methods that are commonly applied from the outside of the pipeline are, in theory, directly applicable from the inside. However, issues such as development of the required equipment to perform repairs remotely and mobilization of equipment through the pipeline to areas that require repair need to be addressed. Several additional repair methods that are commonly applied to other types of pipelines (gas distribution lines, water lines, etc.) also have potential applicability for internal repair of gas transmission pipelines. Many of these require further development to meet the requirements for repair of gas transmission pipelines. The objectives of a project being funded by the National Energy Technology Laboratory are to evaluate, develop, demonstrate, and validate internal repair methods for pipelines; develop a functional specification for an internal pipeline repair system; and prepare a recommended practice for internal repair of pipelines. One of the initial tasks of this project involves conducting a survey to determine the repair needs and performance requirements for internal pipeline repairs. The purpose of this survey is to better understand the needs of the natural gas transmission industry regarding internal repair.

## 2.0 Instructions

Please respond as completely as possible to as many questions as possible. Space is also provided for any comments that you may have.

## 3.0 Survey

### Part 1 – Currently-Used Repair Methods

1. Has your company experienced degradation (corrosion, cracking, etc) of a transmission line?  
  
If so, has your company replaced or repaired pipe because of degradation?
2. What specific repair methods would typically be used to repair different types of degradation?

Comments pertaining to currently-used repair methods –

## Part 2 – Use/Potential Use of Internal Repair

1. Has your company attempted repair of a transmission line from inside the pipe?

If so, describe the repair(s)

2. There are many factors that affect the decision to repair or replace pipe. What circumstances would favor performing a repair from inside the pipe using only one or two excavations rather than excavating the entire length of pipe?

3. If the technology were available to perform a repair from the inside, would your company consider using the technology?

If so, for what application(s) – e.g., specific geographic locations and special situations?

4. At least one excavation will be required to insert the internal repair device into the pipe. From this excavation, the repair device could be travel in each direction from the excavation. About how far from the insertion point should the repair device be able to travel?

What range of pipe diameters should the repair device be capable of operation in?

5. What potential obstructions such as elbows, bends, branches, and taps should the repair system be able to negotiate?

Comments pertaining to the use/potential use of internal repair –

## Part 3 – Need for In-Service Internal Repair

1. How important is the ability to perform a repair from the inside the pipe while the pipeline remains in service?
2. Would internal repair remain attractive if it was necessary to completely shut down the pipeline (depressurized and evacuated) during the repair?

Depressurized but not evacuated?

Out of service (no flow) but remain pressurized?

Comments pertaining to the need for in-service internal repair –

#### **Part 4 – Applicable Types of Damage**

1. What types of external coatings would be found on transmission lines owned by your company?
2. If a repair involving welding from the inside was performed, how important is it to preserve the integrity of the coating?

Is your cathodic protection system capable of compensating for relatively small breaches in the coating?

Comments pertaining to applicable types of damage –

#### **Part 5 – Operational and Performance requirements for Internal Repairs**

1. Two general categories of repairs are being considered, (1) using weld metal to restore a surface and (2) installing an internal sleeve, either metallic or nonmetallic, to provide structural reinforcement of leak tightness. Is it important that the line remain inspectable by pigging after repair?

About how far could the repair protrude into the pipe before it would interfere with pigging?

2. What NDE would your utility require for a repair to an existing longitudinal or circumferential weld?

Could a visual or magnetic particle examination be substituted for radiography in these special circumstances?



What NDE would your utility require for a welded repair to base metal (e.g. corrosion pitting)?

3. Would the use of internal repair be attractive even if it were considered a temporary repair

Comments pertaining to operational and performance requirements for internal repairs –

### **Part 6 - General Comments**

Please provide any general comments that you may have.

**Appendix B: Members of the Pipeline Research Council International**

## Members of the Pipeline Research Council International

Advantica Technologies Ltd  
BP  
Buckeye Pipe Line Company  
Chevron Texaco Pipeline Company  
CMS Panhandle Companies  
Colonial Pipeline Company  
Columbia Gas Transmission Co.  
ConocoPhillips  
Consumers Energy  
Dominion Transmission  
Duke Energy Gas Transmission  
El Paso Corporation  
Enbridge Pipelines  
Enron Transportation Services Corp.  
Explorer Pipeline Company  
ExxonMobil Pipeline Company  
Foothills Pipe Lines Ltd  
Gassco A.S. (Norway)  
Gasum Oy (Finland)  
Gaz de France  
Gulf South Pipeline  
Marathon Ashland Pipe Line LLC  
N.V. Nederlandse Gasunie/Gastransport Services (The Netherlands)  
National Fuel Gas Supply Corporation  
Saudi Aramco  
Sempra Energy Utilities/Southern California Gas Company  
Shell Pipeline Company LP  
Southern Natural Gas Company  
TEPPCO  
TransCanada PipeLines Limited  
Transco (UK)  
TransGas  
Williams Gas Pipeline

**Appendix C: List of Natural Gas Pipeline Operating Companies**  
(from <http://www.ferc.gov/gas/pipecomp.htm>)

## List of Natural Gas Pipeline Operating Companies

Algonquin Gas Transmission Company  
Algonquin LNG, Inc.  
ANR Pipeline Company  
ANR Storage Company  
Black Marlin Pipeline Company  
Blue Lake Gas Storage Company  
Canyon Creek Compression Company  
Carnegie Interstate Pipeline Company  
Chandeleur Pipe Line Company  
Colorado Interstate Gas Company  
Columbia Gas Transmission Corporation  
Columbia Gulf Transmission Company  
Cove Point LNG Limited Partnership  
Crossroads Pipeline Company  
Discovery Gas Transmission LLC  
Dominion Transmission Inc.  
Dynegy Midstream Pipeline, Inc.  
East Tennessee Natural Gas Company  
Egan Hub Partners, L.P.  
El Paso Natural Gas Company  
Equitrans, Inc.  
Florida Gas Transmission Company  
Gas Transport, Inc.  
Granite State Gas Transmission, Inc.  
Great Lakes Gas Transmission Limited Partnership  
Gulf South Pipeline  
Gulf States Transmission Corporation  
High Island Offshore System  
Iroquois Gas Transmission System, L.P.  
Kansas Pipeline Company  
Kentucky West Virginia Gas Company  
Kern River Gas Transmission Company  
KM Interstate Gas Transmission Co.  
KN Wattenberg Transmission  
Maritimes & Northeast Pipeline L.L.C.  
Michigan Gas Storage Company  
Midwestern Gas Transmission Company  
MIGC, Inc.  
Mississippi River Transmission Corporation  
Mojave Pipeline Company  
National Fuel Gas Supply Corporation  
Natural Gas Pipeline Company of America  
Nora Transmission Company  
Northern Border Pipeline Company  
Northern Natural Gas Company  
Northwest Pipeline Corporation

OkTex Pipeline Company  
Overthrust Pipeline Company  
Ozark Gas Transmission System  
Paiute Pipeline Company  
Panhandle Eastern Pipe Line Company  
Petal Gas Storage Company  
PG&E Gas Transmission-Northwest Corporation  
Questar Pipeline Company  
Reliant Energy Gas Transmission Company  
Sabine Pipe Line Company  
Sea Robin Pipeline Company  
Shell Offshore Pipelines  
South Georgia Natural Gas Company  
Southern Natural Gas Company  
Southwest Gas Storage Company  
Steuben Gas Storage Company  
TCP Gathering Co.  
Tennessee Gas Pipeline Company  
Texas Eastern Transmission Corporation  
Texas Gas Transmission Corporation  
Total Peaking LLC  
Trailblazer Pipeline Company  
TransColorado Gas Transmission Company  
Transcontinental Gas Pipe Line Corporation  
Transwestern Pipeline Company  
Trunkline Gas Company  
Trunkline LNG Company  
Tuscarora Gas Transmission Company  
U-T Offshore System  
Vector Pipeline  
Venice Gathering System, L.L.C.  
Viking Gas Transmission Company  
Williams Gas Pipelines Central, Inc.  
Williston Basin Interstate Pipeline Company  
Wyoming Interstate Company, Ltd.  
Young Gas Storage Company, Ltd.

**Appendix D: Lists of Surveyed PRCI Member & Other Gas  
Transmission Companies**

**Including Contact Name, Email, and Telephone Contact Information**

## Members of the Pipeline Research Council International Email Contacts for Survey

(As of 7/9/03 Email of main POC {when determined} for multiple listings, or single listings on Materials Committee)

Organization	POC Email Address
Advantica Technologies Ltd	bob.andrews@advanticatech.com
BP	moskowln@bp.com, moredh@bp.com hammondj3@bp.com,
Buckeye Pipe Line Company	wshea@buckeye.com
Chevron Texaco Pipeline Company	GBKO@ChevronTexaco.com
CMS Panhandle Companies	smgallagher@cmsenergy.com
Colonial Pipeline Company	jgodfrey@colpipe.com
Columbia Gas Transmission Co.	jswatzel@nisource.com
ConocoPhillips	dave.ysebaert@conocophillips.com
Consumers Energy	rswelsh@cmsenergy.com
Dominion Transmission	brian_c_sheppard@dom.com
Duke Energy Gas Transmission	scrapp@duke-energy.com
El Paso Corporation	bennie.barnes@elpaso.com
Enbridge Pipelines	scott.ironside@enbridge.com
Enron Transportation Services Corp.	mcrump@enron.com
Explorer Pipeline Company	jwenzell@expl.com
ExxonMobil Pipeline Company	don.e.drake@exxonmobil.com
Foothills Pipe Lines Ltd	jack.beattie@foothillspipe.com
Gassco A.S. (Norway)	eh@gassco.no
Gasum Oy (Finland)	ilkka.taka-aho@gasum.fi
Gaz de France	gerard.jammes@gazdefrance.com
Gulf South Pipeline	scott.williams@gulfsouthpl.com
Marathon Ashland Pipe Line LLC	tlshaw@mapllc.com
N.V. Nederlandse Gasunie/Gastransport Services (The Netherlands)	w.sloterdijk@gasunie.nl
National Fuel Gas Supply Corporation	pustulkaj@natfuel.com
Saudi Aramco	shuler.cox@aramco.com
Sempra Energy Utilities/Southern California Gas Company	bamend@semprautilities.com
Shell Pipeline Company LP	janiemeyer@shellopus.com
Southern Natural Gas Company	george.benoit@elpaso.com
TEPPCO	lwallett@teppco.com
TransCanada PipeLines Limited	david_dorling@transcanada.com
Transco (UK)	jeremy.bending@uktransco.com
TransGas	btorgunrud@transgas.com
Williams Gas Pipeline	Thomas.R.Odom@Williams.com



## Members of the Pipeline Research Council International Contact Names and Phone Numbers

(As of 7/9/03)

Organization	POC Name	Phone Number
Advantica Technologies Ltd	Bob Andrews	011 44 1509 282749
BP	John Hammond	011 44 1932 775909
BP	David Moore	907 564 4190
BP	Larry Moskowitz	281 366 2924
Buckeye Pipe Line Company	William Shea	610 254 4650
Chevron Texaco Pipeline Company	George Kohut	510 242 3245
CMS Panhandle Companies	Scott Gallagher	713 989 7444
Colonial Pipeline Company	John Godfrey	678 762 2217
Columbia Gas Transmission Co.	Jim Swatzel	304 357 2797
ConocoPhillips	Dave Ysebaert	281 293 2969
Consumers Energy	Robert Welsh	517 788 1928
Dominion Transmission	Brian Sheppard	304 627 3733
Duke Energy Gas Transmission	Steve Rapp	713 627 6394
El Paso Corporation	Bennie Barnes	719 520 4677
Enbridge Pipelines	Scott Ironside	780 420 5267
Enron Transportation Services Corp.	Michael Crump	713 345 1623
Explorer Pipeline Company	Jeff Wenzell	918 493 5140
ExxonMobil Pipeline Company	Don Drake	713 656 2288
Foothills Pipe Lines Ltd	Jack Beattie	403 294 4143
Gassco A.S. (Norway)	Egil Hurloe	011 47 52812500
Gasum Oy (Finland)	Ilkka Taka-Aho	011 358 20 44 78653
Gaz de France	Gerard Jammes	011 33 49 22 54 19
Gulf South Pipeline	Scott Williams	713 544 5220
Marathon Ashland Pipe Line LLC	Thomas Shaw	419 421 4002
N.V. Nederlandse Gasunie/Gastransport	Wytze Sloterdijk	011 31 50 521 2674
National Fuel Gas Supply Corporation	John Pustulka	716 857 7909
Saudi Aramco	Shuler Cox	011 966 3 874 6664
Sempra Energy Utilities/Southern Cal Gas	Bill Amend	213 244 5277
Shell Pipeline Company LP	John Niemeyer	713 241 1856
Southern Natural Gas Company	George Benoit	832 528 4244
TEPPCO	Leonard Mallett	713 759 3615
TransCanada PipeLines Limited	David Dorling	403 948 8147
Transco (UK)	Jeremy Bending	011 44 1689 881479
TransGas	Brian Torgunrud	306 777 9357
Williams Gas Pipeline	Thomas Odom	270 688 6964

## Other Natural Gas Pipeline Operating Companies – Email Contacts

(As of 7/9/03)

Organization	Location	Email Address
Algonquin Gas Transmission Co.	Duke Energy	scrapp@duke-energy.com
Algonquin LNG, Inc.	Duke Energy	scrapp@duke-energy.com
Alliance Pipeline Ltd.		arti.bhatia@alliance-pipeline.com
ANR Pipeline Co.	El Paso	george.benoit@elpaso.com
ANR Storage Co.	El Paso	george.benoit@elpaso.com
Black Marlin Pipeline Co.	Williams	Thomas.R.Odom@Williams.com
Blue Lake Gas Storage Co.	El Paso	robert.white@elpaso.com
Canyon Creek Compression Co.	K. Morgan (KM)	mark_mayworn@kindermorgan.com
Carnegie Interstate Pipeline Co.	Equitrans	amurphy@eqt.com
Chandeleur Pipe Line Co.	ChevronTexaco	GBKO@ChevronTexaco.com
Colorado Interstate Gas Co.	El Paso	bennie.barnes@elpaso.com
Columbia Gas Transmission Corp.	Columbia	jswatzel@nisource.com
Columbia Gulf Transmission Co.	Columbia	jswatzel@nisource.com
Cove Point LNG, L.P.	Dominion	brian_c_sheppard@dom.com
Crossroads Pipeline Co.	Columbia	jswatzel@nisource.com
Discovery Gas Transmission LLC	Williams	Thomas.R.Odom@Williams.com
Dynegy Midstream Pipeline, Inc.		rich.a.mueller@dynegy.com
East Tennessee Natural Gas Co.	Duke Energy	scrapp@duke-energy.com
Egan Hub Partners, L.P.	Duke Energy	scrapp@duke-energy.com
El Paso Natural Gas Co.	El Paso	<a href="mailto:bennie.barnes@elpaso.com">bennie.barnes@elpaso.com</a>
El Paso Field Services	El Paso	<a href="mailto:pat.davis@elpaso.com">pat.davis@elpaso.com</a>
Energy East		spmartin@energyeast.com
EPGT Texas Pipeline, L.P.	El Paso	pat.davis@elpaso.com
Equitrans, Inc.		amurphy@eqt.com
Florida Gas Transmission Co.	Enron	mcrump@enron.com
Granite State Gas Transmission, Inc.	Columbia	jswatzel@nisource.com
Great Lakes Gas Transmission, L.P.		rgrondin@glgt.com
Gulf South Pipeline		scott.williams@gulfsouthpl.com
Gulf States Transmission Corp.	El Paso	george.benoit@elpaso.com
High Island Offshore System	El Paso	george.benoit@elpaso.com
Iroquois Gas Transmission System		ben_gross@iroquois.com
Kansas Pipeline Co.	Midcoast Energy Enbridge	scott.ironside@enbridge.com
Kentucky West Virginia Gas Co.	Equitrans	amurphy@eqt.com
Kern River Gas Transmission Co.	Williams	Thomas.R.Odom@Williams.com
Keyspan Energy		psheth@keyspanenergy.com
KM Interstate Gas Transmission Co.	KM	mark_mayworn@kindermorgan.com
KN Wattenberg Transmission	KM	mark_mayworn@kindermorgan.com
Maritimes & Northeast Pipeline L.L.C.	Duke Energy	scrapp@duke-energy.com
Michigan Gas Storage Co.	Consumers Energy	rswelsh@cmsenergy.com
Midwestern Gas Transmission Co.	Enron	mcrump@enron.com
MIGC, Inc.	Western Gas	jcurtis@westerngas.com

Organization	Location	Email Address
Mississippi River Transmission Corp.	CenterPoint Energy	scott.mundy@centerpointenergy.com
Mojave Pipeline Co.	El Paso	bennie.barnes@elpaso.com
National Fuel Gas Supply Corp.		pustulkaj@natfuel.com
Natural Gas Pipeline Co. of America	KM	mark_mayworn@kindermorgan.com
Nora Transmission Co.	Equitrans	amurphy@eqt.com
North Carolina Natural Gas	Carolina Power & Light	Theodore.hodges@cplc.com
Northern Border Pipeline Co.	Enron	mcrump@enron.com
Northern Natural Gas Co.	Midamerican Energy	paul.fuhrer@nngco.com
Northwest Pipeline Corp.	Williams	Thomas.R.Odom@Williams.com
Overthrust Pipeline Co.	Questar	<a href="mailto:ronji@questar.com">ronji@questar.com</a>
Oncor Gas		mrothba1@oncorgroup.com
Ozark Gas Transmission System		strawnlw@oge.com
Paiute Pipeline Co.	Southwest Gas	jerry.schmitz@swgas.com
Panhandle Eastern Pipe Line Co.	CMS	smgallagher@cmsenergy.com
Petal Gas Storage Co.	El Paso	bennie.barnes@elpaso.com
PG&E Gas Transmission-Northwest Corp.	PG&E	<a href="mailto:WJH7@pge.com">WJH7@pge.com</a>
PG&E Gas Transmission-Northwest Corp.	PG&E	ADE1@pge.com
Questar Pipeline Co.	Questar	ronji@questar.com
Reliant Energy Gas Transmission Co.	CenterPoint Energy	scott.mundy@centerpointenergy.com
Sabine Pipe Line Co.	ChevronTexaco	GBKO@ChevronTexaco.com
Sea Robin Pipeline Co.	CMS	smgallagher@cmsenergy.com
Shell Offshore Pipelines	Shell	janiemeyer@shellopus.com
Southern Natural Gas Co.	El Paso	george.benoit@elpaso.com
Southwest Gas Corp.		jerry.Schmitz@swgas.com
Southwest Gas Storage Co.	CMS	smgallagher@cmsenergy.com
Steuben Gas Storage Co.	ANR/Arlington	george.benoit@elpaso.com
Tennessee Gas Pipeline Co.	El Paso	george.benoit@elpaso.com
Texas Eastern Transmission Corp.	Duke Energy	scrapp@duke-energy.com
Texas Gas Transmission Corp.	Williams	Thomas.R.Odom@Williams.com
Total Peaking LLC	Energy East	spmartin@energyeast.com
Trailblazer Pipeline Co.	KM	mark_mayworn@kindermorgan.com
TransColorado Gas Transmission Co.	KM	mark_mayworn@kindermorgan.com
Transcontinental Gas Pipe Line Corp.	Williams	Thomas.R.Odom@Williams.com
Transwestern Pipeline Co.	Enron	mcrump@enron.com
Trunkline Gas Co.	CMS	smgallagher@cmsenergy.com
Trunkline LNG Co.	CMS	smgallagher@cmsenergy.com
Tuscarora Gas Transmission Co.		<a href="mailto:lcherwenuk@tuscaroragas.com">lcherwenuk@tuscaroragas.com</a>
TXU Gas/TXU Lone Star Pipeline	TXU Gas	mrothba1@oncorgroup.com
Vector Pipeline	Enbridge	scott.ironside@enbridge.com
Venice Gathering System, L.L.C.	Dynegy	rich.a.mueller@dynegy.com

Organization	Location	Email Address
Viking Gas Transmission Co.	Northern Border (Enron)	mcrump@enron.com
Williams Gas Pipelines Central, Inc.	Williams	Thomas.R.Odom@Williams.com
Williston Basin Interstate Pipeline Co.		keith.seifert@wbip.com
Wyoming Interstate Co., Ltd.	El Paso	bennie.barnes@elpaso.com
Young Gas Storage Co., Ltd.	El Paso	bennie.barnes@elpaso.com

## Other Natural Gas Pipeline Operating Companies Contact Names and Phone Numbers

(As of 7/9/03)

Organization	POC Name	Phone Number
Algonquin Gas Transmission Co.	Steve Rapp	713 627 6394
Algonquin LNG, Inc.	Steve Rapp	713 627 6394
Alliance Pipeline Ltd.	Arti Bhatia	403 517 7727
ANR Pipeline Co.	George Benoit	832 528 4244
ANR Storage Co.	George.Benoit	832 528 4244
Black Marlin Pipeline Co.	Thomas Odom	270 688 6964
Blue Lake Gas Storage Co.	Robert White	248 994 4046
Canyon Creek Compression Co. K. Morgan	Mark Mayworn	713 369 9347
Carnegie Interstate Pipeline Co.	Andy Murphy	412 231 4888
Chandeleur Pipe Line Co.	George Kohut	510 242 3245
Colorado Interstate Gas Co.	Bennie Barnes	719 520 4677
Columbia Gas Transmission Corp.	Jim Swatzel	304 357 2797
Columbia Gulf Transmission Co.	Jim Swatzel	304 357 2797
Cove Point LNG Limited Partnership	Brian Sheppard	304 627 3733
Crossroads Pipeline Co.	Jim Swatzel	304 357 2797
Discovery Gas Transmission LLC	Thomas Odom	270 688 6964
Dynegy Midstream Pipeline, Inc.	Rich Mueller	713 507 3992
East Tennessee Natural Gas Co.	Steve Rapp	713 627 6394
Egan Hub Partners, L.P.	Steve Rapp	713 627 6394
El Paso Field Services	Pat Davis	210 528 4244
El Paso Natural Gas Co.	Bennie Barnes	719 520 4677
Energy East	Scott Martin	607 347 2561
EPGT Texas Pipeline, L.P.	Pat Davis	210 528 4244
Equitrans, Inc.	Andy Murphy	412 231 4888
Florida Gas Transmission Co.	Michael Crump	713 345 1623
Granite State Gas Transmission, Inc.	Jim Swatzel	304 357 2797
Great Lakes Gas Transmission L.P.	Ryan Grondin	321 439 1777
Gulf South Pipeline	Scott Williams	713 544 5220
Gulf States Transmission Corp.	George Benoit	832 528 4244
High Island Offshore System	George.Benoit	832 528 4244
Iroquois Gas Transmission System, L.P.	Ben Gross	203 925 7257
Kansas Pipeline Company	Scott Ironside	780 420 5267
Kentucky West Virginia Gas Co.	Andy Murphy	412 231 4888
Kern River Gas Transmission Co.	Thomas Odom	270 688 6964
Keyspan Energy	Perry Sheth	516 545 3844
KM Interstate Gas Transmission Co.	Mark Mayworn	713 369 9347
KN Wattenberg Transmission	Mark Mayworn	713 369 9347
Maritimes & Northeast Pipeline L.L.C.	Steve Rapp	713 627 6394
Michigan Gas Storage Co.	Robert Welsh	517 788 1928
Midwestern Gas Transmission Co.	Michael Crump	713 345 1623
MIGC, Inc.	John Curtis	
Mississippi River Transmission Corp.	Scott Mundy	318 429 3943

<b>Organization</b>	<b>POC Name</b>	<b>Phone Number</b>
Mojave Pipeline Co.	Bennie Barnes	719 520 4677
National Fuel Gas Supply Corp.	John Pustulka	716 857 7909
Natural Gas Pipeline Co. of America	Mark Mayworn	713 369 9347
Nora Transmission Co.	Andy Murphy	412 231 4888
North Carolina Natural Gas	Ted Hodges	919 546 6369
Northern Border Pipeline Co.	Michael Crump	713 345 1623
Northern Natural Gas Co.	Paul Fuhrer	402 398 7733
Northwest Pipeline Corp.	Thomas Odom	270 688 6964
Oncor Gas	Mark Rothbauer	214 875 5574
Overthrust Pipeline Co.	Questar	ronji@questar.com
Ozark Gas Transmission System	Larry Strawn	405 557 5271
Paiute Pipeline Co.	Jerry Schmitz	702 365 2204
Panhandle Eastern Pipe Line Co.	Scott Gallagher	713 989 7444
Petal Gas Storage Co.	Bennie Barnes	719 520 4677
PG&E Gas Transmission-Northwest Corp.	Bill Harris	925 974 4030
PG&E Gas Transmission-Northwest Corp.	Alan Eastman	925 974 4312
Questar Pipeline Co.	Questar	ronji@questar.com
Reliant Energy Gas Transmission Co.	Scott Mundy	318 429 3943
Sabine Pipe Line Co.	George Kohut	510 242 3245
Sea Robin Pipeline Co.	Scott Gallagher	713 989 7444
Shell Offshore Pipelines	John Niemeyer	713 241 1856
Southern Natural Gas Co.	George Benoit	832 528 4244
Southwest Gas Corp.	Jerry Schmitz	702 365 2204
Southwest Gas Storage Co.	Scott Gallagher	713 989 7444
Steuben Gas Storage Co.	George Benoit	832 528 4244
Tennessee Gas Pipeline Co.	George Benoit	832 528 4244
Texas Eastern Transmission Corp.	Steve Rapp	713 627 6394
Texas Gas Transmission Corp.	Thomas Odom	270 688 6964
Total Peaking LLC	Scott Martin	607 347 2561
Trailblazer Pipeline Co.	Mark Mayworn	713 369 9347
TransColorado Gas Transmission Co.	Mark Mayworn	713 369 9347
Transcontinental Gas Pipe Line Corp.	Thomas Odom	270 688 6964
Transwestern Pipeline Co.	Michael Crump	713 345 1623
Trunkline Gas Co.	Scott Gallagher	713 989 7444
Trunkline LNG Co.	Scott Gallagher	713 989 7444
Tuscarora Gas Transmission Co.	Les Cherwenuk	775 834 3674
TXU Gas/TXU Lone Star Pipeline	Mark Rothbauer	214 875 5574
Vector Pipeline	Scott Ironside	780 420 5267
Venice Gathering System, L.L.C.	Rich Mueller	318 429 3943
Viking Gas Transmission Co.	Michael Crump	713 345 1623
Williams Gas Pipelines Central, Inc.	Thomas Odom	270 688 6964
Williston Basin Interstate Pipeline Co.	Keith Seifert	406 359 7223
Wyoming Interstate Company, Ltd.	Bennie Barnes	719 520 4677
Young Gas Storage Company, Ltd.	Bennie Barnes	719 520 4677